Analyse et contrôle de systèmes non linéaires à entrées multiples et à dynamiques couplées par la méthode des formes normales

Tian Tian

École doctorale n° 432 : Science des Métiers de l'ingénieur

Doctorat ParisTech

T H È S E

pour obtenir le grade de docteur délivré par

l'École Nationale Supérieure d'Arts et Métiers

Spécialité "Génie électrique"

présentée et soutenue publiquement par

Tian TIAN

le 15 septembre 2017

Analysis and control of nonlinear multiple input systems with coupled dynamics by the method of normal forms

Application to nonlinear modal interactions and transient stability assessment of interconnected power systems

Directeur de thèse : **Xavier KESTELYN**
Co-encadrement de la thèse : **Olivier THOMAS**

Jury
Mme Manuela SECHILARIU, Professeur des Universités, Université de Technologie de Compiègne   Président
M. Bogdan MARINESCU, Professeur des Universités, Ecole Centrale de Nantes   Rapporteur
M. Claude-Henri LAMARQUE, Professeur ENTPE, Ecole Nationale des Travaux Publics de l'état   Rapporteur
M. Olivier THOMAS, Professeur des Universités, Arts et Métiers ParisTech   Examinateur
M. Xavier KESTELYN, Professeur, Unité de recherche, Arts et Métiers ParisTech   Examinateur

T
H
È
S
E

Arts et Métiers ParisTech - Campus de Xxxx
Nom de l'Unité de recherche

Acknowledgements

Thanks for the initiator, Prof. Xavier KESTELYN, who introduced me to the scientific research. He is a parent-like team-mate. And he gives me great confidence, great patience and a lot of freedom in the scientific exploration. We started from very few resources containing only two reference papers, but we has obtained a lot of achievements, a transaction already published, an another transaction in redaction, 3 IEEE international conference papers, and a PhD dissertation that lays the foundation for several future PhD dissertations. Without the encouragements and the scientific vision of Xavier, we will just end by some fruitless explorations, as the pity that we have seen from some previous researches. Thanks for Prof. Olivier THOMAS, for all the mathematical formulations and theoretical foundations. Since this PhD topic is multi-disciplinary, which mix the electrical engineering, mechanical engineering and automatic engineering, it is the mathematics that link all the domains.

Thanks to the committee members. Mrs. Manuela SECHILARIU kindly accepted to be the president of the committee and designed very interesting questions. Mr. Claude-Henri LAMARQUE and Mr. Bogdan MARINESCU evaluated carefully my PhD dissertation and gave deeper insights than I had expected. Thanks to Mr. Lamarque, who gives insightful remarks to complete the theoretical work. For me, it is a great pleasure to see the person that has achieved a milestone work 26 years ago and with two important papers cited in this PhD dissertation. Thanks to Bogdan, for his insightful comments and inspirations that I have never read, heared, or thought before. I hope that we can collaborate to make some good discoveries. Thanks to Mrs. Manuala SECHILARIU, for your encouragements and especially for your care and suggestions for my future career. During my PhD thesis defense, I was too glad and too excited that I forgot to take a photo with the committee members. It is a great pity. I hope that we can get together again someday.

I would also like to thank an unknown reviewer of PES GM'16, who helps us to find a pile of references papers. Before that (a period of 16 months), we found very few reference papers, we were alone and we work in blind.

I would also like to thank our international collaborators, Mr. Hiroyuki AMANO from Tokyo University, for your inspiration in the nonlinear modal interaction and meticulous scrutiny. Thanks for Mr. Arturo Román MESSINA, you held the torch in the darkness and lighted the way. I'm looking forward to our further collaborations.

ENSAM is a wonderful place to work. Many thanks go to all my colleagues and friends in labo-L2EP and Labo-LSIS. Ngac Ky Nguyen, Adel OLABI, Juliette MORIN, Hussein ZAHR, Tiago MORAES, Martin LEGRY,Jérôme BUIRE, Gabriel MARGALIDA, Oleg Gomozov. Thank you all for making my PhD journey memorable and enjoyable. In addition, I would like to thank the support from our office, the colleagues from LSIS, Emmanuel COTTANCEAU, David BUSSON, Pierre BES-

Simplicity is the ultimate sophistication.

Leonardo da Vinci

List of Abbreviations

- **Dynamical System:** a system in which a function describes the time dependence of a point in a geometrical space

- **Normal Forms:** a "simpler form" of the original system where all the system property is kept

- **Method of Normal Forms (MNF)**: the method that study the dynamical system based on its normal forms

- **Normal Form Transformation:** the transformation of coordinates of state-variables to obtain the normal forms

- **Normal Form Coordinates:** the coordinates where the dynamics of the state-variables are described by the normal forms

- **Normal Dynamics:** the dynamics of the normal forms

- **DAEs:** differential algebraic equations

- **Invariant:** if motion (or oscillation) is initiated on a particular mode, they will remain on this mode without transfer to others

- **Modal Suppersition**

- **Decoupled:** the dynamics of one state-variable is independent of that of others

- **Amplitude-dependent Frequency Shift:** it describes a phenomenon that in system exhibiting nonlinear oscillations, the free-oscilation frequency will vary with respect to the amplitudes

- **Normal Mode:** a basic particular solution of systems in free-oscillations. of motion that move independently to others, the most general motion of a system is a combination of its normal modes.

- **LNM:** Linear Normal Mode

- **NNM:** Nonlinear Normal Mode

- **MS method:** the Modal Series method

- **SP method:** the Shaw-Pierre method

Contents

List of Figures

List of Tables

Introductions générales

Cadre général

Les systèmes électromécaniques industriels à haute performance sont souvent composés d'une collection de sous-systèmes interconnectés travaillant en collaboration, dont la stabilité dynamique est très préoccupante dans l'opération. Plusieurs exemples sont présentés dans la figure 1.

(a) un parc éolien;

(b) un avion plus électrique

(c) un sou-marin;

(d) une véhicule électrique

Figure 1: Examples of Multiple-input with Coupled Dynamics

Du point de vue des systèmes dynamiques, ces systèmes électromécaniques sont dans le cadre «système à entrées multiples avec dynamique couplée», qui sont omniprésents dans tous les aspects de notre vie quotidienne. Leur stabilités méritent d'être étudiées de manière intelligente et méticuleuse pour exploiter leur capacité avec moins de travail humain. Cela donne naissance à l'avenir des technologies avec des bienfaits tels que l'auto-conduite (mieux contrôlé), respect de l'environnement (pour réduire la consommation d'énergie) et etc.

Ce travail de thèse s'inscrit dans le cadre général de l'analyse et la commande des systèmes non-linéaires à entrées multiples ayant dynamiques couplées, qui donne un aperçu sur les comportements dynamiques non-linéaires d'une grande classe des systèmes à entrées multiples, comme illustré sur la figure 1. Ce travail de thèse est multidisciplinaire et la méthodologie systématique proposée analyse et contrôle

les systèmes non-linéaires en simplifiant les non-linéarités par la théorie des formes normales. Des applications sont d'abord réalisées sur l'analyse de la stabilité et la commande des grands réseau électriques.

Analyse de la dynamique des grands réseaux électriques

Un grand réseau électrique (appelé aussi système de puissance interconnectés) se compose d'éléments (générateurs, transformateurs, lignes, ...), plus ou moins nombreux selon la taille du réseau, interconnectés, formant un système complexe capable de générer, de transmettre et de distribuer l'énergie électrique à travers de vastes étendues géographiques.

L'analyse de la dynamique des réseau électriques d'aujourd'hui est un problème difficile et un problème à forte intensité de calcul. Dans la dynamique, de nombreux phénomènes sont intéressants et restent encore à relever.

Cela s'explique en partie par le fait que chacun services d'électricité n'est pas des iles de génération et de contrôle indépendants. Les interconnexions des grandes régions et son utilisation intensive de ces interconnexions faire les ingénieurs de système de puissance d'affronter un système large, poussé à la limite et non-linéaire pour analyser et faire fonctionner.

Par exemple, de plus en plus d'énergie renouvelable a été incluse dans les grands réseaux électriques à ce jour. L'énergie est générée dans des sites distants puis transférée aux zones urbaines avec une longue ligne de transport d'électricité. Ses côtés de l'énergie sont interconnectés pour assurer une répartition optimale de l'énergie. Un exemple du système de puissance interconnecté à grande échelle s'appelle «super grid», qui attire de plus en plus d'attention nationale et globale, comme illustré sur la figure 2.
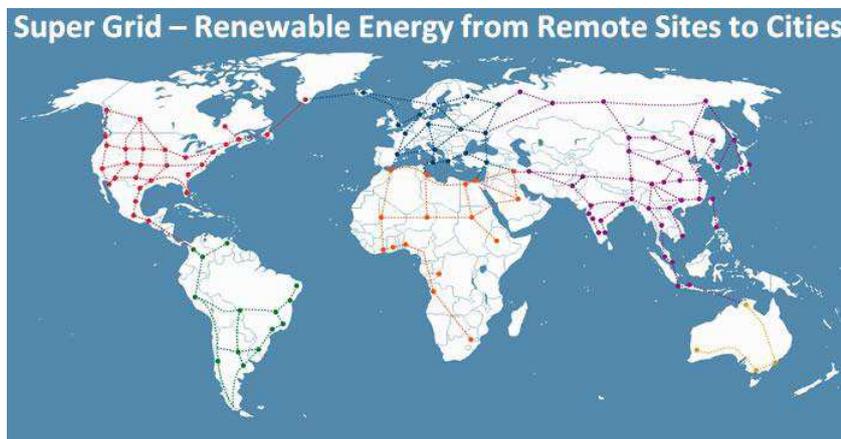
Figure 2: Supergrid– Transfering the Renewable Energy from Remote Sites to the Cities

D'autre part, selon l'exigence de transférer de l'énergie «intelligemment», il s'agit d'exploiter la capacité de transfert en réponse à la crise de l'énergie et d'économiser le travail humain, ce qui conduit à un système de puissance stressé dont la dynamique devrait être examinée afin d'assurer une opération stable. Alors l'étude de la dynamique du système de puissance est nécessaire, surtout, la stabilité des grands réseaux électriques.

La dynamique du système est souvent caractérisée par des oscillations électrique-mécaniques. Analyser la dynamique du système est de répondre à deux questions:

- Comment les composants du système interagissent l'un sur l'autre ? – les interactions modales

- Est-ce que le système arrive finalement un état de stabilité ? –évaluation de stabilité

Les deux questions sont répondu par l'étude de la stabilité du système de puissance.

L'étude de la stabilité des grands réseaux électriques

La stabilité du réseau électrique peut se définir de manière générale comme la propriété d'un système qui lui permet de rester en état d'équilibre opérationnel dans des conditions de fonctionnement normales et de retrouver un état acceptable d'équilibre après avoir subi une perturbation (Étape post-défaut). La stabilité du système dépend de la condition de fonctionnement initiale ainsi que de la nature de la perturbation. Le système est initialement supposé être à une condition d'état de pré-défaut régie par les équations.

Cette thèse se concentre sur la dynamique des angles du rotor quand il y a des perturbations sur la ligne de transport d'électricité, puisque les oscillations électriques-mécaniques sont souvent contastées dans la dynamique des angles rotoriques. Et la dynamique des angle rotoriques caractérise la capacité du système de transférer de l'électricité.

Pour étudier la dynamique des angles rotoriques, on suppose que la stabilité de tension et la stabilité de fréquencie sont déjà assurées.

- **Stabilité de tension**

  On peut définir la stabilité de tension comme la capacité d'un système d'énergie électrique à maintenir des tensions stables à tous ses nœuds après avoir été soumis à une perturbation à partir d'une condition initiale de fonctionnement de ce système. Dans un certain nombre de réseaux, l'instabilité de tension est considérée comme une importante contrainte d'exploitation.

- **Stabilité de fréquence**

Dans un grand système interconnecté, la fréquence subit des variations relativement faibles, même lors d'incidents sévères. L'instabilité de fréquence concerne essentiellement les situations où la perte de plusieurs lignes de transport conduit à un morcélement du système. Si un bloc se détache du reste du système, il évolue vers une fréquence propre et le contrôle de celle-ci peut être difficile en cas de déséquilibre important entre production et consommation au sein de ce bloc. En cas de déficit de production, la chute de la fréquence peut être arrêtée par un délestage de charge (en sous-fréquence). Par contre, en cas de surplus de production, la hausse de la fréquence du système est arrêtée par une déconnexion rapide de certaines unités de productions de sorte que l'équilibre production –consommation soit rétablie.

En effet, selon la nature de la perturbation provoquant l'instabilité, on distingue deux types de stabilité des angles rotoriques que l'on explique ci-après :

- **Stabilité angulaire aux petites perturbations :** Dans les réseaux modernes, l'instabilité angulaire aux petites perturbations prend la forme d'oscillations rotoriques faiblement amorties voire instables. En effet, ces oscillations du rotor qui s'ajoutent au mouvement uniforme correspondant à un fonctionnement normal, ont des fréquences qui se situent entre 0.1 et $2Hz$ suivant le mode d'oscillation.

  L'extension d'une interconnexion et l'incorporation à celle-ci de systèmes moins robustes peut faire apparaître de telles oscillations. Les modes d'oscillation les plus difficiles à amortir sont les modes interrégionaux dans lesquels les machines d'une région oscillent en opposition de phase avec celles d'une autre région.

- **Stabilité angulaire transitoire :** L'instabilité angulaire aux grandes perturbations concerne la perte de synchronisme des générateurs sous l'effet d'un court-circuit éliminé trop tardivement (raté de protection) ou de la perte de plusieurs équipements de transport. La perte de synchronisme se solde par le déclenchement des unités concernées.

Traditionnellement, les études de la dynamique angulaire aux petites perturbations utilisent le modèle linéaire et les études de la dynamique angulaire transitoire utilisent le modèle non-linéaire par contre. Cependant, il est difficile de isoler ces deux parties. Par exemple, les oscillations interrégionaux, qui est un sujet important de la dynamique angulaire aux petites perturbations, sont observées dans l'analyse transitoire (après avoir un défaut de court-circuit triphasé dans la ligne de transport d'électricité), mais sa propriété est étudiée par l'analyse de la stabilité aux petites perturbations.

En outre, lorsque le système éprouve de grandes perturbations, non seulement les limites de transfert sont concernées, mais aussi les sources et les fréquences des oscillations devraient être étudiées. Pour ce problème, l'analyse de la stabilité aux petites perturbations est plus appropriée.

Par conséquent, dans ce travail de thèse, létude de la dynamique angulaire aux petites perturbations est actuellement étendu au domaine non linéaire, pour étudier des oscillations non-linéaires dans des réseaux électriques lorsque le système subi une grande perturbation. Et l'analyse de la stabilité transitoire se concentre sur les limites de transfert, où une stabilité analytique approximative est proposée.

Une analyse bibliographique des recherches de la dynamique angulaire sont présentée dans les parties suivantes.

Analyse de la stabilité angulaire aux petites perturbations basée sur la linéarisation du modèle

La quasi-totalité des systèmes dynamiques réels possède des caractéristiques non-linéaires. Le comportement dynamique d'un système de puissance peut être décrit par un ensemble d'équations différentielles et algébriques (EDA) (1).

$$\boldsymbol{x} = f(\boldsymbol{x}, \boldsymbol{u}) \tag{1}$$
$$g(\boldsymbol{x}, \boldsymbol{u}) = 0$$

Compte tenu que le système de puissance, évolue généralement autour d'un point de fonctionnement donné lors des petites perturbations, il est possible de linéariser ses équations EDA autour de ce point.

Le point de fonctionnement normal du système se définit comme un point d'équilibre ou une condition initiale. Les dérivées des variables d'état en ce point sont donc égales à zéro.

$$\dot{\boldsymbol{x_0}} = f(\boldsymbol{x_0}, \boldsymbol{u_0}) = 0 \tag{2}$$

Où: $\boldsymbol{x_0}$ est le vecteur des variables d'état correspondantes aux points d'équilibre.

Si une petite perturbation se superpose aux valeurs d'équilibre, la série de taylor de (1) en point $\boldsymbol{x_0}$ est la série de fonctions suivante :

$$\triangle\dot{\boldsymbol{x}} = A\triangle\boldsymbol{x} + \mathcal{O}(2) \tag{3}$$

avec matrice d'état A $(n \times n)$ dont $A_{kl} = \frac{\partial f_k}{\partial x_l}$ et $\boldsymbol{u} = \boldsymbol{u_0}$. $\mathcal{O}(2)$ ramasse les termes d'ordre supérieur.

Négliger tout les termes d'ordre supérieur et diagonaliser A par des transformations de similarité unitaires $x = Uy$. Nous obtenons :

$$\triangle\dot{\boldsymbol{y}} = \Lambda\triangle\boldsymbol{y} \tag{4}$$

Où: λ_i est une $i^{\text{ème}}$ valeur propre, U_i est le $i^{\text{ème}}$ valeur propre à droite associé à λ_i, V_i est le $i^{\text{ème}}$ valeur propre à droite associé à λ_i.
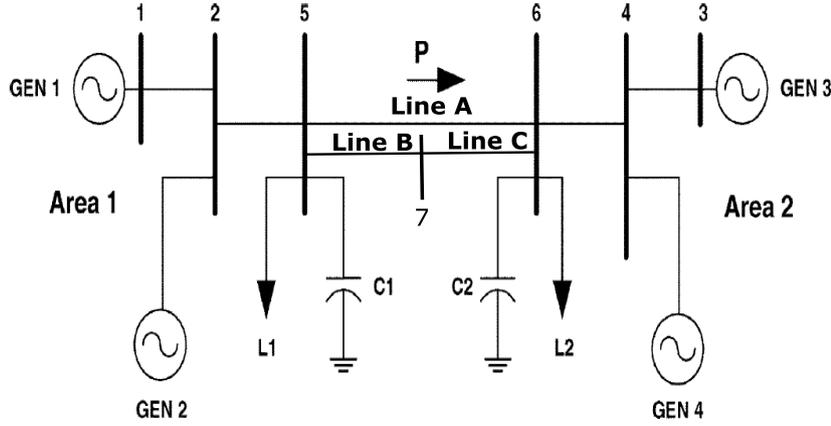
Figure 3: Kundur's 2 Area 4 Machine System

La solution de (4) est une série de $e^{(\lambda_i)t}$, $i = 1, 2, \cdots, N$. C'est-à- dire que la dynamique du système est la supposition des modes indépendants se caractérise par $\lambda_i = \sigma_i + j\omega_i$. La stabilité de mode i se caractérise par σ_i. Si $\sigma_i < 0$, le système est stable en régime dynamique. Et moins σ est, plus stable c'est.

Analyse des interactions modales basée sur la linéarisation du modèle

Vecteur propre à droite U mesure l'influence relative de chaque variable d'état x_k dans un $i^{\text{ème}}$ mode et qu'un vecteur propre à gauche V_i indique la contribution de l'activité de x_k dans le $i^{\text{ème}}$ mode. Par conséquent, une «quantité» caractéristique d'un mode donné peut être obtenue par produit, élément par élément, d'un vecteur propre à droite et d'un vecteur propre à gauche correspondant. Cette quantité, appelée le facteur de participation, est calculée par la relation suivante:

$$p_{ki} = U_{ki}V_{ik} \tag{5}$$

Ainsi, le facteur de participation peut fournir des informations fines sur le problème: il représente une mesure relative de la participation de la $k^{\text{ème}}$ variable d'état dans le $i^{\text{ème}}$ mode, et vice versa [1].

Par le facteur de participation, nous constatons que il y a quatre type d'oscillation dans des grands réseaux électriques:

- **Les oscillations des modes locaux** Les modes locaux sont les modes les plus rencontrés dans les systèmes de puissance. Ils sont associés aux oscillations entre un générateur (ou un groupe des générateurs) d'une centrale électrique et le reste du système. Le terme local est utilisé car les oscillations sont localisées dans une seule centrale ou une petite partie du système, (par exemple : les générateurs G1 par rapport au générateur G2 trouvé dans la même

région (Area 1), figure 3). La gamme de fréquence de ces oscillations est généralement de 1 à 2 Hz. L'expérience montre que ces oscillations tendent à se produire lors de l'utilisation des régulateurs de tension possédant une réponse rapide et quand le lien de transmission entre une centrale et ses charges est très faible. Pour assurer un bon amortissement de ces modes, des sources d'amortissement, tel le stabilisateur de puissance, peuvent être ajoutées aux générateurs à l'origine de ces modes.

- **Les oscillations des modes globaux** Les oscillations des modes globaux, ou oscillations interrégionales, sont associées à l'oscillation entre certains générateurs d'une partie du système et certains générateurs d'une autre partie du système (par exemple : les générateurs, G1 et G2 de la région (area 1) oscillent ensemble par rapport au générateur G3 et G4 de la région (area 2), figure 3).

  Les modes associés à ces oscillations présentent généralement des amortissements très faibles et, si ces derniers sont négatifs, de petites perturbations peuvent exciter des oscillations divergentes.

  Les fréquences de ces oscillations se trouvent généralement dans la gamme de 0.1 à 1 Hz. Cette gamme est inférieure à celle des modes locaux car les réactances des liens entre les systèmes de puissance sont élevées. Généralement, la fréquence naturelle et le facteur d'amortissement d'un mode interrégional décroissent lorsque l'impédance d'une ligne d'interconnexion ou la puissance transmise augmente. Le système d'excitation et les caractéristiques des charges affectent également les oscillations des modes interrégionaux. Ainsi, ces modes présentent des caractéristiques plus complexes que ceux des modes locaux. Étant donné que les modes interrégionaux impliquent plusieurs générateurs, un bon amortissement de tels modes peut exiger l'utilisation de stabilisateurs de puissance pour un grand nombre des générateurs.

- **Les oscillations des modes de contrôle** Les oscillations associées aux modes de contrôle sont dues :

  - soit, aux contrôleurs des générateurs (mauvais réglage des contrôleurs des systèmes

  - soit, aux autres dispositifs contrôleurs (convertisseurs HVDC, SVC,...).

  La fréquence de ces oscillations est supérieure à $4Hz$.

- **Les oscillations des modes de torsion** Ces oscillations sont essentiellement reliées aux éléments en rotation entre les générateurs et leurs turbines. Elles peuvent aussi être produites par l'interaction des éléments de rotation avec le contrôle d'excitation, le contrôle de gouverneur, les lignes équipées avec des compensateurs de condensateurs en série,... La fréquence de ces oscillations est aussi supérieure à $4Hz$.

Un système ayant plusieurs générateurs interconnectés via un réseau de transport se

comporte comme un ensemble de masses interconnectées via un réseau de ressorts et présente des modes d'oscillation multiples. Parmi tout les types de oscillations, les oscillations des modes globaux nous intéressent le plus. Dans les oscillations de modes interrégionaux, plusieurs générateurs de différentes régions sont impliqués et ils peuvent provoquer des défauts en cascade. Étudier les interactions entre les composantes sont très important pour comprendre les comportements dynamique du système et puis améliorer sa performance dynamique, par exemple, l'amortissent des oscillations de modes interrégionaux par l'emplacement optimal de PSS (power system stabilizer).

Évaluation de la stabilité transitoire

Le processus transitoire peut durer longtemps, et ce que nous nous intéressons, c'est le processus de post-perturbation, c'est-à-dire si le système va revenir à l'état d'équilibre après que la perturbation est effacée. Il s'agit de l'évaluation de la stabilité transitoire (TSA).

Une variété d'approches permettant l'évaluation de la stabilité des réseaux d'énergie électrique a été proposée dans la littérature. Les méthode les plus répandue peuvent être classées en deux catégories distinctes :

- Méthodes indirectes d'intégration numérique.

- Méthodes directes énergétiques.

Il y a des méthodes pour TSA où une solution analytique n'est pas fournie. Voyez chapitre 1 pour un examen de la littérature plus détaillé des recherches sur ce sujet.

Méthodes indirectes d'intégration numérique

C'est l'approche la plus largement appliquée dans le marché est l'intégration numérique étape pas-à-pas, mais généralement nécessite beaucoup de calcul pour l'application en ligne. Les algorithmes d'intégration numérique sont utilisés pour résoudre l'ensemble des équations différentielles de premier ordre qui décrivent la dynamique d'un modèle de système. L'intégration numérique fournit des solutions relatives à la stabilité du système en fonction des détails des modèles utilisés.

Dans de nombreux cas, cela suffit pour s'assurer que le système restera synchronisé pour tous les temps après le retour.

Cependant, dans d'autres cas, la dynamique du système peut être telle que la perte de synchronisme ne se produit pas jusqu'à ce que les générateurs aient connu de multiples oscillations. Alors c'est difficile de décider quand s'arrêter une simulation et c'est impossible d'obtenir la marge de stabilité .

Méthodes directes énergétiques

Méthodes graphiques (Critère d'égalité des aires) Considérons un défaut, tel
un défaut sur la ligne de transmission, appliqué au système précédent disparaissant
après quelques périodes du système. Ceci va modifier l'écoulement de puissance et,
par conséquent, l'angle de rotor δ. Retraçons la courbe $(P - \delta)$ en tenant compte
de ce défaut, figure 4. En dessous de cette courbe, nous pouvons considérer deux
zones [1] :

1. La première zone (zone A1, zone d'accélération) se situe au-dessous de la droite
   horizontale correspondante au point de fonctionnement initial (la droite de
   charge). Elle est limitée par les deux angles de rotor (δ_0 et δ_1) correspondants
   à l'apparition et à la disparition de défaut. Cette zone est caractérisée par
   l'énergie cinétique stockée par le rotor du fait de son accélération : $P_m > P_e$.

2. La deuxième zone (zone A2, zone de décélération), qui commence après
   l'élimination du défaut, se situe en dessus de la droite de charge : elle est
   caractérisée par la décélération du rotor : $P_m < P_e$.

Si le rotor peut rendre dans la zone $A2$ toute l'énergie cinétique acquise durant la
première phase, le générateur va retrouver sa stabilité. Mais si la zone $A2$ ne per-
met pas de restituer toute l'énergie cinétique, la décélération du rotor va continuer
jusqu'à la perte de synchronisme. (Voyez [1,2] pour une démonstration mathéma-
tique.)

Durant les trois dernières décennies, les méthodes énergétiques directes ont sus-
cité l'intérêt de plusieurs chercheurs [3]. A.M. Lyapunov a développé une struc-
ture générale pour l'évaluation de la stabilité d'un système régi par un ensem-
ble d'équations différentielles afin d'obtenir une évaluation plus rapide. L'idée de
base des nouvelles méthodes développées est de pouvoir conclure sur la stabilité ou
l'instabilité du réseau d'énergie sans résoudre le système d'équations différentielles
régissant le système après l'élimination du défaut. Elles utilisent un raisonnement
physique simple basé sur l'évaluation des énergies cinétique et potentiel du système.

Contrairement à l'approche temporelle, les méthodes directes cherchent à déterminer
directement la stabilité du réseau à partir des fonctions d'énergie. Ces méthodes
déterminent en principe si oui ou non le système restera stable une fois le défaut
éliminé en comparant l'énergie du système (lorsque le défaut est éliminé) à une
valeur critique d'énergie prédéterminée.

Les méthodes directes énergétiques non seulement permettent de gagner un temps
requis au calcul pas à pas que nécessite l'analyse temporelle, mais donnent égale-
ment une mesure quantitative du degré de stabilité du système. Cette information
additionnelle rend les méthodes directes très intéressantes surtout lorsque la stabil-
ité relative de différentes installations doit être comparée ou lorsque les limites de
stabilité doivent être évaluées rapidement. Un avantage clé de ces méthodes est leur
habilité dans l'évaluation du degré de stabilité (ou d'instabilité). Le second avantage
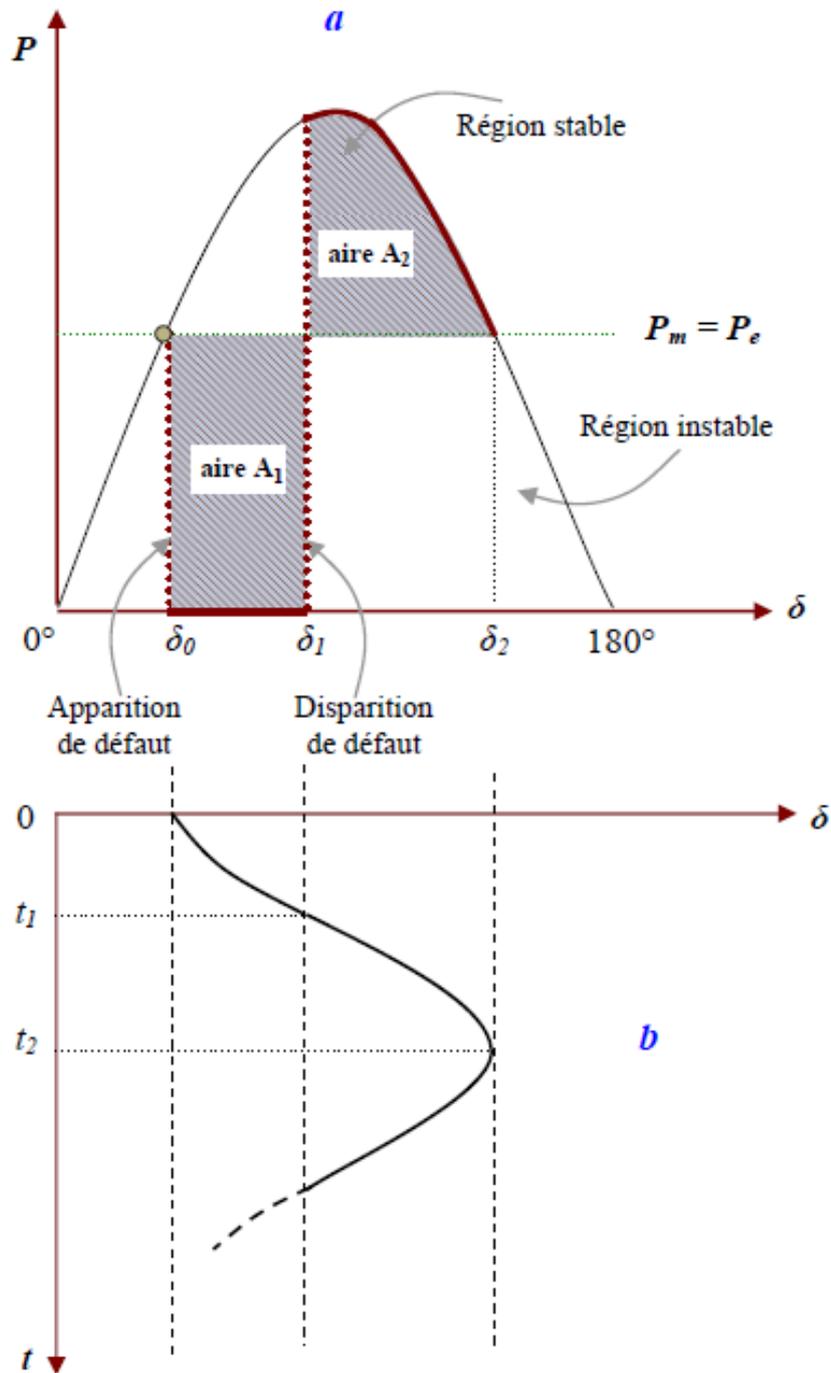
Figure 4: Equal Area Criteria (E-A)

est leur capacité à calculer la sensibilité de la marge de stabilité à divers paramètres du réseau, permettant ainsi un calcul efficient des limites d'exploitation.

Dans la pratique, il existe encore des problèmes non résolus et des inconvénients de cette approche. L'efficacité de cette méthode dépend des simplifications choisies des variables du système. L'intégration de la faute sur les équations du système est nécessaire pour obtenir la valeur critique pour évaluer la stabilité. Il est difficile de construire la fonction appropriée de Lyapunov pour refléter les caractéristiques internes du système. La méthode n'est rigoureuse que lorsque le point de fonctionnement est dans la région de stabilité estimée.

Problème

Depuis une trentaine d'années, les grands réseaux électriques se trouvent obligés de fonctionner à pleine puissance et souvent aux limites de la stabilité. Faire la linéarisation d'un système d'équations entraînerait beaucoup d'erreurs de modélisation et échouerait pour prédire des comportements dynamiques tell que oscillations non-linéaires à fréquence variable [4] et la stabilité [5]. Il a entraîné la nécessité d'une meilleure compréhension des non-linéarités dans le comportement dynamique du réseaux électrique.

Quelques caractéristiques propres aux grands réseaux électriques qui contribuent aux comportements non linéaire en régime dynamique ou transitoire peuvent être citées :

- la relation puissance-angle qui est une relation non-linéaire en sinus;

- étendue géographique des sites jusqu'à plusieurs dizaines d'hectares composée d'une collection de générateurs;

- longueur des connexions, lignes et câbles, jusqu'à centaines de kilomètres pour les différents niveaux de tension;

- une plus forte demande en électricité tel que le système est déjà poussé à la limite.

Alors il faut trouver une méthodologie systématique pour étudier les comportements non-linéaire en utilisant les modelés non-linéaire.

Il aussi nécessite de trouver une méthode afin

- d'identifier les interactions modales nonlinéaires entre les composants du système et les modes d'oscillations non-linéar;

- d'obtenir une évaluation de la stabilité plus rapide et plus facile en tenant compte les non-linéarités.

Cependant, garder tous les termes non-linéaires est laborieux et n'est pas nécessaire. Dans mes travaux, il s'agit de trouver une méthode où les non-linéarités principales

sont gardées afin de conserver l'essentiel du comportement non-linéaire, alors que d'autres sont ignorées pour simplifier les calculs.

Nous conservons notamment les termes qui contribuent à la précision, la stabilité, et la fréquence des oscillations. Cette méthode est basée sur la théorie des formes normales de Poincaré qui élimine des termes non-linéaire par le biais de transformations non-linéaires.

Méthode des formes normales

Théorie des formes normales

Théorème de Poincaré-Dulac : Soit un système dynamique dépendant de X: $\dot{X} = AX + N(X)$. A est linéaire, $N(X)$ est nonlinéaire. Le changement de variable $X = Y + h(Y)$ permet d'éliminer tous les monômes non-résonnants: $\dot{Y} = AY + A_n(Y)$, qui est sous sa forme «la plus simple».

Cette méthode est intéressante pour des systèmes suffisamment différentiables. En prenant successivement les changements de variables $X = Y + h2(Y)$, puis $Y = Z + h3(Z)$ etc, on stabilise bien un terme supplémentaire de degré fixé à chaque étape et obtient les formes normales avec une certaine précision. On a déjà obtenu des réussites sur l'analyse d'un systèmes en mécanique des structures. Nous considérons l'utiliser sur systèmes électromécaniques à dynamiques couplées non-linéaires.

Analyse de la dynamique des grands réseaux électriques par la théorie des formes normales

Des formes normales à l'ordre 2 sont proposée et bien appliquées dans l'analyse des dynamiques de grands réseaux électriques [6–15]. Cependent, il y a des phénomènes non-linéaire restent à relever par des formes normales à l'order 3. Mais des formes normales à l'order 3 n'est pas complétée et n'est pas suffisamment précise [5,16].

Analyse en mécanique des structures basée sur la théorie des formes normales

Notion de mode normal

Pour un système oscillatoire à plusieurs degrés de liberté, un mode normal ou mode propre d'oscillation est une forme spatiale selon laquelle un système excitable (micro ou macroscopique) peut osciller après avoir été perturbé au voisinage de son état d'équilibre stable; une fréquence naturelle de vibration est alors associée à cette forme. Tout objet physique, comme une corde vibrante, un pont, un bâtiment ou

encore une molécule possède un certain nombre, parfois infini, de modes normaux de vibration qui dépendent de sa structure, de ses constituants ainsi que des conditions aux limites qui lui sont imposées. Le nombre de modes normaux est égal à celui des degrés de liberté du système.

Le mouvement le plus général d'un système est une superposition de modes normaux. Le terme «normal» indique que chacun de ces modes peut vibrer indépendamment des autres, c'est-à-dire que l'excitation du système dans un mode donné ne provoquera pas l'excitation des autres modes. En d'autres termes, la décomposition en modes normaux de vibration permet de considérer le système comme un ensemble d'oscillateurs harmoniques indépendants dans l'étude de son mouvement au voisinage de sa position d'équilibre stable.

Mode non-linéaire basée sur des formes normales

Le comportement des systèmes oscillatoires à dynamiques couplées non-linéaires ne peut pas être traités par des modes normaux linéaires car des propriétés non-linéaires seraient perdues. On propose la notion de «Mode non-linéaire» qui conserve variété invariante de l'espace des phases [17–19]. Tous les modes non-linéaires sont «les formes normales» d'un système oscillatoire, calculés en une seule opération basée sur la théorie des formes normales [17–19]. Validé par l'expérimentation, les modes non-linéaires prédisent plus exactement le comportement dynamique non linéaire d'un système mécanique.

Ce que nous proposons dans cette thèse

Dans cette thèse, des méthodes des formes normales sont propoées par deux approches.

Dans une première approche, nous avons employé la méthode des champs vectoriels. L'équation d'un système est sous la forme comme suit:

$$\dot{x} = f(x) \tag{6}$$

L'expérimentation est réalisée dans l'étude de cas: IEEE 2-area 4-machine système (fig. 3). Le travail suscite un intérêt et une collaboration au niveau international: HIROYUKI Amano (Japonais) et MESSINA Arturo Roman (Mexicain). Une publication est acceptée par une revue internationale *IEEE Transactions on Power Systems*.

Dans une deuxième approche, nous avons modifié les modes non-linéaire normaux pour étudier le dynamique d'un système électromécanique tell que convertisseurs

interconnectés. L'équation d'un système est sous la forme de celle d'un oscilla-
teur comme (7) afin d'obtenir une meilleur compréhension physique par rapport
à la méthode des champs vectorielles. Une publication dans revue est en cours de
rédaction.

$$M\ddot{\boldsymbol{q}} + D\dot{\boldsymbol{q}} + K\boldsymbol{q} + f_{nl}(\boldsymbol{q}) = 0 \qquad (7)$$

En réalisant ce travail, nous considérons la généralisation de l'étude du comporte-
ment dynamique non-linéaire du système électromécanique comme suit :

1. de l'analyse à la commande et à la conception: A partir des résultats fournis
   par les analyses nonlinéaire, il est possible de ddévelopper ensuite des méthodes
   pour améliorer la performance dynamique du systéme de puissance, par exem-
   ple, l'emplacement optimal de PSS (power system stabilizer) selon les résultats
   de l'analyse des formes normales [20], étudier l'influences de paramètres prin-
   cipaux pour le réglage de contrôleurs [16] et la conception des grands réseaux
   électriques [21].

   Ailleurs, des explorations très originales dans la commande des entraînements
   électriques utilisant des formes normales ont été effectuées. Ces approches
   consistent à découpler le systéme non-linéaire à sous-systèmes qui peut être
   contrôlé de façon indépendante.

2. de la théorie à la pratique: comment faire l'analyse et la commande du sys-
   tème industriel? Raffiner la méthodologie prenant en compte des apports
   industriels, par exemple, appliquer les méthodologies sur le système à grande
   échelle.

Objectif, organisation et position de cette recherche de doctorat

Objectif et la tâche

L'objectif de cette thèse est de:

- élaborer une méthodologie systématique pour analyser et contrôler les sys-
  tèmes à entrées multiples non linéaires avec une dynamique couplée basée sur
  des méthodes de formes normales à l'ordre 3;

- appliquer la méthodologie systématique pour étudier le comportement dy-
  namique non linéaire des grands réseaux électriques;

- analyser les facteurs que influencent la performance de la méthodologie pro-
  posée et comprendre ses limites et la façon de l'améliorer;

- tirer de conclusions générales pour l'analyse de systèmes dynamiques non-linéaires et développer la stratégie de commande pour améliorer leur performances dynamiques;

La réalisation des objectifs se compose de:

- le développement des méthodes des formes normales (MNF) jusqu'à l'ordre 3;

- la mise en œuvre de programmes génériques de MNF applicables aux systèmes dynamiques avec des dimensions arbitraires;

- la modélisation mathématique des grands réseaux électriques sous forme de série Taylor jusqu'à l'ordre 3;

- l'application des méthode proposée pour étudier les oscillations des modes interrégionaux et la stabilité des grands réseaux électriques.

L2EP et LSIS

Cette thèse est issu d'une collaboration entre deux laboratoires, le L2EP (Laboratoire d'Electrotechnique et d'Electronique de Puissance de Lille) et le LSIS-INSM (Laboratoire des Sciences de l'Information et des Systèmes-Ingénierie Numérique des Systèmes Mécaniques) de l'ENSAM sur le campus à Lille. Le directeur de thèse est Xavier KESTELYN (L2EP) et le co-directeur est Olivier THOMAS (LSIS), dont tous les deux sont professeurs à l'ENSAM-Lille. Il s'agit également d'une collaboration entre les domaines électriques et les domains mécaniques ainsi qu'une collaboration entre le commande et l'analyse, et tous s'appartiennent à mathématiques appliqués.

Cette thèse est basée sur certaines compétences et expertises déjà accumulées à l'intérieur du laboratoire L2EP et LSIS. L2EP a effectué beaucoup de pratiques du contrôle non-linéaire dans le domaine électrique. LSIS-INSM a déjà accumulé beaucoup d'expertise dans l'analyse non-linéaire des structures flexibles et de la validation expérimentale.

Une application de la théorie des formes normales dans l'analyse des structures dans le domaine mécanique consiste à tirer de les modes normals non-linéaire (nonlinear normal mode, NNM) pour le cas spécifique où des systèmes vibratoires présentant des non-linéarités de type polynomial. NNM est un outil théorique utilisé pour réduire le système de degrés finis en un seul degré tout en conservant la propriété essentielle du système et prédire son comportement sous excitation.

Dans l'analyse de la dynamique du système, les principaux avantages bien connus et largement utilisés des modes normaux sont: 1). Les modes et les fréquences naturelles résultent de la résolution (théorique ou numérique) d'un problème des valeurs propres (fréquences) et des vecteurs propres (modes) qui peuvent simultanément indiquer les oscillations modales ainsi que la stabilité ou l'instabilité asympto-

tique. 2). Le modèle peut être réduit pour ne considérer que les modes dominants, ce qui peut largement simplifier l'analyse et le calcul.

LSIS: Analyse en mécanique des structures basée sur la théorie des formes normales

Notion de mode normal

Pour un système oscillatoire à plusieurs degrés de liberté, un mode normal ou mode propre d'oscillation est une forme spatiale selon laquelle un système excitable (micro ou macroscopique) peut osciller après avoir été perturbé au voisinage de son état d'équilibre stable; une fréquence naturelle de vibration est alors associée à cette forme. Tout objet physique, comme une corde vibrante, un pont, un bâtiment ou encore une molécule possède un certain nombre, parfois infini, de modes normaux de vibration qui dépendent de sa structure, de ses constituants ainsi que des conditions aux limites qui lui sont imposées. Le nombre de modes normaux est égal à celui des degrés de liberté du système.

Le mouvement le plus général d'un système est une superposition de modes normaux. Le terme "normal" indique que chacun de ces modes peut vibrer indépendamment des autres, c'est-à-dire que l'excitation du système dans un mode donné ne provoquera pas l'excitation des autres modes. En d'autres termes, la décomposition en modes normaux de vibration permet de considérer le système comme un ensemble d'oscillateurs harmoniques indépendants dans l'étude de son mouvement au voisinage de sa position d'équilibre stable.

Mode non-linéaire basée sur des formes normales

Le comportement des systèmes oscillatoires à dynamiques couplées non-linéaires ne peut pas être traités par des modes normaux linéaires car des propriétés non-linéaires seraient perdues. On propose la notion de «Mode non-linéaire» qui conserve variété invariante de l'espace des phases [17–19]. Tous les modes non-linéaires sont «les formes normales» d'un système oscillatoire, calculés en une seule opération basée sur la théorie des formes normales [17–19]. Validé par l'expérimentation, les modes non-linéaires prédisent plus exactement le comportement dynamique non linéaire d'un système mécanique.

L2EP: laboratoire se concentre sur le système électrique à multiple entrées ayant dynamiques couplées

L2EP a accumulé beaucoup d'expertise dans la modélisation, l'analyse des systèmes de puissance (mais principalement en fonction de l'analyse linéaire des petits signaux) et du contrôle basé sur le modèle. Cela contribue à la modélisation et aux

éléments de contrôle dans le développement d'une méthodologie pour analyser et contrôler le système non linéaire.

Contributions scientifiques

Des contributions scientifiques de cette thèse sont résumés comme suit:

- Du point de vue des domaines disciplinaires: cette thèse est multidisciplinaire, associée aux mathématiques appliquées, à la dynamique non-linéaire, au genie mécanique et au genie mécanique électrique. Et il s'efforce de tirer des propriétés non-linéaires essentielles, qui sont communes aux systèmes dynamiques non-linéaires ayant le type particulier de dynamique couplée, quel que soit le système mécanique ou le système électrique. Par exemple, le phénomène où la fréquence varie avec l'amplitude des oscillations libres est courant pour une structure mécanique [17] et des grands réseaux électriques [22]. Les résultats présentés dans cette theèse peuvent être utilisés pour interpréter la dynamique non-linéaire des autres systèmes.

- Du point de vue des recherches sur le système dynamique:

  1. il a effectué l'analyse non linéaire sur l'oscillation libre ainsi que sur l'oscillation forcée;

  2. il s'efforce de prendre l'analyse ainsi que le contrôle du système dynamique non-linéaire, qui relie l'écart entre l'analyse non-linéaire et le contrôle non-linéaire. Il propose le contrôle non linéaire basé sur l'analyse et le contrôle de la base de découplage.

- Du point de vue de l'application:

  1. c'est la première fois que toutes les méthodes existantes des formulaires normaux jusqu'au l'ordre 3 ont été résumées et que leurs performances ont été évaluées;

  2. c'est la première fois qu'une méthode des formes normales en forme de modes normaux est appliquée pour étudier la stabilité transitoire du système;

  3. c'est la première fois que la modélisation mathématiques du système de puissance dans la série Taylor est fournie;

  4. c'est la première fois que les programmes génériques des méthodes des formes normales présentées dans cette thèse sont partagés en ligne pour faciliter les futurs chercheurs. Ces programmes sont applicables à des systèmes à dimension arbitraire.

Corps de la thèse

Cette thèse est composée de 6 chapitres:

- **Chapitre 1** Dans ce chapitre, le sujet de cette dissertation est introduit avec des exemples concrets, sans utilisant de mots difficiles ou complexes pour faciliter la compréhension. Il commence à partir des concepts et de la théorie classiques et bien connus. Ensuite, il utilise des mathématiques simples et des exemples très concrets et réalistes pour montrer les limites des méthodes conventionnelles et introduit graduellement la problématique. Les approches dans la littérature sont examinée est pour expliquer la nécessité de proposer de nouvelles méthodologies et ce qu'on peut attendre de cette nouvelle méthodologie. Il explique également pourquoi il s'agit de la méthode des formes normales qui devrait être utilisée, plutôt que d'autres méthodes analytiques, telles que les méthodes de la série-modale et les méthodes Shaw-Pierre. L'objectif, l'organisation et le positionnement du travail de doctorat sont également indiqués.

- **Chapitre 2** Dans ce chapitre, deux méthode sont proposées avec des programmes génériques qui sont applicables aux systèmes dynamiques avec des dimensions arbitraires.

- **Chapitre 3-4** Ce chapitre présente l'application des méthode proposée (méthode 3-3-3 et méthode NNM) pour étudier les oscillations des modes interrégionaux et évaluer la stabilité transitoire grands réseaux électriques avec des modélisation mathématiques sous forme de série Taylor jusqu'à l'ordre 3. Les méthodes sont validée sur le réseau test étudié (réseau multimachines interconnecté).

- **Chapitre 5** Ce chapitre tire des conclusions générales sur l'analyse de la dynamique non-linéaire du systéme et se propose d'améliorer la performance dynamique par deux approches:

  1. le réglage des paramètres du contrôleur ou l'emplacement de PSS basée sur l'analyse le modèle non-linéaire du système;

  2. la commande des entraînements électriques utilisant des formes normales

  Les recherches sont encore loin d'être finalisées dans 3 trois sans, mais ils identifient de problèmes intéressants qui peut devenir les sujets d'autres dissertations.

-

- **Chapitre 6** Les conclusions et perspectives sont présentées dans ce chapitre.

Introductions

In this chapter, the topic of this dissertation is introduced with basic definition and daily examples, without using difficult or complex words to facilitate comprehension. It introduces the problems and the conventional linear methods. Then it uses simple mathematics and very concrete and realistic examples from the experimental tests to show the limitations of the conventional methods and the call for nonlinear tools. A state-of-art of nonlinear tools then explain the need to propose new methodologies and what should be expected from this new methodology. It also explains why it is the method of Normal Forms that should be used, rather than other analytical nonlinear methods, such as the Modal Series Methods and Shaw-Pierre Methods. The objective, organization and positioning of the PhD work is also stated.

Keywords: Power System Stability, Rotor Angle Stability, Small-signal Stability, Transient Stability, Methods of Normal Forms, Modal Series Methods

1.1   General Context

1.1.1   Multiple Input System with Coupled Dynamics

High-performance industrial electromechanical systems are often composed of a collection of interconnected subsystems working in collaboration, to increase the flexibility and reliability. Several daily examples are shown in Fig. 1.1.

Fig. 1.1 (a) shows an interconnected power system composed of numerous wind-turbine generators to capture the maximum wind energy and the generators are electrically coupled. Since the wind energy captured by each generator varies drastically in a day, using a collection of generators can smooth the output power. Fig. 1.1 (b) shows a popular European project–"more electric aircrafts" that involves more and more electric motors in the aircrafts which are either electrically coupled or mechanically coupled. Those motors work in collaboration to increase the autonomy of the aircrafts and the comfort of the flight. Fig. 1.1 (c) shows a submarine that is driven by multi-phase electrical drives where the phases are coupled magnetically. When there is fault in one phase, the electrical drive can still work. Fig. 1.1 (d) shows a electric vehicle where the drives are coupled energetically, to give higher flexibility and reliability in driving.

- Interconnected renewable energy generators, Fig.1 (a)

- More electric aircrafts, Fig.1 (b)

- Multi-phase electrical drives, Fig.1 (c)

- Electric vehicles, Fig.1 (d)

(a) Wind Farm   (b) More Electric Aircrafts

(c)Submarine   (d) Electric vehicles

Figure 1.1: Examples of Multiple-input with Coupled Dynamics

From the perspective of dynamical systems, those electromechanical systems can be generalized as "multiple input system with coupled systems dynamics", which is omnipresent in all aspects of our daily life and the analysis and control of its dynamic performance are of great concern.

1.1.2 Background and Collaborations of this PhD Research Work

This PhD research work based on two national laboratories, L2EP (Laboratoire d'Electrotechnique et d'Electronique de Puissance de Lille) and LSIS-INSM (Laboratoire des Sciences de l'Information et des Systèmes - Ingénierie Numérique des Systèmes Mécaniques) in the campus of ENSAM in Lille. The director of this PhD thesis is Xavier KESTELYN (L2EP) and the co-director is Olivier THOMAS(LSIS), both of whom are professors at ENSAM-Lille. This PhD topic is multidisciplinary. It is also a collaboration of people working in electrical and mechanical domains and a collaboration between control and analysis. The common foundation is the applied mathematics and the essential physical properties of system dynamics.

This PhD topic – "Analysis and Control of Nonlinear Multiple Input Systems with Coupled dynamics" is proposed to solve the common problems encountered by L2EP and LSIS. L2EP has performed a lot of nonlinear control practices in electrical domain. LSIS-INSM has already accumulated a lot of expertise in nonlinear analysis of flexible structures and experimental validation.

1.1.2.1 LSIS: Expertise in Normal Form Analysis of Mechanical Structures

An application of Normal Form Theory in structural analysis in mechanical domain is to derive Nonlinear Normal Mode (NNM) for the specific case of vibratory systems displaying a polynomial type of nonlinearities. NNM is a theoretical tool used to reduce the finite-degree system into single-degree while keeping the essential physical property of the system and predict its behaviour under excitation.

Nonlinear normal mode is to extend the notion of linear normal mode. In the linear analysis, the system dynamics is a composition of independent modes, which are named as normal modes. And the NNM proposed by Touzé are invariant modes. It is invariant because when the motion is only initialized in one mode j, other modes will keep zero, and the system dynamics are only contained in the mode j.

In the mechanical domain, it is used to reduce the model, and the system dynamical behaviour can be characterized by a single NNM. Experiments show that a single NNM based on NF predicts the correct type of nonlinearity (hardening/softening behaviour) [17], whereas single linear mode truncation may give erroneous result. Another application is focused on how all the linear modal damping terms are gathered together in order to define a precise decay of energy onto the invariant manifolds, also defined as nonlinear normal modes (NNMs) [18].

1.1.2.2 L2EP and EMR

L2EP is a Laboratory working on multiple input electrical system with coupled dynamics. It has accumulated a lot of expertise in power system modelling and analysis (though mainly based on the linear small signal analysis) [Team: Réseau]; and control of multiple input electrical system with coupled dynamics, such as the electric vehicles, multiphase electrical machines [Team: Commande] and etc.

Although those researches proposed various methodologies to solve the practical problems, most of their researches are based on the Energetic Macroscopic Representation (EMR) and Inversion-Based Control (IBC) Strategy.

Proposed by Prof. Alain BOUSCAYROL, the leader of the control team of lab L2EP, EMR contributes to modelling and control of multi-inputs system with highly coupled dynamics.

EMR is a multi-physical graphical description based on the interaction principle (systemic) and the causality principle (energy), by Prof. Alain BOUSCAYROL. It highlights the relations between the subsystems as actions and reactions decided by the inputs and outputs flowing between each other. It classifies subsystems into sources, accumulation,conversion and distribution elements by their energetic functions. It uses blocks in different colour and shapes to represent subsystems with different functions correspondingly.

A real system, having multiple inputs and strong energetic couplings, can be modelled by a set of decoupled fictitious single-input systems. The control structure, which is deduced from the model, facilitates the control of stored energies, helps to run the system in fault mode and makes it possible to use simple and easy-to-tune controllers, since each of them is assigned to a unique objective.

The EMR classifies the subsystems according to their energetic function in the system dynamics into 4 categories: source, accumulation, conversion, and coupling.

Source elements are terminal elements which deliver or receive energy; they are depicted by green oval pictographs, as in Fig. 1.2 (a). Accumulation elements store energy, e.g. a capacitor, a flywheel, an inductance, etc.; they are depicted by orange rectangular pictogram with an oblique bar inside, Fig. 1.2 (b). Conversion elements transform energy without accumulating it, e.g. an inverter, a lever, a gearbox, etc.; they are depicted by an orange square for a mono-physical conversion, e.g. electrical-electrical; or by an orange circle if the conversion is multi-physical, e.g. electrical-mechanical; as shown in Fig. 1.2 (c). Finally, coupling elements allow distributing energy among subsystems; they are depicted by interleaved orange squares for a mono-physical coupling and by interleaved orange circles for a multi-physical coupling, see Fig. 1.2 (d).
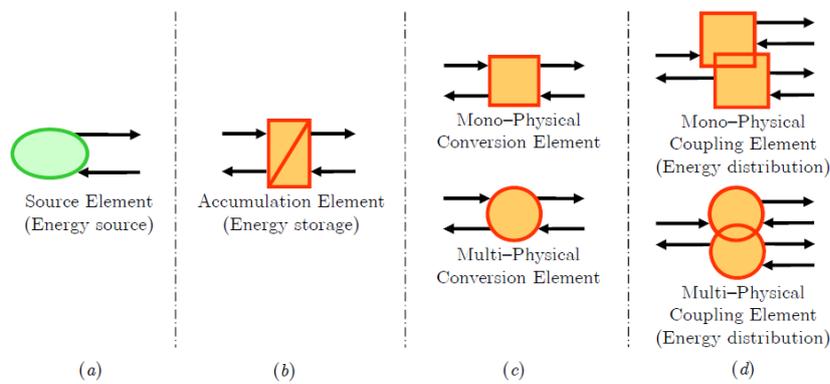
Figure 1.2: EMR elements: (a) source, (b) accumulation, (c) conversion, and (d) coupling

The objective of a control structure is to define an adapted input so to produce the expected output, see Fig. 1.3. In fact, the control has to express the tuning input $u_{tun}(t)$ as a function of the output set-point $y_{ref}(t)$. In consequence, the control can be defined as the inverse of the approximate behavior model describing the relationships between the inputs and outputs.

The effectiveness of EMR and IBC has been proved through many practices of the control team members.

Numerous applications of the proposed methodology have been experimented on prototype test benches, which are equipped with electromechanical systems having multiple inputs and having strong magnetic couplings (*e.g* multiphase synchronous machines), electric couplings (*e.g* multi-leg voltage source inverters) and mechanical couplings (*e.g* multi-actuated positioning gantry systems).

Previously, EMR and IBC are used for linear system, in this PhD research work, it has been extended to the modelling and the control parts in developing methodology to analyze and control the nonlinear system.
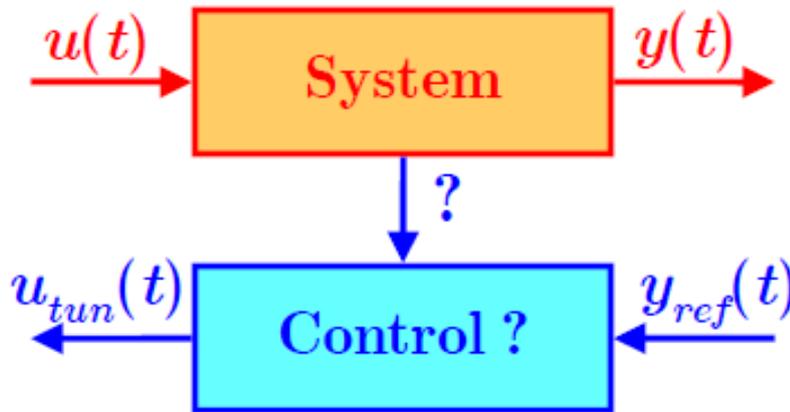
Figure 1.3: Illustration of the Inversion-Based Control Strategy

1.1.2.3 International Collaboration from Japan and Mexico

This PhD research work has also gained international collaboration from Japan and Mexico.

- Hiroyuki Amano, Japanese, Tokyo University, Tokyo, who firstly proposed Method 3-2-3S;

- Arturo Roman Messina, Mexican, Centre for Research and Advanced Studies of the National Polytechnic Institute Mexico City, Mexico, who has achievements in the application of Method 2-2-1, Method 3-3-1

1.1.3 What has been achieved in this PhD research ?

In this PhD thesis, a systematic methodology for the general topic "Analysis and Control of Nonlinear Multiple-Input System with Coupled Dynamics" has been proposed, which casts insights on nonlinear dynamical behaviours of a large class of the multiple-input systems, as shown in Fig. 1.1. This PhD research is multidisciplinary and the proposed systematic methodology can analyze and control the nonlinear systems by simplifying the nonlinearities based on the normal form theory. In this PhD dissertation, applications of the proposed methodology are presented on the nonlinear modal interaction and stability assessment of interconnected power system.

1.2 Introduction to the Analysis and Control of Dynamics of Interconnected Power Systems

1.2.1 Why interconnecting power systems ?

The analysis of the dynamics of today's electric power systems is a challenging and computationally intensive problem that exhibits many interesting and yet to be explained phenomena.

This is due in part to the fact that individual electric utilities are no longer islands of independent generation and control. The interconnections of large regions and the heavy use of these interconnections present to the power system engineer with a large, stressed, nonlinear system to analyse and operate. The physical indicators of stress include the heavy loading of transmission lines, generators working to real or reactive power limits, and the separation of generation and loads by long distances.

Interconnecting the power systems can optimize the exploit of energetic sources and can provide us the electricity with :

- Better generation;

- Better transmission;

- Better distribution.

For example, nowadays, more and more renewable energy has been included in the power grids. The energy is generated in remote sites and then transferred to the urban areas through long transmission lines. Those energy sites are interconnected with each others, as the super grid, which receives more and more attention in the world, as shown in Fig. 1.4. Imagine that we can use the electricity generated in the
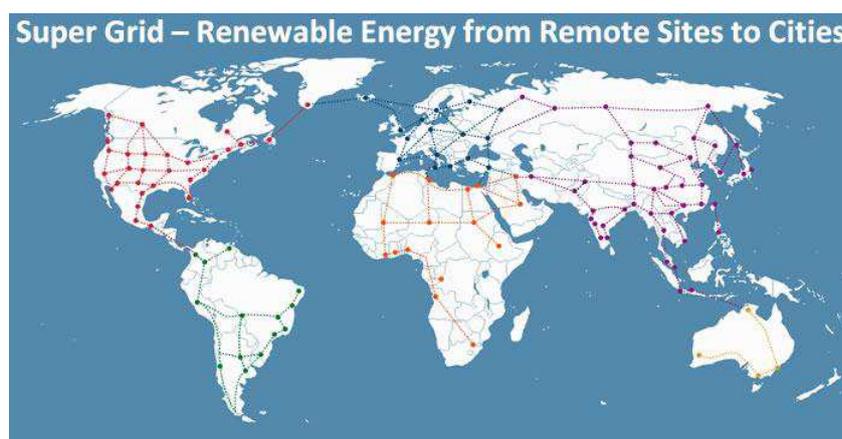
Figure 1.4: Super-grid– Transferring the Renewable Energy from Remote Sites to the Cities

remote areas by the renewable energies in the North Europe, while we are in our

comfortable home in France ! What's more, as shown in Fig. 1.4, an area benefits from the electricity transferred from several electrical sites, therefore, to have a better distribution and more secured electricity supply.

1.2.2 Why do we study the interconnected power system ?

- Its own value: studying the system dynamics of interconnected power system can serve

- Its value as a reference to other systems:

1.2.3 The Questions to be Solved

To analyze and control the dynamic performance, it is to answer two questions:

- Q1: In the microscopic view: How system components interact with each other ? – Modal Interaction

- Q2: In the macroscopic view: Will the system come to the steady state ? – Stability Assessment

Q1 focuses on the details of the system dynamics, such as the source of oscillations (oscillation is a motion that occurs often in system dynamics and normally harmful for system operation). The answer to Q1 can aid us to damp the oscillations (or even to use the oscillations in some cases).

Q2 focuses on the global tendency of the dynamical behaviour of the system. The answer to Q2 can aid us to enhance the stability and to exploit the working capacity of the system.

Normally, to study the system dynamics, there are both the numerical or experimental approach and the analytical approach. By the step-by-step numerical simulation or the experimental measurements, we can observe the system dynamics such as the waveforms of the oscillations, but we cannot identify the sources of the oscillations and predict the stability. And thereby we cannot develop the control strategy to enhance the stability or damp the oscillations. Therefore, analytical analysis tools based on the mathematical model are needed to give physical insights of the oscillations.

If the system is linear or can be linearized, those two questions have been already solved by small-signal (linear modal) analysis.

However, the nonlinearities and couplings in power system make the small-signal (linear modal) analysis fails to study the system dynamics when the system work in a bigger range. Where do the nonlinearities and couplings come from ? To

understand the nonlinearities and couplings, we should first understand the principle of electricity generation.

1.2.4 The Principle of Electricity Generation

The nonlinearities and couplings originate from the electricity generation. The electricity is generated due to the interaction between the stator magnetic field and the rotor magnetic field. A generator is composed of stator and rotor. The stator is composed of windings and the rotor is equivalent to a magnet. The currents induce magnetic fields, and the alternating currents in the stator windings induce a rotating stator magnetic field. If we put the rotor (which is equivalent to a magnet) in the stator magnetic field. The interaction between the stator magnetic field and rotor magnetic field will generate electro-magnetic torque. The rotor is driven by the electro-magnetic torque and the mechanical torque, therefore, the mechanical energy is converted into electricity (generator) or inversely (motor). Fig. 1.5 indicates the interaction between the stator and rotor magnetic fields.
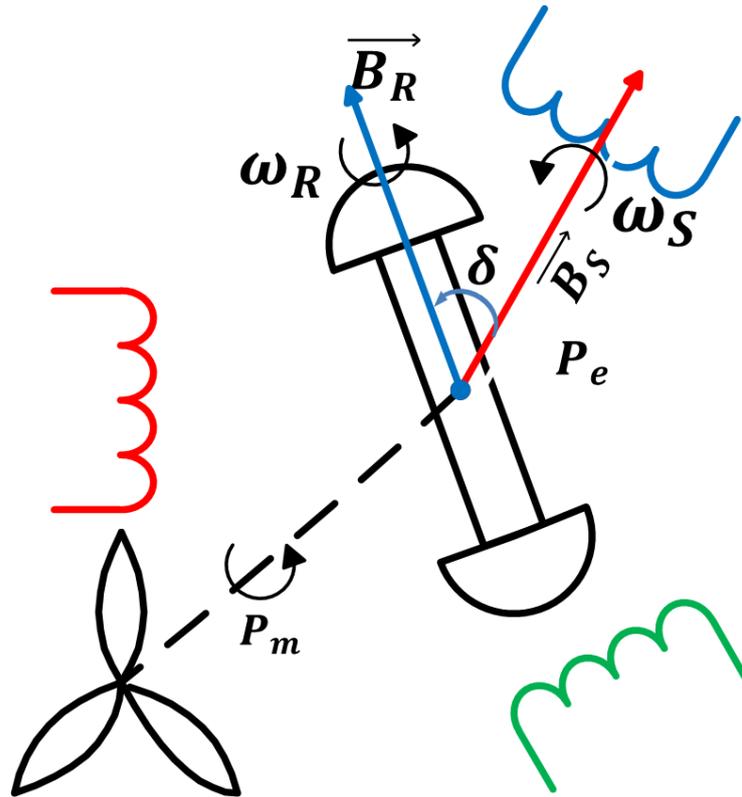
Figure 1.5: The magnetic field of rotor and stator

where $\vec{B_S}$ is the vector representing stator magnetic field and $\vec{B_R}$ is the vector reprenting rotor magnetic field. Therefore, the electrical power is a vector cross product of the stator and rotor magnetic field as Eq. (1.1). If the angular displace-

ment between the stator magnetic field and rotor magnetic field is defined as *Rotor Angle* with the symbol "δ". Then the electric power is a nonlinear function of δ, as indicated by Eq. (1.1).

$$
\begin{cases}
P_e & = k\vec{B_S} \times \vec{B_R} = kB_SB_R\sin\delta \\
\dot{\delta} & = \omega_s\omega \\
\dot{\omega} & = (P_m - P_e - D_\omega(\omega - 1))/(2H)
\end{cases}
\tag{1.1}
$$

To study the power dynamics, we focus on the dynamics of rotor angles. Next, we illustrate the nonlinearities and couplings in the dynamics. To start, we introduce our focus on the rotor angle dynamics and basic assumptions.

1.2.5   The Focus on the Rotor Angle Dynamics

If we connect the stator to the great grid (which is often modelled as the infinite bus), the electricity then can be transferred to the users. The power can be transferred smoothly when the rotor angle is constant. However, when a disturbance occurs on the transmission line, the rotor angle will have oscillations. And its dynamics are shown in Fig. 1.7.
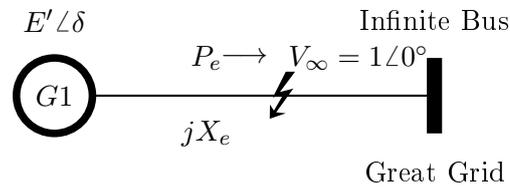
Figure 1.6: A Disturbance Occurs On the Transmission Line
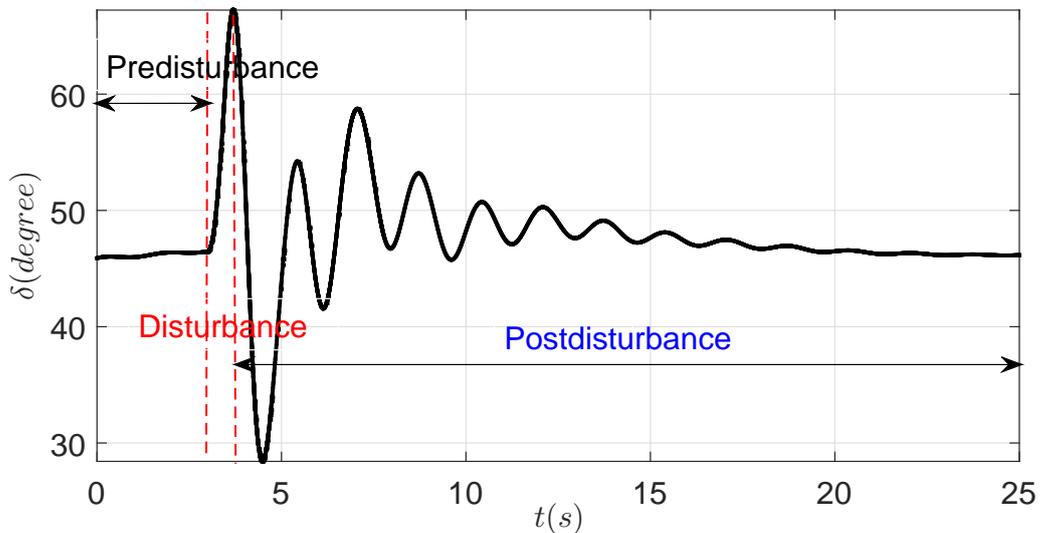
Figure 1.7: The Trajectory of Dynamics

As shown in Fig. 1.7, the disturbance will make the rotor leave the steady-state and cause oscillations. It will then reach to a steady state or become unstable. What we study first is the system dynamics after the fault is cleared, i.e the postdisturbance stage. From the point view of study of dynamical systems, what we focus first is the free-oscillation. In the Chapter 5, we talk about the system dynamics of forced oscillations.

1.2.6   Assumptions to Study the Rotor Angle Dynamics in this PhD dissertation

Several assumptions and simplifications are made in modelling the system dynamics to study the rotor angle dynamics with acceptable complexity and accuracy.

1. **Steady-State Operating Condition:** in the steady state operating condition, we assume that all the state-variables keep constant or change periodically. Though power systems are in fact continually experiencing fluctuations of small magnitudes, for assessing stability when subjected to a specified disturbance, it is usually valid to assume that the system is initially in a true steady-state operating condition.

2. **Disturbance:** the disturbance occurs on the transmission lines, in the form of three-phase short circuit fault. The fault is supposed to be cleared, with or without the line tripped off.

3. **Voltage Stability:** large volume capacitor is installed to avoid the voltage collapse.

4. **Frequency Stability:** the generation and load are balanced to avoid the frequency instability, the load is assumed as constant impedance during the fault.

In the next two subsections, we will first introduce the linear analysis and to show that linear analysis fails to study the system dynamics when there exists nonlinearities and couplings in power system dynamics. Based on which, we illustrate the necessities to develop nonlinear analysis tools and why we choose methods of Normal Forms.

1.3   A Brief Review of the Conventional Small-singal (Linear Modal) Analysis and its Limitations

The system dynamics of rotor angle in the interconnected power system when there is a disturbance in the transmission line are usually caracterized by oscillations.

The numerical simulation tools such as EMTP, Maltab or the monitoring measurements have been widely used to obtain a picture of the system dynamics, especially the oscillations in the interconnected system. However, those tools fail to predict the system dynamical behaviour and identify the sources of oscillations.

Small signal analysis is always an important tool in power system research to study the modal interaction and to assess the stability.

To give the reader an idea of the small-signal analysis, Kundur's 4 machine 2 area system is taken as an example of interconnected power systems, with a tie line power flow from Area 1 to Area 2, as shown in Fig. 1.8. All the generators are equipped with exciters (Automatic Voltage Regulators, VARs) and large capacitance banks to avoid voltage collapose.

Example Case 1
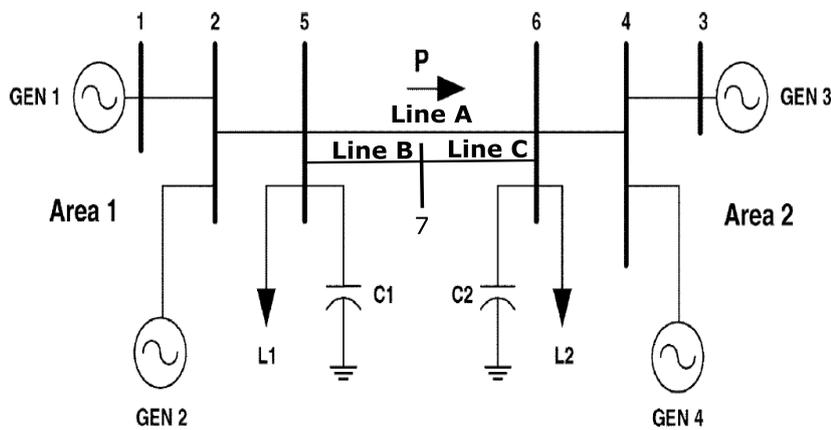
Figure 1.8: Kundur's 2 Area 4 Machine System

When there is a disturbance in Bus 7, all the generators as well as their exciters are involved. For example, if there is a three-phase fault at bus 7 and cleared after $0.15s$, oscillations can occur in the rotors of generators, shown by the black curve in Fig. 1.9, coming from the time-domain step-by-step numerical simulation of the validated demo *pss_Power* (no PSS is equipped). Data for the system and the selected case are provided in the Appendix section.
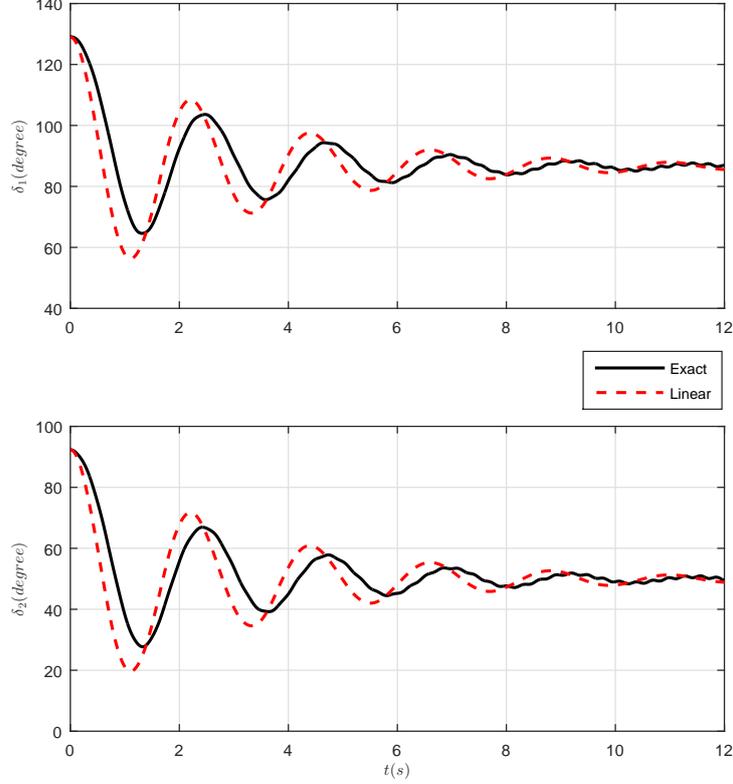
Figure 1.9: Example Case 1: Linear Small Signal Analysis Under Small Disturbance

Since the corresponding mathematical model is a set of high-dimensional nonlinear
differential equations, whose analytical solution is not available in most cases, a
common practice is to linearize this system around the equilibrium point and to use
the linearized model to approximate the system dynamics. This is the principle of
the conventional small-signal analysis, or linear small-signal analysis. With the lin-
earized system, the eigenvalue analysis can be computed. Each eigenvalue indicates
a mode of oscillation that the system can exhibit in the dynamics, and the system
dynamics is a superposition of those modes; local stability properties are given by
the eigenvalues of the linearized system at each equilibrium point.

A brief review is given here, starting by the dynamical system modeled as:

$$\boldsymbol{x} = f(\boldsymbol{x}) \tag{1.2}$$

Linearizing (1.2), it leads:

$$\triangle \dot{\boldsymbol{x}} = A \triangle \boldsymbol{x} \tag{1.3}$$

with A collects all the coefficients of first-order terms in Taylor series: $A_{ij} = \frac{\partial f_i}{x_j}$ and
apply the eigen analysis, which is started by the similarity transformation $\boldsymbol{x} = \boldsymbol{U}\boldsymbol{y}$,

it leads to:

$$\dot{y}_j = \lambda_j y_j \tag{1.4}$$

$\lambda_j = \sigma_j + j\omega$ is the jth eigenvalue of matrix $\boldsymbol{A}$, $\boldsymbol{U}$ and $\boldsymbol{V}$ are the matrices of the right and left eigenvectors of matrix A, respectively.

1.3.1 Small-Signal Stability

In the sense of small-signal stability, the stability of mode j can be predicted by σ_j for $j = 1, 2, \cdots, n$: if the sign of σ_j is negative, it is stable; if possitive, it is unstable. And the stability margin is decided by the eigenvalue closet to the imaginary axis, which is normally named as the critical eigenvalue. One method to improve the system dynamic performance is to tune the controller parameter to obtain the best critical values.

1.3.2 Participation Factor and Linear Modal Interaction

The eigenvectors transform the original system into jordan form, while the linear part is decoupled into independent modes characterized as eigenvalues. Therefore the eigenvectors contain the information that can be used to quantify the contribution of state-values to the modes. The contribution of k-th state variable to the i-th mode can be quantified as participation factor p_{ki}, which is defined as [1]:

$$p_{ki} = u_{ki} v_{ik} \tag{1.5}$$

The matrix P with p_{ki} in the k-th row and i-th column is the participation matrix. Normally, the column vectors of p_{ki} are scaled to have the largest element equals to 1 or are normalized to have a sum of 1 to provide more intuitive physical meanings.

The small-signal stability and the linear modal interaction are the fundamentals of conventional small-signal analysis, by which the frequency of the oscillation and the participation of state-variables keep to the modes can be identified. Based on the participation of state-variables keep, the oscillations fall into four broad categories, which will help us to understand the complex dynamics in power system oscillations.

1. **Local mode oscillations:** these oscillations generally involve nearby power plants in which coherent groups of machines within an area swing against each other. The frequency of oscillations are in the range of 1 to 2 Hz. The dominant state-variables keep are the rotor angle and rotor angular speeds of nearby power plants.

2. **Inter-area mode oscillations:** these oscillations usually involve combinations of many synchronous machines on one part of a power system swinging against machines on another part of the system. Inter-area oscillations are normally of a much lower frequency than local machine system oscillations in

the range of 0.1 to 1 Hz. These modes normally have wide spread effects and are difficult to control;

3. **Control modes oscillations:** these oscillations are associated with generating units and other controls. Poorly tuned exciters, speed governors, HVDC converters and static var compensators are the usual causes of instability of these modes, the frequency is normally higher than 4 Hz;

4. **Torsional modes oscillations:** these oscillations are associated with the turbine-generator shaft system rotational components. Instability of torsional modes may be caused by interaction with excitation controls, speed governors, HVDC controls and series-capacitor-compensated lines, the frequency is also higher than 4 Hz.

Those modes of oscillations can be again illustrated by the example of Kundur's 2 area 4 machine system with the dynamics as shown in Fig. 1.9. The generators are modelled using a two-axis fourth-order model and a thyristor exciter with a Transient Gain Reduction. Loads L1 and L2 are modeled as constant impedances and no Power System Stabilizer is used. The eigenvalues and eigenvectors are calculated by the open source Matlab toolbox PSAT [23] v1.2.10, and all the oscillatory modes are listed in Tab. 1.1.

Table 1.1: Oscillatory Modes: Example Case 1

Mode #	Eigenvalue	Pseudo-Freq (Hz)	Damping Ratio (%)	Time Constant $t = \frac{1}{\zeta \omega_n}$	Dominant States
5,6	$-4.04 \pm j92.09$	14.7	4.39	0.247	$E'_{q1}, E'_{q2}, E'_{q3}, E'_{q4}$
7,8	$-6.53 \pm j87.132$	13.9	7.5	0.153	Control unit G2
9,10	$-18.59 \pm j61.621$	10.2	28.9	0.054	Control unit (G3,G4)
11,12	$-17.64 \pm j63.67$	10.5	26.7	0.057	Control unit G1($\delta_1, \delta_2, \omega_1, \omega_2$)
13,14	$-2.08 \pm j6.74$	1.12	29.5	0.481	Local, Area 2($\delta_3, \delta_3, \omega_4, \omega_4$)
15,16	$-2.39 \pm j6.53$	1.11	34.4	0.418	Local, Area 1($\delta_1, \delta_2, \omega_1, \omega_2$)
17,18	$-0.54 \pm j2.83$	0.45	18.7	1.85	Inter–area ($\delta_1, \delta_2, \delta_3, \delta_4$)

As observed from Tab. 1.1, the system dynamics may contain the local mode oscillation, interarea mode oscillation, and control mode oscillation. By the small signal analysis, it can be identified that the system dynamics in Fig. 1.9 exhibit interarea oscillations at the moment.

By small-signal analysis, the system dynamics can be predicted and quantified without performing the step-by-step time-domain numerical simulation. For example, it can be deduced from the 2nd row in the Tab. 1.1 that, when there is disturbance in the controller, such as the parameter variation, it will cause a control mode oscillation at the frequency around $13.9Hz$. By small-signal analysis, it can also found out that the electromechanical oscillations (whose modes are dominated by the rotor angle and rotor angular speed) are either local mode oscillations or interarea oscillations. Among them, the interarea oscillation is a unique phenomenon presented in interconnected power systems, leading to global problems and having widespread

effects. Their characteristics are very complex and significantly differ from those of local plant mode oscillations.

The eigenvalues and eigenvectors obtained by the linear small signal analysis can provide quantitative results and have several applications as follows.

- **Describing the system's response:** The eigenvalues of the system, indicate the decaying speed and frequencies that may be observed in the oscillations of system variables. For a given initial condition, the linearized system's response can be expressed in a closed form using the eigenvalues and eigenvectors of the system. The eigenvalues are also a tool to analyse the stability of linearized systems. Even the system dynamics can be very complex when several modes are excited under disturbance, it can be approximated by the superposition of the dynamics of several modes. Thus linear analysis completely describes the linearized system's response with reduced complexity.

- **Aiding in the location and design of controls:** When it comes to inter-connected power systems, one would like to figure out the interactions between the system components, which are often referred to as modal interactions in some literatures. Moreover, although the number of inertial modes is equal to the number of system states ($2[n-l]$), typically only a few modes dominate the system response. Under stressed conditions, modes related to groups of machines from different regions begin to dominate. The participation and dominance of some modes will influence the performance of controls, the information being contained in the eigenvectors. The eigenvectors themselves have been used to aid in location of controls [24], and various forms of participation factors [25–27] (which are derived using the eigenvectors) have been used to determine the effectiveness of controls on the system modes. This is referred as modal analysis [1,24–27], and control techniques such as observability and controllability are well developed. Since 1980s, linear modal analysis has been extensively applied to the power system participation factors and measures of modal dominances and are used extensively to characterize linearized power system behaviour.

1.3.3 Linear analysis fails to study the system dynamics when it exhibits Nonlinear Dynamical Behavior

Although the linear analysis can provide answers to modal interaction and stability assessment and therefore we can improve the system dynamic performance. However, it fails to study the system dynamics when it exhibits nonlinear dynamical behavior. We can illustrate this using a SMIB system that has presented in the previous sections.

When the disturbance is small, the oscillations are almost linear as shown in Fig. 1.10 and linear analysis can well approximate the system dynamics.
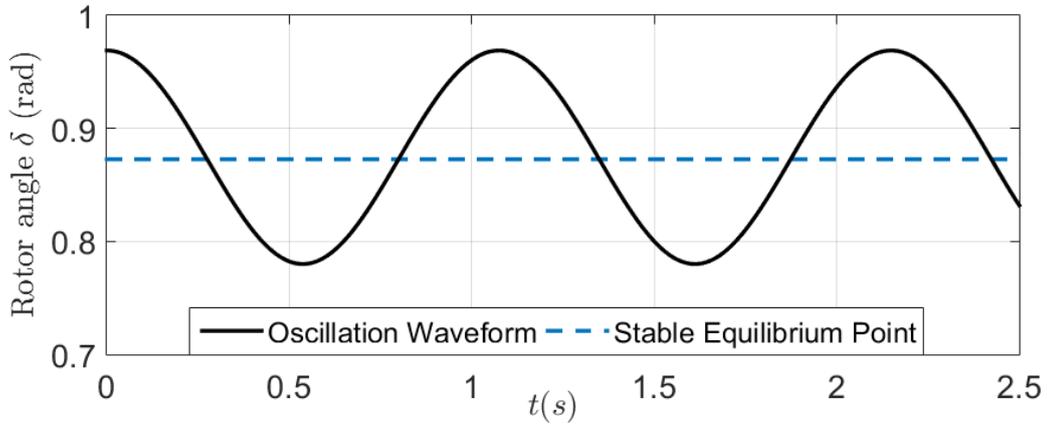
Figure 1.10: Linear Oscillations after Small Disturbance

What happens if the disturbance is bigger ?

When the disturbance is bigger, as shown in Fig. 1.11, the oscillations are predominantly nonlinear, which is unsymmetrical and the frequency doesn't coincide with the imaginary part of the eigenvalue.
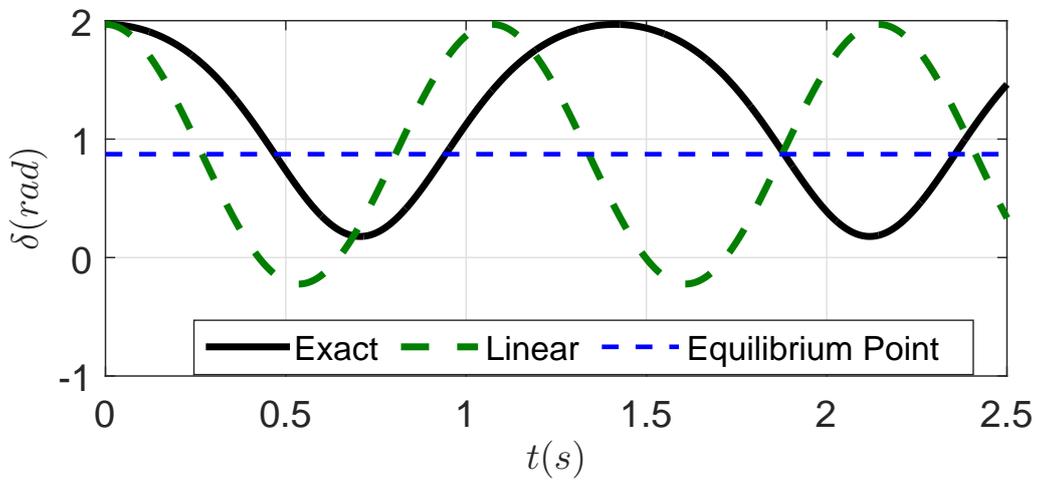
Figure 1.11: Linear analysis fails to approximate the nonlinear dynamics

When the disturbance is even bigger, as shown in Fig. 1.12, the system dynamics indicated by the black curve is unstable, while the linear analysis still predicts a small-signal stability.

This is because that the electric power P_e is a nonlinear function of δ as Eq. 1.6.

$$P_e = \frac{E'V_0}{X} \sin \delta \tag{1.6}$$
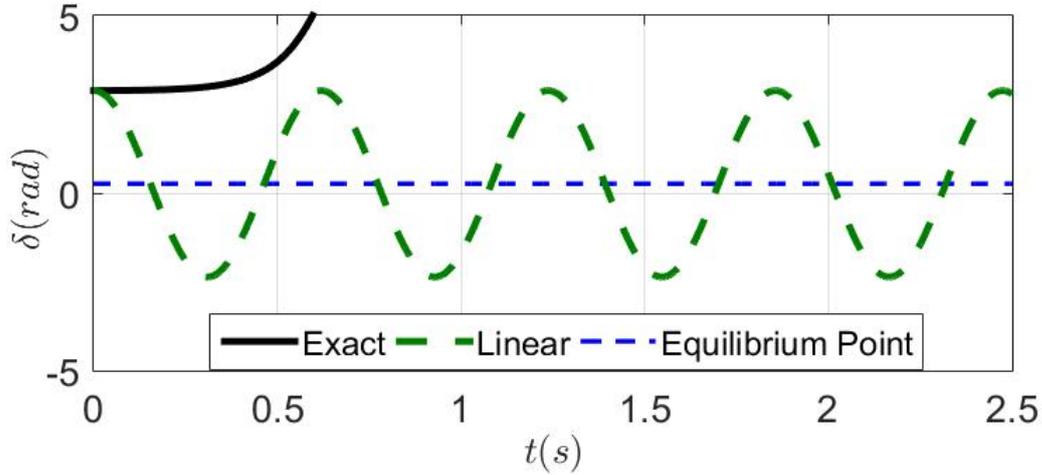
Figure 1.12: Linear analysis fails to predict the stability

When the disturbance is small : $\sin \delta \approx \delta$ and $\triangle \dot{\boldsymbol{x}} = A \triangle \boldsymbol{x}$. The system dynamics can be studied by linear analysis. When the disturbance is bigger, the higher-order terms in Taylor series should be taken into account.

1.3.4 How many nonlinear terms should be considered ?

If nonlinear terms should be kept, then, how many ?

Since Taylor's expansion of $\sin \delta$ around the stable equilibrium point (SEP):δ_{sep} is :

$$
\begin{aligned}
\sin \delta = {} & \sin \delta_{sep} + \cos \delta_{sep}(\delta - \delta_{sep}) \\
& - \frac{\sin \delta_{sep}}{2}(\delta - \delta_{sep})^2 - \frac{\cos \delta_{sep}}{6}(\delta - \delta_{sep})^3 + \cdots
\end{aligned}
\tag{1.7}
$$

If we plot the *power* VS *rotor angle* in Fig. 1.13, we can observe :

- To exploit the power transfer, system has to work in the nonlinear region;

- System dynamics such as the stability should be accurately studied by considering Taylor series terms up to order 3.

1.3.5 Linear Analysis Fails to Predict the Nonlinear Modal Interaction

Linear small signal analysis is accurate in the neighborhood of the equilibrium, but the size of this neighbourhood is not well defined. There is also evidence that the
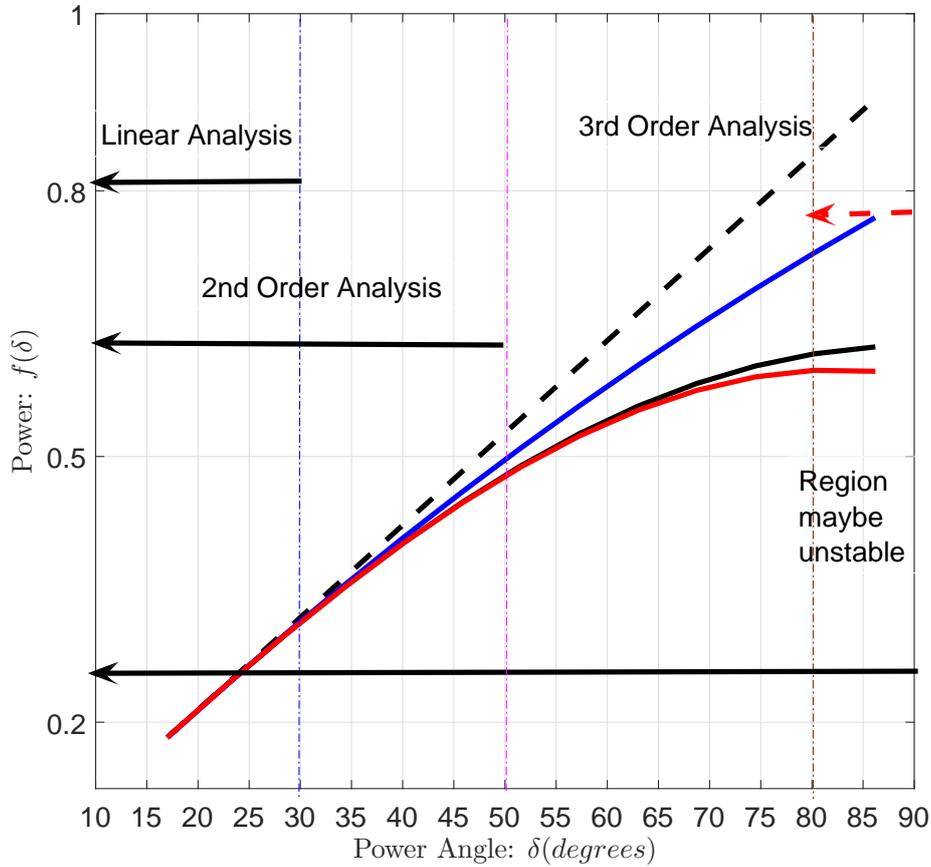
Figure 1.13: Different Order Analysis and the Operational Region of the Power System

nonlinear interactions of the inertial modes increase under stressed conditions [28]. With the emergence of the interarea mode and other problems not explained by linear analysis, there is a need to extend the analysis to include at least some of the effects of the nonlinearities. For example, when for a poorly damped case of the Kundur's 2 area 4 machine system, the linear small-signal analysis fails to approximate the interarea oscillations, as shown in Fig. 1.14, and frequency of oscillations do not corroborate with the results obtained by the linear small-signal analysis as shown in Fig. 1.15.

Example Case 2

The interarea oscillations occur as two groups of generators, in different regions, oscillate with respect to each other. Under a large disturbance (nonlinearities cannot be ignored), interarea-mode response can be described as follows: initially following the large disturbance, generators closed to the disturbance are accelerated; as the
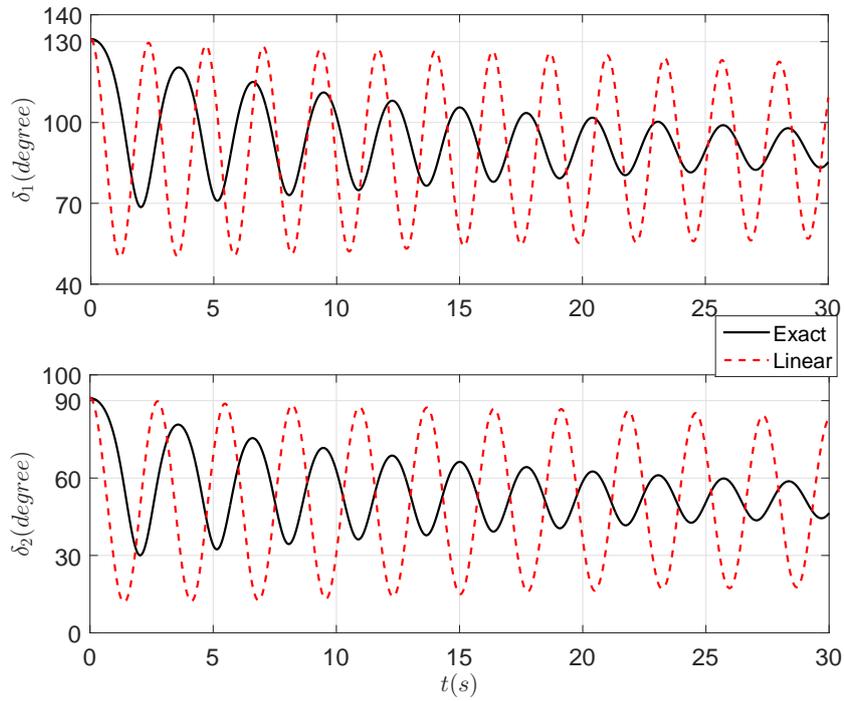
Figure 1.14: Example Case 2: Linear Small Signal Analysis of Stressed Power System Under Large Disturbance
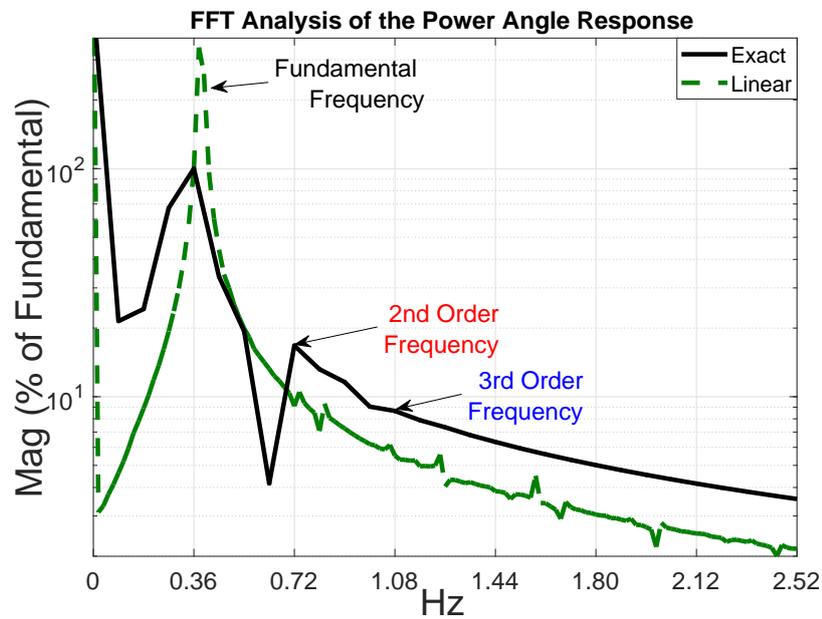
Figure 1.15: Example Case 2: Linear Small Signal Analysis of Stressed Power System Under Large Disturbance

transient continues, other generators, which may be far from the disturbance, also become adversely affected. This system wide response involving a large number of generators is in contrast with the more local response, involving only a few generators and typical of unstressed power systems. In addition, these interarea-mode oscillations may cause cascaded instabilities that occur at some time after the initial swing caused by the fault.

In a word, the interrearea oscillations are due to the interactions between the system components. Understanding the interarea oscillations is to understand the interactions between the system components which is of great significance in optimizing the operation of the whole system. As shown in Fig. 1.14, when the system is stressed, the linear analysis fails to approximates the system dynamics. As observed from Fig. 1.15, there are components at higher-order frequencies. And those higher-order frequency components correspond to nonlinear modal interactions that fails to be captured by linear small-signal analysis.

1.4   Reiteration of the Problems

1.4.1   Need for Nonlinear Analysis Tools

Therefore, considering the nonlinearities and couplings and in the power system, the questions of *Modal Interaction* and **Stability Assessment** are essentially:

- Nonlinear Modal Interaction: how the system components interact with each other nonlinearly ?

- Nonlinear Stability Assessment: how the nonlinearities influence the stability of the system dynamics ?

Since the linear analysis fails to do

1.4.2   Perspective of Nonlinear Analysis

The answers needed to improve the system dynamic performance, i.e to develop the metho

- Nonlinear Modal Interaction $\implies$ Damp the oscillations;

- Nonlinear Stability Assessment $\implies$ Enhance the system stability or increase the power transfer limit.

To give the reader a clear idea of how the control strategy can be implemented, several examples in the linear control are introduced and this PhD work will point that how those applications can also be used to improve the system dynamic performance when it works in the nonlinear region.

1. Aiding in the location and design of controls.

2. Tuning Controller Parameters.

3. Optimizing the Power Transfer.

1.4.2.1   Aid in the Location and Design of Controls

When it comes to interconnected power systems, one would like to figure out the interactions between the system components, which is often referred as modal interactions in some literatures. Moreover, although the number of inertial modes is equal to the number of system states ($2[N - l]$), typically only a few modes dominate the system response. Under stressed conditions, modes related to groups of machines from different regions begin to dominate. The participation and dominance will influence the performance of controls. The information is contained in the eigenvectors. The eigenvectors themselves have been used to aid in location of controls [24], and various forms of participation factors [25–27] (which are derived using the eigenvectors) have been used to determine the effectiveness of controls on the system modes. This is referred as modal analysis [1, 25–27], and control techniques such as observability and controllability are well developed. Since 1980s, linear modal analysis has been extensively applied to power system participation factors and measures of modal dominances, are used extensively to characterize linearised power system behaviour.

1.4.2.2   Automatic Tuning Controller Parameters

Sensibility method based on the small-signal analysis make possible to automatically tuning the controller parameters. The objective is to enhance the small-signal stability. Numerous examples can be found. A recent example can be found in the voltage source converters controlled by strategy of virtual synchronous machine (VSM), where three controller loops are employed and the frequency domain design (appropriate for a maximum number of 2 loops) [29].

1.4.2.3   Optimizing the Power Transfer

Once the power transfer limit of each generator can be figured out, a global optimization of power transfer in the power grid is possible and we can obtain the maximum economic benefits from the whole power grid.

The applications are not confined to the above examples.

1.4.3 The Difficulties in Developing a Nonlinear Analysis Tool

As pointed out in Section 1.3.4, we should consider nonlinear terms in Taylor series up to order 3 to be accurate enough. Therefore, for a N-dimensional system, the nonlinear terms should be in the scale of N^4. How to deal with such an enormous quantity of nonlinear terms ?

1.5 A Solution: Methods of Normal Forms

Extending the small-signal analysis to the nonlinear domain by including the higher order polynomial terms in Taylor series may lead to cumbersome computational burden, since analytical results for nonlinear differential equations are not ensured. And the strong couplings in the nonlinear terms make it difficult to extract useful informations about how the components interact with each other.

One solution is to simplify the nonlinear terms, to obtain "a simplest form" of the system dynamics where system property is maintained with reduced complexity. This "simplest form" is called as "the normal forms", as firstly proposed by Poincaré in 1899. To solve the problem, the first step is to have the mathematical formulation of the system dynamics as Fig. 1.8

$$\dot{\boldsymbol{x}} = f(\boldsymbol{x}, \boldsymbol{u}) \tag{1.8}$$

Doing the Taylor's expansion around the Stable Equilibrium Point (SEP):

$$\triangle\dot{\boldsymbol{x}} = A\triangle\boldsymbol{x} + f_2(\triangle\boldsymbol{x^2}) + f_3(\triangle\boldsymbol{x^3}) \tag{1.9}$$

If linear analysis uses a linear change of state variables (linear transformation) to simplify the linear terms:

$$\triangle\dot{\boldsymbol{x}} = A\triangle\boldsymbol{x} \xrightarrow{\triangle\boldsymbol{x}=U\boldsymbol{y}} \dot{y}_j = \lambda_j y_j \tag{1.10}$$

As indicated by Fig. 1.16, if the system dynamics are nonlinear, after decoupling the linear part, the system of equation is as Eq.(a) with decoupled linear part and coupled nonlinear part. What if we add a nonlinear change of variables(nonlinear transformation) as Eq.(b)? Will we obtain an equation with simplied nonlinearities as Eq.(c) ?

$$\dot{y_j} = \lambda_j y_j + F2^j(\boldsymbol{y^2}) + F3^j(\boldsymbol{y^3}) + \cdots (\mathbf{a})$$

$$\textcolor{red}{\boldsymbol{y} = z + h2(z^2) + h3(z^3) + \cdots (\mathbf{b})}$$

$$\textcolor{blue}{\dot{z_j} = \lambda_j z_j + \mathbf{simpler\ nonlinearities} + \cdots (\mathbf{c})}$$

Figure 1.16: An idea: using nonlinear change of variables to simplify the nonlinearities

The answer is YES. And it is answered by H. Poincaré in 1899 in his book "New Methods of Celestial Mechanics". And the equation of simplied nonlinearities is called as "normal form"(des formes normales).

Poincaré introduced a mathematical technique for studying systems of nonlinear, differential equations using their normal forms [30]. The method provides the means by which a differential equation may be transformed into a simpler form (higher-order terms are eliminated). It also provides the conditions under which the transformation is possible. Although the normal form of a vector field or differential equation may be expressed using a number of forms, the polynomial form is selected because of its natural relationship to the Taylor series. The polynomial normal form of a system of equations contains a limited number of nonlinear terms, which are present due to resonances of system eigenvalues. This normal form is obtained via a nonlinear change of variable (nonlinear transformation) performed on Taylor series of the power system's nonlinear, differential equations. The nonlinear transformation is derived by cancelling a maximum of nonlinearities in the normal forms.

Once the normal form is obtained, the quantitative measures can be used to answer the modal interaction and assess the stability.

1.5.1 Several Remarkable Works on Methods of Normal Forms

During the last decades, there are several remarkable works on methods of normal forms in both electrical engineering and mechanical engineering. Those methods will be reviewed in this PhD dissertation.

Electrical Engineering:

Method 2-2-1 [Vittal et all, 1991] [28]; Method 3-3-1 [Martinez, 2004 [31];Huang, 2009 [32]]; Method 3-2-3S [Amano, 2006] [5].
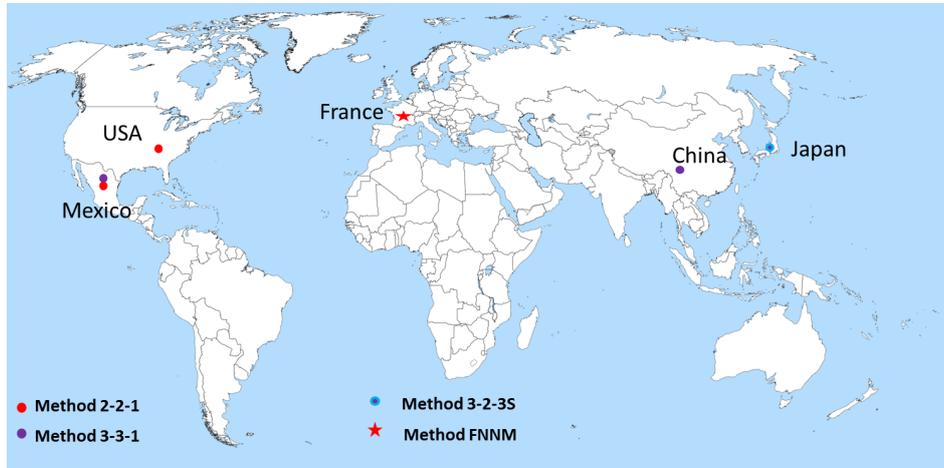
Figure 1.17: The People Working on Methods of Normal Forms

Mechanical Engineering : Method NNM [Jezequel et Lamarque,1991 [33]; Touzé et Thomas, 2004 [17]]

1.5.2 Why choosing normal form methods ?

The existing analytical and statistical tools for nonlinear system dynamics are reviewed in this Section to show the previlege of methods of normal forms.

1.5.2.1 Modal Series Methods for Modal Interaction

Other methods, such as the Modal Series (MS) [34–36], and the Perturbation Technique (PT) [37] have been used to study the power system dynamic performance. These papers have concluded that in the stressed power systems, the possibility of nonlinear interactions is increased, and thereby the performance of power system controllers will be deteriorated. As concluded in [37], the PT and MS method are identical. And as concluded in [35, 38], the MS method exhibits some advantages over the normal form method. Its validity region is independent of the modes resonance, does not require nonlinear transformation, and it can be easily applied on large power systems, leading the MS method once more popular in recent years.

The principle of the MS method is to approximate the system dynamics by a nonlinear combination of linear modes: 1) all the higher-order terms are kept; 2) the stability is predicted by the linear modes.

Therefore, the MS method 1) is not appropriate for nonlinear stability analysis; 2) the complexity increases largely as the order of the nonlinear terms increase.

1.5.2.2 Shaw-Pierre Method

Another method, Shaw-Pierre method, which originated from the center-manifold theory, is popular in studying the nonlinear dynamics of mechanical systems [39]. In [40] nonlinear normal mode is formulated by SP method to study the nonlinear dynamics of interconnected power system. However, the nonlinearities studied is only up to 2nd order, and this approach itself has some drawbacks, making it only applicable in very few cases.

Detailed discussion on MS method and on SP method with mathematical formulation can be found in Chapter 2 (Section 2.3.9).

1.5.2.3 Methods for Transient Stability Assessment for Power Systems

Among all the methods, the direct methods arouse the biggest interest, since it provides the analytical results which quantifies the stability margin. **Direct Methods** These approaches are also referred to as the transient energy function (TEF) methods. The idea is to replace the numerical integration by stability criteria. The value of a suitably designed Lyapunov function V is calculated at the instant of the last switching in the system and compared to a previously determined critical value Vcr. If V is smaller than V_{cr}, the postfault transient process is stable (Ribbens-Pavella and Evans, 1985 [41]). In practice, there are still some unresolved problems and drawbacks of this approach. The efficiency of this method depends on the chosen simplifications of the system variables keep. The integration of the fault on system equations is needed to obtain the critical value for assessing stability. It is difficult to construct the appropriate Lyapunov function to reflect the internal characteristics of the system. The method is rigorous only when the operating point is within the estimated stability region.

Probabilistic Method (Anderson and Bose, 1983 [42]) With these methods, stability analysis is viewed as a probabilistic rather than a deterministic problem because the disturbance factors (type and location of the fault) and the condition of the system (loading and configuration) are probabilistic in nature. Therefore, this method attempts to determine the probability distributions for power system stability. It assesses the probability that the system remains stable should the specified disturbance occur. A large number of faults are considered at different locations and with different clearing schemes. In order to have statistically meaningful results, a large amount of computation time is required (Patton, 1974 [43]). Therefore, this method is more appropriate for planning. Combined with pattern recognition techniques, it may be of value for on-line application.

Expert System Methods (Akimoto, 1989 [44]) In this approach, the expert knowledge is encoded in a rule-based program. An expert system is composed of two parts: a knowledge base and a set of inference rules. Typically, the expertise for the knowledge base is derived from operators with extensive experience on a

particular system. Still, information obtained off-line from stability analyses could be used to supplement this knowledge.

The primary advantage of this approach is that it reflects the actual operation of power systems, which is largely heuristic based on experience. The obvious drawback is that it has become increasingly difficult to understand the limits of systems under today's market conditions characterized by historically high numbers of transactions.

Database or Pattern Recognition Methods The goal of these methods is to establish a functional relationship between the selected features and the location of system state relative to the boundary of the region of stability (Patton, 1974 [43]; Hakim, 1992 [45]; Wehenkel, 1998 [46]). This method uses two stages to classify the system security: (a) feature extraction and (b) classification. The first stage includes off-line generation of a training set of stable and unstable operation states and a space transformation process that reduces the high dimensionality of the initial system description. The second stage is the determination of the classifier function (decision rule) using a training set of labeled patterns. This function is used to classify the actual operating state for a given contingency. Typically, the classifier part of this approach is implemented using artificial neural networks (ANNs).

1.5.2.4 Limitations of the Above Methods

Although there are other methods that can provide analytical solution, they have some limitations.

- Modal Series: nonlinearities are not simplified;

- Shaw-Pierre Method: only for system with non-positive eigenvalues;

- Direct Methods based on Lyapunov theory and other existing methods for TSA: only for stability assessment, not for nonlinear modal interaction.

1.5.2.5 Advantages of Methods of Normal Forms

- It keeps the concept of "modes" for a better understanding of nonlinear modal interaction;

- It is for both stable and unstable system, for not only the nonlinear modal interaction, but also stability assessment;

- The nonlinearities are simplified in the mathematical model, which may contribute to the control.

1.6   A Brief Introduction to Methods of Normal Forms

The principle of methods of normal forms is to obtain the normal forms.   The procedures are shown in Fig. 1.18.

$$\dot{\boldsymbol{x}} = f(\boldsymbol{x}, \boldsymbol{u})$$

Original System

$\boldsymbol{x}$ is a vector of state variables

Expansion by Taylor series

$$\triangle \dot{x} = A\triangle x + f_2(\triangle x^2) + f_3(\triangle x^3) + \cdots$$

Perturbation model

Linear change of state-variables

$$\triangle \boldsymbol{x} = U\boldsymbol{y}$$

Linear decoupling $j = 1, 2, \cdots, N$

$$\dot{y}_j = \lambda_j y_j + F2^j(y^2) + F3^j(y^3) + \cdots$$

Linear Modes with all Nonlin-earities

Nonlinear change of state-variables

$$y_j = z_j + h_2^j(z_k z_l) + h_3^j(z_p z_q z_r) + \cdots$$

Nonlinear Modes with simplified nonlinearities

$$\dot{z}_j = \lambda_j z_j + g_2^j(z^2) + g_3^j(z^3)$$

Figure 1.18: Procedures to Obtain the Normal Forms

The goal of methods of normal forms is to carefully choose the coefficients of the nonlinear transformation $h2, h3, \cdots$, to simplify the nonlinearities in the normal form as much as possible.   The most ideal condition is that all the nonlinearities are cancelled. However, nonlinear terms that satisfy the resonance must be kept. The resonance occurs if the nonlinear term has a frequency equivalent to the frequency of the dominant modes.

1.6.1   Resonant Terms

For the weakly damped modes, $\lambda_j = \sigma_j + j\omega_j$, $\sigma_j \approx 0$, the resonance occurs when the terms have the same frequency of the dominant mode j, $\sum_{k=1}^N \omega_k = \omega_j$.   For mode j :

$$z_k z_l : \quad \omega_j = \omega_k + \omega_l, \omega_j = 2\omega_k \qquad \text{(2nd Order Resonance)}$$
$$z_p z_q z_r : \quad \omega_j = \omega_p + \omega_q + \omega_r, \omega_j = 3\omega_k \qquad \text{(3nd Order Resonance)}$$

terms $z_k z_l$ and $z_p z_q z_r$ are resonant terms.

In this PhD dissertation, the focus is not on resonant terms, and resonances are avoided when selecting the case studies. However, there is a type of resonance that cannot be avoided.

Special Case– trivially resonant terms

If there are conjugate pairs $\lambda_{2k-1} = \lambda_{2k}^*, \omega_{2k-1} + \omega_{2k} = 0.$ then $\omega_{2k} + \omega_{2k-1} + \omega_j \equiv \omega_j$

For mode j, terms $z_j z_{2k} z_{2k-1}$ are trivially resonant terms, which intrinsic and independent of the oscillatory frequencies.

Trivially resonant terms must be kept

1.6.2 How can the methods of normal forms answer the questions ?

Normal forms = Linear mode + resonant terms:

$$\dot{z}_j = \lambda_j z_j + \sum_{\omega_k,\omega_l \in R_2}^{N} \sum^{N} g_{2kl}^{j} z_k z_l + \sum_{\omega_p,\omega_q,\omega_r \in R_3}^{N} \sum^{N} g_{3pqr}^{j} z_p z_q z_r \tag{1.11}$$

- Stability Assessment of mode j can be indicated by λ_j, g_2^j, g_3^j

The system dynamics is to add a nonlinear combination of modes to the linear modes:

$$y_j = z_j + h_2^j(z_k z_l) + h_3^j(z_p z_q z_r) \tag{1.12}$$

- Nonlinear Modal Interaction indicated by h_2 and h_3

Normal form is a simplest form with the most information !

1.6.3 Classification of the Methods of Normal Forms

Different methods of rnormal forms are proposed in the last decades to cater for different requirements. To make their differences obvious, we can classify and name them by the order of Taylor series – order of nonlinear transformation – order of nonlinear terms in normal forms – whether nonlinear terms in the normal forms are simplified (S) or not.

3rd order of Taylor series   keeping all terms in normal forms

$$F_n \qquad h_n \qquad g_n \qquad \text{S or } /$$

order of Nonlinear transformation   order of normal forms
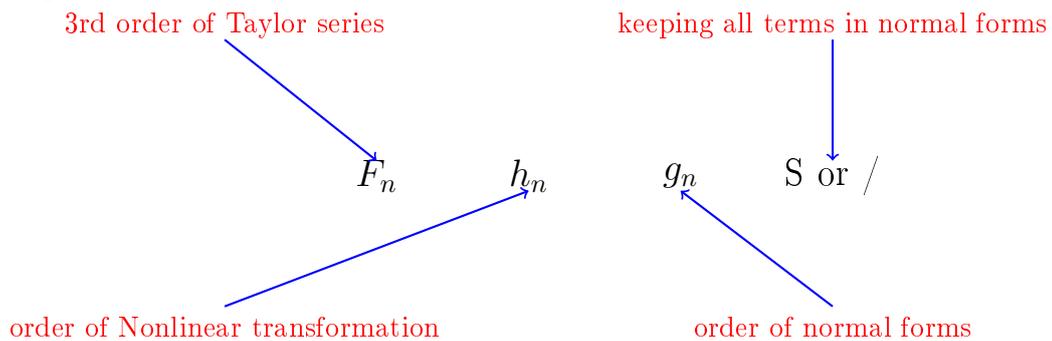
1.7 Current Developments by Methods of Normal Forms: Small-Signal Analysis taking into account nonlinearities

Conventionally, the study of small-signal stability employs small-signal analysis where the power system is not stressed and the disturbance is small. And assessment of transient employs transient analysis where the power system experiences

large disturbance. However, small-signal analysis are not isolated from the transient analysis. For example, the interarea oscillations, which is a big concern in the small signal analysis, is firstly observed in the transient analysis (when there is a three phase short circuit fault in the transmission line of the interconnected power system, and cleared without tripping off the line), but its property is studied by the small-signal analysis. Also, as nowadays, the power system is a more stressed system exhibiting predominantly nonlinear dynamics compared to before. When the system experiences large disturbances, not only the transfer limits are concerned, but also the sources and frequencies of oscillations should be studied. For this issue, the small-signal analysis is more appropriate.

Therefore, in this PhD work, the small-signal stability is extended to the nonlinear domain, to study the nonlinear oscillations in the interconnected power system when the system experiences large disturbance (which is conventionally studied by transient analysis).

Therefore, it essentially leads to:

- Small-signal analysis taking into account nonlinearities;

1.7.1 Inclusion of 2nd Order Terms and Application in Nonlinear Modal Interaction

- Taylor Series: $\dot{y}_j = \lambda_j y_j + F2^j(\boldsymbol{y}^2)$
- Nonlinear Transformation: $\boldsymbol{y} = z + h2(z^2)$
- Normal Form: $\dot{z}_j = \lambda_j z_j$
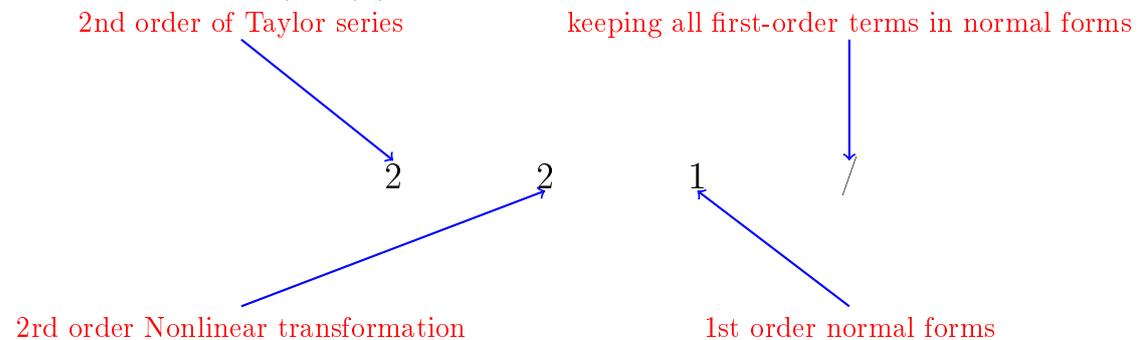
Gradually established and advocated by investigators from Iowa State University in the period 1996 to 2001 [6–15], it opens the era to apply 2nd Order Normal Forms analysis in studying nonlinear dynamics in power system. Its effectiveness has been shown in many examples [6,9–12,14,15,20,47] to approximate the stability boundary [9], to investigate the strength of the interaction between oscillation modes [6,10,47]; to dealt with a control design [11,12]; to analyze a vulnerable region over parameter space and resonance conditions [14,15] and to optimally place the controllers [20]. This method is well summarized by [48] which demonstrated the importance of nonlinear modal interactions in the dynamic response of a power system and the ability of inclusion of 2nd order terms.

In all the referred researches, the general power-system natural response (linear or nonlinear) is often considered to be a combination of the many natural modes of

oscillation present in the system. The linear modes (eigenvalues) represent these basic frequencies that appear in the motions of the system's machines. Even for large disturbances when nonlinearities are significant, the linear modes play an important role in determining the dynamic response of the machine variables. The nonlinear effects should be considered as additions to the linear-modal picture, not as replacements for it [10].

In another word, those referred researches mainly employ the information of 2nd order modal interactions to better describe or improve the system dynamic performance. This is the main advancement of method 2-2-1 compared to the linear analysis.

For the stability, it predicts a small-signal stability as the linear analysis.

1.7.2 Inclusion of 3rd Order Terms

Later, the researchers found that inclusion of nonlinear terms only up to order 2 fails to explain some phenomenon. Therefore, explorations are done in inclusion of 3rd order terms in the small-signal analysis.

1.7.2.1 Method 3-3-1: to study the 3rd order modal interaction

- Taylor Series: $\dot{y}_j = \lambda_j y_j + F2^j(\boldsymbol{y}^2) + F3^j(\boldsymbol{y^3})$
- Nonlinear Transformation: $\boldsymbol{y} = z + h2(z^2) + h3(z^3)$
- Normal Form: $\dot{z}_j = \lambda_j z_j + \text{simpler nonlinearities}$

3rd order of Taylor series   keeping all first-order terms in normal forms

$$3 \quad 3 \quad 1 \quad /$$

3rd order Nonlinear transformation   1st order normal forms
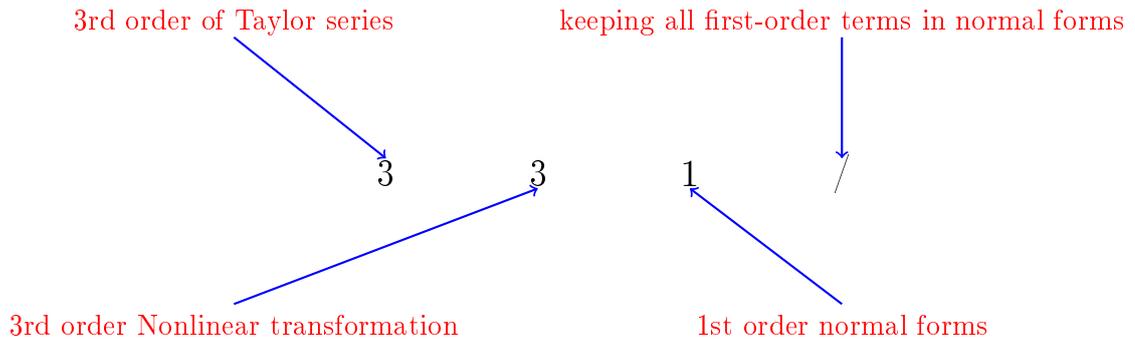
The mathematical formulation of method 3-3-1 is firstly proposed by Martínez in 2004 and then by Huang in 2009 [32] the nonlinear indexes are proposed to quantify the 3rd order modal interaction.

1.7.2.2 Method 3-2-3S: to study the nonlinear stability

- Taylor Series: $\dot{y}_j = \lambda_j y_j + F2^j(\boldsymbol{y}^2) + F3^j(\boldsymbol{y^3})$
- Nonlinear Transformation: $\boldsymbol{y} = z + h2(z^2) + h3(z^3)$
- Normal Form: $\dot{z}_j = \lambda_j z_j + \text{trivially resonant terms for oscillatory modes}$

3rd order of Taylor series   3rd order terms are simplified in normal forms

$$3 \quad 2 \quad 3 \quad S$$

2nd order Nonlinear transformation   3rd order normal forms
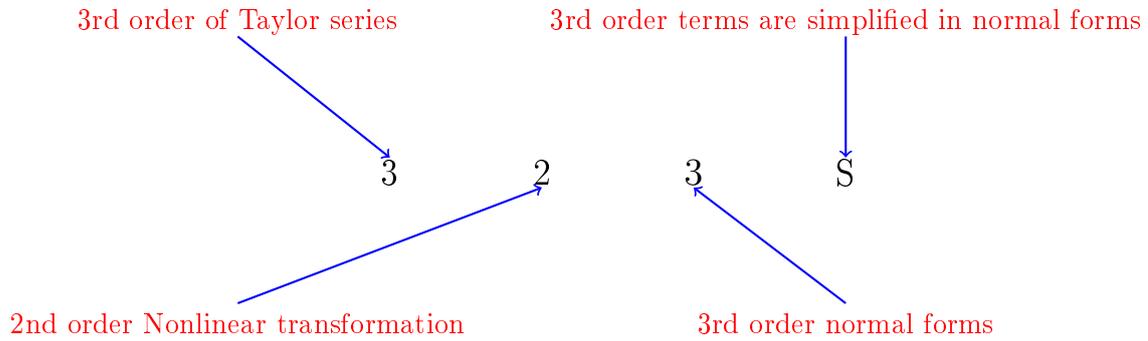
This method is proposed by H.Amano in 2007 [16]. It keeps the trivially resonant terms in the normal forms to study the contribution of the nonlinearities to the system stability. A nonlinear index called stability bound is proposed based on the normal forms which serves as a criteria to tune the controller parameters to improve the system dynamic performance.

1.7.3 What is needed ?

We need a method to include nonlinear terms up to order 3 to study both the **nonlinear modal interaction** and **nonlinear stability**.

1.8 Objective and Fulfilment of this PhD Dissertation

1.8.1 Objective and the Task

The objective of this PhD research work can be sprecified as:
- Develop a systematic methodology to analyze and control nonlinear multiple-input systems with coupled dynamics based on methods of normal forms up to 3rd order;
- Apply the systematic methodology to study the nonlinear dynamical behaviour of interconnected power systems;
- Analyze the factors influencing the performance of the proposed methodology and figure out its limitations and the way to improve it, laying the foundation for future researches.

The fulfilment of the objectives is composed of:
- Derivation of methods of normal forms (MNFs) up to order 3;
- Implementation of generic programs of MNFs applicable for dynamical systems with arbitrary dimensions where;
- Mathematical modelling of interconnected power system in the form of Taylor series up to 3rd order;
- Application of MNFs to study the inter-area oscillations and assess the transient stability of interconnected power system;

1.9 A Brief Introduction to the Achievements of PhD Work with A Simple Example

To give the reader a clear idea of the methods of normal forms and the proposed method 3-3-3 and method NNM we use a concrete example to illustrate those methods.

1.9.1 An example of Two Machines Connected to the Infinite Bus
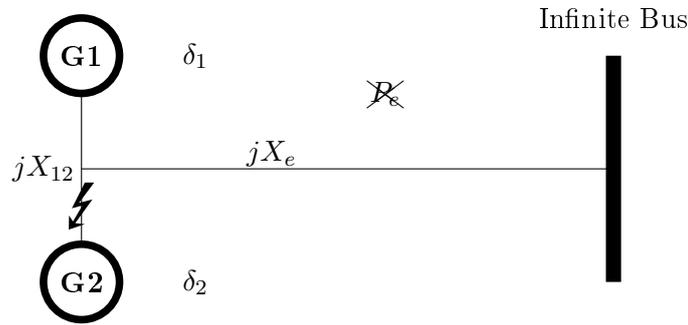
Figure 1.19: A system of Two Machines that are Interconnected and Connected to the Infinite Bus

$$\begin{cases} P_{e1} & = \frac{V_1 V_2}{X_{12}} \sin(\delta_1 - \delta_2) + \frac{V_1 V_\infty}{X_e} X_e \sin \delta_1 \\ \dot{\omega}_1 & = (P_{m1} - P_{e1} - D(\omega_1 - 1))/(2H) \\ \dot{\delta}_1 & = \omega_s(\omega_1 - 1) \\ P_{e2} & = \frac{V_1 V_2}{X_{12}} \sin(\delta_2 - \delta_1) + \frac{V_2 V_\infty}{X_e} X_e \sin \delta_2 \\ \dot{\omega}_2 & = (P_{m2} - P_{e2} - D(\omega_2 - 1))/(2H) \\ \dot{\delta}_2 & = \omega_s(\omega_2 - 1) \end{cases} \tag{1.13}$$

4 state-variables $x = [\delta_1, \delta_2, \omega_1, \omega_2]$
Taylor series around equilibrium point

$$\triangle \dot{\boldsymbol{x}} = A \triangle \boldsymbol{x} + a_2 \boldsymbol{x^2} + a_3 \boldsymbol{x^3} \tag{1.14}$$

Decoupling the linear part, it leads $j = 1, 2, 3, 4$

$$\dot{y_j} = \lambda_j y_j + \sum_{k=1}^{4} \sum_{l=1}^{4} y_k y_l + \sum_{p=1}^{4} \sum_{q=1}^{4} \sum_{r=1}^{4} y_p y_q y_r \tag{1.15}$$

It has at least 28 nonlinear terms, how to solve it ?

1.9.2 The proposed method 3-3-3

Adding a nonlinear transformation : $y_j = z_j + h_2^j(z^2) + h_3^j(z^3)$
Since the maximum number of conjugate pairs are two, λ_1, λ_2 and λ_3, λ_4.

A total maximum of 8 nonlinear terms in the normal forms.

$$\dot{z}_j = \lambda_j z_j + \boxed{g3^j_{j12} z_j z_1 z_2 + g3^j_{j34} z_j z_3 z_4} \tag{1.16}$$
$$\text{Trivially resonant terms}$$

3rd order of Taylor series   3rd order terms are simplified in normal forms

$$3 \qquad 2 \qquad 3 \qquad S$$

2nd order Nonlinear transformation   3rd order normal forms
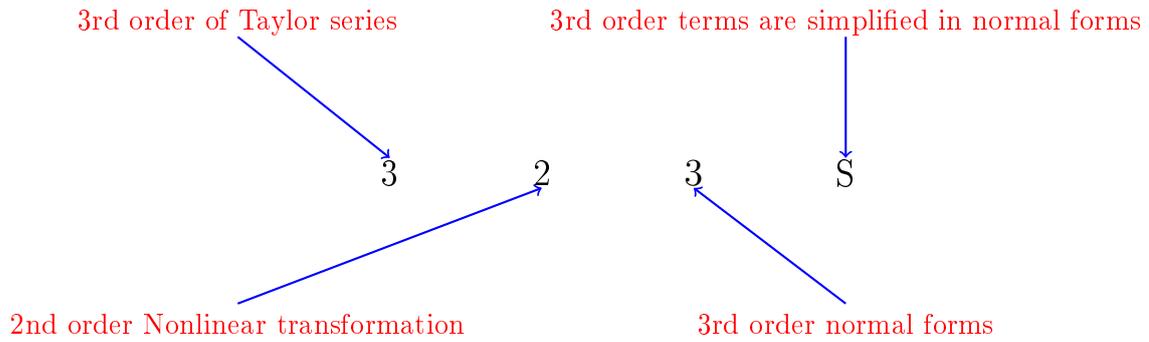
Figure 1.20: Meaning of the name of method 3-3-3

1.9.3 Theoretical Improvements of Method 3-3-3 Compared to existing methods

Tab. 1.2 lists the nonlinear transformations and the normal forms of each method.

Table 1.2: Theoretical Improvements of Method 3-3-3 Compared to existing methods

j=1,2	$y_j = z_j + h_2^j(z^2)$	$y_j = z_j + h_2^j(z^2) + h_3^j(z^3)$
$\dot{z}_j = \lambda_j z_j$	method 2-2-1	method 3-3-1
$\dot{z}_j = \lambda_j z_j + g_3^j z_j z_1 z_2$ $+ g_3^j z_j z_3 z_4$	method 3-2-3S	method 3-3-3

As observed from Tab. 1.2, only method 3-3-3 has both two characteristics as below:
- Method 3-3-3 is up to 3rd order;
- Trivially resonant terms are kept in method 3-3-3.

Having both the two characteristics render method 3-3-3 a better performance in study of system dynamics compared to the existing methods.

1.9.4 Performance of Method 3-3-3 in Approximating the System Dynamics Compared to the Existing Methods

As shown in Fig. 1.21, method 3-3-3 approximates best the system dynamics compared to the existing methods.

By method 3-3-3 Nonlinear terms are reduced from 28 to 8, while keeping all nonlinear properties.

Therefore, we can say:

Method 3-3-3 accurately and largely simplifies the system !
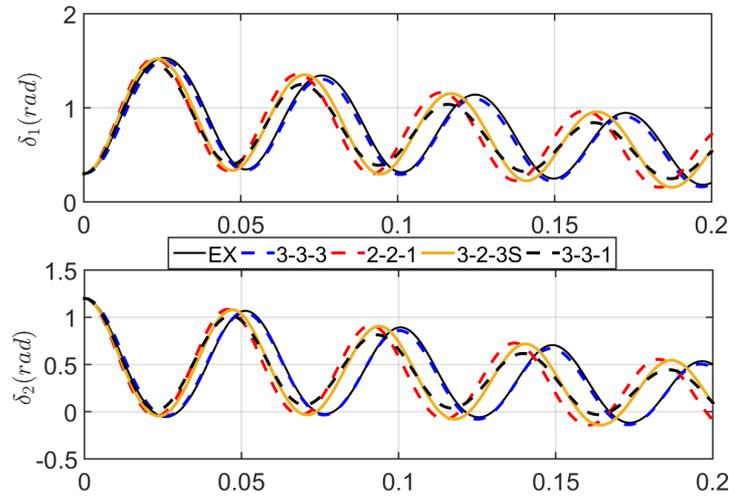
Figure 1.21: Method 3-3-3 approximates best the system dynamics

1.9.5 The Proposed Method NNM

Other than method 3-3-3, another method is proposed, which deals with directly of system modelled by second-order equations. It decouple a N-dimensional system composed of coupled second-order oscillators into a series of second-order oscillators. Its principle can be illustrated by EMR as following.

A N-dimensional system with coupled dynamics can be modelled by second-order differential equations and represented as Fig. 1.22.
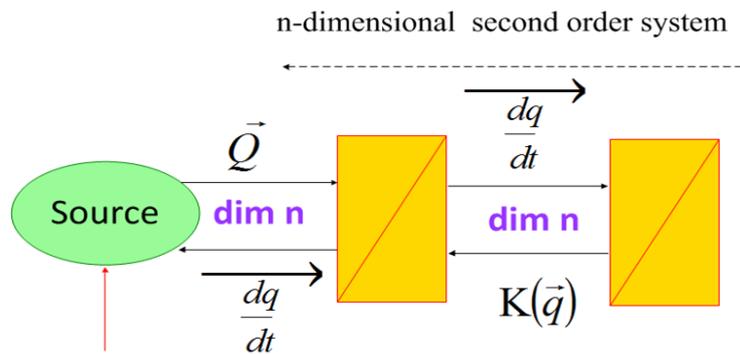
Figure 1.22: N-dimensional System modeled Second-order Differential Equations

If system dynamics are linear, it can be decoupled by a linear transformation as shown in Fig. 1.23.

If system dynamics are nonlinear, it can be approximately decoupled by a nonlinear transformation, as shown in Fig. 1.24.

By Method NNM, the nonlinear system dynamics can be decomposed into two nonlinear modes, as shown in Fig. 1.25.
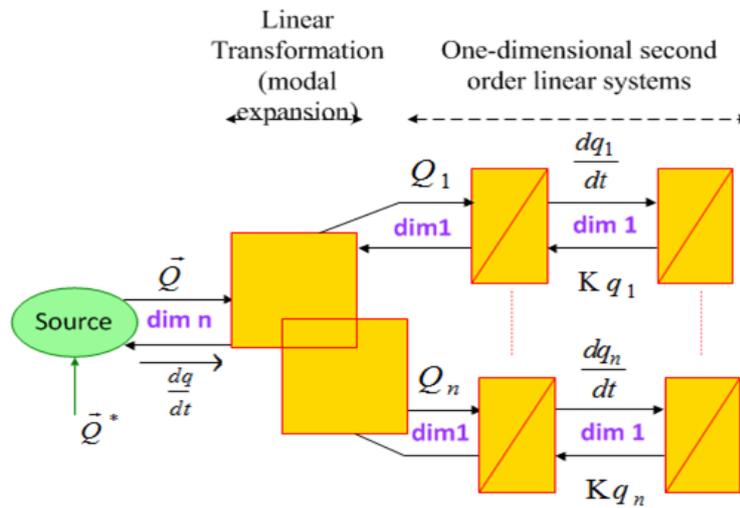
Figure 1.23: Linear system dynamics can be decoupled by linear transformation.
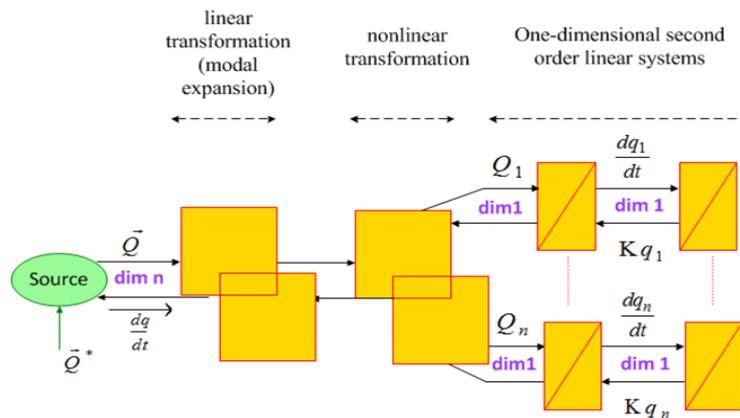
Figure 1.24: Nonlinear system dynamics can be approximately decoupled by non-linear transformation.

1.9.6   Applications of the Proposed Methods

In this PhD work, it has shown how method 3-3-3 and method NNM can be used in nonlinear modal interaction and stability assessment. The method 3-3-3 can quantify the 3rd order nonlinear modal interaction. And by taking into account the trivially resonant terms, it provides a more accurate stability assessment by which the transfer limit can be further exploited. The method NNM (a simplified NNM) has shown its ability to extract the nonlinear properties and predict the stability limit.
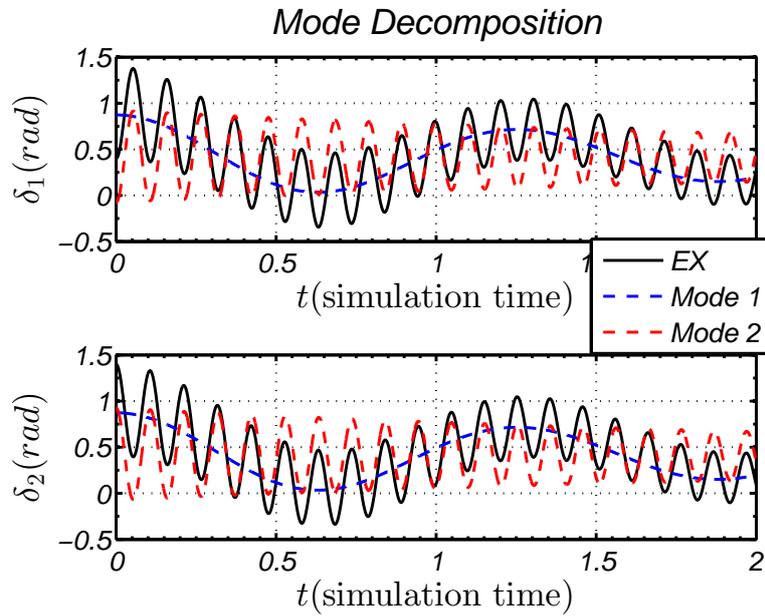
Figure 1.25: System dynamics are approximately decoupled into two modes.

1.10 Scientific Contribution of this PhD Research

In this PhD work, inclusion of 3rd order terms in small-signal analysis is made possible by the proposed method of normal forms. The quantification of 3rd order modal interactions and nonlinear stability assessment is guaranteed by the proposed nonlinear indexes based on normal forms. These points are detailed in Chapter 2 and Chapter 3.

1.10.1 Contribution to Small Signal Analysis

The increased stress in power system has brought about the need for a better understanding of nonlinearities in power-system dynamic behaviour. The higher-order approximation of the system of equations contain significantly more information than the traditionally-used, linear approximation.

However, taking into higher-order terms is extremely complex due to couplings between the terms. It therein desires a methodology to simplify the analysis while providing the most accurate result, leading to:

1. Analytical solution is needed to explain the qualitative properties;
2. Quantitative measures of interactions and nonlinear effects (e.g stability boundary, amplitude-dependent frequency-shift) within the system components are needed;
3. Stability analysis.

1.10.2   Contribution to Transient Stability Assessment

For transient stability analysis, this PhD work studies on the power swing and proposes a stability criterion, which is based on the .

1.10.3   Contribution to Nonlinear Control

As pointed out in the previous sections, the anaylsis of system dynamics can help us find out the essentials of system physical properties. Once a clear picture of system dynamics is obtained, control strategies can be proposed to improve the

1.10.4   Contribution to the Nonlinear Dynamical Systems

Power system dynamics is similar to dynamics of other interconnected system, and has fundamental mathematical underpinnings.
Detailed mathematical models have been derived and concrete applications are demonstrated to show the physical insights rendered by the proposed methodology. Therefore, the significance of this PhD dissertation is not confined in power system stability analysis and control, but can also be used for multiple-input system with differentiable nonlinearities in the mathematical model.

1.10.5   A Summary of the Scientific Contributions

To the author's knowledge, its scientific contributions can be summarized as:
- From the aspect of academic disciplines: this PhD research is multi-discplinary, associated to applied mathematics, nonlinear dynamics, mechanical engineering and electrical enigneering. And it endeavours to extract the essential nonlinear properties, which are common for nonlinear dynamical systems having the particular type of coupled dynamics, whatever the mechanical system or electrical system. For example, the phenomenon where the frequency varies with the amplitude in free-oscillations is common for a mechanical structure [17] and interconnected power systems [22]. The results presented in this PhD research can be used to interpret the nonlinear dynamics of other dynamical systems inside or out of the field of electrical engineering.
- From the aspect of researches on dynamical system:
  1. It conducts the nonlinear analysis on both the free-oscillation and the forced-oscillation;
  2. It endeavours to take the analysis and control of nonlinear dynamical system as a whole, which bridges the gap between nonlinear analysis and nonlinear control. It proposes the analysis-based nonlinear control and the decoupling basis control.
- From the aspect of application and implementation:
  1. It is for the first time that all the existing methods of normal forms up to 3rd order in power system have been summarized and their performances have been evaluated;

2. It is for the first time that a real-form normal form method is applied to study the transient stability of electric power system;

3. It is for the first time that the mathematical modelling of interconnected Power System in Taylor series is provided, from which the origins of the nonlinearities of the system are detected;

4. It is for the first time that the generic programs of the presented methods of normal forms are shared on-line to facilitate the future researchers. Those programs are applicable for systems with arbitrary dimensions.

- From the theoretical part:
- It summarizes the existing MNFs and propose methods of both vector fields and nonlinear normal modes;
- It deduces the normal forms under forced-oscillation and proposes the direction to do the normal forms of the control system (see Chapter 5).

1.11 The Format of the Dissertation

This PhD dissertation is composed of 6 Chapters. In Chapter 2, a general introduction to Normal Form theory is made and two methods are proposed: a novel method 3-3-3 and method NNM. In Chapter 3, method 3-3-3 has been applied to study the nonlinear modal interaction and to predict the nonlinear stability of the interconnected power system. In Chapter 4, method NNM, which is Nonlinear Normal-Mode based approach, is applied to study the transient stability analysis.

Chapter 6 concludes on the nonlinear analysis and points out two approaches to do the nonlinear control: one is the nonlinear analysis based control, the other one is the control on nonlinear model decoupling basis– nonlinear modal control. The Chapter 6 contributes mainly in the study of dynamical system and Normal Form theory.

To make this PhD dissertation as pedagogical as possible, each chapter has an abstract in its front page.

The Methods of Normal Forms and the Proposed Methodologies

This chapter is composed of 4 parts:

Part I: the Normal Form theory, with its basic definitions and general procedures to derive the normal forms are introduced in Section 2.1 & 2.2;

Part II: 3rd order normal forms of vector fields (method 3-3-3) in Section 2.3 and its nonlinear indexes in Section 2.4;

Part III: 3rd order normal forms of nonlinear normal modes (method NNM) in Section 2.5 and its nonlinear indexes in Section 2.6;

Part IV: Practical issues of implementing the methods of normal forms (MNF) are dealt with in Section 2.8. The comparisons on vector fields approach and normal modes approach are conducted in Section 2.9.

Based on the Normal Forms and Normal Form transformation coefficients, nonlinear indexes are proposed in Section 2.4 and Section 2.6, which can be used to study the nonlinear modal interaction and to assess the nonlinear stability, as well as predict and quantify the parameters' influences on the amplitude-dependent frequency shift and the predominance of the nonlinearity in the system dynamics. The programming procedures and computational techniques are also documented in Appendix. To explain why MNFs are chosen to develop the tools to analyse and control the dynamical systems, the competitors– Modal Series (MS) method and Shaw-Pierre (SP) method are reviewed with mathematical formulation in Sections 2.3.9, 2.5.9 and their limitations are pointed out.

This chapter lays the theoretical foundation of the applications presented in Chapter 3 and Chapter 4. The proposed methodologies can also be generally applied to multiple-input systems with nonlinear coupled dynamics. Unlike the previous literatures focused on the bifurcation analysis, this chapter focuses on the analysis of nonlinear modal interaction and nonlinear stability. All the nonlinear indexes are at the first time proposed by this PhD work.

Keywords: Methods of Normal Forms, System of First-order Equations, System of Second-order Equations, Nonlinear Indexes, Nonlinear Modal Interaction, Nonlinear Stability Assessment

2.1 General Introduction to NF Methods

The methods of normal forms can be applied to find out the "simplest form" of a nonlinear system, making it possible to predict accurately the dynamic behaviour, where a complete linearization will lose the nonlinear properties.

2.1.1 Normal Form Theory and Basic Definitions

Normal form theory is a classical tool in the analysis of dynamical systems, and general introductions can be found in many textbooks, see e.g. [30], mainly in the mechanical domain. It is mainly applied in bifurcation analysis [49], to analyze the qualitative influence of parameters on system properties. (Bifurcation analysis comes from the phenomenon that the system properties may be totally different when there is a only small change of parameters at the point of bifurcation.)
It is based on Poincaré-Dulac theorem which provides a way of transformation of a dynamical system into the simplest possible form, which is called "Normal Form" ("formes normales" in French [50]). A normal form of a mathematical object, broadly speaking, is a simplified form of the object obtained by applying a transformation (often a change of coordinates) that is considered to preserve the *essential features* of the object. For instance, a matrix can be brought into Jordan normal form by applying a similarity transformation. This PhD research focuses on Normal Form for non-linear autonomous systems of differential equations (first-order equation on vector fields and second-order equations in form of modes) near an equilibrium point. The starting point is a smooth system of differential equations with an equilibrium (rest point) at the origin, expanded as a power series

$$\dot{x} = Ax + a_2(x) + a_3(x) + \cdots \tag{2.1}$$

where $x \in R_n$ or C_n, A is an $n \times n$ real or complex matrix, and $a_j(x)$ is a homogeneous polynomial of degree j (for instance, $a_2(x)$ is quadratic). The expansion is taken to some finite order k and truncated there, or else is taken to infinity but is treated formally (the convergence or divergence of the series is ignored). The purpose is to obtain an approximation to the (unknown) solution of the original system, that will be valid over an extended range in time. The linear term $A\boldsymbol{x}$ is assumed to be already in the desired normal form, usually the **Jordan** or a **real canonical form**.

2.1.1.1 Normal Form Transformation

A transformation to new variables y is applied, which is referred to as **Normal Form Transformation**, and has the form

$$x = y + h_2(y) + h_3(y) + \cdots \tag{2.2}$$

where h_j is homogeneous of degree j. This transformation can also be done successively, such $x = y + h_2(y)$, $y = z + h_3(z)$, $z = w + h_4(w) \cdots$ to render the

same normal forms. Up to order 3, the coefficients of one-step transformation and sucessive transformation will be the same, a short proof is given as follows:

$$
\begin{aligned}
x &= y + h_2(y) \\
&= z + h_3(z) + h_2(z + h_3(z)) \\
&= [z + h_2(z)] + h_3(z) + Dh_2(z)h_3(z) \\
&= z + h_2(z) + h_3(z) + (O)(4)
\end{aligned}
\tag{2.3}
$$

2.1.1.2 Normal Form

This results in a new system as, which is referred to as **Normal Form** in this thesis.

$$
\dot{y} = \lambda y + g_2(y) + g_3(y) + \cdots,
\tag{2.4}
$$

having the same general form as the original system. The goal is to make a careful choice of the h_j, so that the g_j are "simpler" in some sense than the a_j. "Simpler" may mean only that some terms have been eliminated, but in the best cases one hopes to achieve a system that has additional symmetries that were not present in the original system. (If the normal form possesses a symmetry to all orders, then the original system had a hidden approximate symmetry with transcendentally small error.)

2.1.1.3 Resonant Terms

Resonant terms cannot be cancelled in Normal Form.
If (2.4) has N state-variables, and $\lambda_j = \sigma_j + j\omega_j$ for the , resonance occurs when $\sum_{k=1}^{N} \omega_k = \omega_j$. For example, for the 2nd order and 3rd order resonance.

$$
\omega_k + \omega_l - \omega_j = 0 \qquad \text{\color{red}(2nd Order Resonance)}
$$
$$
\omega_p + \omega_q + \omega_r - \omega_j = 0 \qquad \text{\color{red}(3nd Order Resonance)}
$$

terms $y_k y_l$ and $y_p y_q y_r$ are resonant terms.

2.1.1.4 Normal Dynamics

The solution to the Normal Form (2.4) is normal dynamics. By (2.2), we can reconstruct the solution of $\boldsymbol{x}$, i.e the original system dynamics.

2.1.1.5 Reconstruction of the System Dynamics from the Normal Dynamics

The system dynamics can be reconstructed from the normal dynamics by $x = h_2(y) + h_3(y) + \cdots$. This is a method to verify if the normal dynamics contain the invariance property.
However, this is not an efficient manner to use the Normal Forms. In the engineering practice, indexes can be proposed based on the Normal Forms and Normal Form

transformation to predict, interpret and quantify the system dynamics.

2.1.2 Damping and Applicability of Normal Form Theory

The normal forms are initially proposed for undamped system, i.e $\sigma_j = 0$. And the resonant terms is defined if only $\sigma_i = 0$ [30,50], the no- damped case. However, we can still extend it to weakly-damped case as:

$$
\begin{aligned}
\lambda_j &= -\xi_j \omega_j \pm j\omega_j \sqrt{1 - \xi_j^2} \\
&\approx \pm j\omega_j - \xi_j \omega_j + \mathcal{O}(\xi_j^2)
\end{aligned}
\tag{2.5}
$$

(2.5) shows that the influence of damping on the oscillatory frequency is at least a second-order effect. For computing the normal form, the general formalism can be adopted, excepting that now the eigenvalues are complex number with real and imaginary parts. Physical experiments in [19] proved that approximation of (2.5) when $\xi < 0.4$. In fact, the oscillations of interest in electric power system is $\xi \leq 0.1$, therefore, Normal Form theory can be extended to study the dynamics of electric power system.

2.1.3 Illustrative Examples

2.1.3.1 Linear System

In fact, the eigenvalue matrix is the simplest Normal Form. For a linear system, as before

$$
\dot{x} = Ax
\tag{2.6}
$$

We can use $x = Uy$ to simplify the equation into

$$
y = \Lambda y
\tag{2.7}
$$

where Λ is a diagonal matrix, and the jth equation reads:

$$
\dot{y_j} = \lambda_j y_j
\tag{2.8}
$$

This is the simplest form, and the Normal Dynamic of (2.8) $y(t) = y_j^0 e^{\lambda_j t}$. Therefore, transformation $x = Uy$ renders the system in the simplest form: a linear Normal Form.

2.1.3.2 Nonlinear System

Let us consider a dynamical system [19]:

$$
\dot{X} = sX + a_2 X^2 + a_3 X^3 + \cdots = sX + \sum_{p>1} a_p X^p
\tag{2.9}
$$

where $X \in R$ (phase space of dimension $n = 1$). $X = 0$ is a hyperbolic point as long as $s \neq 0$, otherwise a marginal case is at hand (bifurcation point).

Let us introduce a Normal Form transformation

$$X = Y + \alpha_2 Y^2 \tag{2.10}$$

where α_2 is introduced in order to cancel the quadratic monom of the original system, *i.e.* $a_2 X^2$ in (2.9). Here Y is the new variable, and the goal of the transformation is to obtain a dynamical system for the new unknown Y that is simpler than the original one. Differentiating (2.10) with respect to time and substituting in (2.9) gives:

$$(1 + 2\alpha_2 Y)\dot{Y} = sY + (s\alpha_2 + a_2)Y^2 + \mathcal{O}(Y^3) \tag{2.11}$$

All the calculation are realized in the vicinity of the fixed point. One can multiply both sides by:

$$(1 + 2\alpha_2 Y)^{-1} = \sum_{p=0}^{+\infty} (-2)^p \alpha_2^p Y^p \tag{2.12}$$

Rearranging the terms by increasing orders finally leads to as:

$$\dot{Y} = sY + (a_2 - s\alpha_2)Y^2 + \mathcal{O}(Y^3) \tag{2.13}$$

From that equation, it appears clearly that the quadratic terms can be cancelled by selecting:

$$\alpha_2 = \frac{a_2}{s} \tag{2.14}$$

which is possible as long as $s \neq 0$.

It leads to the Normal Form:

$$\dot{Y} = sY + \mathcal{O}(Y^3) \tag{2.15}$$

Compared to (2.9), (2.15) is simpler in the sense that the nonlinearity has been repelled to order three. And the terms $\mathcal{O}(Y^3)$ arise from the cancellation of 2nd order terms and the 3rd order terms of the original system. According to the specific requirements, all the terms or some terms of $\mathcal{O}(Y^3)$ will be neglected. And it renders a simpler form for which the analytical solution is available or numerical simulation has less computational burden.

Continuing this process, it is possible to propel the nonlinearity to the fourth order. The reader who is curious can be addressed to the reference [51], where Normal Form of a dynamical system is deduced up to order 11.

However, the computational burden increases extraordinarily. Therefore, the Normal Form are always kept up to order 2 or order 3 in practice. And only 2nd Order and 3rd Order Normal Form Transformation will be introduced and deduced in this thesis for , for higher order Normal Form, interested readers may refer to some references as [17, 18, 51] or deduce it by oneself similar to order 2 or order 3.

2.2 General Derivations of Normal Forms for System Containing Polynomial Nonlinearities

Although the methods of normal forms can be applied to system with different types of continuous and differentiable nonlinearities, its applications are primarily in systems containing polynomial nonlinearities, or nonlinearities can be approximated by polynomials after Taylor series expansion. In this PhD work, we focus on system with polynomials up to order 3, and the proposed methodology can be extended to system with higher-order polynomials.

In this section, the general derivations of normal forms up to order 3 will be deduced, which lays the basis for the next two sections, where normal forms are derived for two particular types of systems: system of first order differential equations on vector fields and system of second-order equations on modal space.

2.2.1 Introduction

If the system dynamics can be formalized as:

$$\dot{\boldsymbol{u}} = A\boldsymbol{u} + \epsilon \boldsymbol{F_2}(\boldsymbol{u}) + \epsilon^2 \boldsymbol{F_3}(\boldsymbol{u}) + ... \tag{2.16}$$

where $\boldsymbol{u}$ and F_m are column vectors of length n, A is an $n \times n$ constant matrix, and ϵ is a small nondimensional parameter, which is just a bookkeeping device and set equal to unity in the final result. In this PhD dissertation, it functions as bookkeeping device to separate terms into different degrees. In the literature, the normalization is usually carried out in terms of the degree of the polynomials in the nonlinear terms [31,32,48]. However, some concepts are confused and befuddled in their works [31,32]. By introducing the bookkeeping device ϵ, their mistakes can be deviled.

2.2.2 Linear Transformation

A linear transformation $\boldsymbol{u} = \boldsymbol{Px}$ is first introduced, where $\boldsymbol{P}$ is a non-singular or invertible matrix, in (2.16) and it obtains:

$$P\dot{\boldsymbol{x}} = A\,P\boldsymbol{x} + \epsilon \boldsymbol{F_2}(P\boldsymbol{x}) + \epsilon^2 \boldsymbol{F_3}(P\boldsymbol{x}) + \cdots \tag{2.17}$$

Multiplying (2.17) by P^{-1}, the inverse of P, it reads:

$$\dot{\boldsymbol{x}} = \Lambda \boldsymbol{x} + \epsilon \boldsymbol{f_2}(\boldsymbol{x}) + \epsilon^2 \boldsymbol{f_3}(\boldsymbol{x}) + \cdots \tag{2.18}$$

where

$$\Lambda = P^{-1} A P \qquad \text{and} \qquad f_m(\boldsymbol{x}) = P^{-1} \boldsymbol{F_m}(P\boldsymbol{x})$$

To assure the accuracy of following transformation P should be chosen so that Λ has a simple real form [30] or pure imaginary form [33]. If A is in complex-valued form, extra procedures should be applied to separate the real parts and imaginary

parts [33]. However, to make it as simple as possible, in the previous researches in power system nonlinear analysis, A is always treated as pure imaginary even if it is complex-valued and the researches focus on the oscillatory characteristics brought by the complex conjugate pairs. However, as separating real parts and imaginary parts is technically difficult at present, the previous researches deduced the formula in the assumption that A is in pure imaginary form. This will definitely lead to unexpected errors when try to balance the right side and left side when deducing the normal form transformation coefficients. This issue associated to A has been discussed deeply by the literature in mechanic domain, and will not be addressed in this dissertation (Dumortier,1977 [52]; Guckenheimer and Holemes, 1983 [53]). The practice of this PhD work, is to assume that A is pure imaginary (as assumed in [31, 32, 48]), and pointed out the limitations.

2.2.3 General Normal Forms for Equations Containing Nonlinearities in Multiple Degrees

In our analysis, both quadratic and cubic nonlinearities are concerned. It is proved that a single transformation and successive transformations can produce the same results both theoretically [30] and experimentally on power system [32] up to order 3.

Thus, instead of using a sequence of transformations, a single normal form transformation

$$\boldsymbol{x} = \boldsymbol{y} + \epsilon \boldsymbol{h_2}(\boldsymbol{y}) + \epsilon^2 \boldsymbol{h_3}(\boldsymbol{y}) + \cdots + \epsilon^{k-1} \boldsymbol{h_k}(\boldsymbol{y}) + \cdots \tag{2.19}$$

is introduced into (2.18) and it leads to the so-called normal form (2.20).

$$\dot{\boldsymbol{y}} = \Lambda \boldsymbol{y} + \epsilon \boldsymbol{g_2}(\boldsymbol{y}) + \epsilon^2 \boldsymbol{g_3}(\boldsymbol{y}) + \cdots + \epsilon^{k-1} \boldsymbol{g_k}(\boldsymbol{y}) + \cdots \tag{2.20}$$

h_m is chosen so that $\boldsymbol{g_m}$ takes the simplest possible form. The minimum terms kept in g_m are the resonant terms. In the best case (no resonance occurs), g_n is null and (2.20) turns into $\dot{\boldsymbol{y}} = \Lambda \boldsymbol{y}$ whose solution is ready at hand. Otherwise, g_n is referred to as resonance and near-resonance terms.

Substituting (2.19) into (2.18) yields

$$\begin{aligned}
[I + &D(\epsilon \boldsymbol{h_2}(\boldsymbol{y})) + D(\epsilon^2 \boldsymbol{h_3}(\boldsymbol{y})) + \cdots] \dot{\boldsymbol{y}} \\
=& \Lambda \boldsymbol{y} + \epsilon \Lambda \boldsymbol{h_2}(\boldsymbol{y}) + \epsilon^2 \Lambda \boldsymbol{h_3}(\boldsymbol{y}) + \cdots \\
&+ \epsilon \boldsymbol{f_2}[\boldsymbol{y} + \epsilon \boldsymbol{h_2}(\boldsymbol{y}) + \epsilon^2 \boldsymbol{h_3}(\boldsymbol{y}) + \cdots] \\
&+ \epsilon^2 \boldsymbol{f_3}[\boldsymbol{y} + \epsilon \boldsymbol{h_2}(\boldsymbol{y}) + \epsilon^2 \boldsymbol{h_3}(\boldsymbol{y}) + \cdots] + \cdots
\end{aligned} \tag{2.21}$$

Where Taylor series can be applied

$$\begin{aligned}
\epsilon^{k-1} \boldsymbol{f_k}[&\boldsymbol{y} + \epsilon \boldsymbol{h_2}(\boldsymbol{y}) + \epsilon^2 \boldsymbol{h_3}(\boldsymbol{y}) + \cdots] \\
&= \epsilon^{k-1} \boldsymbol{f_k}(\boldsymbol{y}) + \epsilon^k D\boldsymbol{f_k}(\boldsymbol{y})\boldsymbol{h_2}(\boldsymbol{y}) + \epsilon^{k+1} D\boldsymbol{f_k}(\boldsymbol{y})\boldsymbol{h_3}(\boldsymbol{y}) + \cdots
\end{aligned} \tag{2.22}$$

and

$$[I + D(\epsilon \boldsymbol{h_2}(\boldsymbol{y})) + D(\epsilon^2 \boldsymbol{h_3}(\boldsymbol{y})) + \cdots]^{-1} \tag{2.23}$$
$$= I - \left[D(\epsilon \boldsymbol{h_2}(\boldsymbol{y})) + D(\epsilon^2 \boldsymbol{h_3}(\boldsymbol{y})) + \cdots \right]$$
$$+ \left[D(\epsilon \boldsymbol{h_2}(\boldsymbol{y})) + D(\epsilon^2 \boldsymbol{h_3}(\boldsymbol{y})) + \cdots \right]^2 + \cdots$$

Substituting (2.22) on the right side of (2.21), multiplying (2.23) on both two sides of (2.21), and equating coefficients of like powers of ϵ with the aid of (2.22), it satisfies

$$\epsilon^0 : \quad \dot{\boldsymbol{y}} = \Lambda \boldsymbol{y} \tag{2.24}$$
$$\epsilon^1 : \quad \boldsymbol{g_2}(\boldsymbol{y}) + D\boldsymbol{h_2}(\boldsymbol{y})\Lambda \boldsymbol{y} - \Lambda \boldsymbol{h_2}(\boldsymbol{y}) = \boldsymbol{f_2}(\boldsymbol{y}) \tag{2.25}$$
$$\epsilon^2 : \quad \boldsymbol{g_3}(\boldsymbol{y}) + D\boldsymbol{h_3}(\boldsymbol{y})\Lambda \boldsymbol{y} - \Lambda \boldsymbol{h_3}(\boldsymbol{y}) = \boldsymbol{f_3}(\boldsymbol{y}) \tag{2.26}$$
$$+ D\boldsymbol{f_2}(\boldsymbol{y})\boldsymbol{h_2}(\boldsymbol{y}) - D\boldsymbol{h_2}(\boldsymbol{y})\boldsymbol{g_2}(\boldsymbol{y})$$

$$\vdots$$

$$\epsilon^{k-1} : \quad \boldsymbol{g_k}(\boldsymbol{y}) + D\boldsymbol{h_k}(\boldsymbol{y})\Lambda \boldsymbol{y} - \Lambda \boldsymbol{h_k}(\boldsymbol{y}) = \boldsymbol{f_{k-1}}(\boldsymbol{y}) \tag{2.27}$$

$$+ \sum_{l=2}^{k} [D\boldsymbol{f_l}(\boldsymbol{y})\boldsymbol{h_{k+1-l}}(\boldsymbol{y}) - D\boldsymbol{h_l}(\boldsymbol{y})\boldsymbol{g_{k+1-l}}(\boldsymbol{y})]$$

where terms $\sum_{l=2}^{k}[D\boldsymbol{f_l}(\boldsymbol{y})\boldsymbol{h_{k+1-l}}(\boldsymbol{y}) - D\boldsymbol{h_l}(\boldsymbol{y})\boldsymbol{g_{k+1-l}}(\boldsymbol{y})]$ arise from the cancellation of terms lower than order k. h_m is chosen so that normal dynamics of $\boldsymbol{y}$ will be in the simplest form. Normally, h_m is chosen so that g_m only contain the resonant terms which cannot be cancelled by Normal Form transformations.

It is seen from (2.25) that the transformation at degree ϵ will add terms to degree ϵ^2: $D\boldsymbol{f_2}(\boldsymbol{y})\boldsymbol{h_2}(\boldsymbol{y})$, $D\boldsymbol{h_2}(\boldsymbol{y})\boldsymbol{g_2}(\boldsymbol{y})$, which are important terms obviated in the previous researches in deducing 3rd order normal forms [32, 54].

We would like to remind the reader that it is the degree of nonlinearity rather than the order of nonlinear terms that matters in the normal form transformation.[1]

2.2.4 Summary analysis of the different methods reviewed and proposed in the work

Based on Normal Form theory, different Normal Form methods are developed, depending on h_n- the order of Normal Form Transformation, f_n- the order of terms in Taylor series, and $g_n-$the order of the Normal Form. As some or all terms of n-th order will be neglected in g_n, it can be specified as "Full (F)", meaning that all the terms are kept, and "Simplified(S)", meaning that some terms are neglected.

The methods proposed in this work can be compared on four features. Each method

---

[1]Note: we would like to notify the difference between the order of terms and the degrees of nonlinearities, which is not always the same. For example, if a system of equations only contain cubic nonlinear terms and no quadratic nonlinear terms, its degree of nonlinearity is ϵ, when equating the cubic terms, it is (2.25) instead of (2.26) should be employed.

is then labeled using three digits and one optional letter where:

1. The first digit gives the order of the Taylor expansion of the system's dynamic, i.e the order of f_n;
2. The second digit gives the order of the Normal Form transformation used, i.e, the order of h_n;
3. The third digit gives the order of the Normal Forms, i.e the order of $g(n)$;
4. The optional letter indicates the fact that some terms have not been taken into account in $g(n)$ (S, for Simplified)

In this chapter, Normal Forms are deduced by two approaches, the vector field approach for system of first-order equations, and the normal mode approach for system of second-order equations. All the methods are listed in Tab. 2.1 and Tab. 2.1.

In this PhD dissertation, the vector field methods are labelled as 2-2-1, 3-2-3S and etc. To avoid the ambiguity, the normal mode methods are labelled as LNM, NM2, FNNM, NNM instead of 1-1-1, 2-2-1, 3-3-3 and 3-3-3S.

Tab. 2.1 lists of the four vector field Normal Forms methods proposed in this work.

Table 2.1: List of Existing and Proposed MNFs with Vector Fields Approach

Method	Taylor series	NF Trans.	Normal Form	nth order NF Terms	Related Equation	Cited Reference
2-2-1	2nd order	order 2	order 1	/	(2.41)	[48]
3-2-3S	3rd order	order 2	order 3	S	(2.56)	[5, 16]
3-3-1	3rd order	order 3	order 1	/	(2.58)	[31, 32]
3-3-3	3rd order	order 3	order 3	/	(2.51)(2.52)	

A summary of the existing and proposed normal modes approaches can be found in Tab. 2.2. Since all those methods are the first time to be used in interconnected power system, therefore all those methods are assessed in the Section 2.7 on interconnected VSCs to to give the reader a concrete example.

2.2.5 General Procedures of Applying the Method of Normal Forms in Power System

As illustrated in the previous sections, the Normal Form theory is defined for equation $\dot{x} = f(x)$, however, in the engineering, the x will be constrained by algebraic equations, and normally the differential algebraic equations (DAEs) are formed. By

Table 2.2: List of Existing and Proposed MNFs with Normal Modes Approach

Method	Taylor series	NF Trans.	Normal Form	nth order NF Terms	Related Equation	Cited Reference
LNM (1-1-1)	1st order	order 1	order 1	/	(2.92)	[55]
NM2 (2-1-1)	2nd order	order 2	order 1	/	(2.105)	[56]
FNNM (3-3-3)	3rd order	order 3	order 3	/	(2.123)	[17, 18]
NNM (3-3-3S)	3rd order	order 3	order 3	S	(2.126)	[21, 22]

expanding the equation around the stable equilibrium point (SEP) into Taylor series and substituting by $\boldsymbol{x} - \boldsymbol{x_{SEP}}$ by $\triangle\boldsymbol{x}$, a disturbance model can be formed as $\triangle\dot{\boldsymbol{x}} = A\triangle\boldsymbol{x} +$ Higher-order Terms. The DAE formalism will be discussed further in Section 2.8.3.

The general procedures is well documented in [30, 51] and can be adapted to the power system analysis consisting of eight major steps:

1. Building the differential algebraic equations (DAEs) of the power system– the differential equations and the power flow constraints;
2. Solving the power flow to obtain the stable equilibrium point (SEP) for the post-fault system, i.e the operating point;
3. Expanding the system of equations around the SEP into Taylor series up to third-order;
4. Simplifying the linear part of the system by the use of a linear transformation;
5. Simplifying the non-resonant terms of higher-order terms by successive Normal Form (NF) transformations.
6. Simplifying the Normal Forms by neglecting (if possible) some resonant terms that can not be annihilated by NF transformations;
7. Reconstructing the original system's dynamic from the Normal Forms' dynamics in order to determine the order of the Taylor series and the NF transformations to be selected according to the expected accuracy;
8. Using the chosen Normal Forms for dynamic and stability analysis.

Following the procedures above, the Normal Form formula are deduced in the next sections. Those sections can be roughly divided into two parts. The first part is dedicated to system represented by a set of first order equations, the second part is dedicated to system represented by a set of second-order equations– the oscillators.

2.3   Derivations of the Normal Forms of Vector Fields for System of First Order Equations

The vector fields is a mapping where the dynamics of the system are characterized by a set of first order dynamical equations.

2.3.1   Class of First-Order Equation that can be studied by Normal Form methods

The class of systems that can be studied by MNF are usually modeled using Differential Algebraic Equations (DAEs) [1]. By subsituting the algebraic equations into the differential ones, one transforms those DAEs in a dynamical system, which can be written:

$$\dot{\boldsymbol{x}} = \boldsymbol{f}(\boldsymbol{x}, \boldsymbol{u}), \tag{2.28}$$

where $\boldsymbol{x}$ is the state-variables vector, $\boldsymbol{u}$ is the system's inputs vector and $\boldsymbol{f}$ is a nonlinear vector field. Expanding this system in Taylor series around a stable

equilibrium point (SEP), $\boldsymbol{u} = \boldsymbol{u_{SEP}}$, $x = \boldsymbol{x_{SEP}}$, one obtains:

$$\triangle\dot{\boldsymbol{x}} = \boldsymbol{H1}(\triangle\boldsymbol{x}) + \frac{1}{2!}\boldsymbol{H2}(\triangle\boldsymbol{x}) + \frac{1}{3!}\boldsymbol{H3}(\triangle\boldsymbol{x}) + \mathcal{O}(4) \tag{2.29}$$

where $\boldsymbol{Hq}$ gathers the qth-order partial derivatives of f. i.e., for $j = 1, 2, \cdots, n$, $H1_k^j = \partial f_j/\partial x_k$, $H2_{kl}^j = \left[\partial^2 f_j/\partial x_k \partial x_l\right]$, $H3_{klm}^j = \left[\partial^3 f_j/\partial x_k \partial x_l \partial x_m\right]$ and $\mathcal{O}(4)$ are terms of order 4 and higher.

2.3.2 Step1:Simplifying the linear terms

The linear part of (2.29) is simplified using its Jordan form:

$$\dot{\boldsymbol{y}} = \boldsymbol{\Lambda}\boldsymbol{y} + \boldsymbol{F2}(\boldsymbol{y}) + \boldsymbol{F3}(\boldsymbol{y}) + \cdots \tag{2.30}$$

supposed here to be diagonal, where the jth equation of (2.32) is:

$$\dot{y_j} = \lambda_j y_j + \sum_{k=1}^{N}\sum_{l=1}^{N} F2_{kl}^j y_k y_l + \sum_{p=1}^{N}\sum_{q=1}^{N}\sum_{r=1}^{N} F3_{pqr}^j y_p y_q y_r + \cdots \tag{2.31}$$

λ_j is the jth eigenvalue of matrix $\boldsymbol{H1}$, and $j = 1, 2, \cdots, n$. $\boldsymbol{U}$ and $\boldsymbol{V}$ are the matrices of the right and left eigenvectors of matrix $\boldsymbol{H1}$, respectively: $\boldsymbol{UV} = \boldsymbol{I}$; $\boldsymbol{F2_j} = \frac{1}{2}\sum_{i=1}^{N} v_{ji} \left[\boldsymbol{U^T} h_3^j \boldsymbol{U}\right]$. $F3_{pqr}^j = \frac{1}{6}\sum_{i=1}^{N} v_{ji} \sum_{k=1}^{N}\sum_{k=1}^{N}\sum_{m=1}^{N} H3_{kLNM}^i u_p^l u_q^m u_r^N$, v_{ji} is the element at j-th row and i-th colomn of Matrix $\boldsymbol{V}$. u_p^l is the element at the p-th row and l-th column of matrix $\boldsymbol{U}$.

The fundamentals of linear small-signal analysis uses the sign of the real parts σ_j of the eigenvalues $\lambda_j = \sigma_j + j\omega_j$ to estimate the system stability. $\boldsymbol{U}$ is used to indicate how each mode y_j contribute to the state-variable $\boldsymbol{x}$, and $\boldsymbol{V}$ indicates how the state-variables of $\boldsymbol{x}$ are associated to each mode y_j.

2.3.3 Step 2: Simplifying the nonlinear terms

After the linear transformation to decouple the linear part and obtain the Eigen Matrix, the system equation reads:

$$\boldsymbol{y} = \Lambda\boldsymbol{y} + F(\boldsymbol{y}) \tag{2.32}$$

Λ is the Eigen Matrix, and $F(\boldsymbol{y})$ gathers the higher-order terms of Taylor series after the linear transformation.

2.3.3.1 Method 2-2-1: Cancelling all the 2nd Order Terms

When only 2nd order terms are kept in the Taylor series of the system's dynamics, (2.32) becomes:

$$\dot{\boldsymbol{y}} = \Lambda\boldsymbol{y} + F2(\boldsymbol{y}) \tag{2.33}$$

where the jth equation of (2.33) writes:

$$\dot{y}_j = \lambda_j y_j + \sum_{k=1}^{N}\sum_{l=1}^{N} F2_{kl}^{j} y_k y_l \tag{2.34}$$

To eliminate the second-order terms in (2.33), the following second-order transformation is applied:

$$\boldsymbol{y} = \boldsymbol{z} + h2(\boldsymbol{z}) \tag{2.35}$$

The jth equation of (2.35) being:

$$y_j = z_j + \sum_{k=1}^{N}\sum_{l=1}^{N} h2_{kl}^{j} z_k z_l \tag{2.36}$$

Applying (2.35) to (2.33), it leads to:

$$\dot{\boldsymbol{z}} + \dot{h2}(\boldsymbol{z}) = \Lambda\boldsymbol{z} + \Lambda h2(\boldsymbol{z}) + F2(\boldsymbol{z} + h2(\boldsymbol{z})) \tag{2.37}$$
$$\dot{\boldsymbol{z}}(I + Dh2(\boldsymbol{z})) = \Lambda\boldsymbol{z} + \Lambda h2(\boldsymbol{z}) + F2(\boldsymbol{z}) + DF2(\boldsymbol{z})h2(\boldsymbol{z}) + HF2(\boldsymbol{z})(h2(\boldsymbol{z}))^2$$
$$\dot{\boldsymbol{z}} = (I + Dh2(\boldsymbol{z}))^{-1}(\Lambda\boldsymbol{z} + \Lambda h2(\boldsymbol{z}) + F2(\boldsymbol{z}) + DF2(\boldsymbol{z})h2(\boldsymbol{z}) \qquad + HF2(\boldsymbol{z})(h2(\boldsymbol{z}))^2)$$
$$\dot{\boldsymbol{z}} = (I - Dh2(\boldsymbol{z}) + (Dh2(\boldsymbol{z}))^2 + \mathcal{O}(3))(\Lambda\boldsymbol{z} + \Lambda h2(\boldsymbol{z}) + F2(\boldsymbol{z}) \quad + DF2(\boldsymbol{z})h2(\boldsymbol{z}) + \mathcal{O}(4))$$

Expanding the equation, it obtains:

$$\dot{\boldsymbol{z}} = \Lambda\boldsymbol{z} \qquad\qquad\qquad\qquad\qquad\qquad\qquad\qquad (\text{order } 1)$$
$$- (Dh2(\boldsymbol{z})\Lambda\boldsymbol{z} - \Lambda h2(\boldsymbol{z}) - F2(\boldsymbol{z})) \qquad\qquad\qquad (\text{order } 2)$$
$$+ Dh2(\boldsymbol{z})(Dh2(\boldsymbol{z})\Lambda\boldsymbol{z} - \Lambda h2(\boldsymbol{z}) - F2(\boldsymbol{z})) + DF2(\boldsymbol{z})h2(\boldsymbol{z}) \qquad (\text{order } 3)$$
$$+ (Dh2(\boldsymbol{z}))^2(\Lambda h2(\boldsymbol{z}) + F2(\boldsymbol{z})) - Dh2(\boldsymbol{z})DF2(\boldsymbol{z})h2(\boldsymbol{z}) + \mathcal{O}(4) \quad (\text{order } 4)$$
$$+ (Dh2(\boldsymbol{z}))^2 DF2(\boldsymbol{z})h2(\boldsymbol{z}) \qquad\qquad\qquad\qquad (\text{order } 5)$$

and keeping terms up to the second order leads to:

$$\dot{\boldsymbol{z}} = \Lambda\boldsymbol{z} - Dh2(\boldsymbol{z})\Lambda\boldsymbol{z} + \Lambda h2(\boldsymbol{z}) + F2(\boldsymbol{z}) \tag{2.38}$$

where $Dh2$ is the Jacobin matrix of $h2$. In order to eliminate the second-order terms from (2.38), transformation (2.35) must satisfy the following equation:

$$Dh2(\boldsymbol{z})\Lambda\boldsymbol{z} - \Lambda h2(\boldsymbol{z}) = F2(\boldsymbol{z}) \tag{2.39}$$

If no internal resonance occurs, $h2_{kl}^{j}$ is given by [48]:

$$h2_{kl}^{j} = \frac{F2_{kl}^{j}}{\lambda_k + \lambda_l - \lambda_j} \tag{2.40}$$

Neglecting all terms with order superior to 2, the transformed equation is a set of

decoupled first-order linear differential equations:

$$\dot{z} = \Lambda z + DF2(z)h2(z) + \mathcal{O}(4) \tag{2.41}$$
$$= \Lambda z + \mathcal{O}(3)$$
$$= \Lambda z$$

2.3.3.2 Method 3-2-3S: Keeping some third order terms

Although the second-order method gives a more accurate picture than the linear small-signal analysis, keeping some third-order terms in the Normal Dynamics after the 2nd-order Normal Form transformation can improve the stability analysis [5] and serve as a new criteria to design the system controllers in order to improve the transfer limit [16].

Keeping 3rd order terms in the Taylor series, the j-th state equation of (2.32) becomes:

$$\dot{y}_j = \lambda_j y_j + \sum_{k=1}^{N}\sum_{l=1}^{N} F2_{kl}^{j} y_k y_l + \sum_{p=1}^{N}\sum_{q=1}^{N}\sum_{r=1}^{N} F3_{pqr}^{j} y_p y_q y_r \tag{2.42}$$

Applying the 2nd Order NF transformation $y = z + h2(z)$ to (2.42),it leads to:

$$\dot{z} + \dot{h2(z)} = \Lambda z + \Lambda h2(z) + F2(z + h2(z)) \tag{2.43}$$
$$\dot{z}(I + Dh2(z)) = \Lambda z + \Lambda h2(z) + F2(z) + DF2(z)h2(z) + HF2(z)(h2(z))^2$$
$$\dot{z} = (I + Dh2(z))^{-1}(\Lambda z + \Lambda h2(z) + F2(z) + DF2(z)h2(z)$$
$$+ HF2(z)(h2(z))^2 + F3(z) + DF3zh2(z))$$
$$\dot{z} = (I - Dh2(z) + (Dh2(z))^2 + \mathcal{O}(3))(\Lambda z + \Lambda h2(z) + F2(z)$$
$$+ DF2(z)h2(z) + F3(z) + \mathcal{O}(4))$$

Expanding (2.43), it leads:

$$\dot{z} = \Lambda z \qquad\qquad\qquad\qquad\qquad\qquad\qquad\qquad\qquad\qquad\text{(order 1)}$$
$$- (Dh2(z)\Lambda z - \Lambda h2(z) - F2(z)) \qquad\qquad\qquad\qquad\text{(order 2)}$$
$$+ Dh2(z)(Dh2(z)\Lambda z - \Lambda h2(z) - F2(z)) + DF2(z)h2(z) + F3(z) \qquad\text{(order 3)}$$
$$+ (Dh2(z))^2(\Lambda h2(z) + F2(z)) - Dh2(z)F3(z) - Dh2(z)DF2(z)h2(z) + \mathcal{O}(4)$$
$$\text{(order 4)}$$
$$+ (Dh2(z))^2(DF2(z)h2(z) + F3(z)) \qquad\qquad\qquad\qquad\text{(order 5)}$$

As order 2 has been deleted by the 2nd NF transformation and $Dh2(z)\Lambda z - \Lambda h2(z) - F2(z) = 0$. keeping terms to order 3, (2.43) reduces to:

$$\dot{z} = \Lambda z + DF2(z)h2(z) + F3(z) + \mathcal{O}(4) \tag{2.44}$$

where:

- $DF2(\boldsymbol{z})h2(\boldsymbol{z})$ are third order terms coming from the 2nd Order NF transformation used to cancel the 2nd order terms;
- $F3(\boldsymbol{z})$ are the original 3rd order terms from the system (2.42).

For the jth variable, it reads:

$$
\begin{aligned}
\dot{z}_j =& \lambda_j z_j \hspace{8cm} (2.45)\\
&+ \sum_{p=1}^{N} \sum_{q=1}^{N} \sum_{r=1}^{N} \left(\sum_{l=1}^{N} (F2_{pl}^{j} + F2_{lp}^{j})h2_{qr}^{p} + F3_{pqr}^{j} \right) z_p z_q z_r \\
=& \lambda_j z_j + \sum_{p=1}^{N} \sum_{q=1}^{N} \sum_{r=1}^{N} C_{pqr}^{j} z_p z_q z_r
\end{aligned}
$$

where $C_{pqr}^{j} = \sum_{l=1}^{N} (F2_{pl}^{j} + F2_{lp}^{j})h2_{qr}^{p} + F3_{pqr}^{j}$

2.3.3.3 Method 3-3-3: Elimination of a maximum of third-order terms

To simplify as much as possible the third order terms without neglecting important terms as [16] did, the following third-order NF transformation can be applied to (2.44) [31]:

$$
\boldsymbol{z} = \boldsymbol{w} + h3(\boldsymbol{w}) \tag{2.46}
$$

where $h3$ is a polynomial of w containing only 3rd-order terms. Applying transformation (2.46) to (2.44), it leads to:

$$
\dot{\boldsymbol{w}} + \dot{h3(\boldsymbol{w})} = \Lambda \boldsymbol{w} + \Lambda h3(\boldsymbol{w}) + DF2(\boldsymbol{w}+h3(\boldsymbol{w}))h2(\boldsymbol{w}+h3(\boldsymbol{w})) + F3(\boldsymbol{w}+h3(\boldsymbol{w}))
$$
$$
\tag{2.47}
$$
$$
\begin{aligned}
\dot{\boldsymbol{w}}(I + Dh3(\boldsymbol{w})) &= \Lambda \boldsymbol{w} + \Lambda h3(\boldsymbol{w}) + (DF2(\boldsymbol{w})h2(\boldsymbol{w}) + \mathcal{O}(5)) + (F3(\boldsymbol{w}) + \mathcal{O}(5)) \\
\dot{\boldsymbol{w}} &= (I + Dh3(\boldsymbol{w}))^{-1}(\Lambda \boldsymbol{z} + \Lambda h3(\boldsymbol{w}) + DF2(\boldsymbol{w})h2\boldsymbol{w} + F3(\boldsymbol{w}) + \mathcal{O}(5)) \\
\dot{\boldsymbol{w}} &= (I - Dh3(\boldsymbol{w}) + (Dh3(\boldsymbol{w}))^2 \\
&\quad + \mathcal{O}(5))(\Lambda \boldsymbol{w} + \Lambda h3(\boldsymbol{w}) + DF2(\boldsymbol{w})h2(\boldsymbol{w}) + F3(\boldsymbol{w}) + \mathcal{O}(5))
\end{aligned}
$$

Expanding the equation, it obtains:

$$
\begin{aligned}
\dot{\boldsymbol{w}} = & \Lambda \boldsymbol{w} & \text{\textcolor{red}{(order 1)}} \\
& + DF2(\boldsymbol{w})h2(\boldsymbol{w}) + \Lambda h3(\boldsymbol{w}) - Dh3(\boldsymbol{w})\Lambda \boldsymbol{w} + F3(\boldsymbol{w}) & \text{\textcolor{red}{(order 3)}} \\
& - Dh3(\boldsymbol{w})(DF2(\boldsymbol{w})h2(\boldsymbol{w}) + \Lambda h3(\boldsymbol{w}) - Dh3(\boldsymbol{w})\Lambda \boldsymbol{w} + F3(\boldsymbol{w})) + \mathcal{O}(5) & \\
& & \text{\textcolor{red}{(order 5)}}
\end{aligned}
$$

and keeping only terms up to order 3, it leads to the Normal Dynamics:

$$
\begin{aligned}
\dot{\boldsymbol{w}} =& \Lambda \boldsymbol{w} + DF2(\boldsymbol{w})h2(\boldsymbol{w}) \hspace{4cm} (2.48)\\
& + \Lambda h3(\boldsymbol{w}) - Dh3(\boldsymbol{w})\Lambda \boldsymbol{w} + F3(\boldsymbol{w}) + \mathcal{O}(5)
\end{aligned}
$$

It should be emphasized that there are neither terms of order 2 nor terms of order 4 in (2.48), and that the terms of order 3 are:

- $\boldsymbol{DF2(w)h2(w)}$ that comes from the 2nd-order NF transformation used to cancel the 2nd-order terms
- $\boldsymbol{\Lambda h3(w) - Dh3(w)\Lambda w}$ that comes from the use of transformation (2.46) in order to cancel the 3rd-order terms
- $\boldsymbol{F3(w)}$, the original 3rd order terms of system (2.42).

For the j-th variable, (2.48) can be written as:

$$
\begin{aligned}
\dot{w}_j =& \lambda_j w_j \\
&+ \sum_{p=1}^{N}\sum_{q=1}^{N}\sum_{r=1}^{N}[C_{pqr}^{j} - (\lambda_p + \lambda_q + \lambda_r - \lambda_j)h3_{pqr}^{j}]w_p w_q w_r \\
&+ \mathcal{O}(5)
\end{aligned}
\tag{2.49}
$$

The next step is dedicated to the elimination of a maximum number of 3rd-order terms. The elimination of third-order terms deserves careful attention because resonant terms are systematically present when the system exhibits undamped (or weakly damped) oscillating modes (pairs of complex eigenvalues close the the real axis). (2.49) shows that third order terms can not be eliminated if the condition $\lambda_p + \lambda_q + \lambda_r - \lambda_j \approx 0$ holds. If we consider a weak-damped oscillating mode, composed of two conjugated poles λ_{2l} and λ_{2l-1}, the necessary condition for eliminating the associated third-order term $w_{2k}w_{2l}w_{2l-1}$ will not be met for $j = 2k$. Indeed, in that case, $\lambda_j = \lambda_{2k}$ and the condition $\omega_{2l} + \omega_{2l-1} \approx 0$ holds leading to the impossibility of computing the coefficient $h3_{2k2l2l-1}^{2k}$. As a consequence, term $w_{2k}w_{2l}w_{2l-1}$ cannot then be eliminated and must be kept in the normal dynamics [51,57].

If we consider that the system possesses M weakly-damped oscillatory modes, M third-order terms can thus not be eliminated from the Normal Dynamics of the jth variable ($j \in M$). Apart from internal resonances due to commensurability relationships between eigenvalues, as for example when $\omega_1 = 3\omega_2$, $\omega_1 = 2\omega_2 + \omega_3$ or $\omega_1 = \omega_2 + \omega_3 + \omega_4$, all the other third-order terms are eliminated by third-order transformation (2.46) where coefficients $h3_{pqr}^{j}$ are computed by:

$$
h3_{pqr}^{j} = \frac{F3_{pqr}^{j} + \sum_{l=1}^{N}(F2_{pl}^{j} + F2_{lp}^{j})h2_{qr}^{p}}{\lambda_p + \lambda_q + \lambda_r - \lambda_j}
\tag{2.50}
$$

The normal dynamics of a system composed of M weakly-damped oscillatory modes are then:

$$
\dot{w}_j = \lambda_j w_j + \sum_{l=1}^{M} c_{2l}^{j} w_j w_{2l} w_{2l-1} + \mathcal{O}(5), 2k \in M
\tag{2.51}
$$

$$
\dot{w}_j = \lambda_j w_j + \mathcal{O}(5), j \notin M
\tag{2.52}
$$

where w_{2l-1} is the complex conjugate of w_{2l}, and coefficients c_{2l}^j are defined as for $k \neq l$:

$$
\begin{aligned}
c_{2l}^{j=2k} =&C_{(2k)(2l)(2l-1)}^{2k} + C_{(2k)(2l-1)(2l)}^{2k} + C_{(2l)(2k)(2l-1)}^{2k} \\
&+ C_{(2l)(2l-1)(2k)}^{2k} + C_{(2l-1)(2l)(2k)}^{2k} + C_{(2l-1)(2k)(2l)}^{2k} \\
c_{2k}^{j=2k} =&C_{(2k)(2k)(2k-1)}^{2k} + C_{(2k)(2k-1)(2k)}^{2j} + C_{(2k-1)(2k)(2k)}^{2k}
\end{aligned}
\tag{2.53}
$$

$$
\begin{aligned}
c_{2l}^{j=2k-1} =&C_{(2k-1)(2l)(2l-1)}^{2k-1} + C_{(2k-1)(2l-1)(2l)}^{2k} + C_{(2l)(2k-1)(2l-1)}^{2k-1} \\
&+ C_{(2l)(2l-1)(2k-1)}^{2k-1} + C_{(2l-1)(2l)(2k-1)}^{2k} + C_{(2l-1)(2k-1)(2l)}^{2k-1} \\
c_{2k}^{j=2k-1} =&C_{(2k-1)(2k)(2k-1)}^{2k-1} + C_{(2k)(2k-1)(2k-1)}^{2j} + C_{(2k-1)(2k-1)(2k)}^{2k}
\end{aligned}
\tag{2.54}
$$

(2.51) shows that considering third-order terms in the Normal Dynamic changes the way of making the stability analysis. As shown in [5, 16], the third order terms can have a stabilizing or a destabilizing effect and the inspection of the sign of the eigenvalue real parts is not sufficient to predict the stability of the system.

2.3.4   Analysis of the Normal Dynamics using z variables

To evaluate the gain afforded by the 3rd order method over the 2nd order method, the Normal Dynamics (2.51) and (2.52) have to be reconstructed with the z coordinates. The change of variables gives:

$$
z_j =w_j + \sum_{p=1}^{N}\sum_{q=1}^{N}\sum_{r=1}^{N} h3_{pqr}^j w_p w_q w_r, j \notin M
\tag{2.55}
$$

It can be seen from this reconstruction that 3rd order terms are separated into two sets, one set is w_j whose stability is influenced be coefficients c_{2l}^{2k} in 2.51 that can be used for stability analysis [5,16] and the other set with coefficients $h3_{pqr}^{2k}$ that can be used to quantify the 3rd order modal interaction [32].

The most important issue of Normal Form methods is how they contribute to the approximation of system dynamics, which will be compared with a brief introduction of other works in the next Section 2.3.5.

2.3.5   Other Works Considering Third Order Terms – Summary of all the Normal Form Methods

In [5] and [16], third-order terms are present in the Taylor series but only the second-order transformation is used. Some 3rd order terms are kept on the Normal

Dynamics and leads for the oscillatory modes to :

$$\dot{z}_{(j=2k)} = \lambda_{2k} z_{2k} + \sum_{l=1}^{M} c_{2l}^{2k} z_{2k} z_{2l} z_{2l-1} + \mathcal{O}(3), 2k \in M \qquad (2.56)$$

where z_{2l-1} is the complex conjugate of z_{2l}.

For non-oscillatory modes, the Normal Dynamics keeps the same as expressed by (2.41). Compared to the proposed Normal Dynamics using the third order transformation, only terms with frequency ω_{m+n} are involved in the $z_{j=2k}$ expression, and 3rd-order modal interaction can not be studied.

In [31] and [32], a 3rd order NF transformation is proposed where the terms $\boldsymbol{DF2(w)h2(w)}$ of (2.48) are not taken into account, leading to coefficients given by:

$$\overline{h3_{pqr}^{j}} = \frac{F3_{pqr}^{j}}{\lambda_p + \lambda_q + \lambda_r - \lambda_j} \qquad (2.57)$$

Since some 3rd order terms are omitted, the accuracy of the proposed normal dynamics is worse than the one proposed by the dynamic deduced with using coefficients given by (2.50).

Moreover, the considered Normal Dynamics are:

$$\dot{w}_j = \lambda_j w_j + \mathcal{O}(3) \qquad (2.58)$$

and since all resonant terms in (2.58) are neglected, it fails to give more information about the system stability than the linearized small-signal stability analysis.

2.3.6 Interpretation the Normal Form Methods by Reconstruction of Normal Dynamics into System Dynamics

2.3.6.1 2-2-1 and 3-2-3S

The reconstruction for 2-2-1 and 3-2-3S is the same, as only the 2nd NF transformation is done.

$$\boldsymbol{y} = \boldsymbol{z} + h2(\boldsymbol{z}) \qquad (2.59)$$

As indicated in [48], the initial condition of z and coefficients $h2_{kl}^{j}$ can be used to develop nonlinear indexes to quantify the second-order modal interaction. The application can be found in the placement of stabilizers [20].

For 2-2-1:

$$y_j = \underbrace{z_j}_{\omega_j} + \sum_{k=1}^{N} \sum_{l=1}^{N} \underbrace{h2_{kl}^{i} z_k z_l}_{\omega_k + \omega_l} + \mathcal{O}(3) \qquad (2.60)$$

For 3-2-3S

$$y_j = \underbrace{z_j}_{\omega_j} + \sum_{k=1}^{N} \sum_{l=1}^{N} \underbrace{h2_{kl}^{j} z_k z_l}_{\omega_k + \omega_l} + \mathcal{O}(3) \qquad (2.61)$$

2.3.6.2   3-3-3 and 3-3-1

In fact successive transformation is equivalent to one-step transformation to the same order. Transformation $\boldsymbol{y} = \boldsymbol{z} + h2(\boldsymbol{z})$, $\boldsymbol{z} = \boldsymbol{w} + h3(w)$, is equivalent to $\boldsymbol{y} = \boldsymbol{w} + h2(\boldsymbol{w}) + h3(\boldsymbol{w})$. As:

$$
\begin{aligned}
\boldsymbol{y} =&\Lambda \boldsymbol{w} + h2(\boldsymbol{z}) \\
&\Lambda \boldsymbol{w} + h3(\boldsymbol{w}) + h2(\boldsymbol{w} + h3(\boldsymbol{w})) \\
=&\Lambda \boldsymbol{w} + h3(\boldsymbol{w}) + h2(\boldsymbol{w}) \\
&+ Dh2(\boldsymbol{w})h3(\boldsymbol{w}) + Hh2(\boldsymbol{w})(h3(\boldsymbol{w}))^2 + \cdots \\
=&\Lambda \boldsymbol{w} + h2(\boldsymbol{w}) + h3(\boldsymbol{w}) + \mathcal{O}(4)
\end{aligned}
\tag{2.62}
$$

Therefore the reconstruction can be simplified as:

$$
\boldsymbol{y} = \boldsymbol{w} + h2(\boldsymbol{w}) + h3(\boldsymbol{w})
\tag{2.63}
$$

For 3-3-1

$$
y_j = \underbrace{w_j}_{\omega_j} + \sum_{k=1}^{N}\sum_{l=1}^{N} \underbrace{h2_{kl}^{j} w_k w_l}_{\omega_k + \omega_l} + \sum_{p=1}^{N}\sum_{q=1}^{N}\sum_{r=1}^{N} \underbrace{h3_{pqr}^{j} w_p w_q w_r}_{\omega_p + \omega_q + \omega_r}
\tag{2.64}
$$

For 3-3-3:

$$
y_j = \underbrace{w_j}_{\omega_j} + \sum_{k=1}^{N}\sum_{l=1}^{N} \underbrace{h2_{kl}^{j} w_k w_l}_{\omega_k + \omega_l} + \sum_{p=1}^{N}\sum_{q=1}^{N}\sum_{r=1}^{N} \underbrace{h3_{pqr}^{j} w_p w_q w_r}_{\omega_p + \omega_q + \omega_r}
\tag{2.65}
$$

(2.65) indicates that for the oscillatory modes, the assumed "linear modes" will be changed by c_{2l}^{j}. This violates the assumption in 2-2-1 and 3-3-1 that, taking into nonlinearities by NF will just add nonlinear modes on the linear modes obtained by the small signal analysis.

Stability and Higher-order Interaction

Method 3-2-3S can be used to suggest more information of system stability, both λ_j and c_{2l}^{j} will contribute to the stability of oscillatory mode $j \in M$ and therefore the stability of the whole system [5, 16].

Method 3-3-1 can be used to quantify the 3rd order interaction (if the coefficient $h3M$ has enough resolution) [32]

Method 3-3-3 can do both jobs: the stability analysis by c_{2l}^{2k}; and the 3rd order modal interaction by $h3_{pqr}^{j}$. The insight of physical properties of the system dynamics can be exploited more deeply. And in both aspects, it has a resolution up to 5, while both

Accuracy

Indicated by Eqs. (2.61), (2.64), the accuracy of both method 3-2-3s and 3-3-1 is up to order 3 since some 3rd order terms are neglected in the Normal Dynamics. And the method 3-3-3 is up to order 5.

2.3.7 The significance to do 3-3-3

The discussed methods for systems of first equations in this dissertation are: Linear, 2-2-1, 3-2-3S, 3-3-1, 3-3-3.

Their performances can be evaluated from three theoretical aspects.

1. Describing the power system dynamics with less computational burden compared to the full numerical simulation.
2. Modal interaction: linear modal interaction and nonlinear modal interaction, to see how the system components interact with each other, important for placement of stabilizers.
3. Transient Stability analysis: to predict the stability of the power system, exploit the power transfer capacity and maximize the economical benefits.

Table 2.3: Performance Evaluation of the Reviewed and Proposed MNFs

Method	Accuracy	Order of Modal Interaction	Transient Stability	Applicability to 3rd Order Modes
Linear	$\mathcal{O}(2)$	1st	Linear	None
2-2-1	$\mathcal{O}(3)$	2nd	Linear	None
3-2-3S	$\mathcal{O}(3)$	2nd	Non-linear	Oscillatory
3-3-1	$\mathcal{O}(3)$	3rd	Linear	Non-oscillatory
3-3-3	$\mathcal{O}(5)$	3rd	Non-linear	All

2.3.8 Another Way to Derive the Normal Forms

In some literature [30,58],another way to deduce the NF transformation is presented, though less rigorous in mathematics.

Instead of inverting $(I + Dh2(z))$ by $(I + Dh2(z))^{-1} = I - Dh2(z) + (Dh2(z))^2$, it takes:

$$\dot{(z + h2(z))} = \dot{z} + Dh2(z)\dot{z} = \dot{z} + Dh2(z)\Lambda z \tag{2.66}$$

Therefore, there is no need to inverse the nonlinear transformation. However, (2.66) is wrong because it will cause error in the deducing Normal Forms higher than 2nd order.

2.3.9 Comparison to the Modal Series Methods

Despite the Methods of Normal Forms (MNF), several other methods are used by the researchers to study the nonlinear dynamics of interconnected power system, such as Perturbation Techniques (PT) and Modal Series (MS) Methods (As concluded in [37], the PT techniques and MS methods are identical). Having proposed by Shanechi in 2003 [35], the 2nd MS method has declared a better method than MNF [35,37,38,59,60] since it can suggest the closed form solution when resonance occurs. The reader may have a question:

Why MNF, rather than MS is used to study the 3rd order nonlinearities?

As it is difficult to find a satisfying answer in the literatures, the author will answer this question by deducing the 3rd order MS methods.

2.3.9.1   A Brief Review of the MS Methods

Let's start by a brief review of the MS methods. The princple of MS method is to approximate the solution of the nonlinear differential equation by power series.

Let the solution of (2.42), for initial condition $\boldsymbol{y_0}$, be $y_j(y_0, t)$. Let ψ denote the convergence domain of Maclaurin expansion of $y_j(y_0, t)$ in term of y_0 for all $t \in [0, T] \subset R$. $\mu \in C_n$ is the convergence domain of y when expanding the Taylor series. If $\theta = \mu \cap \psi$ is nonempty, then the solution of (2.42) for $y_0 \in \theta$ and for some interval $t \in [0, T] \subset R$ is:

$$y_j(t) = f_j^1(t) + f_j^2(t) + f_j^3(t) + \cdots \tag{2.67}$$

where the right hand side of (2.67) can be found by solving the following series of differential equations with initial conditions, $f^1(0) = [f_1^1(0), f_2^1(0), \cdots, f_N^1(0)]^T = \boldsymbol{y_0}$ and $f_j^k(0) = 0$ for each $j \in 1, 2, \cdots, N$.

$$\dot{f}_j^1 = \lambda_j f_j^1 \tag{2.68}$$

$$\dot{f}_j^2 = \lambda_j f_j^2 + \sum_{k=1}^{N} \sum_{l=1}^{N} C_{kl}^j f_k^1 f_l^1 \tag{2.69}$$

$$\dot{f}_j^3 = \lambda_j f_j^3 + \sum_{k=1}^{N} \sum_{l=1}^{N} C_{kl}^j (f_k^1 f_l^2 + f_k^2 f_l^1) + \sum_{k=1}^{N} \sum_{l=1}^{N} \sum_{k=1}^{N} D_{pqr}^j f_p^1 f_q^1 f_r^1 \tag{2.70}$$

$$\vdots$$

The solution of (2.68) can be easily found as:

$$f_j^1(t) = y_j^0 e^{\lambda_j t} \tag{2.71}$$

Substituting (2.71) into (2.69) reads:

$$\dot{f}_j^2 = \lambda_j f_j^2 + \sum_{k=1}^{N} \sum_{l=1}^{N} C_{kl}^j y_k^0 y_l^0 e^{(k+l)t} \tag{2.72}$$

By Multi-dimensional Laplace Transform,

$$f_j^2(s_1, s_2) = \sum_{k=1}^{N} \sum_{l=1}^{N} C_{kl}^j \frac{1}{s_1 + s_2 - \lambda_j} f_k^1(s_1) f_l^1(s_2) \tag{2.73}$$

the solution of f_j^2 can be found as:

$$f_j^2 = \sum_{k=1}^{N}\sum_{l=1}^{N}C_{kl}^j f_k^1(0)f_l^1(0)S_{kl}^j(t) \tag{2.74}$$

$$= \sum_{k=1}^{N}\sum_{l=1}^{N}C_{kl}^j y_k^0 y_l^0 S_{kl}^j(t)$$

where,

$$S_{kl}^j(t) = \frac{1}{\lambda_k + \lambda_l - \lambda_j}(e^{(\lambda_k+\lambda_l)t} - e^{\lambda_j t})$$

$$S_{kl}^j(t) = te^{\lambda_j t}, \text{for } (k,l,j) \in R_2$$

and the set R_2 contains all the 2nd order resonances.

As observed from (2.74), the solution of f_j^2 is a polynomial series of $e^{(\lambda_j)t}$, $e^{(\lambda_k+\lambda_l)t}$. Similarly, substituting (2.72) into (2.70), using three-dimensional Laplace transform:

$$f_j^3(s_1,s_2,s_3) = \sum_{k=1}^{N}\sum_{l=1}^{N}C_{kl}^j \frac{1}{s_1+s_2+s_3-\lambda_j}(f_k^2(s_1+s_2)f_l^1(s_3) + f_k^1(s_1)f_l^2(s_2+s_3)) +$$

$$\tag{2.75}$$

$$\sum_{k=1}^{N}\sum_{l=1}^{N}\sum_{r=1}^{N}D_{pqr}^j \frac{1}{s_1+s_2+s_3-\lambda_j}f_p^1(s_1)f_q^1(s_2)f_r^1(s_3)$$

Substituting (2.73) into (2.75), it leads:

$$f_j^3(s_1,s_2,s_3) = \sum_{k=1}^{N}\sum_{l=1}^{N}C_{kl}^j \frac{1}{s_1+s_2+s_3-\lambda_j}\left[\sum_{k=1}^{N}\sum_{l=1}^{N}C_{kl}^j \frac{1}{s_1+s_2-\lambda_j}f_k^1(s_1)f_l^1(s_2)\right]f_l^1(s_3)$$

$$\tag{2.76}$$

$$+ f_k^1(s_1)\left[\sum_{k=1}^{N}\sum_{l=1}^{N}C_{kl}^j \frac{1}{s_1+s_2-\lambda_j}f_k^1(s_2)f_l^1(s_3)\right]$$

$$+ \sum_{k=1}^{N}\sum_{l=1}^{N}\sum_{r=1}^{N}D_{pqr}^j \frac{1}{s_1+s_2+s_3-\lambda_j}f_p^1(s_1)f_q^1(s_2)f_r^1(s_3)$$

As observed from the (2.72) and (2.75), the solution of f_j^3 will be a polynomial series of $e^{\lambda_j t}$, $e^{(\lambda_k+\lambda_l)t}$ and $e^{(\lambda_p+\lambda_q+\lambda_r)t}$.

Continuing the above procedures to order n, the solution of $y_j(t)$ is a polynomial series of $e^{\lambda_j t}$, $e^{(\lambda_k+\lambda_l)t}$ and $e^{\lambda_p+\lambda_q+\lambda_r},\ldots e^{(\lambda_1+\lambda_2+\cdots+\lambda_n)t}$.

As observed from the procedures above, it can be concluded that:

1. The solution is a linear combination of $e^{\lambda_j t}$, $e^{(\lambda_k+\lambda_l)t}$, $e^{(\lambda_p+\lambda_q+\lambda_r)t}$,...; or, equivalently speaking, it is a nonlinear combination of linear modes since the basic component is $e^{(\lambda_i)t}$ with constant eigenvalue. Therefore, the nonlinearities will

not change the decaying speed and oscillatory frequency of the fundamental modes.

2. For each mode j, all the nonlinear terms are taken into account when solving the equations, in the scale of $(C^j)^2$.

3. Closed form results are always available.

2.3.9.2 Advantages and Disadvantages

Therefore, compared to MS method, the MNF is preferred since:

1. the MNF can take the minimum nonlinear terms while the MS method has to keep all the nonlinear terms, since for N-dimensional system, the scalability for 2nd order nonlinear terms is N^3, and for 3rd order modal series N^5 ($N \times \dim(C^j)^2$), this makes the MS method nonapplicable for large-scale system; while MNF is more capable for study of large-scale problem and can be extended to take into account higher-order nonlinear terms;

2. the MNF can predict the system's behaviour without offering closed-form results, therefore, offering the closed form results when resonance occurs is not a privilege of MS method;

3. the Normal Forms makes possible to assess the nonlinear stability, while the MS methods only work on the convergence domain.

Though nonlinear indexes can be proposed without solving the modal series based on C_{kl}^j and D_{kl}^j and etc, they can only quantify the nonlinear modal interaction, and cannot perform the nonlinear stability assessment.

2.4 Nonlinear Indexes Based on the 3rd order Normal Forms of Vector Fields

The objective of NF methods is to quantify modal interaction and to predict the system stability. To evaluate the gain obtained by the 3rd order method over the 2nd order method, normal dynamics (2.51) and (2.52) have to be reconstructed with the z coordinates as:

$$z_j = w_j + \sum_{p=1}^{N}\sum_{q=1}^{N}\sum_{r=1}^{N} h3_{pqr}^j w_p w_q w_r \qquad (2.77)$$

with $|\lambda_j - \lambda_p - \lambda_q - \lambda_r| \gg 0$.

It can be seen from the reconstruction that z_j is separated into two sets; a first set with coefficients $h3_{pqr}^j$ that can be used to quantify the 3rd order modal interactions [32]; a second set is w_j which may be influenced by c_{2l}^j that can be used for stability analysis [5, 16].

Based on the Normal Forms and $h3_{pqr}^j$, c_{2l}^j, nonlinear indexes are proposed to quantify the 3rd order modal interaction and nonlinear stability margin.

2.4.1 3rd Order Modal Interaction Index

As observed from (2.55), the 3rd order oscillation is caused by $h3^j_{pqr}w_p w_q w_r$. Then the third order Modal Interaction index $MI3^j_{pqr}$ can be defined as:

$$MI3^j_{pqr} = \frac{|h3^j_{pqr}w^0_p w^0_q w^0_r|}{|w^0_j|} \tag{2.78}$$

which indicates the participation of 3rd order modal interaction with the frequency $\omega_p + \omega_q + \omega_r$ in the mode j. Introducing $MI3^j_{pqr}$ leads to a more clear picture of how the system components interact with each other, and a more precise identification of the source of the oscillations. Those additional informations are crucial, especially when some fundamental modal interaction, 2nd order modal interactions and 3rd order modal interactions may exhibit the same oscillatory frequency (as indicated in the Chapter 3, the 16 machine 5 area test system), and it is difficult to identify the order of modal interaction from the FFT analysis frequency spectrum, let alone to identify the source of oscillation. NF analysis plays a role more than that of time-domain simulation plus signal processing, in the sense that FFT can only identify the oscillatory frequency of the frequency spectrum, while NF analysis can also identify the source of oscillatory frequency.

2.4.2 Stability Index

Since the stability of oscillatory modes in (2.29) is consistent with (2.51) (2.52), the stability can be assessed without performing the time-domain simulation assessment. For the non-oscillatory modes, $\dot{w}_j = \lambda_j w_j$, the stability is determined by λ_j. And for the oscillatory modes $j \in M$:

$$\dot{w}_j = \lambda_j w_j + \sum_{l=1}^{M} c^j_{2l} w_j w_{2l} w_{2l-1}, \tag{2.79}$$

$$= (\lambda_j + \sum_{l=1}^{M} c^j_{2l} |w_{2l}|^2) w_j$$

$$\tag{2.80}$$

where $|w_{2l}|$ is the magnitude of w_{2l}.
A stability interaction index can be defined as:

$$SII^j_{2l} = c^j_{2l} |w^0_{2l}|^2, j \in M \tag{2.81}$$

Since

$$\lambda_j + \sum_{l=1}^{M} c^j_{2l} |w_{2l}|^2 = \sigma_j + real(\sum_{l=1}^{M} SII^j_{2l}) + j(\omega_j + imag(\sum_{l=1}^{M} SII^j_{2l})) \tag{2.82}$$

the real part of SII will contribute to the stability of the mode and the imaginary part of SII will contribute to the fundamental frequency.

2.4.3 Nonlinear Modal Persistence Index

The nonlinear indexes proposed in the previous sections just indicate the nonlinear interaction at the point when the disturbance is cleared. To quantify the 3rd order modal interaction in the overall dynamics, a persistence index is defined to indicate how long a nonlinear interaction will influence the dominant modes. Similar to (23), (24) in [48], the $Tr3$ is the ratio of the time constants to the combination modes and the dominant mode.

$$Tr3 = \frac{\text{Time constant for combination mode}(\lambda_p + \lambda_q + \lambda_r)}{\text{Time constant for dominant mode}(\lambda_j)} \tag{2.83}$$

A small $Tr3$ indicates a significant presence of the combination mode. For example, if $Tr3 = 1$, it means that the nonlinear interactions decay at the same speed as the dominant mode. if $Tr3$ is very large, it means that the influence of combination mode (p, q, r) decays too quickly compared to the dominant mode. A relatively high value of the product $SII \times Tr3, MI3 \times Tr3$ tends to reveal a condition of persistent modal interaction.

2.4.4 Stability Assessment

As indicated from (2.79), it is both the eigenvalues λ_j and the stability indexes SII_{2l}^j contribute to the system stability. However, λ_j will keep constant during the system dynamics, while SII_{2l}^j will decay as time goes by with time constant of $Tr3_{j(2l-1)(2l)}^j$. If the SII_{2l}^j is large, but $SII_{2l}^j \times Tr_{j(2l)(2l-1)}^j$ is small, the 3rd-order terms may stabilize the system at the beginning, but leaves a long-term instability. This will lead to a wrong stability assessment. Therefore, the time constant of SII_{2l}^j must be taken into account when assessing the overall stability; and an index of stability assessment can be defined as:

$$SI_j = \sigma_j + \sum_{l=1}^{M} Re(SII_{2l}^j) \times Tr_{j(2l-1)(2l)}^j, j \in M \tag{2.84}$$

with σ coming from $\lambda_j = \sigma_j + j\omega_j$. It immediately follows from this definition, that

$$\begin{cases} SI_j > 0, & \text{unstable} \\ SI_j < 0, & \text{stable} \end{cases} \tag{2.85}$$

when $SI_j = 0$ the system may stay in limit cycles, or switch between the stable and the unstable phase. Different cases should be discussed and further investigations should be made.

Inversely, letting $SI_j \geq 0, \forall j \in M$, a set of equation will be formed, with the stability bound $|w_j|, \forall j \in M$ as the variables, solving this set of equation, the stability bound

can be obtained.

Compared to [5], this proposed method is more accurate as: 1) it takes into account the time pertinence; 2) it is appropriate to case where $\sigma_j = 0$.

2.5 Derivations of Normal Forms of Nonlinear Normal Modes for System of Second-Order Differential Equations

In the previous section, derivation of normal forms for first-order equations has been performed. A drawback of this method is that the state variables may have complex form values in the normal form coordinates and lose the physical meanings. For example, the displacement x is naturally a real form number, however, by the normal form transformations, it may be in complex form, fails to direct correspond to physical phenoma.

In this section, derivation of normal forms for second-order equations will be performed. The normal forms for second-order equations have been found in nonlinear structure analysis [17–19], and will be applied to transient analysis of power system in Chapter 4.

This approach is mainly used to deduce the nonlinear normal modes in the mechanical engineering, and it can be referred to as Normal Mode approach. Or, it can also be referred to as normal mode approach, since in the normal transformations, the state-variables always have real form values.

2.5.1 Class of Second-Order Equations that can be studied by Methods of Normal Forms

The nonlinear electromechanical oscillations in interconnected power system can be modeled as second-order coupled oscillators. If the variables of the power system, around a given equilibrium point, are gathers in a N dimensional vector $\boldsymbol{q}$, the basic model under study writes:

$$\boldsymbol{M}\ddot{\boldsymbol{q}} + \boldsymbol{D}\dot{\boldsymbol{q}} + \boldsymbol{K}\boldsymbol{q} + \boldsymbol{f}_{nl}(\boldsymbol{q}) = 0 \tag{2.86}$$

In the above equation, $\boldsymbol{M}$ and $\boldsymbol{D}$ are constant symmetric inertia and damping matrix, whose values depend on the physical parameters of the power system and controller parameters. $\boldsymbol{K}$ and $\boldsymbol{f}_{nl}$ indicate the coupling between the variables, where $\boldsymbol{K}$ is a constant matrix, including the linear terms and $\boldsymbol{f}_{nl}$ gathers the nonlinear terms.

If $\boldsymbol{f}_{nl}$ is developed in a Taylor series up to the third order, it comes:

$$f_{nl}^p(q) = \sum_{i=1,j\geq i}^{N} f2_{ij}^p q_i q_j + \sum_{i=1,j\geq i,k\geq j}^{N} f3_{ijk}^p q_i q_j q_k \tag{2.87}$$

where f_{ij}^p and f_{ijk}^p $(i, j, k, p = 1 \ldots N)$ are coefficients of the quadratic and cubic terms. Components of $\boldsymbol{K}$ and $\boldsymbol{f}_{nl}$ depend on the chosen equilibrium point and the system structure, for example, the network connectivity of the power grids.

It is seen that (2.86) is a N-dimensional nonlinear dynamical problem.

2.5.2 Linear Transformation

Viewed from (2.86), the dynamics physical property (oscillatory frequency, damping, friction, etc) is obscured by the mathematical model.

In order to decouple the equation into second-order oscillators, a linear transformation $\triangle \boldsymbol{q}(t) = \boldsymbol{\Phi} \boldsymbol{x}(t)$ can be used. To obtain $\boldsymbol{\Phi}$ is to solve the following eigen-value problem.

$$\left(\boldsymbol{K_S} - \Omega^2 \boldsymbol{M} \right) \boldsymbol{\Phi} = 0 \tag{2.88}$$

where Ω^2 is a diagonal matrix collecting the natural frequency of the oscillators.

After decoupling the linear terms, the system dynamics is therefore characterized by a group of oscillators with coupled nonlinearities.

$$\ddot{X}_p + 2\xi_p \omega_p \dot{X}_p + \omega_p^2 X_p \tag{2.89}$$

$$+ \sum_{i=1}^N \sum_{j \geq i}^N g_{ij}^p X_i X_j + \sum_{i=1}^N \sum_{j \geq i}^N \sum_{k \geq j}^N h_{ijk}^p X_i X_j X_k = 0$$

where ξ_p is the p-th modal damping ratio. And g_{ij}^p and h_{ijk}^p are quadratic and cubic nonlinearities coming from decoupling of K_S, which are given as:

$$[g^p] = \sum_{i=1}^N \frac{\Phi_{pi}^{-1}(\Phi^T K_{2S}^p \Phi)}{\Phi_i^{-1} M_i \Phi} [\Phi^{-1} M \Phi]_{pp} \tag{2.90}$$

$$h_{ijk}^p = \sum_{i=1}^N \Phi_{pi}^{-1} (\sum_{P=1}^N \sum_{Q=1}^N \sum_{R=1}^N K_{3Sijk}^p \Phi_{iP} \Phi_{jQ} \Phi_{kR}) / [\Phi^{-1} M \Phi]_{pp} \tag{2.91}$$

Φ_{pi} is the element of p-th row and i-th column of matrix Φ.

2.5.3 Normal Modes and Nonlinear Normal Modes

Neglecting all the nonlinearities, the (2.89) reads a Linear Normal Mode (LNM):

$$\ddot{X}_p + 2\xi_p \omega_p \dot{X}_p + \omega_p^2 X_p = 0 \tag{2.92}$$

The physical meaning and physical properties of normal mode :
- The basic particular solution of the motion of oscillations of system, and the system dynamics is a combination of normal modes.
- The free motion described by the linear normal modes takes place at the fixed frequencies. These fixed frequencies of the normal modes of a system are

known as its natural frequencies;

- All the normal modes are orthogonal to each other, i.e, when the motion is initialized at one normal mode, its motion will always contains in that mode.

The most general motion of a linear system is a superposition of its normal modes. The modes are normal in the sense that they can move independently, that is to say that an excitation of one mode will never cause motion of a different mode. In mathematical terms, normal modes are orthogonal to each other. By normal modes, the complex system dynamics are decomposed into normal modes with fixed frequency.

However, in oscillations with large amplitudes, the system dynamics are predominantly nonlinear where the theorem of supposition of normal modes fails and the nonlinear property of system dynamics cannot be extracted from the normal modes. In order to extend the physical insights of normal modes to nonlinear domain, the concept of "nonlinear normal modes" are proposed [61, 62]. Rosenberg [61] firstly define "nonlinear normal modes" as specific periodic solutions in which the modal coordinates exhibit particular features. Using center manifold theory, Shaw and Pierre [62] define a NNM as an invariant manifold in phase space, tangent at the origin to their linear counterpart. This definition is used in this PhD thesis. The derivation of nonlinear normal modes by normal form theory are based the works [17–19], which have been technically verified within the mechanical context for an assembly of nonlinear oscillators thanks to a real formulation of the normal form.

2.5.4 Second-Order Normal Form Transformation

Taking into account of the quadratic nonlinearities of (2.89), it reads:

$$\ddot{X}_p + 2\xi_p\omega_p\dot{X}_p + \omega_p^2 X_p + \sum_{i=1}^{N}\sum_{j\geq i}^{N} g_{ij}^{p} X_i X_j = 0 \tag{2.93}$$

which can be rewritten as:

$$\dot{X}_p = Y_p \tag{2.94}$$

$$\dot{Y}_p = -2\xi_p\omega X_p - \omega^2 X_p - \sum_{i=1}^{N}\sum_{j\geq i}^{N} g_{ij}^{p} X_i X_j \tag{2.95}$$

(the mention: $\forall p = 1 \cdots N$ will be omitted when not confusing).
The first step consists of defining a second-order polynom with $2N$ variables (N pairs displacement-velocity). It is chosen tangent to the identity, and is written:

$$\begin{cases} X & = U + \epsilon(\boldsymbol{a(U^2)} + \boldsymbol{b(V^2)} + \boldsymbol{c(U,V)}) \\ \\ Y & = V + \epsilon(\boldsymbol{\alpha(U^2)} + \boldsymbol{\beta(V^2)} + \boldsymbol{\gamma(U,V)}) \end{cases} \tag{2.96}$$

where ϵ is a small nondimensional parameter, which is just a bookkeeping device to equal the terms in the same degree in the normal form transformation. For example, polynomial terms with ϵ are in the same polynomial degree, and polynomial terms with ϵ^2 indicate a higher polynomial degree.

$\forall p = 1 \ldots N, Y_p = \dot{X}_p$,then

$$X_p = U_p + \sum_{i=1}^{N} \sum_{j \geq i}^{N} (a_{ij}^p U_i U_j + b_{ij}^p V_i V_j) + \sum_{i=1}^{N} \sum_{j=1}^{N} c_{ij} U_i V_j$$

$$Y_p = V_p + \sum_{i=1}^{N} \sum_{j \geq i}^{N} (\alpha_{ij}^p U_i U_j + \beta_{ij}^p V_i V_j) + \sum_{i=1}^{N} \sum_{j=1}^{N} \gamma_{ij} U_i V_j \qquad (2.97)$$

(U_p, V_p) are the new variables. The polynoms (2.97) are written in this form to take commuting and non-commuting terms into account.

The unknown of the problem are now the $2N^2(2N + 1)$ coefficients $\left\{ a_{ij}^p, b_{ij}^p, c_{ij}^p, \alpha_{ij}^p, \beta_{ij}^p, \gamma_{ij}^p \right\}$. They are determined by introducing (2.97) to (2.93). This generates terms of the form $\dot{U}_i U_j, \dot{V}_i V_j, \dot{U}_i V_j$, which can be remedied by observing that, at lower order:

$$\dot{U}_j = V_j + O(U_i^2, V_i^2) \qquad (2.98)$$

$$\dot{V}_j = -\omega_j^2 U_j + O(U_i^2, V_i^2) \qquad (2.99)$$

It therefore renders:

$$D(a_{ij}^p U_i U_j) = a_{ij}^p U_i \dot{U}_j + a_{ij}^p \dot{U}_i U_j = (a_{ij}^p + a_{ji}^p) U_i V_j + \mathcal{O}(U_i^3, V_i^3) \quad (2.100)$$

$$D(b_{ij}^p V_i V_j) = b_{ij}^p V_i \dot{V}_j + b_{ij}^p \dot{V}_i V_j = -\omega_j^2 (b_{ij}^p + b_{ji}^p) U_i V_j$$

$$D(c_{ij}^p U_i V_j) = c_{ij}^p U_i \dot{V}_j + c_{ij}^p \dot{U}_i V_j = -\omega_j^2 c_{ij}^p U_i U_j + c_{ij}^p V_i V_j$$

$$D(\alpha_{ij}^p U_i U_j) = \alpha_{ij}^p U_i \dot{U}_j + \alpha_{ij}^p \dot{U}_i U_j = (\alpha_{ij}^p + \alpha_{ji}^p) U_i V_j + V_i U_j + \mathcal{O}(U_i^3, V_i^3)$$

$$D(\beta_{ij}^p V_i V_j) = \beta_{ij}^p V_i \dot{V}_j + \beta_{ij}^p \dot{V}_i V_j = -\omega_j^2 (\beta_{ij}^p + \beta_{ji}^p) U_i V_j$$

$$D(\gamma_{ij}^p U_i V_j) = \gamma_{ij}^p U_i \dot{V}_j + \gamma_{ij}^p \dot{U}_i V_j = \gamma_{ij}^p U_i(-\omega_j^2 U_j) + \gamma_{ij}^p V_i V_j$$

They are cumbersome for the identification of the different monomials, because involving the derivative of a variable against time. This is remedied by observing that, at lower order:

Letting $V_p = \dot{U}_p$,Equating the 2nd order terms, there is:

$$D(\boldsymbol{a} + \boldsymbol{b} + \boldsymbol{c}) = \boldsymbol{\alpha} + \boldsymbol{\beta} + \boldsymbol{\gamma} \qquad (2.101)$$

$$D(\boldsymbol{\alpha} + \boldsymbol{\beta} + \boldsymbol{\gamma}) + 2\xi\omega D(\boldsymbol{a} + \boldsymbol{b} + \boldsymbol{c}) \qquad (2.102)$$

$$= -\omega^2(\boldsymbol{a} + \boldsymbol{b} + \boldsymbol{c}) - \boldsymbol{g}(\boldsymbol{U}^2)$$

To degree ϵ^1:

$$\begin{cases} D\boldsymbol{a}(\boldsymbol{U^2}) - \omega^2 D\boldsymbol{b}(\boldsymbol{V^2}) & = \boldsymbol{\gamma} & (UV) \\[2mm] D\boldsymbol{c}(\boldsymbol{UV})_{\boldsymbol{V}} & = \boldsymbol{\alpha} & (U^2) \\[2mm] D\boldsymbol{c}(\boldsymbol{UV})_{\boldsymbol{U}} & = \boldsymbol{\beta} & (V^2) \end{cases} \tag{2.103}$$

$$\begin{cases} D\boldsymbol{\alpha}(\boldsymbol{U^2}) - \omega^2 D\boldsymbol{\beta}(\boldsymbol{V^2}) & = -2\xi\omega D\boldsymbol{a}(\boldsymbol{U^2}) + 2\xi\omega^3 D\boldsymbol{b}(\boldsymbol{V^2}) - \omega^2 \boldsymbol{c}(\boldsymbol{UV}) & (UV) \\[2mm] -\omega^2 D\boldsymbol{\gamma}(\boldsymbol{UV})_{\boldsymbol{V}} & = 2\xi\omega^3 D\boldsymbol{c}(\boldsymbol{UV})_{\boldsymbol{V}} - \omega^2 \boldsymbol{a}(\boldsymbol{U^2}) - \boldsymbol{g}(\boldsymbol{U^2}) & (U^2) \\[2mm] D\boldsymbol{\gamma}(\boldsymbol{UV})_{\boldsymbol{U}} & = -\omega^2 \boldsymbol{b}(\boldsymbol{V^2}) - 2\xi\omega \boldsymbol{c}(\boldsymbol{UV})_{\boldsymbol{U}} & (V^2) \end{cases}$$
$$\tag{2.104}$$

where $D\boldsymbol{c}(\boldsymbol{UV})_{\boldsymbol{V}}$ indicates $\frac{\partial \boldsymbol{c}(\boldsymbol{UV})}{\partial V}$ There are six equations with six variables, solving (2.103)(2.104), $\left\{ a_{ij}^p, b_{ij}^p, c_{ij}^p, \alpha_{ij}^p, \beta_{ij}^p, \gamma_{ij}^p \right\}$ can be solved. The coefficients are listed in the Appendix for case where no resonance occurs. When there occurs internal resonance occurs, i.e $\omega_k + \omega_l \neq \omega_j$, the corresponding second-order terms will be kept in the normal forms, and corresponding coefficients will be zero.

If all the 2nd-order terms can be cancelled, then the Normal Forms is:

$$\ddot{U}_p + 2\xi_p\omega_p\dot{U}_p + \omega_p^2 U_p + \mathcal{O}(3) = 0 \tag{2.105}$$

with

$$\mathcal{O} = \sum_{i=1}^{N}\sum_{j\geq1}^{N}\sum_{k\geq j}^{N}(H_{ijk}^p + A_{ijk}^p)U_iU_jU_k \tag{2.106}$$

$$+ \sum_{i=1}^{N}\sum_{j\geq i}^{N}\sum_{k\geq j}^{N} B_{ijk}^p U_i\dot{U}_j\dot{U}_k + \sum_{i=1}^{N}\sum_{j\geq i}^{N}\sum_{k\geq j}^{N} C_{ijk}^p \dot{U}_iU_jU_k$$

A_{ijk}^p, B_{ijk}^p, C_{ijk}^p are coefficients of terms $DG(U)a(U)$, $DG(U)b(U,V)$ and $DG(U)c(V)$, arising from the cancellation of 2nd order terms.

$$A_{ijk}^p = \sum_{l\geq i}^{N} g_{il}^p a_{jk}^l + \sum_{l\leq i} g_{li}^p a_{jk}^l \tag{2.107}$$

$$B_{ijk}^p = \sum_{l\geq i}^{N} g_{il}^p b_{jk}^l + \sum_{l\leq i} g_{li}^p b_{jk}^l \tag{2.108}$$

$$C_{ijk}^p = \sum_{l\geq i}^{N} g_{il}^p c_{jk}^l + \sum_{l\leq i} g_{li}^p c_{jk}^l \tag{2.109}$$

Therefore, by cancelling the quadratic nonlinearities and neglecting all the cubic nonlinearities, the normal dynamics is obtained in the 2nd order normal mode (2.105) is labelled as NM2.

2.5.5   Third-order Normal Form Transformation

However, when the disturbance is predominantly nonlinear, a second approximation is not sufficient, $\mathcal{O}(3)$ can contain terms that contribute to the nonlinear stability of the system dynamics. In Refs [17, 18, 21, 22] a 3rd order NF transformation is proposed, by which the state-variables are transformed into Nonlinear Normal Modes represented as RS.

$$\begin{cases} U & = R + \epsilon^2(\boldsymbol{r}(\boldsymbol{R^3}) + \boldsymbol{s}(\boldsymbol{S^3}) + \boldsymbol{t}(\boldsymbol{R^2}, \boldsymbol{S}) + \boldsymbol{u}(\boldsymbol{R}, \boldsymbol{S^2})) \\[2mm] V & = S + \epsilon^2(\boldsymbol{\lambda}(\boldsymbol{R^3}) + \boldsymbol{\mu}(\boldsymbol{S^3}) + \boldsymbol{\nu}(\boldsymbol{R^2}, \boldsymbol{S}) + \boldsymbol{\zeta}(\boldsymbol{R}, \boldsymbol{S^2})) \end{cases} \tag{2.110}$$

Equating the terms at different degrees by assuming $\dot{\boldsymbol{R}} = \boldsymbol{S}, \dot{\boldsymbol{S}} = -2\xi\omega\dot{\boldsymbol{R}} - \omega^2\boldsymbol{R} + \mathcal{O}(2)$, the expressions for the coefficients can be obtained.

To cancel the 3rd order terms, there is:

$$D(\boldsymbol{r} + \boldsymbol{s} + \boldsymbol{t} + \boldsymbol{u}) = \boldsymbol{\lambda} + \boldsymbol{\mu} + \boldsymbol{\nu} + \boldsymbol{\zeta} \tag{2.111}$$

$$D(\boldsymbol{\lambda} + \boldsymbol{\mu} + \boldsymbol{\nu} + \boldsymbol{\zeta}) + 2\xi\omega D(\boldsymbol{r} + \boldsymbol{s} + \boldsymbol{t} + \boldsymbol{u}) \tag{2.112}$$
$$= -\omega^2(\boldsymbol{r} + \boldsymbol{s} + \boldsymbol{t} + \boldsymbol{u}) + D\boldsymbol{g}(\boldsymbol{R^2})(\boldsymbol{a} + \boldsymbol{b} + \boldsymbol{c}) - \boldsymbol{h}(\boldsymbol{R^3})$$

To degree ϵ^2:

$$\begin{cases} D\boldsymbol{r_R} - \omega^2 D\boldsymbol{u_s} & = \boldsymbol{\nu} \qquad (R^2, S) \\[2mm] -\omega^2 D\boldsymbol{s_S} + 2D\boldsymbol{t_R} & = \boldsymbol{\zeta} \qquad (R, S^2) \\[2mm] -\omega^2 D\boldsymbol{t_S} & = \boldsymbol{\lambda} \qquad (R^3) \\[2mm] D\boldsymbol{u_R} & = \mu \qquad (S^3) \end{cases} \tag{2.113}$$

$$\begin{cases} D\boldsymbol{\lambda_R} - \omega^2 D\boldsymbol{\zeta_S} & = -2\xi\omega(D\boldsymbol{r_R} - \omega^2 D\boldsymbol{u_S} - \omega^2\boldsymbol{t} + D\boldsymbol{g}(\boldsymbol{R^2})\boldsymbol{c} \qquad (R^2, S) \\[2mm] -\omega^2 D\boldsymbol{\mu_S} + D\boldsymbol{v_R} & = -2\xi\omega(-\omega^2 D\boldsymbol{s_S} + D\boldsymbol{t_R}) - \omega^2\boldsymbol{u} + D\boldsymbol{g}(\boldsymbol{R^2})\boldsymbol{b} \qquad (R, S^2) \\[2mm] -\omega^2 D\boldsymbol{\nu_S} & = -2\xi\omega(-\omega^2 D\boldsymbol{t_S}) - \omega^2\boldsymbol{r} + D\boldsymbol{g}(\boldsymbol{R^2})\boldsymbol{a} - h(R)^3 \qquad (R^3) \\[2mm] D\boldsymbol{\zeta_R} & = -2\xi\omega(-\omega^2 D\boldsymbol{u_R}) - \omega^2\boldsymbol{s} \qquad (S^3) \end{cases}$$
$$\tag{2.114}$$

There are 8 coefficients described by 8 different equations, and the coefficients can be solved by symbolic programming with the coefficients of trivially resonant terms set as zero:

$$\forall p = 1 \cdots N :$$

$$r^p_{ppp} = s^p_{ppp} = t^p_{ppp} = u^p_{ppp} = 0$$

$$\lambda^p_{ppp} = \mu^p_{ppp} = \nu^p_{ppp} = \zeta^p_{ppp} = 0$$

$$\forall j \geq p \cdots N :$$

$$r^p_{pjj} = s^p_{pjj} = t^p_{jpj} = t^p_{pjj} = u^p_{pjj} = u^p_{jpj} = 0 \qquad (2.115)$$

$$\lambda^p_{pjj} = \mu^p_{pjj} = v^p_{pjj} = v^p_{jpj} = \zeta^p_{pjj} = \zeta^p_{jpj} = 0$$

$$\forall i \leq p :$$

$$r^p_{iip} = s^p_{iip} = t^p_{iip} = t^p_{pii} = u^p_{iip} = u^p_{pii} = 0$$

$$\lambda^p_{iip} = \mu^p_{iip} = v^p_{iip} = v^p_{pii} = \zeta^p_{iip} = \zeta^p_{pii} = 0$$

The detailed calculation of the coefficients and their values can be found in [18, 19] and are listed in Appendix.

2.5.6 Eliminating the Maximum Nonlinear Terms

To eliminate the maximum nonlinear terms, the issue is to identify the resonant terms.

2.5.6.1 Internal Resonance

Like the approach for systems of first order equations, all the terms can be eliminated when there is no *internal resonances* between the eigenfrequencies of the system. For example, order-two internal resonances reads, for arbitrary (p, i, j):

$$\omega_p = \omega_i + \omega_j, \omega_p = 2\omega_i \qquad (2.116)$$

while third-order (linked to cubic nonlinear coupling terms) writes, (p, i, j, k)

$$\omega_p = \omega_i + \omega_j \pm \omega_k, \omega_p = 2\omega_i \pm \omega_j, \omega_p = 3\omega_i \qquad (2.117)$$

There are also two characteristics of *internal resonant terms*: 1)dependent of the oscillatory frequency;2)can be brought by either the quadratic terms or cubic terms or both.

2.5.6.2 Trivial Resonance Introduced by Conjugate Pairs

Indeed, if only one oscillator equation is considered, the one can always fulfill the following relationship between the two complex conjugate eigenvalues $+i\omega, -i\omega$.

$$+i\omega = +i\omega + i\omega - i\omega \tag{2.118}$$

i.e a relationship of the form (2.89) with order $p = 3$. Coming back to the oscillator equation, this means that the Duffing equation:

$$\ddot{X} + \omega^2 X + \alpha X^3 = 0 \tag{2.119}$$

is under its normal form, the cubic terms (monom associated with the resonance relation (2.118)) cannot be canceled through a nonlinear transform. On a physical viewpoint, this stands as a good news. Indeed one of the most important observed feature in nonlinear oscillations is the frequency dependence upon oscillation amplitude. If the system could be linearized, this would mean that the underlying dynamics is linear, hence the frequency should not change with the amplitude. And this will violate the well-established common-sense in mechanical dynamics that the solution of (2.119) is $X(t) = a\cos(\omega_{NL}t + \phi) + \mathcal{O}(a^2)$

Neglecting the trivially resonant terms, the proposed Normal Transform renders the equations too simple to contain the basic characteristics of nonlinear dynamics, it is useless.

In fact, the normal dynamics contain the *trivially* resonant terms which exist whatever the values of the frequencies of the studied structures are.

In the general case, where N oscillator-equations are considered, numerous resonance relationships of the form

$$+i\omega_p = +i\omega_p + i\omega_k - i\omega_k \tag{2.120}$$

are possible, for arbitrary $p, k \in [1, N]^2$. This means that the original system can be simplified, but numerous terms will remain at the end of the process, in the normal form, following Poincarè-Dulac theorem. However, as it will be shown next, this effort is worthy as numerous important terms will be canceled and also because the remaining terms can be easily interpreted.

The resonance relationships put forward through the (2.118), (2.119), (2.120) are denoted as *trivial* and there are two characteristics: 1) independent of the values of the frequencies of the studied oscillations; 2) only for the cubic terms.

2.5.6.3 Damping and Resonance

The *internal resonance* is firstly defined for conservative oscillation, i.e $\forall p = 1, 2, \cdots N, \xi_p = 0$. However, they can be extended to case with viscous damping as the oscillatory frequency writes [18, 19]

$$\lambda_p^{\pm} = -\xi_p\omega_p \pm i\omega_p\sqrt{1 - \xi_p^2} \tag{2.121}$$

Besides the real part of (2.121) which controls the decay rate of energy along the pth linear eigenspace, the imaginary part shows that the damping also have an effect on the oscillation frequency. However, in the oscillatory case we study, the damping ratio ξ_p is always very small compared to ω_p, so that the assumption of a lightly damped system could be considered. In that case, a first-order development of (2.121) shows that:

$$\lambda_p^{\pm} = \pm i\omega_p - \xi_p\omega_p + \mathcal{O}(\xi_p^2) \tag{2.122}$$

Therefore, the definition of internal resonance and trivial resonance relationship can be extended to damped oscillators.

2.5.7 Invariance Property

Like the case of system of first-order equations, all the higher-order terms are neglected in the previous researches [30] when no internal resonance occurs. And the normal dynamics are depicted by linear differential equations. However, the nonlinear terms contain qualitative effect of the original nonlinear dynamics, such as the amplitude-dependent frequency shift, which cannot be represented by the linear equations. In fact, there exists resonant terms that cannot be neglected in normal normals and an complete linearization is impossible.

In fact, the normal dynamics contain the *trivially* resonant terms which exist whatever the values of the frequencies of the studied structures are. By keeping the trivially resonant terms, the invariance property is conserved.

If no internal resonances are present in the eigen spectrum, this nonlinear transformation weakens the couplings by shifting all the nonlinearities to the cubic terms, The new dynamical system writes, for all $p = 1, \ldots N$:

$$\ddot{R}_p + 2\xi_p\omega_p\dot{R}_p + \omega_p^2 R_p \tag{2.123}$$
$$+ (h_{ppp}^p + A_{ppp}^p)R_p^3 + B_{ppp}^p R_p\dot{R}_p^2 + C_{ppp}^p R_p^2\dot{R}_p$$
$$+ R_p\mathcal{P}^{(2)}(R_i, \dot{R}_j) + \dot{R}_p\mathcal{Q}^{(2)}(R_i, \dot{R}_j) = 0$$

where $\mathcal{P}^{(2)}$ and $\mathcal{Q}^{(2)}$ are second order polynomials in R_j and $\dot{R}_j$, $j \neq p$, $j \neq p$ and write:

$$\mathcal{P}^{(2)} = \sum_{j \geq p}^{N} \left[(h_{pjj}^p + A_{pjj}^p + A_{jpj}^p)R_j^2 + B_{pjj}^p\dot{R}_j^2 + (C_{pjj}^p + C_{jpj}^p)R_j\dot{R}_j \right] \tag{2.124}$$

$$+ \sum_{i \leq p} \left[(h_{iip}^p + A_{iip}^p + A_{pii}^p)R_i^2 + B_{pii}^p\dot{R}_i^2 + (C_{pii}^p + C_{ipi}^p)R_i\dot{R}_i \right]$$

$$\mathcal{Q}^{(2)} = \sum_{j \geq p}^{N}(B_{jpj}^p R_j\dot{R}_j + C_{jjp}^p R_j^2) + \sum_{i \leq p}^{N}(B_{iip}^p R_i\dot{R}_i + C_{iip}^p R_i^2) \tag{2.125}$$

and the coefficients $(A_{ijk}^p, B_{ijk}^p, C_{ijk}^p)$ arise from the cancellation of the quadratic

terms [17, 18] and are defined in (2.109). This model can be called as full NNM (FNNM).

Compared to (2.89), all the oscillators are *invariants* in the new dynamical FNNM system (2.123).

Observed from (2.123), all the nonlinear terms can be classified into two types: cross-coupling nonlinearities (terms with $\mathcal{P}^{(2)}$ and $\mathcal{Q}^{(2)}$) and self-coupling nonlinearities (the other nonlinear terms with coefficients: $h_{ppp}^p + A_{ppp}^p, B_{ppp}^p, C_{ppp}^p$).

If the dynamics is initiated on a given mode (say the p-th., $X_j = \dot{x}_j = 0, \forall j \neq p$ at $t = 0$), the system dynamics will only be influenced by this given mode, the system oscillates as an *invariant* second-order oscillator . Equivalently speaking, in this case, $\mathcal{P}^{(2)}$ and $\mathcal{Q}^{(2)}$ are null, leading to the property of invariance.

For the cases where several modes have non zero initial conditions, cross-coupling nonlinearities are not zero. However, their effect on the dynamics can be weak compared to the any self-coupling nonlinearities. Thus a series of decoupled subsystem is obtained, which can be generally expressed as:

$$\ddot{R}_p + 2\xi_p\omega_p\dot{R}_p + \omega_p^2 R_p \tag{2.126}$$
$$+ (h_{ppp}^p + A_{ppp}^p)R_p^3 + B_{ppp}^p R_p \dot{R}_p^2 + C_{ppp}^p R_p^2 \dot{R}_p = 0$$

Model ((2.126)) is labelled as NNM, and can be viewed as a type of nonlinear normal mode, as all the modes are decoupled and nonlinear . The solution of each mode can be approximated by an analytical perturbation method.

2.5.8   One-Step Transformation of Coordinates from XY to RS

As indicated in Section 2.2, sequential transformations render the same results as one-step transformation, therefore, once the coefficients are calculated the normal forms in RS coordinates can be obtained by:

$$X_p = R_p + \sum_{i=1}^{N}\sum_{j\geq i}^{N}(a_{ij}^p R_i R_j + b_{ij}^p R_i R_j) + \sum_{i=1}^{N}\sum_{j=1}^{N}c_{ij}R_i S_j$$
$$+ \sum_{i=1}^{N}\sum_{j\geq i}^{N}\sum_{k\geq j}^{N}(r_{ijk}^p R_i R_j R_k + s_{ijk}^N S_i S_j S_k)$$
$$+ \sum_{i=1}^{N}\sum_{j\geq i}^{N}\sum_{k\geq j}^{N}(t_{ijk}^p S_i R_j R_k + u_{ijk}^p S_i S_j R_k)$$

$$Y_p = S_p + \sum_{i=1}^{N}\sum_{j\geq i}^{N}(\alpha_{ij}^{p}R_iR_j + \beta_{ij}^{p}S_iS_j) + \sum_{i=1}^{2}\sum_{j=1}^{2}\gamma_{ij}R_iS_j$$

$$+ \sum_{i=1}^{N}\sum_{j\geq i}^{N}\sum_{k\geq j}^{N}(\lambda_{ijk}^{p}R_iR_jR_k + \mu_{ijk}^{p}S_iS_jS_k)$$

$$+ \sum_{i=1}^{N}\sum_{j\geq i}^{N}\sum_{k\geq j}^{N}(\nu_{ijk}^{p}S_iR_jR_k + \zeta_{ijk}^{p}S_iS_jR_k) \tag{2.127}$$

2.5.9 Comparison with Shaw-Pierre Method where Nonlinear Normal Modes are Formed

Another method to form nonlinear normal mode is the Shaw-Pierre method, firstly proposed by Shaw & Pierre [39] and applied in both structural analysis in mechanical engineering [39] and power system analysis in electrical engineering [40].

This method originates from the master-slave coordinates transformation of the Center Manifold method. However, it only works for slave-coordinates where $Re(\lambda_s) < 0$ i.e the linearized system must be stable.

Its principle is to reduce the N-dimensional nonlinear system with N variables $\boldsymbol{x}$ into N_c dimensional systems with N_c variables $\boldsymbol{x_c}$. And the other N_s variables $\boldsymbol{x_s}$ expressed as static functions of $\boldsymbol{x_s} = f(\boldsymbol{x_c}), N_s + N_c = N$. With the SP method, some dynamics of $\boldsymbol{x_s}$ are lost.

To illustrate such a point, a simple example of a 2-dimensional nonlinear system is presented [63]:

$$\begin{pmatrix} \dot{x} \\ \dot{y} \end{pmatrix} = \begin{bmatrix} \mu & 0 \\ 0 & -1 \end{bmatrix} \begin{pmatrix} x \\ y \end{pmatrix} + \begin{pmatrix} xy + cx^3 \\ bx^2 \end{pmatrix} \tag{2.128}$$

where the μ is a parameter dependent of the point at which the system dynamics would be studied the "critical point". For example, in power system dynamics, μ depends on "operating point".

If the critical point, critical state variable and stable coordinates are as:

$$\mu_c = 0, \quad \boldsymbol{x_c} = \boldsymbol{x}, \quad \boldsymbol{x_s} = \boldsymbol{y} \tag{2.129}$$

The equation of center manifold is $y = h(x, \mu)$, substituting it into $\dot{y} = -y + bx^2$ and equating like power terms, it leads to:

$$y = bx^2 + (|x, \mu|^3) \tag{2.130}$$

and (2.128) can be reduced into the bifurcation equation:

$$\dot{x} = \mu x + (b+c)x^3 \tag{2.131}$$

As observed from (2.131), the system dynamic is dominated by state-variable x, and the dynamics of y is under the slave of x. Therefore, the coordinates of x is also referred to as master coordinates, and y is also referred to as slave coordinates. As observed in (2.131), the dynamics of y totally depend on the x. y is the passive state-variables and x the active state-variables. (2.131) fails to study the case when

y is excited, or matrix $\begin{bmatrix} \mu & 0 \\ 0 & -1 \end{bmatrix}$ has positive eigenvalues.

Center manifold theorem has been successfully applied to bifurcation analysis [49] where only a few of critical state-variables are concerned in the mechanical systems [39]. However, in power system dynamic analysis, it is difficult to decide which one is the critical state-variable, as all state-variables can be excited simultaneously in some scenario, and positive eigenvalue may exist even when the system is stable [5, 16]. Therefore, the SP method which originates from center-manifold method is not applicable for a lot of cases. In [40], nonlinear normal modes are formed to study the inter-area oscillations in power system when only one inter-area mode is excited, however, in interconnected power systems, several inter-area modes can be excited simultaneously even when only one system component is disturbed [64]. In those cases, the center-manifold method is not that efficient.

2.5.10 Possible Extension of the Normal Mode Approach

Compared to (2.29) from a mathematical view, some generalities are lost in (2.86), for example, nonlinear couplings such as $Y_i X_j$ and $Y_i Y_j$ are not considered. However, the similar normal form transformations can be applied to deduce the normal forms.

2.5.11 A Summary of the Existing and Proposed MNFs Based on Normal Mode Approaches

The reviewed and proposed normal-mode-based MNFs are summarized in Tab. 2.4, which are assessed on an example of interconnected VSCs in Section 2.7.

2.6 Nonlinear Indexes Based on Nonlinear Normal Modes

From the normal forms, several nonlinear properties can be extracted, such as the amplitude-dependent frequency-shift [21, 22] and the stability assessment.

Table 2.4: A Summary of the Presented Normal-Mode-Based MNFs

Method	Transformation	Decoupled/Invariant	Normal Dynamics	Related Equation
LNM [55]	linear	decoupled	linear	(2.92)
NM2 [48]	order 2	decoupled	linear	(2.105)
FNNM [18]	order 3	invariant	order 3	(2.123)
NNM ([21, 22]	order 3	decoupled	order 3	(2.126)

2.6.1 Amplitude Dependent Frequency-Shift of the Oscillatory Modes

$$R_p(t) = C_p e^{-\sigma_p t} \cos(\omega_p^{\mathrm{nl}} t + \varphi) = a \cos(\omega_p^{\mathrm{nl}} t + \varphi) \tag{2.132}$$

Where, the parameter C_p represents the amplitudes of the nonlinear oscillations respectively, which is a function of the initial conditions R_p^0, S_p^0 [18]. And R_p^0, S_p^0 satisfies $X_p^0 = R_p^0 + \mathcal{R}^{(3)}(R_i^0, S_i^0), Y_p^0 = S_p^0 + \mathcal{S}^{(3)}(R_i^0, S_i^0)$.
ω_p^{nl} is the damped natural frequency of the oscillation. Compared to the previous research [40], it is not a constant value but amplitude-dependent, which reads,

$$\omega_p^{\mathrm{nl}} = \omega_p \left(1 + \frac{3(A_{ppp}^p + h_{ppp}^p) + \omega_p^2 B_{ppp}^p}{8\omega_p^2} a^2 \right) \tag{2.133}$$

The frequency-shift is an important property of the nonlinear dynamical system. (2.132) (2.133) indicate how the nonlinear interactions between the state variables brought by nonlinear couplings influence both the amplitude and frequency of the R_p. Unlike the previous researches, where all the coupling terms are canceled after normal from transformation, the NNM approach concentrates nonlinearities into the self-coupling terms while weakens the cross-coupling terms. This simplifies the system while reserving the nonlinear essence to the maximum.

2.6.2 Stability Bound

On the stability bound, the amplitude of R_p reaches the maximum, and $\dot{R}_p = 0$, therefore, (2.126) reads:

$$\begin{aligned} \ddot{R}_p &= -\omega_p^2 R_p + (h_{ppp}^p + A_{ppp}^p) R_p^3 \\ &= -\left[\omega_p^2 + (h_{ppp}^p + A_{ppp}^p) R_p^2\right] R_p \end{aligned} \tag{2.134}$$

Therefore, for the p-th mode, to ensure the stability the R_p should meet

$$\omega_p^2 + (h_{ppp}^p + A_{ppp}^p) R_p^2 \geq 0 \tag{2.135}$$

with

$$R_p \le \sqrt{-\frac{\omega_p^2}{h_{ppp}^p + A_{ppp}^p}} \tag{2.136}$$

As R_p is the nonlinear projection of X_p in the Normal-Mode coordinate, we should calculate the bound in the physical coordinate taking into account of the scaling of the coordinates.

To predict the stability bound in the physical coordinate, the scaling problem introduced by the nonlinear transformation should be considered.

Strictly speaking, the stability bound in XY coordinates is a nonlinear mapping of that in RS coordinates.

Since there is no "an inverse nonlinear transformation", a nonlinear factor is introduced to facilitate the calculation, which is as follows.

Since, when only p-th mode is excited, $R_i \ne 0, R_j \ne 0$ when, $i \ne 0, j \ne 0$.

$$X_p = R_p + R_p^3 + a_{pp}^p R_p^2 + r_{ppp}^p R_p^3 \tag{2.137}$$

The nonlinear can be calculated as X_p/R_p when assuming $R_p = 1$ which reads:

$$K_{nl} = \frac{R_p}{X_p} = \frac{1}{1 + a_{ppp}^p + r_{ppp}^p} \tag{2.138}$$

Therefore, the proposed stability bound (PSB) can be defined as:

$$PSB = R_p K_{nl} \Phi + \boldsymbol{q}_{SEP} \tag{2.139}$$

2.6.3 Analysis of Nonlinear Interaction Based on Closed-form Results

The difference between the nonlinear approach and linear approach are demonstrated in two aspects.

- Vibration amplitudes;
- Amplitude-dependent frequency-shift.

Thus, when analyzing the nonlinear interaction in the system, nonlinear index should be defined both for vibration amplitude and vibration frequency. Compared to the previous research, which assumes that there is no frequency-shift, the proposed method is more accurate in predicting nonlinear dynamics.

Based on the work of [59, 65], the nonlinear index for vibration amplitude can be defined as (2.140).

$$NI_p = \frac{\sqrt{\sum_{k=1}^N \sum_{j=1}^N \left| R_{p0} + a_{ij}^p R_{i0} R_{j0} - X_{p0} \right|^2}}{|X_{p0}|} \tag{2.140}$$

Where R_{p0}, X_{p0} is the initial value of LNM and NNM correspondingly, which can be calculated algebraically.

NI_p can measure the biggest error caused by the linear approach to study the nonlinear dynamics with respect to the nonlinear vibration amplitudes. In fact, the definition of NI_p is based on the assumption that the vibration frequency captured by X_p and R_p is the same. Thus, when there is a big frequency-shift in the nonlinear dynamics, NI_p may lead to wrong predictions.

As the nonlinear frequency of each mode is indicated in (2.133) [18], the frequency-shift index of each mode p is therefore defined, which writes:

$$FS_p = \frac{3(A^p_{ppp} + h^p_{ppp}) + \omega_p^2 B^p_{ppp}}{16\pi\omega_p} \tag{2.141}$$

If the cubic terms in (2.126) are neglected, it reads a "linear" equation, which fails to capture the amplitude-dependent frequency-shift in nonlinear dynamics. In the previous researches, the nonlinearities are truncated in the equations after the normal form transformation [59,65], which is correct only when FS_p is small.

The impacts of parameters on the nonlinear interaction can be studied analytically, in avoidance of time-consuming and high-cost numerical simulations. When the nonlinear indices are small, it means that linear analysis is not that far from being accurate, whose technique is more mature and simple .

2.7 The Performance of Method NNM Tested by Case Study

A small example of the interconnected VSCs is used to show the physical insights brought by the NNM and the proposed nonlinear indexes.

2.7.1 Interconnected VSCs

The interconnection of power systems and injection of wind energy into the transmission grid are realized by large capacity Voltage Source Converters (VSCs). The proposed case study is composed of two VSCs, VSC_1 and VSC_2, which are interconnected by a short connection line with the reactance X_{12} and are both connected to the transmission grid by long transmission lines with reactance X_1, X_2, as shown in Fig. 2.1.

To study the nonlinear interactions of the power angle δ_1, δ_2 under disturbances, the detailed mathematical model is first made, which consists of the physical structure as well as the current, voltage and power loops. To design the power loop, since the conventional PLL controller can cause synchronization problems when facing connections using long transmission lines [66], the Virtual Synchronous Machine (VSM) control strategy is adopted [29].

Linear stability analysis shows that this system works well under different operating points. However, when there is a large disturbance, the linear analysis tools fail to offer satisfying results.

The overall control is composed of three cascaded loops, where only the power loop
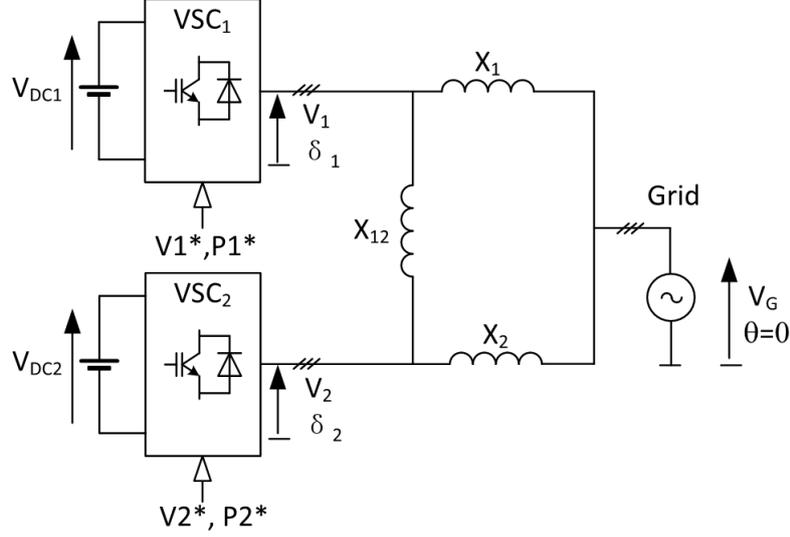
Figure 2.1: The Interconnected VSCs

is considered since voltage and current loops dynamics decays to steady state rapidly compared to the power loops. After reducing the model,the system can be expressed as (2.142). The procedures to reduce the model and all the parameters can be found in Appendix.

$$J_1 \frac{d^2\delta_1}{dt^2} + D_1(\dot{\delta}_1 - \omega_g) + \frac{V_1 V_g}{L_1}\sin\delta_1 + \frac{V_1 V_2}{L_{12}}\sin(\delta_1 - \delta_2) = P_1^*$$

$$J_2 \frac{d^2\delta_1}{dt^2} + D_2(\dot{\delta}_2 - \omega_g) + \frac{V_2 V_g}{L_2}\sin\delta_2 + \frac{V_1 V_2}{L_{12}}\sin(\delta_2 - \delta_1) = P_2^*$$

$$(2.142)$$

Where J_1, D_1, J_2, D_2 are the controller parameters of the power loop, δ_1, δ_2 are the power angles, V_1, V_2 are the voltages, P_1^*, P_2^* are the references values of the power of the two VSCs. ω_g is the angular frequency of the grid, and L_1, L_2 is the impedance of the cable connecting VSC to the grid, and L_{12} is the impedance of the transmission line connecting the two VSCs to each other. L_1, L_2 is very high ($0.7pu$), leading a very big power angle of VSC to transfer the electricity. L_{12} is very low due to high voltage of the transmission system, leading to strong coupling between the two VSCs. When there is a large disturbance on one VSC, there will be drastic nonlinear oscillations between the two VSCs.

Perturbing (2.142) around the stable equilibrium point (SEP) and applying the transformations of coordinates, it reads in RS coordinates:

$$\ddot{R}_1 + 2\xi_1\omega_1\dot{R}_1 + \omega_1^2 R_1 + (h_{111}^1 + A_{111}^1)R_1^3 + B_{111}^1 R_1 \dot{R}_1{}^2 + C_{111}^1 R_1^2 \dot{R}_1$$
$$+ R_1((A_{212}^1 + A_{122}^1 + h_{122}^1)R_2^2 + B_{122}^1 \dot{R}_2{}^2 + (C_{122}^1 + C_{212}^1)R_2\dot{R}_2) + \dot{R}_1(B_{212}^1 R_2\dot{R}_2 + C_{221}^1 R_2^2) = 0$$
$$\ddot{R}_2 + 2\xi_2\omega_2\dot{R}_2 + \omega_2^2 R_2 + (h_{222}^2 + A_{222}^2)R_2^3 + B_{222}^2 R_2 \dot{R}_2{}^2 + C_{222}^2 R_2^2 \dot{R}_2$$
$$+ R_2((A_{112}^2 + A_{211}^2 + h_{112}^2)R_2^2 + B_{211}^2 \dot{R}_1{}^2 + (C_{211}^2 + C_{121}^2)R_1\dot{R}_1)) + \dot{R}_2(B_{112}^2 R_1\dot{R}_2 + C_{112}^2 R_2^2) = 0$$
$$(2.143)$$

(2.143) appears longer on the page than (2.89), but it is much simpler in essence. To analyze the relation between the two modes, we can rewrite the equation into the form as (2.144), where $\widetilde{Q_p^2}, \widetilde{P_p^2}$ represent quadratic polynomials.

$$\ddot{R}_1 + 2\xi_1\omega_1\dot{R}_1 + \omega_1^2 R_1 + (h_{111}^1 + A_{111}^1)R_1^3 + B_{111}^1 R_1 \dot{R}_1{}^2 + C_{111}^1 R_1^2 \dot{R}_1 + R_2\widetilde{P_1^{(2)}}(R_i, \dot{R}_i) + \dot{R}_2\widetilde{Q_1^{(2)}}(R_i, \dot{R}_i) = 0$$
$$\ddot{R}_2 + 2\xi_2\omega_2\dot{R}_2 + \omega_2^2 R_2 + (h_{222}^2 + A_{222}^2)R_2^3 + B_{222}^2 R_2 \dot{R}_2{}^2 + C_{222}^2 R_2^2 \dot{R}_2 + R_1\widetilde{P_2^{(2)}}(R_i, \dot{R}_i) + \dot{R}_1\widetilde{Q_2^{(2)}}(R_i, \dot{R}_i) = 0$$
$$(2.144)$$

(2.144) highlights the couplings between R_1 and R_2. Although this equation still has nonlinear coupling, it puts all the nonlinearities to cubic terms, and the strength of coupling is largely reduced. What is more, when only one mode is excited, for example $R_1 \neq 0$ but $R_2 = 0, \dot{R}_2 = 0$, there will be no couplings. This is shown in (2.145).

$$\ddot{R}_1 + 2\xi_1\omega_1\dot{R}_1 + \omega_1^2 R_1 + (h_{111}^1 + A_{111}^1)R_1^3 + B_{111}^1 R_1 \dot{R}_1{}^2 + C_{111}^1 R_1^2 \dot{R}_1 = 0 \qquad (2.145)$$

Now the dynamic of the system will just exhibit vibration under one single mode. The complex dynamics are decomposed. This is the invariance. In the (2.89), even when $X_2 = 0, \dot{X}_2$ at $t = 0$, the motion of X_1 will definitely influence the value of $X_2, \dot{X}_2$, making it impossible to analyze and control X_1, X_2 independently. Also, if we make some approximations when $R_1 \neq 0, R_2 \neq 0$, Equation ((2.143)) will be:

$$\ddot{R}_1 + 2\xi_1\omega_1\dot{R}_1 + \omega_1^2 R_1 + (h_{111}^1 + A_{111}^1)R_1^3 + B_{111}^1 R_1 \dot{R}_1{}^2 + C_{111}^1 R_1^2 \dot{R}_1 = 0 \qquad (2.146)$$
$$\ddot{R}_2 + 2\xi_2\omega_2\dot{R}_2 + \omega_2^2 R_2 + (h_{222}^2 + A_{222}^2)R_2^3 + B_{222}^2 R_2 \dot{R}_2{}^2 + C_{222}^2 R_2^2 \dot{R}_2 = 0$$

Now, we can see that the system is decoupled. Although it has some quantitative error compared to the original equation, it represents the nonlinear behavior of the system with great accuracy and can be used to decompose the complex dynamics for analysis and decouple the system for control.

The 2-dimension second-order problem is reduced to 1-dimension second-order problem. The complexity of the problem is largely reduced. We can solve these two independent nonlinear equations by numerical integration with much lower complexity, or perturbation methods to obtain analytical results of R_1, R_2. And then by (2.127),

the system dynamics can be obtained.

Then, in our case, the dynamics of R_1, R_2 can be studied independently and analytical results can be obtained by perturbation method. Thus the nonlinear behavior can be predicted by the analytical results (discussed in Section 2.7.5) and the dynamics are decomposed (Section 2.7.4) and it is possible to analyze the nonlinear influences of parameters to suggest the analysis based control (discussed in Section 2.7.6 and Chapter 6).

2.7.2   Analysis based on EMT Simulations

The proposed system is simulated using a EMT (Electromagnetic transient) software. The test consists in experiencing at $t = 0$ a large disturbance in the power angle of VSC$_2$. Before the disturbance, the two VSCs are working under different operating points.
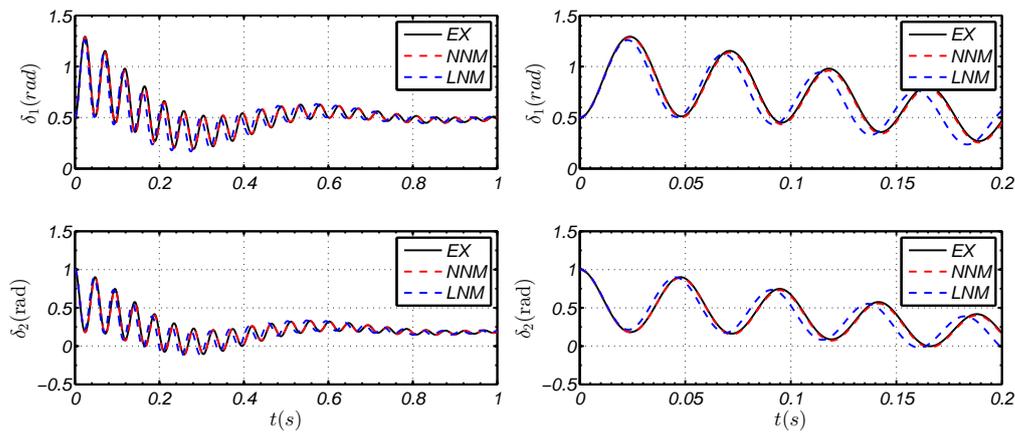
Figure 2.2: Comparison of LNM and NNM models with the exact system (EX): Full dynamics (left) and Detail (right)

The nonlinear dynamics of the system are shown in Fig. 2.2, where the Exact Model (named EX and based on (2.86)) is compared to the LNM and NMM models. It shows that the large disturbance imposed on only one VSC causes drastic power angle oscillations in both VSCs. This shows the significance of studying the nonlinear oscillations caused by the interconnection of VSCs in weak grid conditions. Moreover, the NNM model match the exact model much more better than the LNM, not only on the vibration amplitudes but also on the frequency shift due to the nonlinearities.

2.7.3   Coupling Effects and Nonlinearity

The accuracies of Model FNNM (2.123), NNM (2.126) and NM2 (2.105) to the exact model are compared in Fig. 2.3 to study the coupling effect and nonlinear essence of the studied system. It seen that NNM is almost as good as FNNM, convincing that
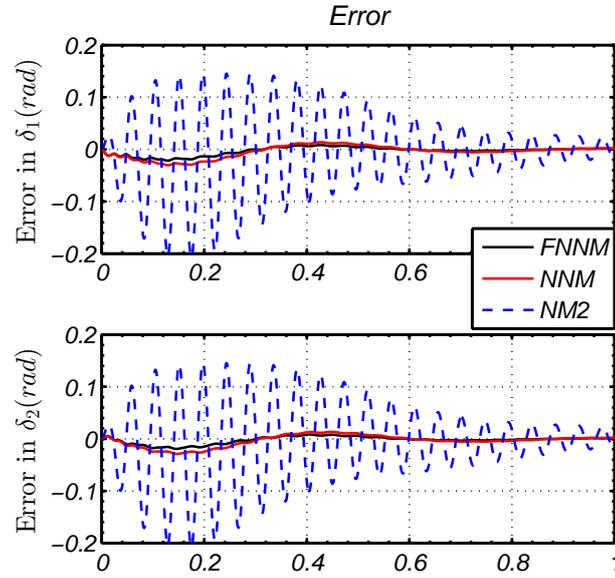
Figure 2.3: The Effect of the Cubic and Coupling Terms in the Nonlinear Modal Model

the coupling can be neglected. The LNM cannot track the nonlinear dynamics, because the cubic terms are neglected, which are responsible of the amplitude-dependent frequency-shifts [17]. The present NNM method appears very accurate and keep the advantage of linear normal modes as it approximately decomposes the dynamics into independent (nonlinear) oscillators.

2.7.4 Mode Decomposition and Reconstruction

As NNM method makes possible to model the nonlinear dynamics by decomposing the model into two independent nonlinear modes R_1, R_2 whose nonlinear dynamics are described by (2.126), the complex dynamics can be viewed as two independent modes. Fig. 2.4 shows those two modes projected on the generalized coordinates δ_1 and δ_2. As with linear modes that decompose a N-dimensional linear system into a linear sum of 1-dimensional linear systems, nonlinear modes make possible to decompose a N-dimensional nonlinear system into a nonlinear sum of nonlinear 1-dimensional nonlinear system.

2.7.5 Amplitude-dependent Frequency-shift

Another important characteristic in nonlinear dynamics is the amplitude-dependent frequency-shift, shown in Fig. 2.2, not captured by Model LNM and NM2, nor even by FFT analysis. The natural frequencies of the two linear modes (X_1, X_2) are extracted as $\omega_1 = 11.4 rad/s$, $\omega_2 = 137.4 rad/s$ at the equilibrium point. There is slight frequency-shift in the mode frequency according to the vibration amplitudes.
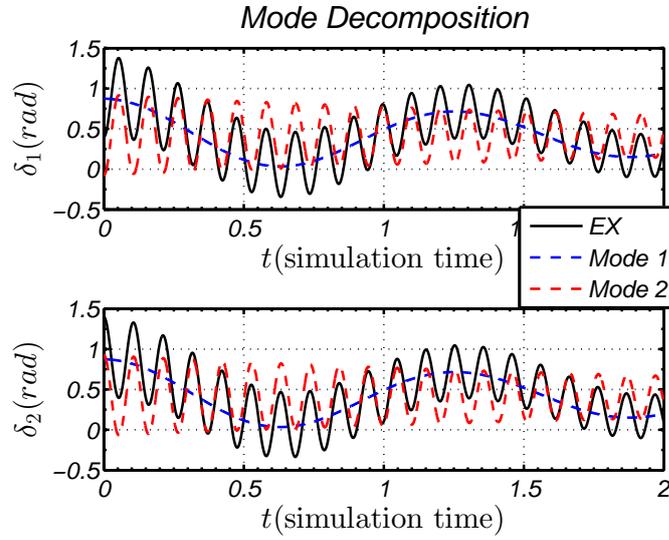
Figure 2.4: Mode Decomposition: An Approximate Decoupling of Nonlinear System

Based on (2.133), it can be predicted that if nonlinear modal frequency ω_2 is almost constant, frequency ω_1 experiences variations around 1 rad/s, as shown by Fig. 2.5.

2.7.6 Analytical Investigation on the Parameters

In our case, the nonlinear interaction is mainly determined by the reactances of transmission and connection lines. It is seen from Fig. 2.6 that the reactances of transmission lines X_1, X_2 mainly influence the nonlinear vibration amplitudes. While the reactance of connection line is more responsible for the frequency-shift of the modes, shown in Fig. 2.7.
Furthermore, it is also seen from Fig. 2.6 that Mode -1 is more sensitive to the reactance of the transmission lines than Mode -2. This corresponds to the fact shown in Fig. 2.4 that the vibration amplitude is decided by Mode -1.
It is seen from Fig. 2.7 that NI_p keeps aLNMost constant, while Mode-2 shows great variance in the frequency-shift indicated by FS_2. When only NI_p is considered, this characteristic cannot be captured and this will lead to great error.

2.7.6.1 Verification by EMT

The predictions of nonlinear dynamics by nonlinear indices are verified by the EMT simulation. Both the dynamics and errors are plotted out, shown in Fig. 2.8 and Fig. 2.9. To make the plots more clear and with the limitation of space, the dynamics are just shown for an interval $0.2s$, while the errors are plotted out in a longer interval: $1s$, to give more information in comparing the performance of nonlinear analysis and its linear counterpart.
Plots in Fig. 2.8 and Fig. 2.9 verify the predictions made by the nonlinear indexes. As NI_p indicates, the performance of linear analysis in cases of $X_{12} = 0.001$ and
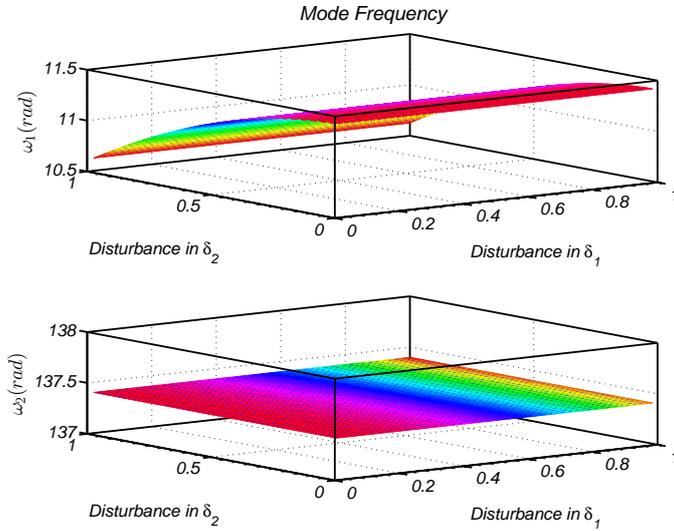
Figure 2.5: Amplitude-dependent Frequencies of the Nonlinear Modes
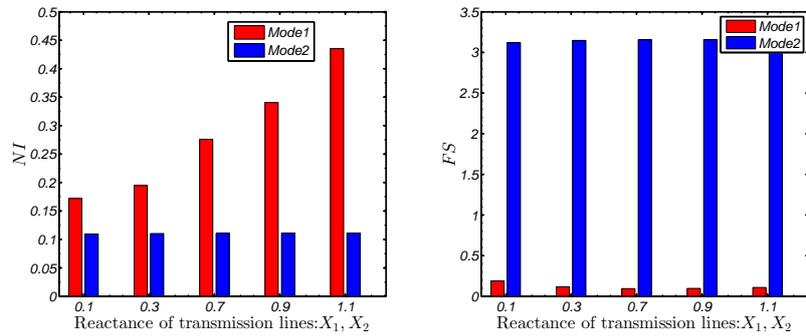
Figure 2.6: X_1, X_2 vary from 0.1 to 1.1 while X_{12} keeps 0.01
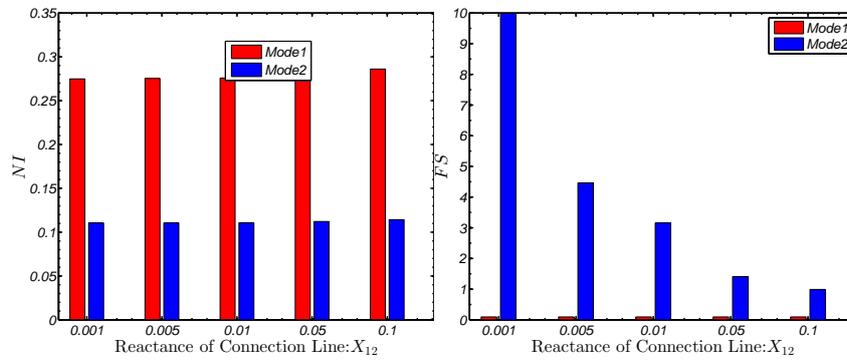
Figure 2.7: X_1, X_2 keep 0.7, while X_{12} varies from 0.001 to 0.1

(a) $X_1 = X_2 = 0.1$

(b) $X_1 = X_2 = 1.1$
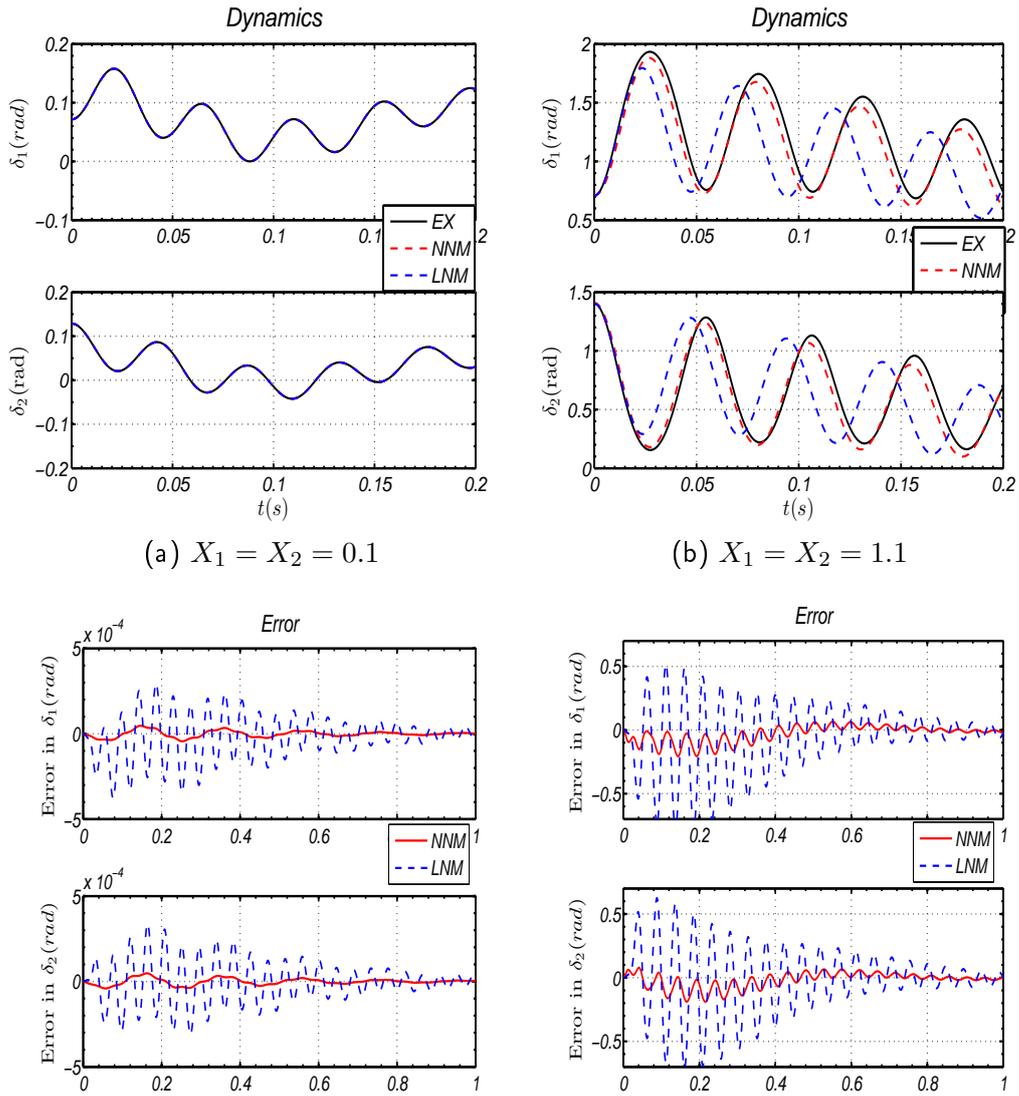
Figure 2.8: Dynamics Verified by EMT, when X_{12} keeps 0.01

(a) $X_{12} = 0.001$ (b) $X_{12} = 0.1$
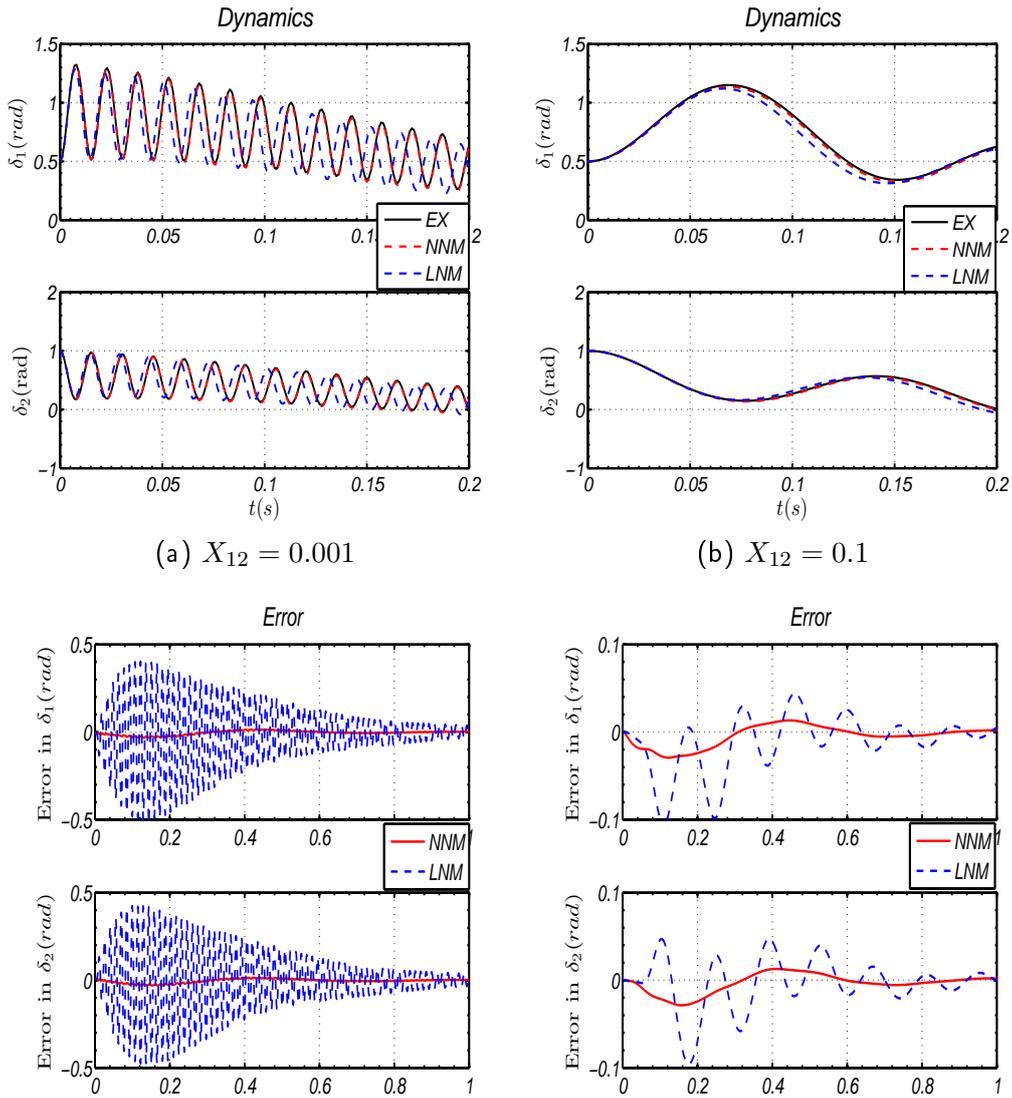
Figure 2.9: Dynamics Verified by EMT, when X_1, X_2 keeps 0.7

$X_{12} = 0.1$ should be same. However, it is seen from Fig. 2.9 the error of linear analysis in case of $X_{12} = 0.001$ can be as big as 0.5, while in case of $X_{12} = 0.1$, the error is less than 0.1. Compared to the methodology proposed in the previous research, it is convinced that our method is more accurate by considering both vibration amplitudes and frequency-shift.

2.7.7 Closed Remarks

Verified by EMT simulation, this example shows that the NNM has a good performance in approximating the nonlinear dynamics of the system. And it weakens the nonlinear couplings by normal form transformations and approximately decouples the nonlinear system, reducing the complexity of the system.

Third-order based analytical investigation on the influence of the parameters on the nonlinear dynamics taking into accounts of both vibration amplitudes and frequency-shift, in avoidance of numerical simulations. In recent works [59, 65], nonlinear index is defined as the criteria to quantify the influence of controller parameters on nonlinear interaction. However, failing to take into account the frequency-shift, their prediction can be wrong in some cases. Thus, in this PhD work, nonlinear indices are for the first time defined both for the vibration amplitude and the frequency-shift, rendering the nonlinear predictions more precise.

2.8 Issues Concerned with the Methods of Normal Forms in Practice

The methods of normal forms are firstly proposed by Poincaré in 1899, its application in analysis of system dynamics . Though the methods of normal forms theoretically render a "simplest form" of nonlinear dynamical systems, several issues are concerned in the practice.

2.8.1 Searching for Initial Condition in the Normal Form Coordinates

The analytical expression of normal form transformation, normal forms and nonlinear indexes are derived in the previous sections. However, the analytical expressions of the initial condition in the normal form coordinates are not available.

Since there is no analytical inverse of the normal form transformation, the numerical solution is obtained by formulating a nonlinear system of equations of the form.

$$f(z) = z - y^0 + h(z) = 0 \qquad (2.147)$$

The solution z (which is w for method 3-3-1 and method 3-3-3, respectively) to the above equation (2.147) provides the initial condition z^0. This system of equations is directly related to the nature of the second-order nonlinear terms and/or third-order nonlinear terms. And it describes how the z-variable differ from y^0 as a result

of the nature of the higher-order terms. The numerical solution of these equations is complicated. It requires a robust algorithm and is sensitive to the choice of the initial conditions for the solution.

The most popular algorithm is the Newton-Raphson method, which is adopted in this PhD work. A more robust algorithm is proposed in [47] to circumvent some disadvantages of NR method, which can be adopted also for the 3rd order NF methods.

It is recommended that y^0 be selected as the choice of the initial condition, based on the nature of the system of (2.147) where the variables z differ from y^0 according to the higher-order nonlinear terms, i.e, $z^0 = y^0$ where there is no higher-order term. From the analysis on a variety of test systems, the choice of $z^0 = y^0$ provides the most robust results. The pseudo-code of searching for the initial condition of 3rd order normal form methods is listed as follows, which is an extension of the search algorithm for method 2-2-1 [48].

2.8.1.1 The Search Algorithm of Initial Condition for method 3-3-3

The algorithm begins:
1. x^0: x^0 is the initial condition of the system dynamics at the end of the disturbance, e.g, when the fault is cleared in the power system, this value can be obtained from measurement or time-domain simulation.

2. y^0: $y^0 = U^{-1}x^0$, the initial condition in the Jordan coordinate.

3. z^0: the system of (2.147) is solved for z^0 using the Newton-raphson method as follows:

a: formulate a nonlinear solution problem of the form $j = 1, 2, \cdots, N$:

$$f_j(w) = w_j + \sum_{k=1}^{N}\sum_{l=1}^{N} h2_{kl}^j h2_{kl}^j w_k w_l + \sum_{p=1}^{N}\sum_{q=1}^{N}\sum_{r} h3_{pqr}^j h3_{pqr}^j w_p w_q w_r = 0$$

;

b. choose y^0 as the initial estimate for w^0. Initialize the iteration counter:$s = 0$;

c. compute the mismatch function for iteration s, $j = 1, 2, \cdots, N$:

$$f_j(w^{(s)}) = w_j^{(s)} + \sum_{k=1}^{N}\sum_{l=1}^{N} h2_{kl}^j h2_{kl}^j w_k^{(s)} w_l^{(s)} + \sum_{p=1}^{N}\sum_{q=1}^{N}\sum_{r} h3_{pqr}^j h3_{pqr}^j w_p^{(s)} w_q^{(s)} w_r^{(s)} = 0,$$

;

d.compute the Jacobian of $f(z)$ at $w^{(s)}$:

$$[A(w^s)] = \left[\frac{\partial f}{\partial w}\right]_{w=w^{(s)}}$$

;

e.compute the Jacobian of $f(z)$ at $w^{(s)}$:

$$\triangle w^{(s)} = -\left[A(w^s)\right]^{-1} f(w^{(s)})$$

;

f. determine the optimal step length ρ using cubic interpolation or any other appropriate procedure and compute:

$$w^{(s+1)} = w^{(s)} + \rho \triangle w^{(s)}$$

;

g. continue the iterative process until a specified tolerance is met. The value of w^s when the tolerance is met provides the solution w^0.

The algorithm ends.

2.8.1.2 Search for Initial Condition of the Normal Mode Approach

When it comes to the normal mode approach, the search for initial condition is the same except the nonlinear solution problem should be formulated as: $\forall p = 1, 2, \cdots, N$

$$f_p = R_p + \sum_{i=1}^{N}\sum_{j\geq i}^{N} a_{ij}^p R_i R_j + \sum_{i=1}^{N}\sum_{j\geq i}^{N}\sum_{k\geq j}^{N} r_{ijk}^p R_i R_j R_k - X^p \tag{2.148}$$

with $Y^0 = 0$, $S^0 = 0$.
In fact, there are well validated Newton-Raphson software package on line [67] which can determine the optimal step length to avoid the non-convergence, and what is needed in practice is just formulate the nonlinear solution problem in the form of (2.147).The codes for all the methods presented in this PhD thesis can be found in the Appendix.

2.8.2 The Scalability Problem in Applying Methods of Normal Forms on Very Large-Scale System

One concern of the methods of normal forms is the scalability problem when is applied on the large-scale system or huge dimensional system. One solution is to reduce the model by focusing on only the critical modes, which will be illustrated in details in Chapter 3.

2.8.3 The Differential Algebraic Equation Formalism

In practice, the dynamic power flow models are often formulated as DAE with nonlinear algebraic part (for instance due to constant power loads with small time constants). And generalizations of normal form approach that would be applicable to these systems are available.

In fact, the differential equations $\dot{x} = f(x)$ of system dynamics essentially comes from a set of DAE equation composed of the differential equations representing the machine dynamics and the algebraic equations representing the network connectivity and power flow constraints. Using the power flow analysis, the stable equilibrium point (SEP) is obtained, and the differential equation is the DAE perturbed around the SEP.

There is an alternate formalism in [54], which transforms DAEs into an explicit set of differential equations by adding an appropriate singularly perturbed dynamics. It points out the interests to take DAE into normal form methods as:

1. Sparsity can be taken into account;
2. DAE models are compatible with current small signal stability commercial software, i.e PSSE, DSAT tolos, etc.

2.9   Comparisons on the two Approaches

2.9.1   Similarity and Difference in the Formalism

For methods of normal mode approach, (2.89) can be rewritten into an equivalent
first-order form with state-variables $[X_p \quad Y_p]$:

$$
\begin{bmatrix} \dot{X}_1 \\ \dot{Y}_1 \\ \vdots \\ \dot{X}_p \\ \dot{Y}_p \\ \vdots \\ \dot{X}_N \\ \dot{Y}_N \end{bmatrix} = \begin{bmatrix} \begin{bmatrix} 0 & 1 \\ -\omega_1^2 & -2\xi_1\omega_1 \end{bmatrix} & 0 & 0 & \cdots & 0 \\ 0 & & \vdots & \vdots & \vdots & \vdots \\ \vdots & \vdots & \begin{bmatrix} 0 & 1 \\ -\omega_p^2 & -2\xi_p\omega_p \end{bmatrix} & \vdots & 0 \\ 0 & \vdots & \vdots & \vdots & \vdots \\ 0 & 0 & \cdots & \vdots & \begin{bmatrix} 0 & 1 \\ -\omega_N^2 & -2\xi_N\omega_N \end{bmatrix} \end{bmatrix} \begin{bmatrix} X_1 \\ Y_1 \\ \vdots \\ X_p \\ Y_p \\ \vdots \\ X_N \\ Y_N \end{bmatrix} + \begin{bmatrix} g(X_1)+h(X_1) \\ 0 \\ \vdots \\ g(X_p)+h(X_p) \\ 0 \\ \vdots \\ g(X_N)+h(X_N) \\ 0 \end{bmatrix}
$$

$$(2.149)$$

2.9.1.1   Linear Transformation

As observed from (2.149), the linear matrix is composed with N $[2{\times}2]$ blocks at the
principle diagonal. In such a way, X_p are independent of $X_j(j \neq p)$, but dependent
of Y_p.

Diagonalizing the linear matrix, the diagonal element may have complex conjugate
values and X_p will be independent of Y_j, which is exactly the vector field approach.
As observed from (2.149) and (2.30), the difference between the two approaches
lays in the linear transformation, i.e the way to decouple the linear terms.

In the vector field approach, the basic unit is differential equations of each state-
variable y_p: y_p is linearly uncoupled with y_j, $j \neq p$; in the normal mode approach,
the basic unit is differential equations of the state-variable pair $[U_p, V_p]$: $[U_p, V_p]$ is
linearly uncoupled with $[U_p, V_p]$, but U_p are coupled with V_p.

As indicated in Section 2.9.1.1, since the simplified linear matrix should have a
simple real form [30] or pure imaginary form [33] to ensure the accuracy, the vector
field approach which involves the complex form numbers, is less accurate than the
normal mode approach.

2.9.1.2   Normal Form Transformation

The essentials of the normal form transformation of those two approaches are equat-
ing the like power systems, as generalized in Eqs. (2.19) to (2.27).

The difference in the normal form transformation is that: in the vector field ap-
proach, $\dot{y}_j$ is canceled by the replacement $\dot{y}_j = \lambda_j y_j + \sum_{k=1}^{N}\sum_{l=1}^{N} F2_{kl}^j y_k y_l + \sum_{p=1}^{N}\sum_{q=1}^{N}\sum_{r=1}^{N} F3_{pqr}^j y_p y_q y_r + \cdots$, the equating of like power terms involves only

the state-variable y_p;in the normal mode approach, $\dot{U}_p$ is canceled by letting $\dot{U}_p = V_p$, and $\dot{V}_p$ is canceled by letting $\dot{V}_p = -\omega_p^2 U_p - 2\xi_p \omega_p V_p$, the equating of like power terms involves the state-variable pair $[U_p, V_p]$.

2.9.2 Applicability Range and Model Dependence

Second-order (or order higher than 2nd order) equations definitely have equivalent first-order equations, but the equivalent second-order (or order higher than 2nd order) equations of first-order equations are not guaranteed. From the mathematical view, the applicability range of the normal mode approach is a subset of that of the vector field approach.

However, from the engineering view, the normal mode approach may do a better job since it represents better the physical properties of inter-oscillations and highlights the relations between the state variables. Also, the complex-form will cause some error in the computation compared to the normal mode approach, which will be illustrated by case studies in Chapter 4.

The vector field approach is the most widely used approach in analysis and control of nonlinear dynamical systems and aLNMost applicable for all types of power system models with differentiable nonlinearities. First applied and advocated by investigators from Iowa State University in the period 1996 to 2001 [6–15], it opens the era to apply Normal Forms analysis in studying nonlinear dynamics in power system. Its effectiveness has been shown in many examples [6, 9–12, 14, 15, 20, 31, 47, 54].

The normal mode approach proposed in this PhD work is found mostly in mechanical engineering [17–19, 56], and can be adopted to study the electromechanical oscillations in interconnected power system, which will be illustrated in Chapter 4.

2.9.3 Computational Burden

When comes to the issue of computational burden, the normal mode approach is advantaged over the vector field approach, since calculating the complex-form values is much heavier than that of the real-form values when:

1. Formulating the nonlinear matrices: calculating $F2$, $F3$ may be quite laborious compared to calculation of $H2$, $H3$ by both two possible approaches:
   - approach 1: firstly calculating the matrix $H2$, $H3$, ($H2$, $H3$ are calculated by doing the Hessian matrix and 3rd order differentiation of $f(x)$), secondly calculating $F2$, $F3$ by $\boldsymbol{F2_j} = \frac{1}{2}\sum_{i=1}^{N} v_{ji}\left[\boldsymbol{U^T h_3^j U}\right]$. $F3_{pqr}^j = \frac{1}{6}\sum_{i=1}^{N} v_{ji}\sum_{k=1}^{N}\sum_{k=1}^{N}\sum_{m=1}^{N} H3_{kLNM}^i u_p^l u_q^m u_r^N$;
   - approach 2: firstly calculating the nonlinear equation $F(y)$ on the vector fields by $\boldsymbol{F(y) = U^{-1} f(Uy)}$, secondly doing the Hessian matrix and 3rd order differentiation of $F(y)$ to obtain $\boldsymbol{F2(y)}$, $\boldsymbol{F3(y)}$.

   Both those two approaches involve complex-form matrix multiplication, leading to heavy computational burden.
2. Searching for the initial conditions: The state-variables x^0 are real-form values, and the state-variables y^0 contain complex-form values as far as there exists

oscillations in the system dynamics, and the terms $h2$, $h3$ are in complex-form, therefore the mismatch function contain complex-values, this will add to the computational burden in searching for the initial conditions.

2.9.4   Possible Extension of the Methods

As indicated in Section 2.2, both method 3-3-3 and method NNM can be extended to include terms higher than 3rd order.

The method NNM may be also extended to system with state-variable pair consisting of M state-variables $[q_1, q_2, \cdots, q_M]$, $M > 2$ i.e, system of higher-order equations. In such a case, when represented by first-order equations, the linear matrix is composed of $[M \times M]$ blocks at the principle diagonal.

2.10   Conclusions and Originality

In this chapter, two approaches are proposed to deduce the normal forms of system of nonlinear differential equations. One is the most classical vector-field approach, method 3-3-3, working for system of first-order equations. The other approach is the normal mode approach, method NNM, working for system of second-order equations.

Method 3-3-3 makes possible the quantification of 3rd order modal interaction and the assessment of nonlinear stability, and will be applied to the interconnected power system in Chapter 3.

By method NNM, nonlinear interaction can be described by a N-dimensional coupled second-order problem, which involves highly computational numerical simulation and analytical results are rare. In this chapter, a methodology is proposed to solve this problem by decoupling it into a series of 1-dimensional independent second-order problems whose analytical solutions are available and by which complex dynamics are decomposed into several simpler ones. Moreover, nonlinear behavior can be accurately predicted by the defined nonlinear indexes in avoidance of numerical simulation. The application of this method may be:

1. Providing information in designing system parameters by quantifying their influence on the nonlinearities of the system with the nonlinear indexes; as shown in Section 2.7;

2. Transient stability analysis of interconnected power systems, which will be illustrated in Chapter 4.

The similarities and differences between the vector-field approach and normal mode approach have been made, to go further in illustrating the principle of normal form theory. And possible extensions of method 3-3-3 and method NNM have been pointed out, to cater for further demands in future researches.

All the nonlinear properties can be predicted by one approach can be revealed by the other, which are summarized in Tab. 2.5 for mode j.

What's more, the competitors of methods of normal forms (MNF) has been reviewed, such as the MS method in the vector field approach and Shaw-Pierre (SP) method in

Table 2.5: The Nonlinear Properties Quantified by Method 3-3-3 and Method NNM

Properties	Nonlinear Modal Interaction	Amplitude-dependent Frequency-shift	Nonlinear Stability
3-3-3	$h2_{kl}^j, h3_{pqr}^j$	$Im(SII^j)$	SI^j
NNM	$a^j, b^j, c^j, \cdots$	FS	PSB

forming the NNM. As it is difficult to find literature comparing MNF to MS method and SP method, we hope that the comparisons made in this PhD thesis bridge a bit the gaps in the literature.

Concerning the originality, it is for the first time that method 3-3-3 is proposed to study the system dynamics. And for method NNM, though its FNNM has been proposed in mechanical domain, it is mainly for bifurcation analysis. The nonlinear properties extracted from the method NNM, such as the amplitude-frequency shift and nonlinear mode decomposition are firstly found in power system. What's more, all the nonlinear indexes are at the first time proposed by this PhD work.

In the previous researches, the methods of normal forms are conventionally used for bifurcation analysis [49]. And their derivations of normal forms focus more on the variation of parameters, i.e., the parameters can be viewed as state-variables, but in different-scales with the physical state-variables of the system. In this chapter, we focus on the influence of physical state-variables on the system dynamics.

Application of Method 3-3-3: Nonlinear Modal Interaction and Stability Analysis of Interconnected Power Systems

The inclusion of higher-order terms in Small-Signal (Modal) analysis has been an intensive research topic in nonlinear power system analysis. Inclusion of 2nd order terms with the Method of Normal Forms (MNF) has been well developed and investigated, overcoming the linear conventional small-signal methods used in the power system stability analysis and control. However, application of the MNF has not yet been extended to include 3rd order terms in a mathematically accurate form to account for nonlinear dynamic stability and dynamic modal interactions. Due to the emergence of larger networks and long transmission line with high impedance, modern grids exhibit predominant nonlinear oscillations and existing tools have to be upgraded to cope with this new situation.

In this chapter, the proposed method 3-3-3 is applied to a standard test system, the IEEE 2-area 4-generator system, and results given by the conventional linear small-signal analysis and existing MNFs are compared to the proposed approach. The applicability of the proposed MNF to larger networks with more complex models has been evaluated on the New England New York 16 machine 5 area system.

Keywords: Interconnected Power System, Power System Dynamic, Nonlinear Modal interaction, Stability, Methods of Normal Forms

3.1 Introduction

Today's standard electrical grids are composed of several generators working in parallel to supply a common load. An important problem associated with interconnected power systems is the presence of oscillations that could have dangerous effects on the system. The multiplication of distributed generation units, usually composed of renewable-energy-based-generators, and the increase of energy exchanges through long distance lead to highly stressed power systems. Due to the large amount of power flowing through the lines, the low-frequency oscillations, called in classical power system studies electromechanical oscillations, exhibit predominant nonlinear behaviors. Since these oscillations are essentially caused by modal interactions between the system components after small or large disturbances, they are called nonlinear modal oscillations, higher order modes or higher order modal interactions, inaccurately modelled by the linear analysis based on a linearized model.

Although intensive research has been conducted on the analytical analysis of nonlinear modal oscillations based on the Normal Form Theory with inclusion of 2nd order terms in the system's dynamics, this chapter proposes to show that in certain stressed conditions, as modern grids experience more and more, inclusion of 3rd order terms offer some indubitable advantages over existing methods.

The Method of Normal Forms (MNF) being based on successive transformations of increasing orders, the proposed 3rd order-based method inherits the benefits of the linear and the 2nd order-based methods, i.e.:

1. Analytical expressions of decoupled (or invariant) normal dynamics;
2. Physical insights keeping the use of modes to study the contribution of system components to inter-area oscillations;
3. Stability analysis based on the evaluation of the system parameters.

3.1.1 Need for inclusion of higher-order terms

Small-signal analysis is the conventional analysis tool for studying electromechanical oscillations that appear in interconnected power systems. It linearizes the power system's equations around an operating point by including only the first-order terms of the Taylor series of the system's dynamics. The eigenanalysis is made to obtain analytical expressions of the system's dynamic performances and the stability analysis is realized on the basis of the first Lyapunov Method (Analysis of the real parts of the poles). Besides, modal analysis uses the eigenvectors to give an insight of the modal structure of a power system, showing how the components of the power system interact. Thanks to modal analysis, power system stabilizers can be placed at the optimal location in order to stabilize the whole system, ensuring then a small-signal stability [1].

Later, researchers suggested that in certain cases, such as when the system is severely stressed, linear analysis techniques might not provide an accurate picture of the power system modal characteristics. From 1996 to 2005, numerous papers [6–15] have been published proving that higher order modal interactions must be studied

in case of certain stressed conditions. MNF with the inclusion of 2nd order terms shows its great potential in power system stability analysis and control design. Those achievements are well summarized in the Task-force committee report [48], whose formalism is referred to as the method 2-2-1 in Chapter 2.

The existing 2nd-order-based method gives a better picture of the dynamic performance and the mode interactions than the classical linear modal analysis. However, it fails to take benefit of the system's nonlinearities for studying the stability where the conventional small-signal stability analysis fails. Based on this, [5] proposed to keep a second order transformation but with including some of the third-order terms in order to improve the system stability analysis.

The emergence of renewable energy (unbalanced energy generation and weak grid) and fast control devices [59] increases the nonlinearity, and inclusion of 3rd order terms is demanded.

Finally, some 3rd-order-based MNFs have been proposed in [31,32] but have not been fully developed yet, not leading to a more useful tool than the ones using linear-based and second-order-based methods. For nonlinear mechanical systems, that often include lightly damped oscillatory modes and possible internal resonances, Normal Forms up to third order are widely used, either to classify the generic families of bifurcations in dynamical systems [53,68] or to define Nonlinear Modes of vibration and to build reduced-order models [17,18,33].

Taking into account the 3rd order nonlinearities will increase the expected model accuracy in most cases while keeping the overall complexity at a relatively low level. This can be illustrated by a simple example. Primitive as the example is, it visualizes the need of inclusion of higher-order terms and the increased stress due to the increased power transferred.

As an illustration of the gains afforded by inclusion of higher-order-terms, the transferred active power through a power grid as a function of the power angle δ: $P = \frac{V^2}{X} \sin \delta$ is analyzed in steady state. Considering the voltage V at the terminals and the reactance X of the line both constant, the transmitted power can be simplified as $P = k \sin \delta, k = constant$. The exact system (Exact) and its Taylor series, up to the first order (Linear), up to the second order (Tayl(2)) and up to the third order (Tayl(3)) are plotted in Fig. 3.1. Depending on the power angle values, inclusion of higher-order terms by nonlinear analysis, especially up to 3rd order terms, is necessary to maximize the transfer capacity of the modern power system with ever-increasing stress.
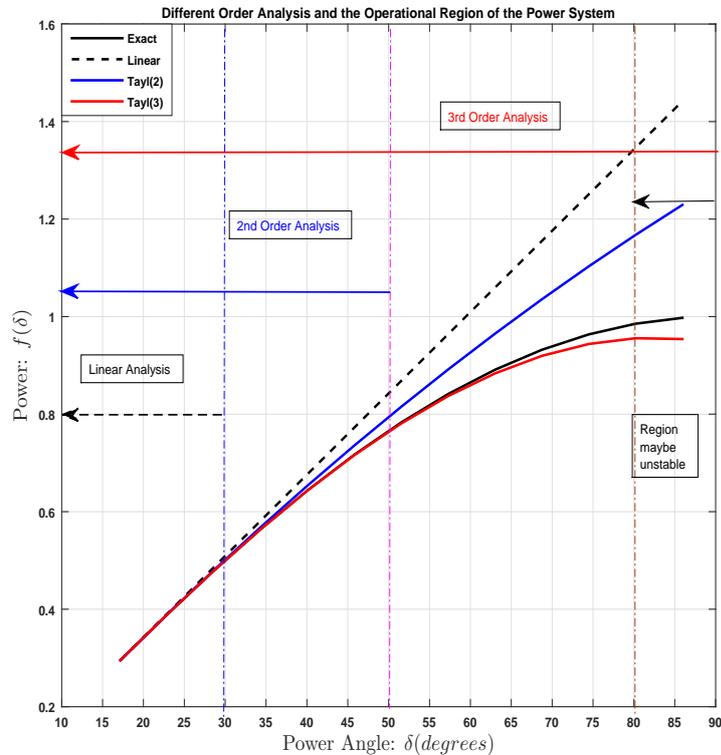
Figure 3.1: The Need of Inclusion of Higher-Order Terms

The Chapter 3 is organized as follows. A brief review of the existing normal forms on vector field and proposed method 3-3-3 is conducted in Section 3.2. The test benches are presented in Section 3.3 with mathematical modelling. The applications of method 3-3-3 will be conducted on interconnected power systems in Section 3.4 and Section 3.5, where the performance of reviewed and proposed MNFs on vector fields will be assessed. And the benefits promised in Chapter 2 will be demonstrated. Section 3.6 discusses the factors influencing the Normal Form analysis. Section 3.7 proposes some conclusions and possible applications of the proposed method are suggested.

3.2   A Brief Review of the existing Normal Forms of Vector Fields and the Method 3-3-3

The Methods of Normal Forms (MNF) was initially developed by Poincaré [50] to simplify the system dynamics of nonlinear systems by successive use of near-identity changes of coordinates. The transformations are chosen in such a way as to eliminate the nonresonant terms of a corresponding order. The principle is to transform the system dynamics into invariant *normal dynamics*. The word *invariant* means that qualified property is the same in the system dynamics and normal dynamics. It was

proved by Poincaré that linear invariants are eigenvalues and nonlinear invariants are the homogeneous resonant terms [69].

In Chapter 2, the existing methods: linear small-signal analysis, method 2-2-1, method 3-2-3S, method 3-3-1, and the proposed method 3-3-3 have already illustrated with detailed derivations. In this section, for the compactness, a simple review is made, and the assessment of those methods is performed in the following sections.

3.2.1 Modeling of the System Dynamics

The class of systems that can be studied by MNF are usually modeled by Differential Algebraic Equations (DAEs) [1]. By subsituting the algebraic equations into the differential ones, one transforms those DAEs in a dynamical system, which can be written:

$$\dot{\boldsymbol{x}} = \boldsymbol{f}(\boldsymbol{x}, \boldsymbol{u}), \tag{3.1}$$

where $\boldsymbol{x}$ is the state-variables vector, $\boldsymbol{u}$ is the system's inputs vector and $\boldsymbol{f}$ is a nonlinear vector field. Expanding this system in Taylor series around a stable equilibrium point (SEP), $u = u_S EP$, $x = x_S EP$, one obtains:

$$\triangle\dot{\boldsymbol{x}} = \boldsymbol{H1}(\triangle\boldsymbol{x}) + \frac{1}{2!}\boldsymbol{H2}(\triangle\boldsymbol{x}) + \frac{1}{3!}\boldsymbol{H3}(\triangle\boldsymbol{x}) + \mathcal{O}(4) \tag{3.2}$$

where $\boldsymbol{Hq}$ gathers the qth-order partial derivatives of f. i.e., for $j = 1, 2, \cdots, n$, $H1_k^j = \partial f_j/\partial x_k$, $H2_{kl}^j = \left[\partial^2 f_j/\partial x_k \partial x_l\right]$, $H3_{klm}^j = \left[\partial^3 f_j/\partial x_k \partial x_l \partial x_m\right]$ and $\mathcal{O}(4)$ are terms of order 4 and higher.

3.2.1.1 The Linear Small Signal Analysis

The linear part of (3.2) is simplified into its Jordan form:

$$\dot{\boldsymbol{y}} = \boldsymbol{\Lambda}\boldsymbol{y} + \boldsymbol{F2}(\boldsymbol{y}) + \boldsymbol{F3}(\boldsymbol{y}) + \cdots \tag{3.3}$$

supposed here to be diagonal, where the jth equation of (3.3) is:

$$\dot{y}_j = \lambda_j y_j + \sum_{k=1}^{N}\sum_{l=1}^{N} F2_{kl}^j y_k y_l + \sum_{p=1}^{N}\sum_{q=1}^{N}\sum_{r=1}^{N} F3_{pqr}^j y_p y_q y_r + \cdots \tag{3.4}$$

λ_j is the jth eigenvalue of matrix $\boldsymbol{H1}$, and $j = 1, 2, \cdots, n$. $\boldsymbol{U}$ and $\boldsymbol{V}$ are the matrices of the right and left eigenvectors of matrix $\boldsymbol{H1}$, respectively: $\boldsymbol{UV} = \boldsymbol{I}$; $\boldsymbol{F2_j} = \frac{1}{2}\sum_{i=1}^{N} v_{ji}\left[\boldsymbol{U^T}h_3^j\boldsymbol{U}\right]$. $F3_{pqr}^j = \frac{1}{6}\sum_{i=1}^{N} v_{ji}\sum_{k=1}^{N}\sum_{k=1}^{N}\sum_{m=1}^{N} H3_{klm}^i u_p^l u_q^m u_r^n$, v_{ji} is the element at j-th row and i-th colomn of Matrix $\boldsymbol{V}$. u_p^l is the element at the p-th row and l-th column of matrix $\boldsymbol{U}$.

The fundamentals of linear small-signal analysis uses the sign of the real parts σ_j of the eigenvalues $\lambda_j = \sigma_j + j\omega_j$ to estimate the system stability. $\boldsymbol{U}$ is used to indicate how each mode y_j contribute to the state-variable $\boldsymbol{x}$, and $\boldsymbol{V}$ indicates how

the state-variables of $\boldsymbol{x}$ are associated to each mode y_j.

$$x = Uy \Rightarrow \dot{y}_j = \lambda_j y_y + \mathcal{O}(2) \tag{3.5}$$

3.2.2 Method 2-2-1

Gradually established and advocated by investigators from Iowa State University, the period 1996 to 2001 [6–15] opens the era to apply Normal Forms analysis in studying nonlinear dynamics in power system. This method is labelled 2-2-1 according to our classification.

Its effectiveness has been shown in many examples [6, 9–12, 14, 15, 20, 47], to approximate the stability boundary [9], to investigate the strength of the interaction between oscillation modes [6,10,47], to dealt with a control design [11,12], to analyze a vulnerable region over parameter space and resonance conditions [14, 15] and to optimally place controllers [20].

This method is well summarized in [48], which demonstrated the importance of nonlinear modal interactions in the dynamic response of a power system and the utility of including 2nd order terms. Reference [70] propose an extension of the method to deal with resonant cases. It has become a mature computational tool and other applications have been developed [36,54], or are still emerging [71].

Method 2-2-1 can be summarized as:

$$y_j = z_j + h2^j_{kl} z_k z_l \Rightarrow \dot{z}_j = \lambda_j z_j + \mathcal{O}(3) \tag{3.6}$$

with $h2^j_{kl} = \frac{F2^j_{kl}}{\lambda_k + \lambda_l - \lambda_j}$ where $\mathcal{O}(3) = (DF2)h2 + F3$.

It is very important to note that the normal dynamics given by (3.6) uses the linear modes of the linearized system. The nonlinearities are then taken into account only through the nonlinear 2nd-order transform $\boldsymbol{y} = \boldsymbol{z} + h2(\boldsymbol{z})$ and results in a quadratic combination of linear modes, leading to 2nd-order modal interactions. Then, the stability analyses conducted using this linear normal dynamics give the same conclusion than the analysis that can be conducted using the linear dynamics.

3.2.3 Method 3-2-3S

Although the second-order-based method gives a more accurate picture of the system's dynamics than the linear small-signal analysis, keeping some of the 3rd order terms in $(DF2)h2 + F3$ contributes some important features to the method. As examples, improvements in the stability analysis have been proved in [5] and new criteria to design the system controllers in order to improve the transfer capacity of transmissions lines have been established in [16], where some 3rd order terms are kept in (3.7).

The normal forms of a system composed of M weakly-damped oscillatory modes are

then:

$$
y = z + h2(z) \Rightarrow
\begin{cases}
\dot{z}_j = \lambda_j w_j + \sum_{l=1}^{M} c_{2l}^j w_j w_{2l} w_{2l-1} + \mathcal{O}(5), j \in M \\
\\
\dot{w}_j = \lambda_j w_j + \mathcal{O}(5), j \notin M
\end{cases}
\tag{3.7}
$$

where c_{2l}^j is the sum of coefficients associated with term $w^j w_{2l} w_{2l-1}$ of $DF2h2+F3$, more details are found in Chapter 2.

It should be noted that the normal dynamics given by (3.7) is nonlinear, contributed by the third-order terms $c_{2l}^j w_j w_{2l} w_{2l-1}$, depending on oscillatory amplitude $|w_{2l}|$. Therefore, 3rd order terms contain the nonlinear property such as the stability bound [5, 5] and amplitude-frequency dependent [21, 22, 55]. However, it is not the "simplest form" up to order 3.

3.2.4   Method 3-3-1

Later, to study the 3rd order modal interaction, method 3-3-1 has been proposed [31, 32] and 3rd order indexes are proposed [32].

$$
y = w + h2(w) + \overline{h3}(w) \Rightarrow \dot{w}_j = \lambda_j w_j
\tag{3.8}
$$

where $\overline{h3_{pqr}^j} = \frac{F3_{pqr}^j}{\lambda_p + \lambda_q + \lambda_r - \lambda_j}$

However, it is not an accurate 3rd order normal form, since 1) it neglects the term $DF2h2$ and may lead to a big error in quantifying the 3rd order modal interaction; 2) it fails to study the oscillatory interaction between oscillatory modes, and may lead to strong resonance.

3.2.5   Method 3-3-3

To overcome those disadvantages, the proposed method 3-3-3, takes into account both the M oscillatory modes and $N - M$ non-oscillatory modes.

$$
y = w + h2(w) + h3(w) \Rightarrow
\begin{cases}
\dot{w}_j = \lambda_j w_j + \sum_{l=1}^{M} c_{2l}^j w_j w_{2l} w_{2l-1} + \mathcal{O}(5), j \in M \\
\\
\dot{w}_j = \lambda_j w_j + \mathcal{O}(5), j \notin M
\end{cases}
\tag{3.9}
$$

As observed from (3.9), method 3-3-3 approximates the system dynamics by a nonlinear combination of nonlinear modes. Based on the normal forms, nonlinear indexes $MI3$ and SI are proposed to quantify the 3rd order modal interaction and assess the stability of the system dynamics.

In this chapter, all the presented methods have been assessed on the IEEE standard test systems.

3.3   Chosen Test Benches and Power System Modeling

In this PhD work, two IEEE standard test systems are chosen, the first is the Kundur's 4-machine 2-area system, whose mechanism is easy to understand and which serves as a classic example for small-signal analysis and modal analysis. It serves as a didactic example to show how the proposed method 3-3-3 does a better job in quantifying the nonlinear modal interaction and assessing the stability of system dynamics than the existing methods. The second test bench is the New England New York 16 machine 5 area system, used to assess the applicability of the proposed method 3-3-3 to large scale power system.

For both two test benches, the chosen mathematical model is built with reasonable simplification and is well validated. Power systems are nonlinear dynamic systems, whose behaviors are usually modelled by differential-algebraic equations(DAEs).
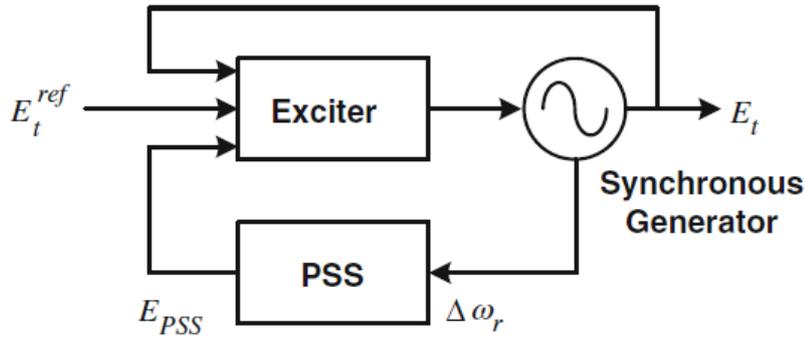
Figure 3.2: The Relationships Between the Generator, Exciter and PSS

The study of a general power system model might be difficult and unnecessary, since the time constants of different dynamic elements are quite different, ranging from $10^{-3}s$, e.g. the switching time constant of power electronic devices like FACTS, voltage source converters (VSCs). to $10s$. e.g, the governor system for controlling the active power input to generators. Thus, for a specific study purpose, a common handling is to consider the fast and slow dynamics separately, which means only part of the dynamic equations corresponding to the elements with interesting behaviors will be remained. In particular, for studying the electromechanical oscillation and angle stability of a power system, which decides the overall power transfer limit, equations associated with the generator, exciter and power system stabilizer models are usually remained, while the amplitude of terminal voltages and the network parameters are assumed as constant. The generator which is the source of the electro-mechanical oscillations, the exciter, which largely contributes to the transient and sub-transient process in the system dynamics, and the power system stabilizer (PSS) which is used to stabilize the electromechanical oscillations. Their relationships are shown in Fig. 3.2.

For any stable interconnected power system, the rotor angles of all generators are

kept still to each other but constantly changing at a certain synchronized speed/frequency which is slightly floating around 60Hz/50Hz. Since the electromechanical oscillation will last for tens of seconds, which is caused by the relative motions among different power angles of concern, a rotating coordinate system with d and q axes at the synchronized speed/frequency is commonly used to represent the generator equations, where the rotor is placed at the d axis.

For power flow analysis, the model used in this work is a phasor model, where the voltages and currents are placed in the synchronization frame with x axes and y axes. This simplifies the power flow analysis and facilitates the analysis of the system dynamics.

For the 4 machine system, the transient generator model is adopted, and for the 16 machine system, the sub-transient generator model is adopted. The transient generator model and sub-transient generator model are among the most widely used generator models with a relatively high accuracy and low complexity.

3.4 Assessing the Proposed Methodology on IEEE Standard Test system 1: Kundur's 4 machine 2 area System

The chosen test system to assess the proposed method is a well known IEEE standard system, the Kundur's 2–area 4–machine system shown in Fig. 3.3. It is a classical system suitable for the analysis of modal oscillations for the validation of small-signal analysis [1], and for the validation of 2nd order Normal Form analysis [48].
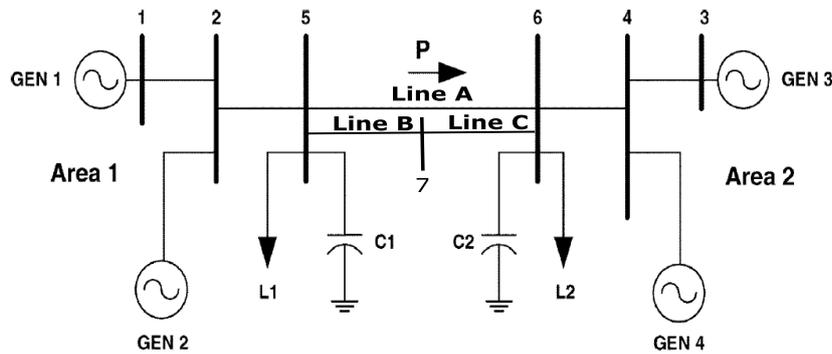
Figure 3.3: IEEE 4 machine test system: Kundur's 2-Area 4-Machine System

The generators are modelled using a two-axis fourth-order model and a thyristor exciter with a Transient Gain Reduction. Loads L1 and L2 are modeled as constant impedances and no Power System Stabilizer (PSS) are used. To make the system robust, each area is equipped with large capacitor banks to avoid a voltage collapse. The data for the system and the selected case are provided in the Appendix section. The full numerical time domain simulation is used to assess the performance of the MNFs in approximating the nonlinear system dynamics, based on the well validated

demo *power_PSS* in Matlab 2015a.

The test case is modeled as a 27th order system with the rotor angle of $G4$ taken as the reference.

3.4.1 Modelling of Mutli-Machine Multi-Area Interconnected Power System

The difficulty in modelling of Multi-Machine Multi-Area interconnected power system lays in the need of unifying the angle reference frame.

For each generator, the rotating frame is different, therefore, a common reference frame with xy orthogonal axes is demanded to do the power flow analysis. The difficulty lays in the transformation between the common reference frame with xy orthogonal axes and the rotating frame ,shown as Fig. 3.4, which consists of the i-th dq rotating frame for generator i, the dq rotating frame for generator k, and the common reference frame xy. All those three frames rotate at the synchronization speed ω_s.

There are different dq rotating frames and depending on which the expression of transient and sub-transient models are established. In this chapter, two most widely used common reference frames are introduced. One is presented with the 4 machine case, and other other is presented with the 16 machine case.
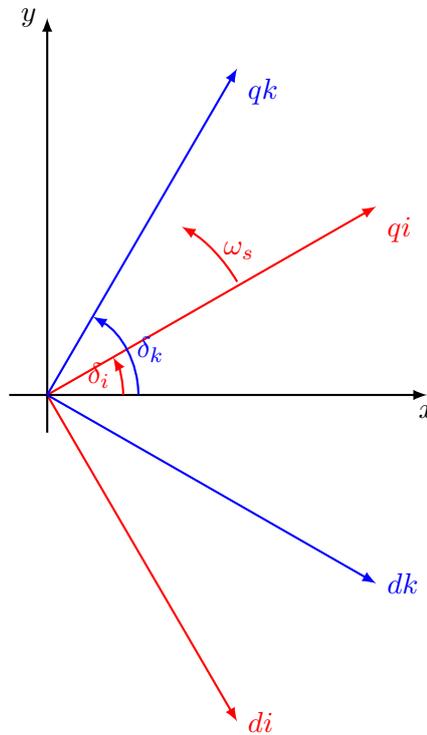
Figure 3.4: The Rotating Frame and the Common Reference Frame of 4 Machine System

3.4.1.1 Transient Generator Model

Exciters (automatic voltage regulators) are considered for the IEEE 4 machine system to represent the industrial situation to the maximum. Therefore, the classical generator model is not appropriate and the 4th order generator model is introduced, along with the 3th order exciter model containing the voltage regulator.
The 4th order generator model in i-th dq rotating frame reads:

$$
\begin{cases}
\dot{\delta}_i = & \omega_s \omega_k \\[2mm]
\dot{\omega}_i = & \frac{1}{2H_i}(P_{mi} - P_{ei} - D_i \omega_i) \\[2mm]
\dot{e}'_{qi} = & \frac{1}{T'_{d0i}}(E_{fqi} - (X_{di} - X'_{di})i_{di} - e'_{qi}) \\[2mm]
\dot{e}'_{di} = & \frac{1}{T'_{q0i}}((X_{qi} - X'_{qi})i_{qi} - e'_{di})
\end{cases}
\tag{3.10}
$$

where $\delta_i, \omega_i, e'_{qi}$ and e'_{di} are the rotor angle, rotor speed, transient voltages along q and d axes respectively of generator i. They are state-variables for each generator, which are crucial in the transient analysis and rotor angle stability. P_{mi} is the mechanical power of generator and ω_s is the synchronized frequency of the system. Then the transformation matrix $\triangle^i_{dq-xy}$ from i-th dq rotating frame to the common reference frame and its inverse can be defined as:

$$
\triangle^i_{dq-xy} = \begin{bmatrix} \sin\delta_i & \cos\delta_i \\ -\cos\delta_i & \sin\delta_i \end{bmatrix} \quad \triangle^i_{xy-dq} = \begin{bmatrix} \sin\delta_i & -\cos\delta_i \\ \cos\delta_i & \sin\delta_i \end{bmatrix}
\tag{3.11}
$$

with $\triangle^i_{dq-xy} = (\triangle^i_{xy-dq})^T$. The generator parameters consist of H_i, D_i, T'_{d0}, T'_{q0}. H_i and D_i are inertia and damping coefficient of generator. T'_{q0} and T'_{d0} are the open-circuit time constants, X_d and X_q are the synchronous reactance, X'_d and X'_q are the transient reactance respectively for d and q axes of generator i.
The power flows are indicated by P_{ei}, i_{di} and i_{qi}, which are the electric power, stator currents of d and q axes respectively of generator i, which depend on both the state variables of i-th generator, as well as the rotor angle of other generators and the network connectivity.

3.4.1.2 Modelling of Exciter (Automatic Voltage Regulators)

To enhance the stability of power system, exciter, which serves as Automatic Voltage Regulator (AVR) is added, as shown as Fig. 3.5. E_{fqi} becomes a state variable described by the differential equation associated with the exciter. And the voltage
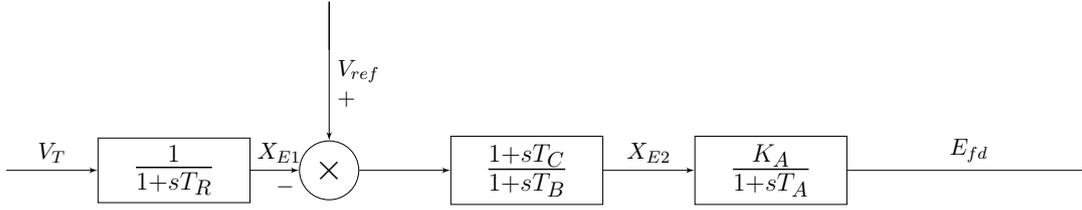
Figure 3.5: Control Diagram of Exciter with AVR

regulators will add up to the exciter model, which reads:

$$
\begin{cases}
\dot{E}_{fdi} = & \frac{K_{Ai}X_{E2i}}{T_{Ai}} - \frac{1}{T_{Ai}}E_{fdi} \\[2mm]
\dot{X}_{E1i} = & -\frac{1}{T_{Ri}}X_{E1i} + \frac{1}{T_{Ri}}V_{Ti} \\[2mm]
\dot{X}_{E2i} = & \frac{1}{T_{Bi}}(\frac{T_{Ci}}{T_{Ri}} - 1)X_{E1i} - \frac{1}{T_{Bi}}X_{E2i} - \frac{T_{Ci}}{T_{Bi}T_{Ri}}V_{Ti} + \frac{1}{T_{Bi}}V_{refi}
\end{cases}
\tag{3.12}
$$

where,
V_T: generator terminal voltage. V_T is given by

$$
V_{Ti} = \sqrt{(e'_{qi} + X'_{di}i_{di})^2 + (e'_{di} - X'_{qi}i_{qi})^2}, i = 1, 2, \cdots, m
\tag{3.13}
$$

V_{ref}: exciter reference voltage

3.4.1.3   Modelling of the Whole System

As indicated in Chapter 1, the power angle stability of the interconnected power system which is composed of generators equivalently means the synchronism of the rotor angles of the generators. And lacking of infinite bus in the multi-machine system leads to zero eigenvalue. In the conventional small signal analysis, the solution is to neglect the zero eigenvalues or taking the rotor angle of one generator as the However, when taking into account the nonlinearities, the zero eigenvalues can not be neglected, since the "zero eigenvalues" may have non-zero nonlinearities and become saddle points.
Therefore, we choose the new state-variables $\delta_{iN} = \delta_i - \delta_N$ with the N-th generator as reference instead of δ_i.
And the equation of the rotor angle is:

$$
\delta_{iN} = \omega_s(\omega_i - \omega_N);
\tag{3.14}
$$

For a detailed model considering the transient voltages and influence of exciter and voltage regulators, the i-th generator has 7 state-variables, $\left[\delta_{iN}, \omega_i, e'_d, e'_q, E_{fdi}, X_{E1i}, X_{E2i}\right]$.

3.4.1.4 Possibility to Add Other Components

As the time constant of turbo governor is much larger than the electro-mechanical time constants, the model of turbo governor is not included. However, it can be added by taken into account the differential equations related to T_m.

3.4.2 Network Connectivity and Nonlinear Matrix

Although the dynamics are described by (3.10) (3.12), it is still far from forming a multi-machine dynamic system for interconnected power system.
The question is:

how the interconnections influence the dynamics?

The answer lays in the network connectivity and the reference frame of the generators. The biggest challenge in dealing with the interconnected power system is the network connectivity
To calculate P_{ei}, a common reference frame (with synchronous speed) is used, where voltages and currents are placed in the $x - y$ frame.
The expressions of P_{ei}, i_{di} and i_{qi} are a system having n generators are [72]:

$$
\begin{cases}
\begin{bmatrix} e'_{xi} \\ e'_{yi} \end{bmatrix} = \triangle^i_{dq-xy} \begin{bmatrix} e'_{di} \\ e'_{qi} \end{bmatrix} \\
I_t = Y \left[e'_{x1}, e'_{y1}, \cdots, e'_{xn}, e'_{yn} \right]^T \\
(\text{denote}) I_t = [i_{x1}, i_{y1}, \cdots, i_{xn}, i_{xn}] \\
P_{ei} = e'_{xi} i_{xi} + e'_{yi} i_{yi}
\end{cases}
\tag{3.15}
$$

where e'_{qi}, e'_{qi} are the transient internal bus voltages of generator i. e'_{xi}, e'_{yi} are their projections in the common reference frame. Y is the admittance matrix of the reduced network to the internal bus of each generator i, including source impedances of generators and constant-impedance loads. I_t is the terminal current of generators. Viewed from all the equations above, assume that all the parameters are constant, the nonlinearities of the power system comes from $\sin \delta$,$\cos \delta$.
(3.15) indicates the network constraints of the 4th order generator model, for which the key point is to derive the admittance matrix Y.
The calculation of Y is in next Section, with programming procedures. Even with all the equations above, the modelling for the power system is not ready for computer-based analysis, since the matrix Y still needs a lot of work and the terms Taylor polinomial terms $H1(\boldsymbol{x})$, $H2(\boldsymbol{x})$, $H3(\boldsymbol{x})$ in (3.1) are not available.
Since it is difficult to find a reference to present the details in modelling the interconnected power system with nonlinearities by a systematic procedures (although insightful mathematical modellings are presented in Refs. [1, 73], some technique

details are not sufficiently illustrated), this job is done in this PhD book.

3.4.2.1 Calculation of Y Matrix

Calculation of Y matrix is composed of two steps:

- Step1: Calculate Y_t from Y_{bus}, reducing the bus admittance matrix to the terminals of the generators;
- Step2: Calculate Y from Y_t, reducing the terminal admittance to the internal bus of generators.

Step1: from Y_{bus} to Y_t

If a system has $m + n$ nodes among which, n nodes are terminals of generators, Y_{bus} is a $[(m + n) \times (m + n)]$ matrix describing the relation between the currents and voltages at each node, and Y_t is a $[n \times n]$ matrix describing the Current-Voltage relation at each terminal.

Y_{bus} is defined by node voltage equation, using the ground potential as reference gives:

$$I_{bus} = Y_{bus}V_{bus} \tag{3.16}$$

$$
\begin{bmatrix}
I_1 \\
I_2 \\
\vdots \\
I_m \\
\hline
I_{m+1} \\
\vdots \\
I_{m+n}
\end{bmatrix}
=
\left[
\begin{array}{ccc|ccc}
Y_{11} & \cdots & Y_{1m} & Y_{1(m+1)} & \cdots & Y_{1(n+m)} \\
Y_{21} & \cdots & Y_{2m} & Y_{2(m+1)} & \cdots & Y_{2(n+m)} \\
\vdots & \ddots & \vdots & \vdots & \ddots & \vdots \\
Y_{m1} & \cdots & Y_{2m} & Y_{m(m+1)} & \cdots & Y_{2(n+m)} \\
\hline
Y_{(m+1)1} & \cdots & Y_{(m+1)m} & Y_{(m+1)(m+1)} & \cdots & Y_{(m+1)(m+n)} \\
\vdots & \ddots & \vdots & \vdots & \ddots & \vdots \\
Y_{(m+n)1} & \cdots & Y_{(m+n)m} & Y_{(m+n)(m+1)} & \cdots & Y_{(m+n)(m+n)}
\end{array}
\right]
\begin{bmatrix}
V_1 \\
V_2 \\
\vdots \\
V_m \\
\hline
V_{m+1} \\
\vdots \\
V_{m+n}
\end{bmatrix}
$$

$$\tag{3.17}$$

where I_{bus} is the vector of the injected bus currents; V_{bus} is the vector of bus voltages measured from the reference node; Y_{bus} is the bus admittance matrix: Y_{ii} (diagonal element) is the sum of admittances connected to bus i; Y_{ij} (off-diagonal element) equals the negative of the admittance between bus i and j.

The admittance matrix depicts the relation between the injected currents and the node voltage. The injected bus currents may come from the generators, loads, batteries, etc. Taking the load at node k as constant impedance, it adds the shunt impedance to the element Y_{kk}.

Since only the generators inject currents into the grid, rewriting (3.16) into (3.18), then all nodes other than the generator terminal nodes are eliminated as follows:

$$
\begin{bmatrix} 0 \\ I_n \end{bmatrix} = \begin{bmatrix} Y_{mm} & Y_{mn} \\ Y_{nm} & Y_{nn} \end{bmatrix} \begin{bmatrix} V_m \\ V_{t,n} \end{bmatrix}
\tag{3.18}
$$

Therefore, from (3.18), it obtains

$$
I_n = \left[Y_{nn} - Y_{nm} Y_{mm}^{-1} Y_{mn} \right] V_{t,n}
\tag{3.19}
$$

Then, the admittance matrix of the reduced network to the terminal bus of generator is defined as:

$$
Y_t = \left[Y_{nn} - Y_{nm} Y_{mm}^{-1} Y_{mn} \right]
\tag{3.20}
$$

However, Y_t is not appropriate for computer-aided calculation as Y_t is a complex matrix and V_t is also a complex matrix.

As $I_{t,i} = i_{xi} + ji_{yi} = \sum_{j=1}^{N} Y_{t,ij} e_j = \sum_{j=1}^{N} (G_{ij}^t + jB_{ij}^t)(e_{xi} + je_{yi}) = \sum_{j=1}^{N} \left[(G_{ij}^t e_{xi} - B_{ij}^t e_{yi}) + j(B_{ij}^t e_{xi} + G_{ij}^t e_{yi}) \right]$

we can therefore define a $[(2N) \times (2N)]$ matrix Y_r as:

$$
Y_r = \begin{pmatrix} \begin{bmatrix} G_{11}^t & -B_{11}^t \\ B_{11}^t & G_{11}^t \end{bmatrix} & \cdots & \begin{bmatrix} G_{1n}^t & -B_{1n}^t \\ B_{1n}^t & G_{1n}^t \end{bmatrix} \\ \vdots & \ddots & \vdots \\ \begin{bmatrix} G_{n1}^t & -B_{n1}^t \\ B_{n1}^t & G_{n1}^t \end{bmatrix} & \cdots & \begin{bmatrix} G_{nn}^t & -B_{nn}^t \\ B_{nn}^t & G_{nn}^t \end{bmatrix} \end{pmatrix}
\tag{3.21}
$$

By Y_t we calculate I_t once the $V_{t,n} = [e_1, e_2, \cdots, e_n]$ is known.

However, as in the dynamics, the state variables are $\left[e_1', e_2', \cdots, e_n' \right]$, an admittance matrix Y is needed which defines as

$$
I_t = Y_r \left[e_{xi}, e_{yi}, \cdots, e_{xn}, e_{yn} \right] = Y \left[e_{xi}', e_{yi}', \cdots, e_{xn}', e_{yn}' \right]
\tag{3.22}
$$

Step2: Obtaining Y from Y_t

Therefore, to obtain Y, the transformation between $[e_{xi}, e_{yi}, \cdots, e_{xn}, e_{yn}]$, $\left[e_{xi}', e_{yi}', \cdots, e_{xn}', e_{yn}' \right]$ should be found at first.

Since

$$\begin{bmatrix} e_{di} \\ e_{qi} \end{bmatrix} = \begin{bmatrix} e_{di}' \\ e_{qi}' \end{bmatrix} - \begin{bmatrix} R_{ai} & -X_{qi}' \\ X_{di}' & R_{ai} \end{bmatrix} \begin{bmatrix} i_{di} \\ i_{qi} \end{bmatrix} = \begin{bmatrix} e_{di}' \\ e_{qi}' \end{bmatrix} - Z_i \begin{bmatrix} i_{di} \\ i_{qi} \end{bmatrix} \qquad (3.23)$$

multiplying both sides by the matrix $\triangle_{dq-xy}^i$

$$\triangle_{dq-xy}^i \begin{bmatrix} e_{di} \\ e_{qi} \end{bmatrix} = \triangle_{dq-xy}^i \begin{bmatrix} e_{di}' \\ e_{qi}' \end{bmatrix} - \triangle_{dq-xy}^i Z_k \begin{bmatrix} i_{di} \\ i_{qi} \end{bmatrix} \qquad (3.24)$$

it therefore leads:

$$\begin{bmatrix} e_{xi} \\ e_{yi} \end{bmatrix} = \begin{bmatrix} e_{xi}' \\ e_{yi}' \end{bmatrix} - \triangle_{dq-xy}^i Z_k \triangle_{xy-dq}^i \begin{bmatrix} i_{xi} \\ i_{yi} \end{bmatrix} \qquad (3.25)$$

Defining $T_1 = \text{diag}\left[\triangle_{dq-xy}^1, \triangle_{dq-xy}^2, \cdots, \triangle_{dq-xy}^i, \cdots, \triangle_{dq-xy}^n\right]$, $T_2 = \text{diag}\left[Z_1, Z_2, \cdots, Z_i, \cdots, Z_n\right]$, and using (3.22), it leads to:

$$\begin{bmatrix} e_{x1} \\ e_{y1} \\ e_{x2} \\ e_{y2} \\ \vdots \\ e_{xn} \\ e_{yn} \end{bmatrix} = \begin{bmatrix} e_{x1}' \\ e_{y1}' \\ e_{x2}' \\ e_{y2}' \\ \vdots \\ e_{xn}' \\ e_{yn}' \end{bmatrix} - T_1 T_2 T_1^{-1} \begin{bmatrix} i_{x1} \\ i_{y1} \\ i_{x2} \\ i_{y2} \\ \vdots \\ i_{xn} \\ i_{yn} \end{bmatrix} \implies Y_r^{-1} \begin{bmatrix} i_{x1} \\ i_{y1} \\ i_{x2} \\ i_{y2} \\ \vdots \\ i_{xn} \\ i_{yn} \end{bmatrix} = Y^{-1} \begin{bmatrix} i_{x1} \\ i_{y1} \\ i_{x2} \\ i_{y2} \\ \vdots \\ i_{xn} \\ i_{yn} \end{bmatrix} - T_1 T_2 T_1^{-1} \begin{bmatrix} i_{x1} \\ i_{y1} \\ i_{x2} \\ i_{y2} \\ \vdots \\ i_{xn} \\ i_{yn} \end{bmatrix}$$
$$(3.26)$$

$$\implies Y_r^{-1} + T_1 T_2 T_1^{-1} = Y^{-1}$$

Therefore, it obtains:

$$Y = (Y_r^{-1} + T_1 T_2 T_1^{-1})^{-1} \qquad (3.27)$$

If $X_q' = X_d'$, then $\triangle_{dq-xy}^i Z_i = Z_i \triangle_{dq-xy}^i$, then $T_1 T_2 = T_2 T_1$, so

$$Y = (Y_r^{-1} + T_2)^{-1} \qquad (3.28)$$

In our test systems, $X'_{di} = X'_{qi}$ for simplicity, and the calculation of matrix Y is as (3.28).

3.4.2.2 Calculating the Nonlinear Matrix

The next step is to calculate the nonlinear matrix $H1, H2, H3$ in (3.2).
Since Y is obtained, the function of $I_{dq} = [i_{d1}, i_{q1}, \cdots, i_{dn}, i_{qn}]$ on $e' = \left[e'_{d1}, e'_{q1}, \cdots, e'_{dn}, e'_{qn} \right]$ can be obtained as:

$$\left[i_{d1}, i_{q1} \cdots, i_{di}, i_{qi}, \cdots, i_{dn}, i_{qn} \right]^T = T_1^{-1} Y T_1 \left[e'_{d1}, e'_{q1}, \cdots, e'_{di}, e^{qi}, \cdots, e'_{dn}, e'_{qn} \right]^T \tag{3.29}$$

Therefore Y_δ is defined as

$$Y_\delta = T_1^{-1} Y T_1 \tag{3.30}$$

, where Y_δ is a nonlinear matrix and is time-variant in the system dynamics, as $\sin \delta_i, \cos \delta_i$ varies as the rotor oscillates. In (3.29), only state-variables will exist in (3.10) (3.12). And the system can be formed as:

$$\begin{cases} \dot{\delta_i} &= \omega_s(\omega_k - 1) \\[2mm] \dot{\omega_i} &= \frac{1}{2H_i}(P_{mi} - P_{ei} - D_i\omega_i) \\[2mm] \dot{e}'_{qi} &= \frac{1}{T'_{d0i}}(E_{fqi} - (X_{di} - X'_{di})i_{di} - e'_{qi}) \\[2mm] \dot{e}'_{di} &= \frac{1}{T'_{q0i}}((X_{qi} - X'_{qi})i_{qi} - e'_{di}) \\[2mm] \dot{E}_{fdi} &= \frac{K_{Ai}X_{E2i}}{T_{Ai}} - \frac{1}{T_{Ai}}E_{fdi} \\[2mm] \dot{X}_{E1i} &= -\frac{1}{T_{Ri}}X_{E1i} + \frac{1}{T_{Ri}}V_{Ti} \\[2mm] \dot{X}_{E2i} &= \frac{1}{T_{Bi}}(\frac{T_{Ci}}{T_{Ri}} - 1)X_{E1i} - \frac{1}{T_{Bi}}X_{E2i} - \frac{T_{Ci}}{T_{Bi}T_{Ri}}V_{Ti} + \frac{1}{T_{Bi}}V_{refi} \end{cases} \tag{3.31}$$

which can be rewritten as (3.31)

$$
\begin{bmatrix} \dot{\delta_i} \\ \dot{\omega_i} \\ \dot{e}'_{qi} \\ \dot{e}'_{di} \\ \dot{E_{fdi}} \\ \dot{X_{E1i}} \\ \dot{X_{E2i}} \end{bmatrix} = \begin{bmatrix} 0 & \omega_s & 0 & 0 & 0 & 0 & 0 \\ 0 & -\frac{D_i}{2H_i} & 0 & 0 & 0 & 0 & 0 \\ 0 & 0 & -\frac{1}{T'_{d0i}} & 0 & \frac{1}{T'_{d0i}} & 0 & 0 \\ 0 & 0 & 0 & -\frac{1}{T'_{q0i}} & 0 & 0 & 0 \\ 0 & 0 & 0 & 0 & -\frac{1}{T_{Ai}} & 0 & \frac{K_{Ai}}{T_{Ai}} \\ 0 & 0 & 0 & 0 & 0 & -\frac{1}{T_{Ri}} & 0 \\ 0 & 0 & 0 & 0 & 0 & \frac{1}{T_{Bi}}(\frac{T_{Ci}}{T_{Ri}}-1) & -\frac{1}{T_{Bi}} \end{bmatrix} \begin{bmatrix} \delta_i \\ \omega_i \\ e'_{qi} \\ e'_{di} \\ E_{fdi} \\ X_{E1i} \\ X_{E2i} \end{bmatrix} + \begin{bmatrix} 0 \\ -\frac{e'_{di}i_{di}+e'_{qi}i_{qi}}{2H_i} \\ -\frac{X_{di}-X'_{di}}{T'_{d0i}}i_{di} \\ \frac{X_{qi}-X'_{qi}}{T'_{q0i}}i_{qi} \\ 0 \\ \frac{V_{Ti}}{T_{Ri}} \\ -\frac{T_{Ci}}{T_{Bi}T_{Ri}}V_{Ti} \end{bmatrix} + \begin{bmatrix} 0 \\ \frac{P_{mi}}{2H_i} \\ 0 \\ 0 \\ 0 \\ 0 \\ \frac{V_{refi}}{T_{Bi}} \end{bmatrix}
$$

(3.32)

when there is no disturbance in the voltage reference and power reference.
As $[I_{dq}] = Y_\delta \left[e'_{dq} \right]$, are nonlinear functions of $\delta_i, e'_{di}, e'_{qi}$, (3.31) can be rewritten as:

$$
x_i = \begin{bmatrix} \delta_i \\ \omega_i \\ e'_{qi} \\ e'_{di} \\ E_{fdi} \\ X_{E1i} \\ X_{E2i} \end{bmatrix}, A^g_i = \begin{bmatrix} 0 & \omega_s & 0 & 0 & 0 & 0 & 0 \\ 0 & -\frac{D_i}{2H_i} & 0 & 0 & 0 & 0 & 0 \\ 0 & 0 & -\frac{1}{T'_{d0i}} & 0 & 0 & 0 & 0 \\ 0 & 0 & 0 & -\frac{1}{T'_{q0i}} & 0 & 0 & 0 \\ 0 & 0 & 0 & 0 & -\frac{1}{T_{Ai}} & 0 & \frac{K_{Ai}}{T_{Ai}} \\ 0 & 0 & 0 & 0 & 0 & -\frac{1}{T_{Ri}} & 0 \\ 0 & 0 & 0 & 0 & 0 & \frac{1}{T_{Bi}}(\frac{T_{Ci}}{T_{Ri}}-1) & -\frac{1}{T_{Bi}} \end{bmatrix}, N_i(X) = \begin{bmatrix} 0 \\ -\frac{e'_{di}i_{di}+e'_{qi}i_{qi}}{2H_i} \\ -\frac{X_{di}-X'_{di}}{T'_{d0i}}i_{di} \\ \frac{X_{qi}-X'_{qi}}{T'_{q0i}}i_{qi} \\ 0 \\ \frac{V_{Ti}}{T_{Ri}} \\ -\frac{T_{Ci}}{T_{Bi}T_{Ri}}V_{Ti} \end{bmatrix}, U_i = \begin{bmatrix} 0 \\ \frac{P_{mi}}{2H_i} \\ 0 \\ 0 \\ 0 \\ 0 \\ \frac{V_{refi}}{T_{Bi}} \end{bmatrix}
$$

(3.33)

Therefore, the whole system can be written as:

$$
\begin{bmatrix} \dot{x_1} \\ \dot{x_2} \\ \vdots \\ \dot{x_n} \end{bmatrix} = \begin{bmatrix} A^g_1 & 0 & \cdots & 0 \\ 0 & A^g_2 & \cdots & 0 \\ \vdots & \vdots & \ddots & \vdots \\ 0 & 0 & \cdots & A^g_n \end{bmatrix} \begin{bmatrix} x_1 \\ x_2 \\ \vdots \\ x_n \end{bmatrix} + \begin{bmatrix} N_1(x) \\ N_2(x) \\ \vdots \\ N_n(x) \end{bmatrix} + \begin{bmatrix} U_1 \\ U_2 \\ \vdots \\ U_n \end{bmatrix}
$$

(3.34)

$$
\dot{x} = A_g x + N(x) + U
$$

(3.35)

where $N_i(x)$ is the ith row of $N(x)$, which can be calculated by (3.29).
Therefore, doing the Taylor series with the stable equilibrium point (SEP) as the point of expansion. The SEP is calculated by the power flow analysis.

Free Oscillation

If free oscillation is studied (i.e $U = 0$) (3.35) becomes:

$$\triangle\dot{x} = A_g\triangle x + N1(\triangle x) + \frac{1}{2!}N2(\triangle x) + \frac{1}{3!}N3(\triangle x) \tag{3.36}$$

where $N1,N2,N3$ are first-order, second order and third-order derivative of $N(x)$. Then, for the definition in (3.2), the nonlinear coefficients can be extracted as:

$$H1 = Ag + N1, H2 = N2, H3 = N3 \tag{3.37}$$

As observed from (3.37), the linearization matrix is $Ag + N1$ for the multi-machine system instead of Ag for the single machine system. $N1$ counts for the influence of power flows between the generators on the eigenvalue analysis. $N2, N3$ account for the second order nonlinear interactions and third order nonlinear interactions. Therefore, all the procedures of Normal From transformations can be followed.

3.4.3 Programming Procedures for Normal Form Methods

3.4.3.1 How to Initialize the Normal Form Methods Calculation

1. Forming the system dynamic equation: it is a 28th model.
   - For each generator station: it is 4th for generator, 3 for the AVR and Thyristor Exciter.
   - For the network: the systems of equations of 4 generator are concatenated by the Bus voltage and Flow currents in the network.
2. Equilibrium Points: Doing the Power Flow Analysis for the steady state, and obtaining the equilibrium points $\boldsymbol{x_{eq}}$ to calculate all the normal form coefficients. (Software: PSAT)
3. Perturbation Condition: Recording all the disturbances of the state-variables when the generator power angle reaches the maximum $\boldsymbol{x_{init}}$.

3.4.3.2 Programming Steps of the Normal Form Methods

The steps can be detailed as:
1. Forming the system of equations with the first Taylor polynomial term, 2nd Taylor polynomial term $F2_{kl}^{j}$ and 3rd Taylor polynomial term $F3_{pqr}^{j}$ calculated with the equilibrium point;
2. Calculate Eigen-matrix Λ.
3. Normal Form Coefficients Calculation: $h2_{kl}^{j}$ and $h3_{pqr}^{j}$.
4. Using x_{init} search the initial values for z_{init}, w_{init} by Newton-Raphson Method.
5. Calculating the Normal Dynamics by Runge-Kutta Method.
6. Reconstruction the system using dynamic coefficients $h2_{kl}^{j}$ and $h3_{pqr}^{j}$.

3.4.3.3 The Procedures of Calculating the Matrices

1. Initialize the parameters and input the matrix Y_{bus}

2. Calculate $Y_{bus} \rightarrow Y_t \rightarrow Y$, by Eqs. (3.20) (3.28)
3. Calculate Y_{delta} from (3.30).
4. Calculate $N(x)$ from A_g from (3.34)
5. Calculate $N1(x), N2(X), N3(x)$ from (3.36)
6. Calculate coefficients $H1, H2, H3$ from (3.37)

3.4.4 Cases Selected and Small Signal Analysis

The oscillatory modes for the selected cases are listed in Tab. 3.1 and 3.2 with the associated pseudo frequency, time-constant and dominate states. It gives a clear picture of the physical property of the system dynamics by small-signal analysis. Some stable real modes are not listed for the sake of compactness.

The cases analyzed in this section have been selected to highlight information provided by the 3rd order Normal Form analysis. The selected system operating conditions for the study are highly stressed cases where the system is close to the voltage collapse, characterized by a tie line flow of 420MW from Area1 to Area2. To consider the emergence of renewable energy based generators, some modifications are made compared to the conventional small-signal and 2nd-order-based NF analysis that have been already conducted on the same test case. The powers generated by generators G1 and G2 in Area1 are unbalanced to consider the production of energy from distant renewable energy based generators in large areas.

The results of conventional small-signal analysis are shown in Tab. 3.1 and Tab. 3.2, where the damping, frequency, time-constant and the dominant states of the oscillatory modes are listed.

Those results come from two cases that are considered:
1. Case 1: This case represents a poorly damped situation, where the damping ratio of the inter-area mode is only 5.9% and the system is at its limit of stability according to a linear analysis. A three phase short-circuited fault is applied at Bus 7 and after 0.41s, line B and line C are tripped. The exciter gain Ka is set as 150 for all generators.
2. Case 2: This case represents a situation where the damping ratio of two oscillatory modes is negative (modes (5,6) and (7,8), as indicated in Tab. 3.2). The negative damping is introduced by changing the gain of the 4 thyristor exciters by a higher value ($K_a = 240$). A three phase short-circuited fault is applied at Bus 7 and after $0.10s$, line B and line C are tripped.

The transient analysis of the overall system based on the NF analysis is presented in the next section, where G1 and G2 exhibit predominant electromechanical oscillations.

Table 3.1: Oscillatory Modes: Case 1

Mode #	Eigenvalue	Pseudo-Freq (Hz)	Damping Ratio (%)	Time Constant $t = \frac{1}{\zeta \omega_n}$	Dominant States
5,6	$-3.46 \pm j93.2$	14.8	3.17	0.289	$E'_{q1}, E'_{q2}, E'_{q3}, E'_{q4}$
7,8	$-5.94 \pm j88.3$	14.0	6.71	0.168	Control unit G2
9,10	$-18.1 \pm j62.8$	9.99	27.7	0.055	Control unit (G3,G4)
11,12	$-17.3 \pm j64.5$	10.3	25.9	0.057	Control unit G1
13,14	$-1.51 \pm j6.73$	1.07	21.9	0.662	Local, Area $2(\delta_1, \delta_2, \omega_1, \omega_2)$
15,16	$-1.69 \pm j6.51$	1.03	25.1	0.593	Local, Area $1(\delta_1, \delta_2, \omega_1, \omega_2)$
17,18	$-0.135 \pm j2.28$	0.36	5.9	7.41	Inter–area $(\delta_1, \delta_2, \delta_3, \delta_4)$

Table 3.2: Oscillatory Modes: Case 2

Mode #	Eigenvalue	Pseudo-Freq (Hz)	Damping Ratio (%)	Time Constant $t = \frac{1}{\zeta \omega_n}$	Dominant States
5,6	$3.61 \pm j107.9$	17.2	-3.34	-0.277	$E'_{q1}, E'_{q2}, E'_{q3}, E'_{q4}$
7,8	$1.73 \pm j104.1$	16.6	-1.66	-5.79	Control unit G2
9,10	$-11.4 \pm j77.8$	12.4	14.5	0.088	Control unit (G3,G4)
11,12	$-10.3 \pm j79.9$	12.7	12.8	0.097	Control unit G1
13,14	$-1.56 \pm j6.64$	1.05	22.9	0.641	Local, Area $2(\delta_1, \delta_2, \omega_1, \omega_2)$
15,16	$-1.72 \pm j6.44$	1.02	25.8	0.581	Local, Area $1(\delta_1, \delta_2, \omega_1, \omega_2)$
17,18	$-0.132 \pm j2.23$	0.36	5.92	7.55	Inter–area $(\delta_1, \delta_2, \delta_3, \delta_4)$

3.4.5   Case 1-2:   Benefits of using 3rd order approximation for modal interactions and stability analysis
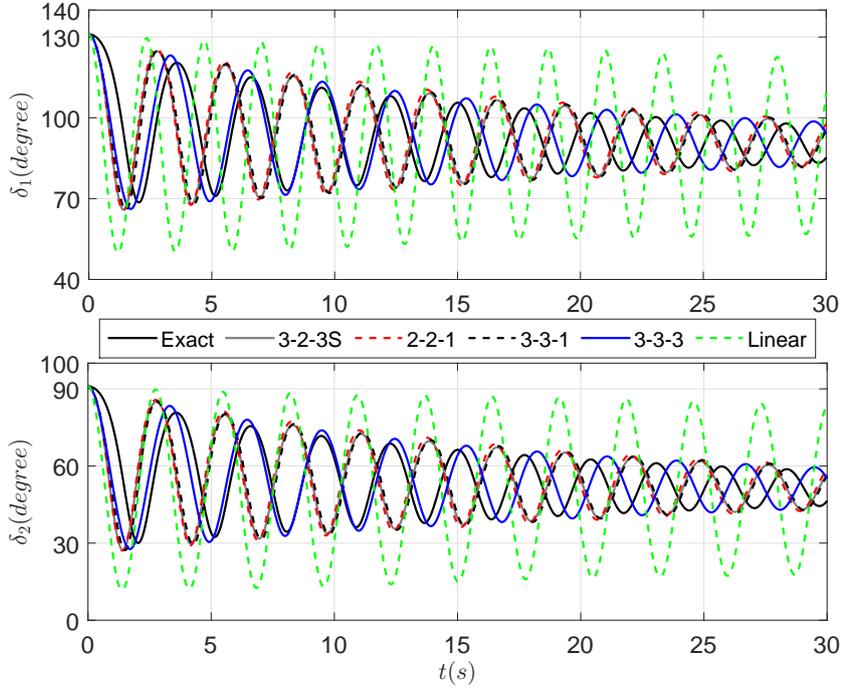
Figure 3.6: Comparison of different NF approximations: Case 1

When the system is close to its limits of stability as depicted by Case 1, Fig.3.6 shows that the linear analysis gives wrong predictions concerning the dynamic behavior of the system. 2nd-order and 3rd-order Normal Form approximations can both better model the system dynamic response than the Linear Method.

The proposed third-order approximation, called 3-3-3, is superior over the other methods since it makes possible to model the interactions of oscillatory of non-oscillatory modes up to order 3, contributing to a better modeling of the frequency variation of the oscillations as recently formulated in [4], [74].

Concerning Case 2, the system is such that the linear analysis leads to the computation of two oscillatory modes with a negative damping (See modes (5,6) and (7,8) given by Tab. 3.2). According to the conventional small-signal stability analysis, the overall system is then considered as unstable. However, as shown in Fig. 3.8, the system's nonlinearities contribute to the overall stability of the system [5]. The comparison of the different NF approximations shows that only methods keeping 3rd-order terms in the normal dynamics are able to predict the stability of the system (3-2-3S and proposed 3-3-3 approximations).

The inear analysis predicts that Gen 1 loses its synchronization (the power angle reaches 180°), at around 19s. In the physical meaning, it indicates that the synchronization torque is weak if only its linear part is considered. From the eigineering view, considering that the power system works in the nonlinear domain, its working
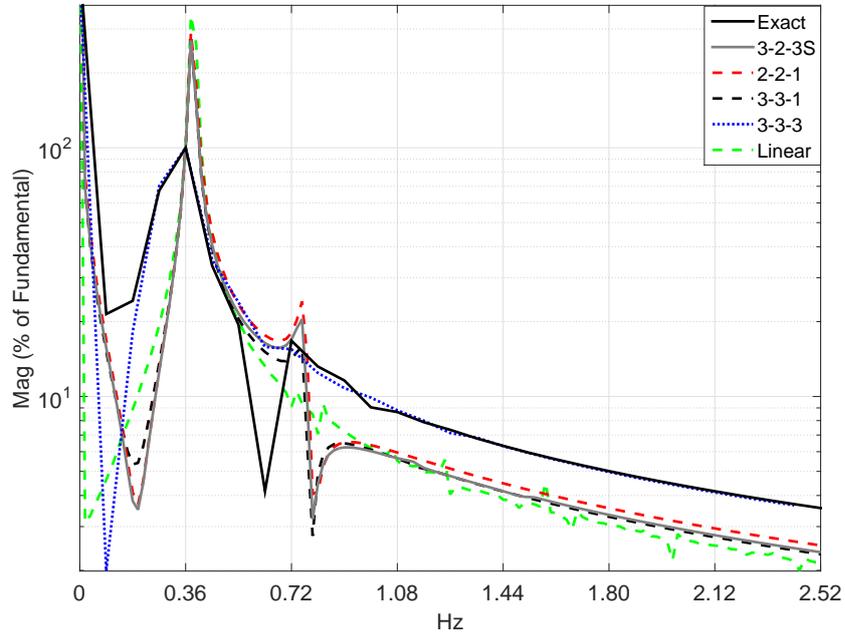
Figure 3.7: FFT Analysis of different NF approximations: Case 1
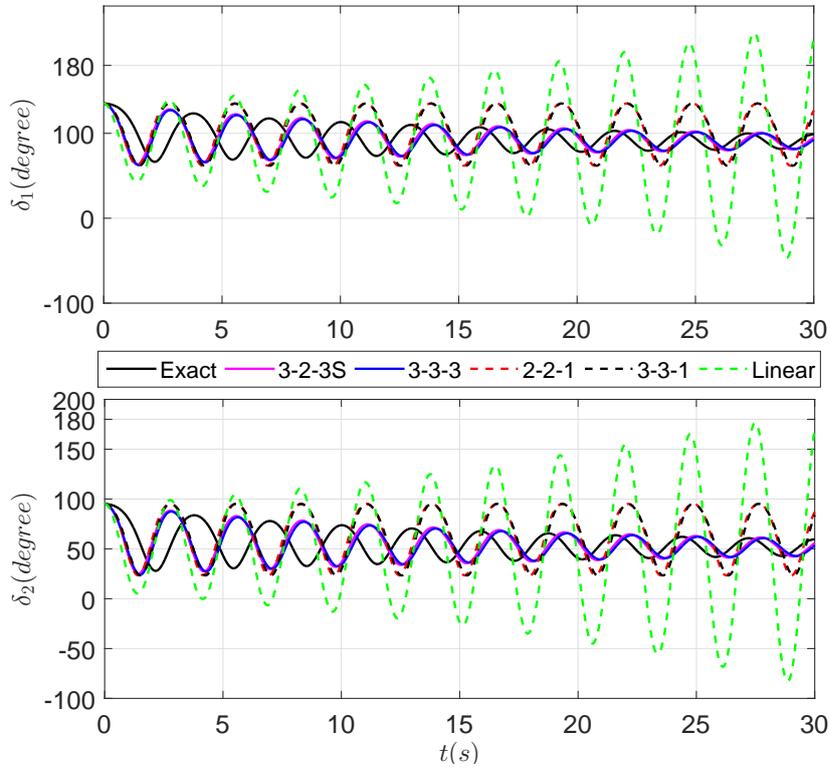
Figure 3.8: Comparison of different NF approximations: Case 2

capacity can be exploited to the maximum.

Although 2-2-1 and 3-3-1 have done a better job in considering the higher-order modal participation, they cannot predict the stability as their Normal Dynamic is linear and the stability only depends on the eigenvalues.

By keeping trivially resonant 3rd order terms in the Normal Dynamics, 3-2-3S and 3-3-3 can better predict the stability of the system. Shown in all the cases, method 3-3-3 is more accurate and the results are more realistic.
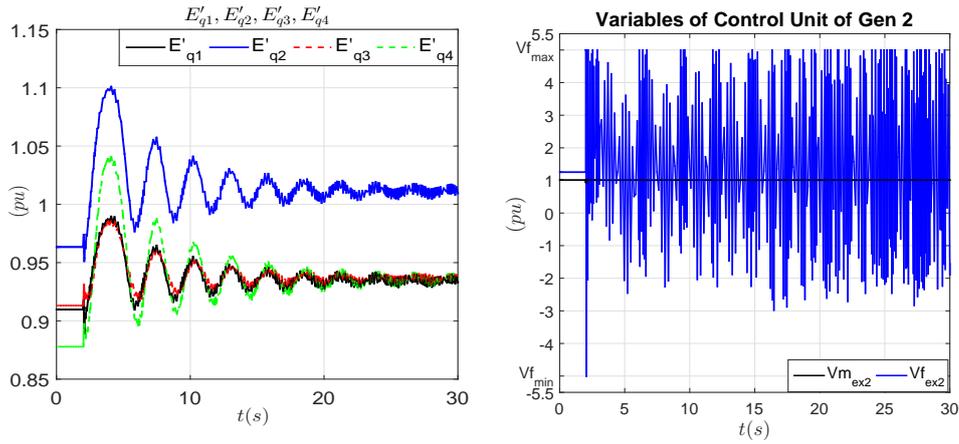
Figure 3.9: Dynamics of Dominant State Variables Associated to Positive Eigenvalue Pairs: Case 2

The dynamic responses by numerical simulation of the state-variables associated with the modes having a negative damping are shown in Fig. 3.9 (the left for $E'_{q1}, E'_{q2}, E'_{q3}, E'_{q4}$ and the right for the Control Unit of Gen2). Even if some eigenvalues have a negative real part, the damping afforded by the nonlinearities have to be taken into account for a correct stability analysis.

3.4.6   Nonlinear Analysis Based on Normal Forms

It has been validated by the time-domain simulation in the previous section that the normal dynamics well approximate the system dynamics. In this section, the MNF is used to make quantitative analyses of the system dynamics using the nonlinear indexes.

3.4.6.1   Initial Condition and Magnitude at Fundamental Frequency

The initial conditions in the Jordan form (y^0) and for methods 2-2-1 ($z0221$), 3-3-1 ($z0331$) and 3-3-3 ($z0333$) are listed in Tab. 3.3. It has to be noticed that method 3-2-3S has the same initial conditions as method 2-2-1, i.e. $z0323 = z0221$. From the initial condition, it can be seen that the magnitude of the ratio of y^0_{17}, $z0221_{17}$, $z0331_{17}$, $z0333_{17}$ over $z0333_{17}$ is respectively equals to $124\%, 107.8\%, 107.7\%$ and 100%, which approximately matches the ratios at the fundamental frequency of the different curves in Fig. 3.7.

Table 3.3: Initial Conditions

j	$y0$	$z0221$	$z0331$	$z0333$
5	$5.14 + j2.93$	$3.89 + j2.38$	$3.88 + j2.38$	$0.3105 + j0.3263$
7	$-6.36 - j2.73$	$-3.24 - j0.95i$	$-3.24 - j0.95$	$-0.36 - j2.49$
9	$-1.35 - j1.39$	$0.48 - j3.14$	$0.58 - j2.3$	$0.75 - j1.59$
11	$-9.84 - j4.25$	$-6.07 - j4.58$	$-6.27 - j4.58$	$-0.54 - j3.84$
13	$-0.25 - j0.21$	$-0.27 - j0.08$	$-0.226 - j0.085$	$-0.20 - 0.22i$
15	$0.32 + j0.10$	$0.04 - 0.0012i$	$0.05 - j0.0012$	$0.072 + j0.05$
17	$0.87 + j2.52$	$0.82 + j2.16$	$0.84 + j2.10$	$1.70 + j1.31i$

Table 3.4: 3rd Order Coefficients for Mode $(17, 18)$

p, q, r	$(DF2h2)^j_{pqr}$	$F3^j_{pqr}$	$h3^j_{pqr}$
(17,17,17)	$0.046 - j0.118$	$0.029 + j0.034$	$0.017 - j0.019$
$MI3^j_{pqr}$	$\overline{h3^{17}_{17,17,17}}$	$\overline{MI3^j_{pqr}}$	$Tr3$
0.1220	$0.0068 + j0.008$	0.0560	0.33

3.4.6.2 Distribution of the Frequency Spectrum

The third order spectrum can be found by $MI3^j_{pqr}$. Among all the $MI3^j_{pqr}$, $MI3^{17}_{(17)(17)(17)}$ and $MI3^{18}_{(18)(18)(18)}$ contribute most to the 3rd order spectrum of the rotor angle oscillations. The 3rd order coefficients for mode $(17, 18)$ are listed in Tab. 3.4, with $\overline{MI3^j_{pqr}}$ calculated by $\overline{h3^j_{pqr}}$.

Comparing results of Tab. 3.4 with data extracted frm Fig. 3.7, it is seen that: 1) $MI3^{17}_{17,17,17} = 0.11 = 11\%$ approximately matches the magnitude ratio of the 3rd order component at approximately $1Hz$; 2) ignoring $DF2h2$, $\overline{h3^j_{pqr}}$ is small and leads to a too modest prediction of the 3rd order interaction $\overline{MI3^j_{pqr}} = 0.056 = 5.6\%$.

A deeper analysis can be made using NF methods compared to FFT analysis. For example, $MI3^{17}_{17,26,27} = 0.45$ indicates a strong nonlinear interaction, however, since $Tr = 6.7341 \times 10^{-4}$ and $MI3 \times Tr = 3.03 \times 10^{-4}$ such a short duration will be difficult to be captured by FFT analysis.

3.4.6.3 Frequency Shift of the Fundamental Component

It can be also noted that there is a shift in the fundamental frequency. As already mentioned, it is indicated by the imaginary part of index SII^j_{2l}. Among all those coefficients, coefficients SII^j_{18} are predominant and $Tr3$ indicates a long-time influence as listed in Tab. 3.5. Although the real part of SII^j_{18} are too small to contribute

to the stability compared to λ_j, its imaginary part indicates that the there is a frequency shift added to the eigen-frequency.

Table 3.5: Resonant Terms associated with Mode $(17, 18)$

j	SII_{18}^j	$\lambda_j + \lambda_{2l} + \lambda_{2l-1}$	$Tr3$
5	$-1.30 - j2.59$	$-3.73 + j93.2$	0.93
7	$0.48 + j0.96$	$-6.21 + j88.3$	0.96
9	$0.0117 + j0.17$	$-18.37 + j62.8$	0.98
11	$-0.51 - j1.52$	$-17.57 + j64.5$	0.98
13	$0.074 - j0.25$	$-1.78 + j6.73$	0.85
15	$0.89 + j0.532$	$-1.96 + j6.51$	0.86
17	$0.12 - j0.678$	$-0.405 + j2.28$	0.33

This analysis corroborates with the analysis of the frequency spectrum in Fig. 3.7. If there are no resonant terms in the normal forms, the fundamental frequency of the system oscillatory dynamics will be exactly as ω_j.

3.4.6.4   Stability Assessment

Seen from Tab. 3.6, the nonlinear interactions can enhance (e.g $MI3_{5,5,6}^5$) or weaken the stability (e.g $MI3_{7,17,18}^j$). Only taking into account one specific $MI3$ without considering its time pertinence will lead to a wrong prediction. In this sense, the stability assessment proposed by method 3-3-3 is more rigorous and comprehensive than method 3-2-3. As $SI^5 \ll 0, SI^7 \ll 0$, modes $(5,6)$ and $(7,8)$ are essentially stable, as validated by the time domain analysis, as shown in Fig. 3.8.

The proposed nonlinear stability indicators make possible to better use the power transfer capability of the power grid. For example, in the studied case, the high-gain exciter can improve the system response to a fault, which is not shown using the conventional eigen-analysis.

3.5   Applicability to Larger Networks with More Complex Power System Models

For larger networks with more complex models, method 3-3-3 is more demanding since the modeling of modal interactions is more complex, such as for the case of the New England New York 16 machine 5 area system [75], whose typology is shown in

Table 3.6: Stability Indexes of Mode $(5,6),(7,8)$

$2l-1$	SII_{2l}^5	$Tr3$	$real(SII) \times Tr3^5$
5	$-53.54 - j109.77$	0.33	-17.6682
9	$-3.37 - j6.34$	-0.18	-0.63
13	$-3.06 - j7.56$	7.50	-22.95
15	$-6.5 - j11.7$	22.50	-146.25
17	$-1.60 - j4.15$	1.08	-1.72

$$SI^5 = 3.61 - 17.6682 - 0.63 + 22.95 - 146.25 - 1.72 = -185.6082$$

$2l-1$	SII_{2l}^7	$Tr3$	$real(SII) \times Tr3^7$
5	$-105.3 - j221.7$	0.2	-21.06
9	$-5.0 - j8.94$	0.0821	-0.41
13	$-3.21 - j8.81$	1.24	-3.99
15	$-4.57 - j8.67$	1.01	-4.62
17	$0.29 + j1.31$	1.1801	0.34

$$SI^7 = 1.73 - 21.06 - 0.41 - 3.99 - 4.62 + 0.34 = -28.01$$

Fig. 3.10. It is composed of five geographical regions out of which NETS and NYPS are represented by a group of generators whereas, the power import from each of the three other neighboring areas are approximated by equivalent generator models (G14 to G16). G13 also represents a small sub-area within NYPS. Generators G1 to G8 and G10 to G12 have DC excitation systems (DC4B); G9 has a fast static excitation (ST1A), while the rest of the generators (G13 to G16) have manual excitation as they are area equivalents instead of being physical generators [75]. The realistic parameters and well validated Simulink models can be found in [75, 76], where the generators are modeled with the sub-transient models with four equivalent rotor coils. There are 15 pairs of electromechanical modes, among which there are 4 inter-area modes. This system is unstable when no PSS or only one PSS is installed [75].
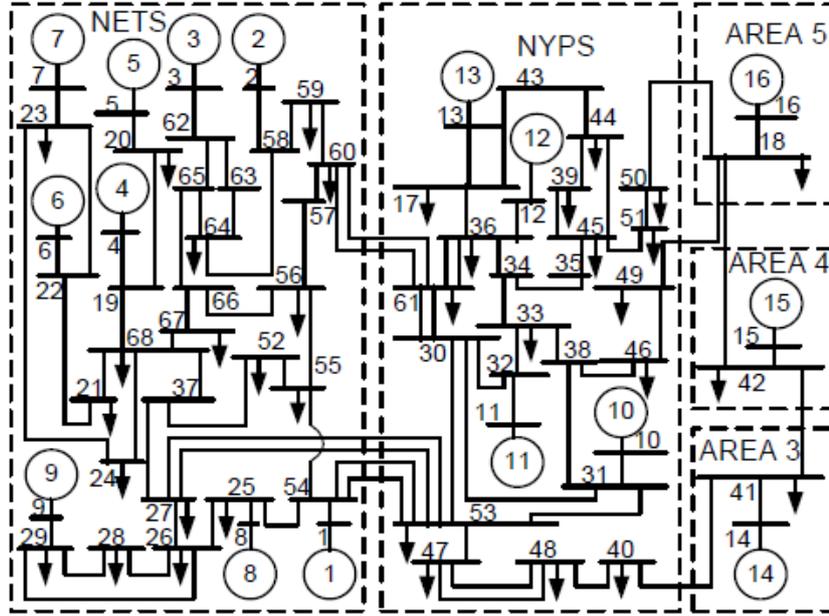
Figure 3.10: New England New York 16-Machine 5-Area Test System [75]

3.5.1   Modelling of the System of Equations

3.5.1.1   The Sub-transient Generator Model

A frequently used generator model is the sub-transient model with four equivalent rotor coils as per the IEEE convention. The slow dyanmics of the governors are ignored, and the mechanical orques to the generators are taken as constant inputs. Standard notations are followed in the following differential equations which represent the dynamic behavior of the ith generator [77]:

$$
\begin{cases}
\frac{d\delta_i}{dt} = \omega_s(\omega_i - 1) = \omega_s S_{mi} \\[2mm]
2H_i\frac{S_{mi}}{dt} = (T_{mi} - T_{ei}) - D_i S_{mi} \\[2mm]
T'_{q0i}\frac{dE'_{di}}{dt} = -E'_{di} + (X_{qi} - X'_{qi})\{-I_{qi} + \frac{(X'_{qi}-X''_{qi})}{(X'_{qi}-X_{lsi})^2}((X'_{qi} - X_{lsi})I_{qi} - E'_{di} - \psi_{2qi})\} \\[2mm]
T'_{d0i}\frac{dE'_{qi}}{dt} = E_{fdi} - E'_{qi} + (X_{di} - X'_{di})\{I_{di} + \frac{(X'_{di}-X''_{di})}{(X'_{di}-X_{lsi})^2}(\psi_{1di} + (X'_{di} - X_{lsi})I_{di} - E'_{qi})\} \\[2mm]
T''_{d0i}\frac{d\psi_{1di}}{dt} = E'_{qi} + (X'_{di} - X_{lsi})I_{di} - \psi'_{1di})\} \\[2mm]
T''_{q0i}\frac{d\psi_{2qi}}{dt} = -E'_{di} + (X'_{qi} - X_{lsi})I_{qi} - \psi'_{2qi})\} \\[2mm]
T_{ci}\frac{dE'_{dci}}{dt} = I_{qi}(X''_{di} - X''_{qi}) - E'_{dci}
\end{cases}
\tag{3.38}
$$

where, $T_{ei} = E'_{di}I_{di}\frac{(X''_{qi}-X_{lsi})}{(X'_{qi}-X_{lsi})} + E'_{qi}I_{qi}\frac{(X''_{di}-X_{lsi})}{(X'_{di}-X_{lsi})} - I_{di}I_{qi}(X''_{di} - X''_{qi}) + \psi_{1di}I_{qi}\frac{(X''_{di}-X''_{di})}{(X'_{di}-X_{lsi})} - \psi_{2qi}I_{di}\frac{(X''_{qi}-X''_{qi})}{(X'_{qi}-X_{lsi})}$

and $I_{qi}+jI_{di} = 1/(R_{ai}+jX''_{di})\{E'_{qi}\frac{(X''_{di}-X_{lsi})}{(X'_{di}-X_{lsi})}+\psi'_{1di}\frac{(X'_{di}-X''_{di})}{(X'_{di}-X_{lsi})}-V_{qi}+j[E'_{di}\frac{(X''_{qi}-X_{lsi})}{(X'_{qi}-X_{lsi})} - \psi'_{2qi}\frac{(X'_{qi}-X''_{qi})}{(X'_{qi}-X_{lsi})} - V_{di} + E'_{dci}]\}$
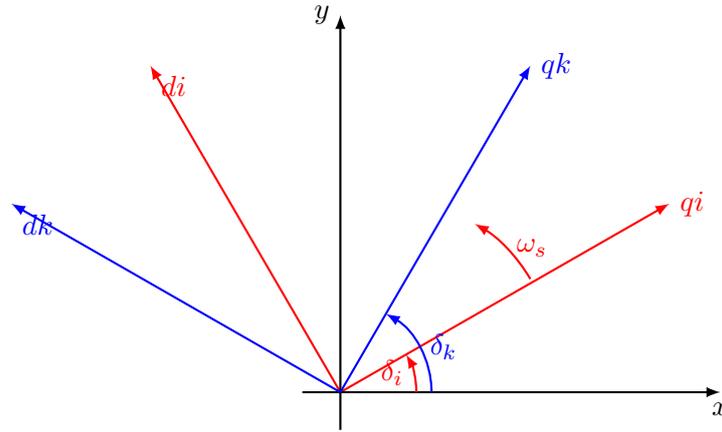
Figure 3.11: The Rotating Frame and the Common Reference Frame of 16 Machine System

The reference frame transformation from the DQ frame to dq frame is

$$I = I_q + jI_d = e^{j\delta_i}(I_x + I_y); V_g = V_x + jV_y = e^{j\delta_i}(V_{qi} + jV_{di});$$

3.5.1.2 Excitation Systems (AVRs)

Two types of automatic voltage regulators (AVRs) are used for the excitation of the generators. The first type is an IEEE standard DC exciter (DC4B) (shown in Fig. 3.12) and the second type is the standard static exciter (ST1A).

The differential equations governing the operation of the IEEE-DC4B excitation system are given by (3.39), while for the IEEE-ST1A are given by (3.40):

$$\begin{cases} T_e\frac{dE_{fd}}{dt} = V_a - (K_eE_{fd} + E_{fd}A_{ex}e^{B_{ex}E_{fd}}) \\ \\ T_a\frac{dV_a}{dt} = K_aV_{PID} - V_a \\ \\ V_{PID} = (V_{ref} + V_{ss} - V_r - \frac{K_f}{T_f}(E_{fd} - V_f))(K_p + \frac{K_i}{s} + \frac{sK_d}{T_d+1}) \\ \\ T_r\frac{dV_r}{dt} = V_t - V_r \\ \\ T_f\frac{dV_f}{dt} = E_{fd} - V_f \end{cases} \quad (3.39)$$

where $E_{fdmin} \leq V_a \leq E_{fdmax}; E_{fdmin}/K_a \leq V_{PID} \leq E_{fdmax}/K_a$.
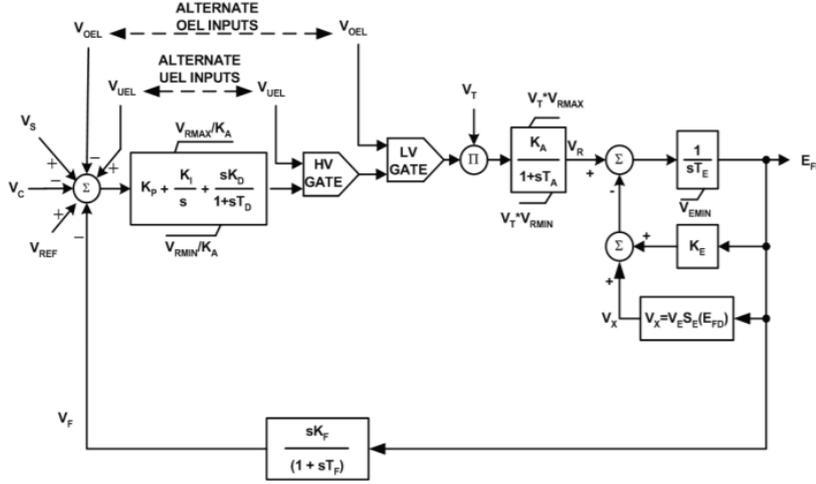
Figure 3.12: Exciter of Type DC4B [78]

$$E_{fd} = K_A(V_{ref} + V_{ss} - V_r)$$

$$T_r \frac{dV_r}{dt} = V_t - V_r$$

(3.40)

where $E_{fdmin} \leq E_{fd} \leq E_{fdmax}$.

Here, E_{fd} is the field excitation voltage, K_e is the exciter gain, T_e is the exciter time constant, T_r is the input filter time constant, V_r is the input filter emf, K_f is the stabilizer gain, T_f is the stabilizer time constant, V_f is the stabilizer emf, A_{ex} and B_{ex} are the saturation constants, K_a is the dc regulator gain, T_a is the regulator time constant, V_a is the regulator emf, K_p, K_i, K_d and T_d are the PID-controller parameters, K_A is the static regulator gain, V_{ref} is the reference voltage and V_{ss} is output reference voltage from the PSS.

3.5.1.3 Modeling of Power System Stabilizers (PSSs)

Besides, the excitation control of generators, we use PSSs as suppelements to damp the local modes. The feedback signal to a PSS may be the rotor speed (or slip), terminal voltage of the generator, real power or reactive power generated etc. Signal is chosen which has maximum controllability and observability in the local mode. If the rotor slip S_m is used as the feedback signal then the dynamic equation of the PSS is given by (3.41)

$$V_{ss} = K_{pss} \frac{sT_w}{1 + sTw} \frac{(1 + sT_{11})}{(1 + sT_{12})} \frac{(1 + sT_{21})}{(1 + sT_{22})} \frac{(1 + sT_{31})}{(1 + sT_{32})} S_m$$

(3.41)

Here K_{pss} is the PSS gain, T_w is the washout time constant, T_{i1} and T_{i2} are the ith stage lead and lag time constants respectively.

3.5.2 Case-study and Results

Using (3.14) to avoid the zero eigenvalues and neglecting the zero eigenvalues caused by the exciter and PSS controller parameters (the time constant of exciter and PSS controller are much more smaller than that of the electromechanical modes), the eigenvalue analysis shows that this system has 15 pairs of electromechanical modes among which there are 4 inter-area modes, as shown in Tab. 3.13 and Tab. 3.14 .

Figure 3.13: The Electromechanical Modes of the 16 Machine System When No PSS is Equipped [75]

No.	Damping Ratio(%)	Frequency (Hz)	State State	Participation Factor	State	Participation Factor	State State	Participation Factor	State State	Participation Factor
1	-0.438	0.404	$\delta(13)$	1	$\omega(13)$	0.741	$\omega(15)$	0.556	$\omega(14)$	0.524
2	0.937	0.526	$\delta(14)$	1	$\omega(16)$	0.738	$\omega(14)$	0.5	$\delta(13)$	0.114
3	-3.855	0.61	$\delta(13)$	1	$\omega(13)$	0.83	$\delta(12)$	0.137	$\omega(6)$	0.136
4	3321	0.779	$\delta(15)$	1	$\omega(15)$	0.755	$\omega(14)$	0.305	$\delta(14)$	0.149
5	0.256	0.998	$\delta(2)$	1	$\omega(2)$	0.992	$\delta(3)$	0.913	$\omega(3)$	0.905
6	3.032	1.073	$\delta(12)$	1	$\omega(12)$	0.985	$\omega(13)$	0.193	$\delta(13)$	0.179
7	-1.803	1.093	$\delta(9)$	1	$\omega(9)$	0.996	$\delta(1)$	0.337	$\omega(1)$	0.333
8	3.716	1.158	$\delta(5)$	1	$\omega(5)$	1	$\omega(6)$	0.959	$\delta(6)$	0.958
9	3.588	1.185	$\omega(2)$	1	$\delta(2)$	1	$\delta(3)$	0.928	$\omega(3)$	0.928
10	0.762	1.217	$\delta(10)$	1	$\omega(10)$	0.991	$\omega(9)$	0.426	$\delta(9)$	0.42
11	1.347	1.26	$\omega(1)$	1	$\delta(1)$	0.996	$\delta(10)$	0.761	$\omega(10)$	0.756
12	6.487	1.471	$\delta(8)$	1	$\omega(8)$	1	$\omega(1)$	0.435	$\delta(1)$	0.435
13	7.033	1.487	$\delta(4)$	1	$\omega(4)$	1	$\omega(5)$	0.483	$\delta(5)$	0.483
14	6.799	1.503	$\delta(7)$	1	$\omega(7)$	1	$\omega(6)$	0.557	$\delta(6)$	0.557
15	3.904	1.753	$\delta(11)$	1	$\omega(11)$	0.993	$\Psi_1 d(11)$	0.056	$\omega(10)$	0.033

Figure 3.14: The Electromechanical Modes of the 16 Machine System When all 12 PSSs are Equipped [75]

No.	Damping Ratio (%)	Frequency (Hz)	State	Participation Factor	State	Participation Factor	State	Participation Factor	State	Participation Factor
1	33.537	0.314	$\omega(15)$	1	$\omega(16)$	0.982	$\delta(7)$	0.884	$\delta(4)$	0.857
2	3.621	0.52	$\delta(14)$	1	$\omega(16)$	0.645	$\omega(14)$	0.521	$\delta(15)$	0.149
3	9.625	0.591	$\delta(13)$	1	$\omega(13)$	0.83	$\omega(16)$	0.111	$\omega(12)$	0.096
4	3.381	0.779	$\delta(15)$	1	$\omega(15)$	0.755	$\omega(14)$	0.304	$\delta(14)$	0.148
5	27.136	0.972	$\omega(3)$	1	$\delta(3)$	0.962	$\omega(2)$	0.924	$\delta(2)$	0.849
6	18.566	1.08	$\omega(12)$	1	$\delta(12)$	0.931	$E_q'(12)$	0.335	PSS4(11)	0.196
7	23.607	0.939	$\delta(9)$	1	$\omega(9)$	0.684	PSS3(9)	0.231	PSS2(9)	0.231
8	30.111	1.078	$\delta(5)$	1	$\omega(5)$	0.928	$\omega(6)$	0.909	$\delta(6)$	0.883
9	28.306	1.136	$\omega(2)$	1	$\delta(2)$	0.961	$\delta(3)$	0.798	$\omega(3)$	0.777
10	13.426	1.278	$\omega(1)$	1	$\delta(1)$	0.969	$E_q'(1)$	0.135	$\omega(8)$	0.111
11	18.83	1.188	$\delta(10)$	1	$\omega(10)$	0.994	$E_q'(10)$	0.324	PSS3(10)	0.19
12	32.062	1.292	$\delta(8)$	1	$\omega(8)$	0.935	$E_q'(8)$	0.61	PSS2(8)	0.422
13	39.542	1.288	$\delta(4)$	1	$\omega(4)$	0.888	$E_q'(4)$	0.706	PSS4(4)	0.537
14	33.119	1.367	$\delta(7)$	1	$\omega(7)$	0.909	$\delta(6)$	0.653	$\omega(6)$	0.612
15	23.87	5.075	$\omega(11)$	1	$E_q'(11)$	0.916	$\Psi_1 d(11)$	0.641	PSS4(10)	0.464

This system is unstable with positive eigenvalues of electromechanical modes as shown in Tab. 3.13. And the PSS is therefore used to stabilise this system. When placing PSSs on G1 to G12 (the maximum number of possible PSSs), all the local modes are damped, and 3 inter-modes are poorly damped, as shown in Tab. 3.14. No more information is available from the linear analysis to damp the inter-area modes [75]. When a three-phase fault is applied to G13 and cleared in 0.25s, the machines exhibit nonlinear inter-area oscillations and finally damp out to a steady-state equilibrium in $50s$, as shown by the frequency spectrum in Fig. 3.15. As all the local-modes are well damped, the components at frequency higher than $1Hz$ are expected as nonlinear interactions.

When placing PSSs only on G6 and G9 (the minimum number of PSSs to ensure the stability of the system), all inter-area modes are poorly damped as listed in Tab. 3.7. When there is a three-phase short circuit fault applied near the end of G13, generators in all the 5 areas exhibit poorly damped electromechanical oscillations and finally damp out to a steady-state equilibrium in a large time. Since the linear participation factor of G13 is [0.0075   0.7997   0.0214   0.6871] on the inter-area modes 1-4, only Mode 2 and Mode 4 will be effectively excited, while Mode 1 and Mode 3 are trivially excited. However, as observed from the frequency spectrum in Fig. 3.16, there are significant components at $0.5Hz$ (G14, the fundamental frequency of Mode 3), at $0.8Hz$ (G15, the fundamental frequency of Mode 1), around $1.0Hz$ (G6,G9,G13,G14,G15, the frequency is not corroborated with any inter-area mode). Therefore, SII and $MI3$ are expected to give additional information to identify the modal interactions.
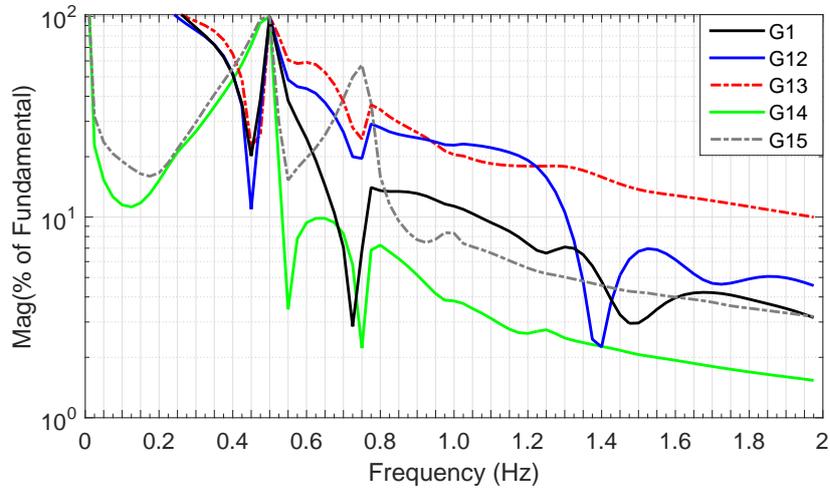
Figure 3.15: FFT Analysis of Generator Rotor Angles' Dynamics when G1 to G12 are equipped with PSSs

Table 3.7: Inter-area Modes of the 16 Machine 5 Area System with PSSs Present on G6 and G9

Mode	1	2	3	4
damping ratio	3.35%	0.55%	1.58%	2.76%
frequency (Hz)	0.7788	0.6073	0.5226	0.3929
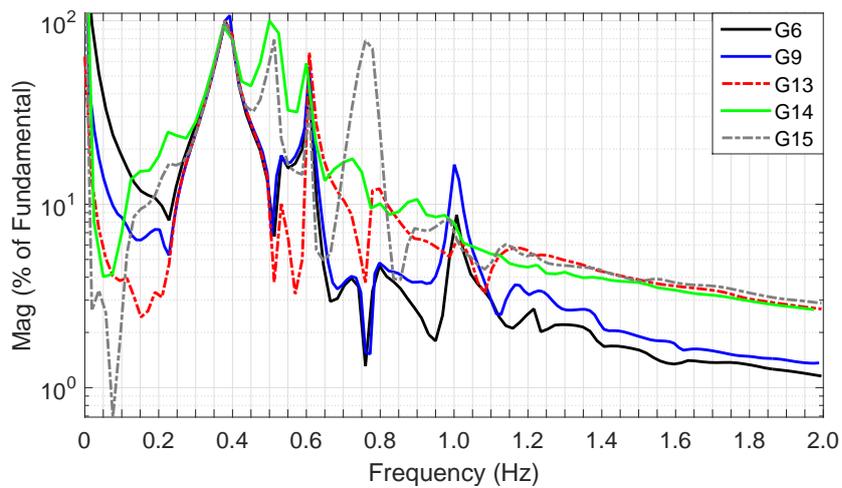
Figure 3.16: FFT Analysis of Generator Rotor Angles' Dynamics when G1 to G12 are equipped with PSSs

Table 3.8: Search for Initial Conditions in the NF Coordinates

Method	Case 1		Case 2	
	Iterations	Resolution	Iterations	Resolutions
3-3-3	12	1.294e-12	17	1.954e-6
2-2-1/3-2-3	3	1.799e-11	6	1.838e-06
3-3-1	7	1.187e-09	11	7.786e-09

In this case, method 3-3-3 may provide more information to: 1) reduce the number of PSSs; 2) damp the inter-area modes. The siting of PSSs based on NF analysis is not the issue to be dealt with in this chapter, and it can be found in [20].

3.6   Factors Influencing Normal Form Analysis

3.6.1   Computational Burden

The essence of NF analysis is to calculate the nonlinear indexes to predict the modal interactions and to give information on the parameters influencing the system stability, which is composed of two phases of computations:

1. the SEP Initialization in order to obtain the eigen matrix λ and matrices $F2$ and $F3$, which depends on the post-fault SEP;
2. the Disturbance Initialization in order to obtain the initial points in the NF coordinates, which depend on the disturbances the system experiences.

The values of nonlinear indexes depend both on the SEP and the disturbances. Item 2 has been discussed in detail in [47, 48] while Item 1 is somewhat neglected in the literature.

3.6.1.1   Search for the Initial Conditions

In this chapter, the search for the initial conditions is performed using the Newton-Raphson (NR) method [67], the starting search point is y^0, and it converges in several iterations, as shown in Tab. 3.8. This is because the normal coefficients $h2$ and $h3$ are small in size. When these coefficient are large in size (near strong resonance case), the search for z^0, w^0 can be extremely slow and even fails to converge.

A more robust algorithm is proposed in [47] to circumvent some disadvantages of NR method, which can be adopted also for the 3rd order NF methods.

3.6.1.2 SEP Initialization

If the power load changes, the SEP initialization must be restarted. The calculation of the nonlinear matrices $F2$ and $F3$ can be extremely tedious. The problem is that matrices $F2$ and $F3$ are composed of complex values. Using the same Matlab function to calculate matrices A, $H2$, $H3$, Λ, $F2$ and $F3$ for the IEEE 4 machine case it leads to differences from $200s$ to $2000s$. Reducing the time needed to multiply complex matrix can be a direction to optimize the program.

Once the perturbation model around the SEP is established in Jordan form, calculation of nonlinear indexes can be computed in a short time.

3.6.2 Strong Resonance and Model Dependence

Validated using 4th order or higher order generator models, the proposed method 3-3-3 also inherits the applicability to systems modeled by 2nd order generator models as method 3-3-1 used in [54], and 3rd order generator as method 3-2-3S used in [5]. The technique works where method 3-3-1 is not applicable. For example, using classical models with zero mechanical dampings, the eigenvalues will be pure imaginary, i.e $\sigma_{j=0}$. In this case, method 3-3-1 fails to be applied, since $\overline{h3^j_{j2l-12l}} = \infty$, (Mode (2l-1,2l) being a conjugate pair that leads to a strong resonance).

In addition, as the eigenvalues are purely imaginary, the stability boundary proposed in [5,16] (see Eqs.(13) and (22)) will be wrongly predicted, as the stability boundary will be calculated as $R_j = \sqrt{-\frac{real(\lambda_j)}{real(c^{j=2k}_{2k})}} = 0$.

Method 3-3-3 is more complete, as it can make possible to predict both the importance of modal interactions and to proposes nonlinear stability indexes for a broader ranges of implemented models.

3.7 Conclusion of the Reviewed and Proposed Methods

3.7.1 Significance of the Proposed Research

With the nonlinear indexes, the proposed method 3-3-3 makes possible to quantify the third-order modal interactions and offers some pertinent information for stability analysis, providing a better tool compared to the linear or other existing normal forms methods. The indication given by the nonlinear indexes are validated by time-domain simulation and FFT analysis.Factors influencing NF analysis, such are the computational burden and the model dependency are discussed.

Besides, this chapter gives a good review of existing MNFs along with a performance evaluation of the different NF approximations studied in this work (see Tab. 3.9).

3.7.2 Future Works and Possible Applications of Method 3-3-3

Based on the proposed 3rd-order NF approximations, potential applications could be emerged such as:

Table 3.9: Performance evaluation of the studied NF approximations

Method	Resolution	Order of Modal Interaction	Transient Stability	Applicability to 3rd Order Modes
Linear	$\mathcal{O}(2)$	1st	Linear	None
2-2-1	$\mathcal{O}(3)$	2nd	Linear	None
3-2-3S	$\mathcal{O}(3)$	2nd	Non-linear	Oscillatory
3-3-1	$\mathcal{O}(3)$	3rd	Linear	Non-oscillatory
3-3-3	$\mathcal{O}(5)$	3rd	Non-linear	All

1. Methods to find the optimal location of Power System Stabilizers;
2. Sensibility analysis based on the higher-order participation factors to aid in the design of the power system structure and controller's parameters tuning;
3. Nonlinear stability analysis to better predict the power transfer limits of the system. Transferring as much as possible power with an existing grid is of major interest.

Application of Method NNM: Transient Stability Assessment

Transient stability assessment, is one of the most important issue for power systems composed of generators. The existing popular tools are either the time-domain simulation or direct methods. Time-domain simulation stability analysis is time-consuming and therefore makes the on-line assessment impossible. The current direct methods involving the energy function formulation to calculate the energy threshold of rotor angle is difficult to implement due to the quadratic nonlinearities. In this chapter, analytical stability bound is provided by method NNM for transient stability assessment. Taking into account the 3rd order nonlinearities from the Taylor series, the proposed method NNM cancels the quadratic nonlinearities and conserves only the self-conserving cubic nonlinearities in the nonlinear normal modes by nonlinear transformations, leading to a conservative prediction of the stability bound.

The proposed stability bound has been assessed in SMIB system and Kundur's 2 area 4 machine system. Conclusions and Perspectives are given.

Keywords: Analytical Transient Stability Analysis, Stability Bound, 3rd Normal Forms, Nonlinear Normal Mode

4.1   Introduction

Nowadays the electricity is transferred and distributed in a more smart way, leading to interconnected power grid which is a complex and large-scale system with rich nonlinear dynamics. Local instabilities arising in such a power network can trigger cascading failures and ultimately result in wide-spread blackouts.

The detection and rejection of such instabilities will be one of the major challenges faced by the future "smart power grid". The envisioned future power generation will rely increasingly on renewable energies such as wind and solar power. Since these renewable power sources are highly stochastic, there will be an increasing number of transient disturbances acting on an increasingly complex power grid. Thus, an important issue of power network stability is the so-called transient stability, which is the ability of a power system to remain in synchronism when subjected to large transient disturbances (event disturbances) such as faults or loss of system components or severe fluctuations in generation or load.

The power system under such a large disturbance can be considered as going through changes in configuration in three stages: from prefault, to fault-on, and then to postfault systems. The prefault system is usually in a stable equilibrium point (SEP). The fault occurs (e.g a short circuit), and the system is then in the fault-on condition before it is cleared by the protective system operation. Stability analysis is the study of whether the postfault trajectory will converge (tend) to an acceptable steady-state as time passes [3].

Transient stability has become a major operating constraint of the interconnected power system. The existing practical tools for transient stability analysis are either time-domain simulation or direct methods based on energy-function and Lyapounov direct method. For other tools, a literature review can be found in Section 1.5.2.

4.2   Study of Transient Stability Assessment and Transfer Limit

The transient stability analysis focus more on the electromechanical oscillations caused by large disturbances. The classical models of generators that are used in that case are:

$$\dot{\delta} = \omega \tag{4.1}$$
$$2H\dot{\omega} = T_m - T_e - D(\omega - \omega_s)$$

In alternating current (AC) systems, the generators must all operate in synchronism in steady state. When a fault occurs on the system, the electrical power output of some generators T_e (usually those near the fault) will tend to decrease. Since the turbine power input T_m does not change instantaneously to match this, these generators will accelerate above the nominal synchronous speed. At the same time, the electrical power output of other generators may increase, resulting in decelera-
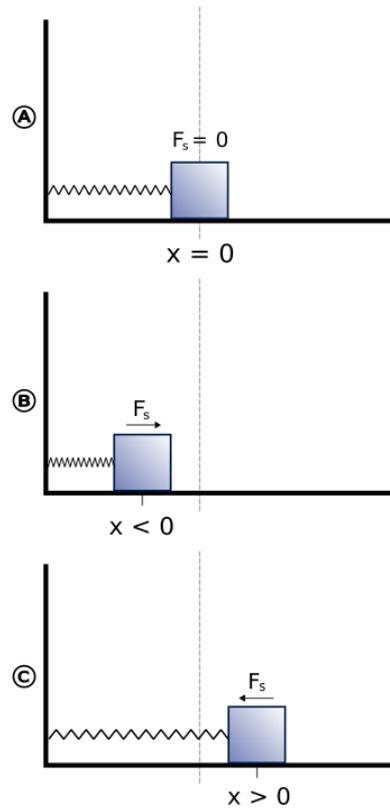
Figure 4.1: The Spring Mass System for the Illustration of the Transient Process When the System Experiences Large Disturbances

tion below the nominal synchronous speed. As a fundamental property of rotating equipment, the generators must all reverse their trends before the energy imbalances become so large that return to synchronous operation is impossible.

Transient stability analysis focuses on this phenomenon, which is analogues to the experience with a spring-mass system, as shown in Fig. 4.1.

When we pull the mass away from its equilibrium point $x = 0$, the spring will give a resistance that once we lease it, it will be pulled back, shown as Fig. 4.1.©; the further it deviates from the equilibrium point, the bigger the resistance. When it returns back to the equilibrium, the force is zero, but the speed $\dot{x}$ is not zero, therefore, the mass continues to move, and the spring gives it a resistance to decrease $\dot{x}$ until $\dot{x} = 0$, shown as Fig. 4.1.b. When $\dot{x} = 0$, the resistance reaches to the maximum, and it pushes the mass to move from Fig. 4.1. ⓑ to Fig. 4.1.©. If there is a damping, after several oscillations, the mass will stop at the equilibrium after several oscillations, and the spring-mass system comes to steady state. If there is no damping, the spring-mass system will continue the periodic oscillation. Both the damped oscillation and the periodic oscillation indicate a transient stability. However, when the displacement x is too much big, the mass will not go back to the equilibrium point, and the system is not stable anymore. In the power system, the
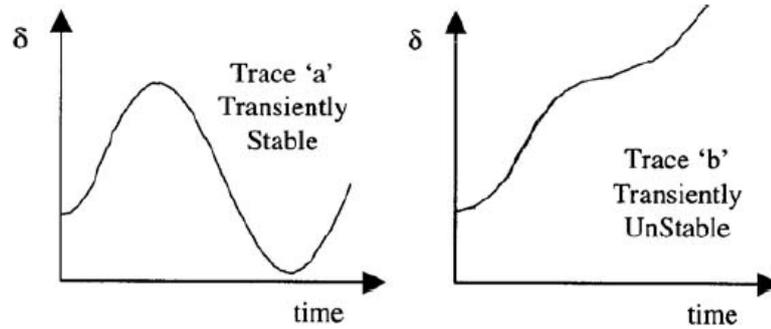
Figure 4.2: Typical Swing Curves [79]

resistance is the synchronizing torque, and the damping is equivalent to mechanical damping, damping winding, etc. The objective is to figure out the stability bound of x, which is the transfer limit of the interconnected power system.

When generators accelerate or decelerate with respect to each other, their speed deviations (and the corresponding angle deviations) constitute swings. If two or more generators swing apart in speed and then reverse, their return to synchronism could be considered "first-swing stable" if the analysis concludes at the point of return. The transient stability and the "the first-swing unstable" is illustrated in Fig. 4.2. (However, it happens that the system becomes unstable after the first swing [3], as shown in Fig. 4.3 and Fig. 4.4, which is difficult to explain. This may be explained by the proposed stability assessment index and time pertinance index.)

A time domain simulation is performed on the well validated matlab simulink model [76] to assess the transient stability. When there is a three-phase short circuit fault applied on Bus 13 and cleared in $0.30s$, generators in all the 5 areas exhibit oscillations, with the dynamics of rotor angles shown in Fig. 4.4. The oscillations firstly damp, and nearly converge to the steady state in $32s$, but then they begin to dissipate later. For such a case, it is difficult to decide when to stop the simulation and analytical tools are needed.

Compared to the nonlinear analysis conducted the Chapter 3, the biggest difference between the small-signal analysis and the transient analysis is that:

The nonlinearity in the small signal analysis is mainly contributed by x_{SEP}, and the nonlinearity in the transient analysis is mainly contributed by $\triangle x$

Example Case 3

Taking the single-machine infinite-bus (SMIB) system as an example with classical model as (4.2):

$$\dot{\delta} = \omega_s \omega \tag{4.2}$$
$$\dot{\omega} = (P_m - P_e - D_\omega(\omega - 1))/(2H)$$
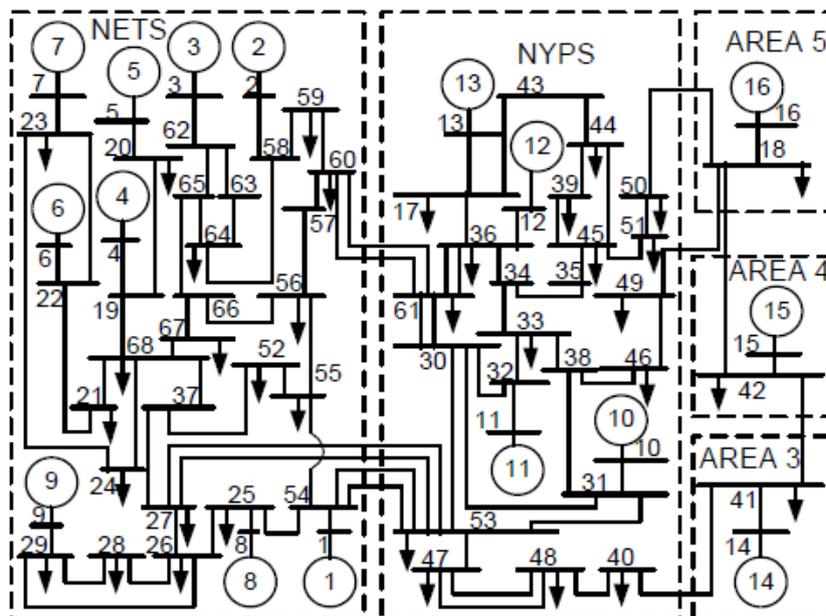
Figure 4.3: New England and New York 16-Machine 5-Area Test System [75]
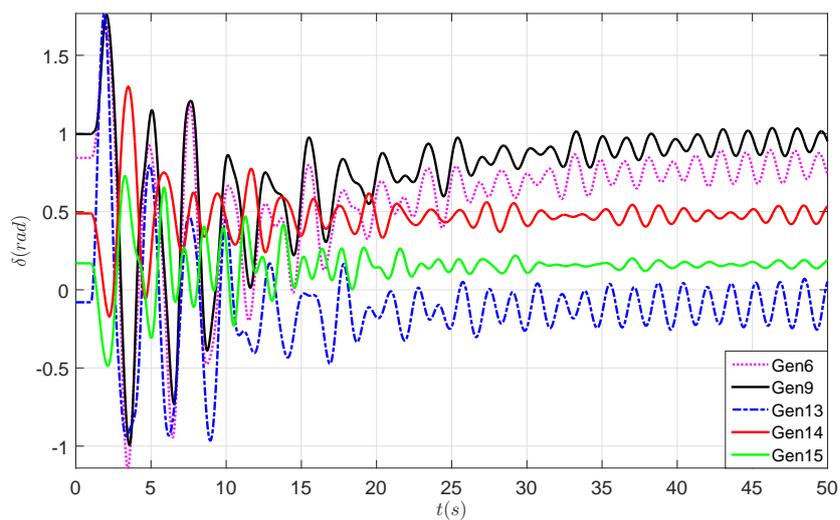
Figure 4.4: Example Case 4: Simulation of Rotor Angles' Dynamics of the New England New York 16-Machine 5-Area System
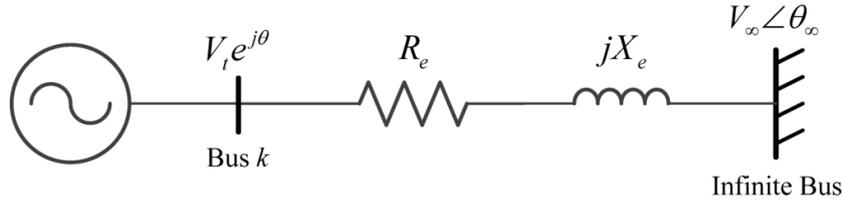
Figure 4.5: Representative Example of SMIB System

with

$$P_{max} = \frac{E_q' E_0}{X} \quad , P_e = P_{max} \sin \delta \quad , P_m = P_{max} \sin \delta_{ep} \qquad (4.3)$$

where P_m is the mechanical input in the machine, P_e is the electrical power supplied by the machine, δ_{ep} is the equilibrium point. D_ω is the damping on the rotor speed. The parameters are set as $E_0 = 1, E_q' = 1.7, X = 1, 2H = 3, D = 0$.

When there is a three-phase short circuit fault applied on the transmission line, as observed from Fig. 4.6, the system behavior is predominantly nonlinear that the linear analysis fails to approximate, though this system is unstressed. When the
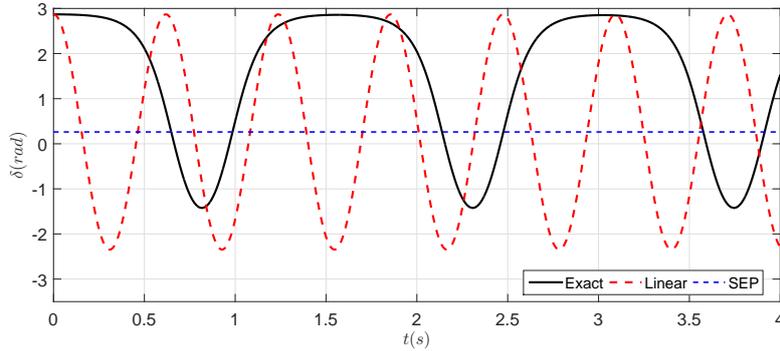
Figure 4.6: Example Case 3: The Unstressed SMIB System under Large Disturbance

disturbance is big enough, the system will be unstable. The objective of Transient Stability Assessment (TSA) is to predict the maximum disturbance that the system can experience while maintaining the stability.

4.2.1   Existing Practical Tools

4.2.1.1   Time-domain simulation tools

Until recently, transient stability analysis has been performed in power companies mainly by means of numerical integrations to calculate generator behaviours relative to a given disturbance. EMTP software such as PSCAD, phasor-type software such as Matlab/SymPower have to be used. By those time-domain simulation programs, a clear picture of the post-fault trajectory can be obtained. The time-domain

simulation is advantaged in the sense that:

1. it is directly applicable to any level of detail of power system models;
2. all the information of state variables during transient process as well as steady-state is available;
3. the results are visual and can be directly interpreted by system operators.

However, the main disadvantages are that:

1. it is time-consuming;
2. it fails to offer analytical results, i.e., it tells whether the system is stable, but fails to tell the degrees of the stability, e.g the stable margin [3] which is crucial to exploit the power transfer limit and maximize the economic opportunities.

Therefore analytical methods are required to do the on-line stability assessment and serve as a preventive tool.

4.2.1.2 Direct Methods(Ribbens-Pavella and Evans, 1985 [41]; Chiang, 1995 [3])

An alternative approach is the direct methods employing the energy functions (Lyapounov's second method for stability). It avoids the step-by-step time-domain stability analysis of the post-fault system, and also provides a quantitative measure of the degree of system stability to provide guide in the power system planing and operating.

There are three main steps needed for direct methods:

1. Constructing an energy function for the post-fault system, say $V(\delta, \omega)$
2. Computing the critical energy value V_{cr} for a given fault-on trajectory (say, based on the controlling u.e.p method).
3. Comparing the energy value of the state when the fault is cleared, say $V(\delta_{cl}, \omega_{cl})$, with the critical energy value V_{cr}. If $V(\delta_{cl}, \delta_{cl}) < V_{cr}$, the postfault trajectory will be stable. Otherwise, it may be unstable.

By direct methods, conservative transient stability is found.

For the single-machine infinite-bus(SMIB) direct methods are easy to be implemented, one method is named the equal-area (E-A) criterion [1] with good visualization and good interpretation.

However, for the high-dimension systems (a multi-swing case, which is widespread in the inter-area oscillations in the interconnected large-scale problem), formulating the energy function (multi-variable function) is a challenging work, demanding very skilful interpretors and operators.

What's more, the Lyapounov second method for stability analysis requires the equilibrium point *hyperbolic* (there is no eigenvalue having zero-real part), making it not appropriate for the weakly-damping or zero-damping case.

Those drawbacks make the direct methods academically prospective but impractical for industry until 1990s.

After 1990s, with the development of computing algorithms, the applicability range of direct methods is enlarged. However, the computing development benefits more the time-domain simulation tools than the direct methods tools. The current market

is still a: small-signal analysis + time-domain analysis.

However, it is also difficult to interpret the results obtained by direct methods, as the physical meanings are obscured by the energy concept. The recently proposed tool such as the F-A curve [4] is an effort to make the direct method visual by using the direct methods to establish the one-to-one mapping between the oscillation amplitude and frequency. However, it is based on the assumption that the nonlinear behaviour of the global system is the sum of the individual behaviour of each system component, which is not mathematically proved, and far from our experience with the physical systems.

When interpreting the physical motion by energy concept, the direct methods are not that "direct".

4.2.1.3   Problem Formulating

In essence, the problem of transient stability analysis can be translated into the following: given a set of non-linear equation with an initial condition, determine whether or not the ensuing trajectories will settle down to a desired steady-state. In this sense, time-domain simulation is too time-consuming in providing unnecessary details and direct-methods employing the energy functions not to highlight the physical motion of the power dynamics.

Let's go to the fundamentals and we will note that: the couplings in the nonlinearities make the analytical solutions unavailable. To settle this problem, a method based on Normal Form (NF) Theory is proposed to simplify the nonlinearities by the use of nonlinear transformations. The procedure is well documented in [30,51] and consists of 4 major steps:

1. Simplifying the linear part of a system by the use of a linear transformation;
2. Simplifying the nonresonant terms of higher-order terms by successive Normal Form (NF) transformations.
3. Simplifying the Normal Dynamics by neglecting (if possible) some resonant terms that can not be annihilated by NF transformations;
4. Using the chosen Normal Dynamics for dynamic and stability analysis.

4.2.1.4   Existing Normal Form Methods

In [5,16,48] the formulas of different NF methods are derived, the normal dynamics are in the Jordan form where complex numbers are involved. For [48], the normal dynamics are linear and the stability analysis is a linear analysis plus higher-order fluctuations. In [5,16], some 3rd order terms are kept to render a more accurate prediction of the nonlinear stability based on which the stability bound is proposed. However, as the stability bound is the threshold of the rotor angle, which is a real number, extra effort is made to transform the complex number to the real number, leading to additional computational errors. Those methods are summarized as methods on vector fields in Chapter 2.

Another approach is to keep the differential equation in the second-order form, and to decouple the linear matrix in [2 × 2] blocks to avoid the computation of complex

numbers. It originates from the Touzé's method to formulate the nonlinear normal mode [17]. The nonlinear normal mode (NNM) is the basic particular solution of the nonlinear dynamics. By studying NNM, the nonlinear properties of the system dynamics are revealed and quantified.

In [40], it also formulates the nonlinear normal mode to study the power system dynamics. However, it is based on the Shaw-Pierre method, and fails to suggest accurately the nonlinear system stability. Discussions on SP method can be found in Section 2.5.9.

The comparisons between the time-domain simulation, direct methods employing energy functions and the proposed NF method are listed in Tab. 4.1. The advantages and disadvantages of each method are summarized in the Sections. 4.2.2, 4.2.3.

4.2.2   Advantages of the Presented Methods

4.2.2.1   Advantages of Time-domain Simulations

1. it is directly applicable to any type of power system models;
2. all the information of state variables during transient as well as steady-state is available;
3. the results are visual and can be directly interpreted by system operators.

4.2.2.2   Advantages of TEF Methods

1. It avoids time-consuming numerical integration of a postfault power system.
2. It makes quantitative measure of the degree of system stability available
   - It provides information to designing network configuration plans to push the power system to its operating limits
   - The derivation of preventive control actions

4.2.2.3   Advantages of Methods of Normal Forms

1. Analytical conservative stability bound is predicted;
2. It provides clear physical insights: notion of modes is kept in the normal dynamics, which is better to predict the motion compared to the energy equation based methods.
3. It is easy to be implemented with clear physical meanings that anyone who has knowledge with nonlinear differential equations can implement it.
4. It is applicable for high-dimensional system: the complexity does not increase drastically with the high-dimensional systems.

4.2.3   Challenges for the Presented Methods

4.2.3.1   Challenges for Time domain simulations

1. It is difficult to be applied for large-dimensional system;
2. It is difficult to decide when to stop the simulation.

Table 4.1: Comparisons of the Presented Methods

Methods	Time-domain Step-by-step Integration	Direct Methods employing energy functions	NF methods employing Normal Modes
Principle	The post-fault trajectory obtained by step-by-step simulation tells the stability	The potential energy decides the stability	The Normal Forms of the system (obtained by nonlinear transformation conserving the "invariance property") tells the stability
Trajectories and dynamics	Prefault trajectory, fault-on trajectory, post-fault trajectory	trajectory is unknown	postfault trajectory of electromechanical oscillations
State-variables	rotor angle, currents, voltages...	Energy: $V(\delta_{cl})$	Rotor angle: δ
Computation	1. Numerical, off-line 2. Step-by-step integration 3. The computational time is typically between 10-30s 4. Qualitative stability assessment	1. Mostly-Numerical 2. No integration of post-fault trajectory but 3. computational time: milliseconds 4. Calculation of $V(cr), V(X(t_{cl}^+))$, if $V(X(t_{cl}^+)) < V_{cr}$, then $x(t)$ is stable; otherwise, unstable.	1. Explicitly analytical results 2. Systematic procedure 3. stability bound can be systematically calculated out in microseconds.

4.2.3.2   Challenges for TEF Methods

1. The modelling: not every (post-fault) transient stability model admits an energy function, e.g the model contains the quadratic nonlinearities;
2. The function: only applicable to first swing stability analysis of power system transient stability models described by pure differential equations;
3. The reliability: the reliability of a computational method in computing the controlling UEP for every study contingency.

4.2.3.3   Challenges for Methods of Normal Forms

1. The modelling: real-form approach is just for network-reduction model, vector-field approach can cover network-preserving model [48]
2. The function:only applicable to first swing stability analysis
3. The reliability:the reliability of a computational method in computing the controlling UEP for every study contingency

4.2.4   A Brief Review of the Proposed Tool: Method NNM

The nonlinear electromechanical oscillations in interconnected power system can be modelled as second-order coupled oscillators. If the variables of the power system, around a given equilibrium point, are gathers in a N dimensional vector $\boldsymbol{q}$, the basic model under study writes:

$$\boldsymbol{M\ddot{q}} + \boldsymbol{D\dot{q}} + \boldsymbol{Kq} + \boldsymbol{f}_{nl}(\boldsymbol{q}) = 0 \tag{4.4}$$

In the above equation, $\boldsymbol{M}$ and $\boldsymbol{D}$ are constant symmetric inertia and damping matrix, whose values depend on the physical parameters of the power system and controller parameters. $\boldsymbol{K}$ and $\boldsymbol{f}_{nl}$ indicate the coupling between the variables, where $\boldsymbol{K}$ is a constant matrix, including the linear terms and $\boldsymbol{f}_{nl}$ gathers the nonlinear terms.
If $\boldsymbol{f}_{nl}$ is developed in a Taylor series up to the third order, it comes:

$$f_{nl}^p(q) = \sum_{i=1,j\geq i}^N f2_{ij}^p q_i q_j + \sum_{i=1,j\geq i,k\geq j}^N f3_{ijk}^p q_i q_j q_k \tag{4.5}$$

where f_{ij}^p and f_{ijk}^p $(i,j,k,p = 1\ldots N)$ are coefficients of the quadratic and cubic terms. Components of $\boldsymbol{K}$ and $\boldsymbol{f}_{nl}$ depend on the chosen equilibrium point and the system structure, for example, the network connectivity of the power grids.
It is seen that (4.4) is a N-dimensional nonlinear dynamical problem.

4.2.4.1   LNM

As viewed from (2.86), the dynamics physical property (oscillatory frequency, damping, friction, etc) is obscured by the mathematical model.

In order to decouple the equation into second-order oscillators, a linear transformation $\triangle \boldsymbol{q}(t) = \boldsymbol{\Phi}\boldsymbol{x}(t)$ can be used.

After decoupling the linear terms, the system dynamics is therefore characterized by a group of oscillators with coupled nonlinearities.

$$\ddot{X}_p + 2\xi_p\omega_p\dot{X}_p + \omega_p^2 X_p \tag{4.6}$$
$$+ \sum_{i=1}^{N}\sum_{j\geq i}^{N} g_{ij}^p X_i X_j + \sum_{i=1}^{N}\sum_{j\geq i}^{N}\sum_{k\geq j}^{N} h_{ijk}^p X_i X_j X_k = 0$$

where ξ_p is the p-th modal damping ratio. And g_{ij}^p and h_{ijk}^p are quadratic and cubic nonlinearities coming from decoupling of K_S, which are given in Chapter 2. Neglecting all the nonlinearities, the (4.6) reads a Linear Normal Mode (LNM):

$$\ddot{X}_p + 2\xi_p\omega_p\dot{X}_p + \omega_p^2 X_p = 0 \tag{4.7}$$

4.2.4.2   NM2

Using a second order NF transformation to cancel all the 2nd-order terms, the Normal Forms in the new coordinate $U - V$ is:

$$\ddot{U}_p + 2\xi_p\omega_p\dot{U}_p + \omega_p^2 U_p + \mathcal{O}(3) = 0 \tag{4.8}$$

4.2.4.3   NNM

Using a 3rd order NF transformation to cancel all the 2nd-order terms and the non-resonant 3rd order terms, the Normal Forms in the new coordinate $R - S$ is:

$$\ddot{R}_p + 2\xi_p\omega_p\dot{R}_p + \omega_p^2 R_p \tag{4.9}$$
$$+ (h_{ppp}^p + A_{ppp}^p)R_p^3 + B_{ppp}^p R_p \dot{R}_p^2 + C_{ppp}^p R_p^2 \dot{R}_p = 0$$

with the coefficients $(A_{ijk}^p, B_{ijk}^p, C_{ijk}^p)$ arise from the cancellation of the quadratic terms [17, 18] and are defined in (2.109).

4.2.4.4   Analytical Stability Bound for Transient Stability Assessment

Since the bound of R_p indicates the bound the X_p, in Section 2.6.2, the proposed stability bound (PSB) is defined as:

$$PSB = R_p K_{nl}\Phi + \boldsymbol{q}_{SEP} \tag{4.10}$$

with

$$R_p \leq \sqrt{-\frac{\omega_p^2}{h_{ppp}^p + A_{ppp}^p}} \tag{4.11}$$

and K_{nl} is defined to consider the nonlinear scaling bround by the NF transformation:

$$K_{nl} = \frac{R_p}{X_p} = \frac{1}{1 + a_{ppp}^p + r_{ppp}^p} \qquad (4.12)$$

4.2.5 Technical Contribution of the Method NNM

The proposed method NNM uses nonlinear transformation up to 3rd order to cancel all the 2nd order and part of 3rd order nonlinearities in the normal dynamics.

It deals with the second-order equation directly, the complex numbers are avoided, and the computational burden is reduced while better physical meanings are preserved. Compared to the reviewed methods, it has the advantages as:

1. it provides analytical conservative stability bound;
2. it keeps the notion of modes, which is better to predict the motion compared to the energy equation based methods;
3. it is easy to be implemented with clear physical meanings, anyone who has knowledge with nonlinear differential equations can implement it;
4. its complexity does not increase drastically with the high-dimensional systems.

4.2.6 Structure of this Chapter

In Section 4.1, an introduction to the problematic is made with a bibliographical review of the existing practical tools.

The mathematical modelling of test systems are established in Section 4.3.

In Section 4.4, it shows how the normal-mode based MNFs can work on the transient stability assessment of interconnected power systems.

The conclusions and perspectives are made in Section 4.5.

4.3 Network Reduction Modelling of the Power System

4.3.1 Modelling of SMIB System

The classic electro-mechanical model of one single machine connected to the grid with voltage V_0 (as shown in Fig. 4.7), with constant amplitude e.m.f E'_q and the state variables are δ and ω, which can be descibed by the differential equations are as follows:

$$\dot{\delta} = \omega_s \omega \qquad (4.13)$$

$$\dot{\omega} = (P_m - P_e - D_\omega(\omega - 1))/(2H) \qquad (4.14)$$

with

$$P_{max} = \frac{E'q V_0}{X_e} \quad , P_e = P_{max} \sin \delta \quad , P_m = P_{max} \sin \delta_{ep} \qquad (4.15)$$

where P_m is the mechanical input in the machine, P_e is the electrical power supplied by the machine, δ_{ep} is the equilibrium point. D_ω is the damping coefficient on the rotor speed.
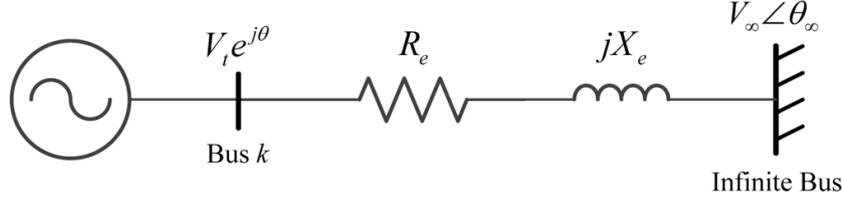
Figure 4.7: Representative Example of SMIB System

4.3.2   Modeling of Multi-Machine System

By reducing the network, the interconnected power system exhibiting oscillations can be essentially characterized as a multi-machine model.

$$\frac{2H_i}{\omega_b}\ddot{\delta}_i = P_{mi} - P_{ei} - \frac{D_{\omega i}}{\omega_b}\dot{\delta}_i \tag{4.16}$$

where

$$P_{ei} = E_i^2 Gg_{ii} + \sum_{\substack{k=1 \\ k \neq i}}^{N} E_i E_k \left[Gg_{ik} \cos \delta_{ik} + Bg_{ik} \sin \delta_{ik} \right] \tag{4.17}$$

E^i is the terminal voltage of the i-th machine and Gg_{ik} is the conductance between machine i and k, Bg_{ik} is the susceptance between machine i and k.

4.3.3   Taylor Series Around the Equilibrium Point

For a perturbation around the equilibrium point (δ_i^0), the state-variable is changed into $\triangle\boldsymbol{\delta} = \boldsymbol{\delta} - \boldsymbol{\delta^0}, \triangle\boldsymbol{\omega} = \boldsymbol{\omega} - \boldsymbol{\omega^0}$. As in the free-oscillation case, $\omega^0 = 1$. (4.16) can therefore be written as (4.4).

4.3.3.1   Synchronization Torque for SMIB System

The synchronization torque is given as the first, second and third derivative of P_e.

$$K_S = \cos \delta_{ep} \quad , K_{2S} = -\frac{\sin \delta_{ep}}{2} \quad , K_{3S} = -\frac{\cos \delta_{ep}}{6} \tag{4.18}$$

4.3.3.2   Synchronization Torque for Multi-Machine System

$$
\begin{aligned}
[K_{Sij}] &= \frac{\partial P_{ei}}{\partial \delta_j} \\[2ex]
&= \begin{cases}
\sum_{\substack{k=1 \\ k \neq i}}^{N} E_i E_j \left[-Gg_{ik} \sin \delta_{ik}^0 + Bg_{ik} \cos \delta_{ik}^0 \right], j = i \\[3ex]
E_i E_j \left[Gg_{ik} \sin \delta_{ik}^0 - Bg_{ik} \cos \delta_{ik}^0 \right], j \neq i
\end{cases}
\end{aligned} \tag{4.19}
$$

For i-th machine, $K^i_{2Sij}] = \frac{1}{2}\frac{\partial^2 P_{ei}}{\partial\delta_i\delta_j}$ reads:

$$
\begin{cases}
K^i_{2Sii} & = -\sum_{\substack{k=1\\k\neq i}}^{N} E_i E_k \left[Gg_{ik}\cos\delta^0_{ik} + Bg_{ik}\sin\delta^0_{ik}\right] \\[2mm]
K^i_{2Sij} & = E_i E_j \left[Gg_{ij}\cos\delta^0_{ij} + Bg_{ij}\sin\delta^0_{ij}\right], j \neq i \\[2mm]
K^i_{2Sjj} & = -E_i E_j \left[Gg_{ij}\cos\delta^0_{ij} + Bg_{ij}\sin\delta^0_{ij}\right], j \neq i
\end{cases}
\tag{4.20}
$$

For i-th machine, $K^i_{3Sijk} = \frac{1}{6}\frac{\partial^3 P_{ei}}{\partial\delta_i\delta_j\delta_k}$, it reads:

$$
\begin{cases}
K^i_{3Siii} & = \frac{1}{6}\sum_{\substack{k=1\\k\neq i}}^{N} E_i E_k \left[Gg_{ik}\sin\delta^0_{ik} - Bg_{ik}\cos\delta^0_{ik}\right] \\[2mm]
K^i_{3Siij} & = -\frac{1}{2}E_i E_j \left[Gg_{ij}\sin\delta^0_{ij} - Bg_{ij}\cos\delta^0_{ij}\right], j \neq i \\[2mm]
K^i_{3Sijj} & = \frac{1}{2}E_i E_j \left[Gg_{ij}\sin\delta^0_{ij} - Bg_{ij}\cos\delta^0_{ij}\right], j \neq i \\[2mm]
K^i_{3Sjjj} & = -\frac{1}{6}E_i E_j \left[Gg_{ij}\sin\delta^0_{ij} - Bg_{ij}\cos\delta^0_{ij}\right]
\end{cases}
\tag{4.21}
$$

4.3.4 Reducing the State-Variables to Avoid the Zero Eigenvalue

In the multi-machine system composed of N generators, if no infinite bus exists, there is zero-eigenvalue, in such a case, the proposed Stability Bound is not efficient. In another word, if all the variables $\delta_i, \delta_j, \forall i, j \in N$ are unstable, the global system can still be stable if δ_{ij} is stable. i.e., the stability is ensured once the synchronization is ensured.

To avoid the zero-eigenvalue, we can use δ_{in}, δ_{jn} instead of δ_i, δ_j, therefore $\delta_{ij} = \delta_{in} - \delta_{jn}$.

Starting from the differential equations:

$$
\frac{2H_i}{\omega_b}\delta_i - \frac{D_{w_i}}{\omega_b}\dot\delta_i = P_{mi} - P_{ei}
\tag{4.22}
$$

$$
\frac{2H_n}{\omega_b}\delta_n - \frac{D_{w_n}}{\omega_b}\dot\delta_n = P_{mn} - P_{en}
\tag{4.23}
$$

When $H_i = H_j = H$, $D_i = D_j = D$, Eq. (4.22)-Eq. (4.23) leads to

$$
\frac{2H}{\omega_b}(\ddot\delta_i - \ddot\delta_n) - D(\dot\delta_i - \dot\delta_n) = P_{mi} - P_{mn} - (P_{ei} - P_{en})
\tag{4.24}
$$

Calculating Taylor series around the equilibrium point, $\forall i = 1, 2, \cdots, n-1$:

$$
\frac{2H}{\omega_b}\triangle\dddot{\boldsymbol\delta}_{\boldsymbol N} + \frac{D}{\omega_b}\triangle\dot{\boldsymbol\delta}_{\boldsymbol N} + \boldsymbol K'_{\boldsymbol S}\triangle\boldsymbol\delta_{\boldsymbol N} + \boldsymbol K'_{\boldsymbol{2S}}\triangle\boldsymbol\delta^{\boldsymbol 2}_{\boldsymbol N} + \boldsymbol K'_{\boldsymbol{3S}}\triangle\boldsymbol\delta^{\boldsymbol 3}_{\boldsymbol N} = 0
\tag{4.25}
$$

where $\triangle\delta_N = \triangle\delta_i - \triangle\delta_n$, and $\triangle\delta_N^2$ contains the quadratic terms such as $\triangle\delta_{iN}\triangle\delta_{jN}$ and $\triangle\delta_N^3$ contains the cubic terms such as $\triangle\delta_{iN}\triangle\delta_{jN}\triangle\delta_{kN}$
Then the coefficients K_S, K_{2S}, K_{3S} are replaced as:

$$K'_{Sij} = \frac{\partial(P_{ei} - P_{en})}{\partial\delta_{jN}} = K_{Sij} + E_n E_i \left[Gg_{ni}\sin\delta_{ni}^0 - Bg_{ni}\cos\delta_{ni}^0 \right] \tag{4.26}$$

For i-th machine, $K'^i_{2Sij}] = \frac{1}{2}\frac{\partial^2(P_{ei} - P_{en})}{\partial\delta_{iN}\delta_{jN}}$ reads:

$$\begin{cases} K'^i_{2Sii} &= K^i_{2Sii} + E_n E_i \left[Gg_{ni}\cos\delta_{ik}^0 + Bg_{ik}\sin\delta_{ik}^0 \right] \\ K'^i_{2Sij} &= K^i_{2Sij}j \neq i \\ K^i_{2Sjj} &= K^i_{2Sjj} + E_n E_j \left[Gg_{nj}\cos\delta_{nj}^0 + Bg_{nj}\sin\delta_{nj}^0 \right] j \neq i \end{cases} \tag{4.27}$$

For i-th machine, $K^i_{3Sijk} = \frac{1}{6}\frac{\partial^3 P_{ei}}{\partial\delta_i\delta_j\delta_k}$, it reads:

$$\begin{cases} K'^i_{3Siii} &= K^i_{3Siii} + E_n E_i \left[Gg_{ni}\sin\delta_{ni}^0 - Bg_{ni}\cos\delta_{ni}^0 \right] \\ K'^i_{3Siij} &= K^i_{3Siij}, j \neq i \\ K'^i_{3Sijj} &= K^i_{3Sijj}, j \neq i \\ K'^i_{3Sjjj} &= K^i_{3Sjjj} + \frac{1}{6}E_n E_j \left[Gg_{nj}\sin\delta_{nj}^0 - Bg_{nj}\cos\delta_{nj}^0 \right] \end{cases} \tag{4.28}$$

4.4 Case-studies

4.4.1 SMIB Test System

4.4.1.1 Nonlinearity and Asymmetry

Fig. 4.8 and Fig. 4.9 show how the different methods approximate the rotor angle dynamics in the transient process, where the NNM captures the two nonlinear properties of the electromechanical oscillations: 1)asymmetry; 2)amplitude dependent frequency-shift [4,21,22].
In all the figures, the curve LNM is symmetric, as it is in the linear case.
For $\delta_{SEP} = \frac{\pi}{2.4}$, the oscillatory frequency is $f = 0.836 hZ$, and the nonlinear oscillatory frequency calculated by (2.133) is $f = 0.78 hZ$ is closer to the exact system dynamics.
For $\delta_{SEP} = \frac{\pi}{12}$, the oscillatory frequency is $f = 1.62 hZ$, and the nonlinear oscillatory frequency calculated by (2.133) is $f = 1.24 hZ$ is closer to the exact system dynamics.
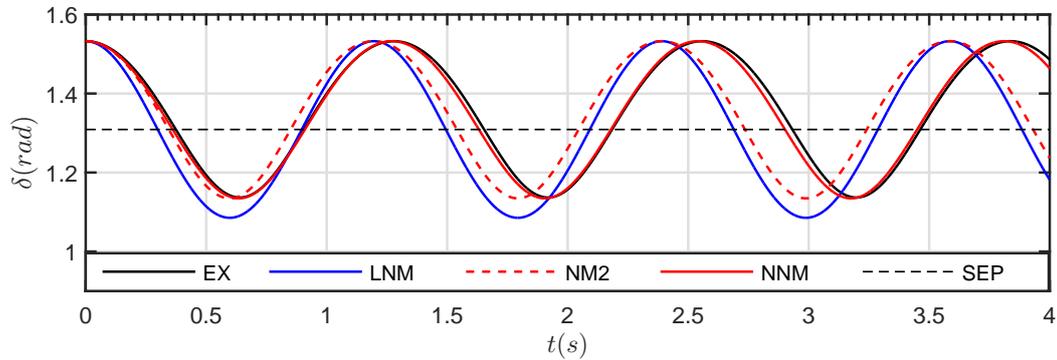
Figure 4.8: A Case Where the System Works to its limit: $\delta_{SEP} = \frac{\pi}{2.4}$
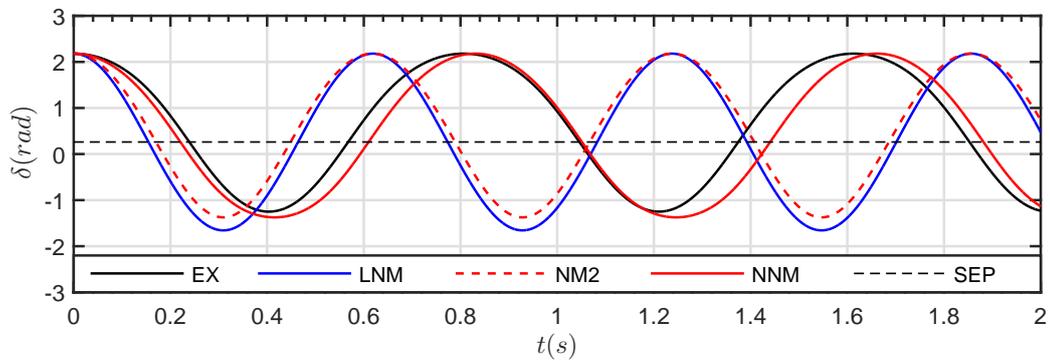
Figure 4.9: A Case Where the System Works to its limit: $\delta_{SEP} = \frac{\pi}{12}$

4.4.1.2 Analytical Stability Bound for Transient Stability Assessment

More results are listed in Tab. 4.2, where the stability bound predicted by the method NNM is labeled as "PSB" and the stability bound predicted by the E-A criteria is labelled as "EAB". To illustrate the influence of the nonlinear scaling factor K_{nl}, the stability bound predicted in the $R - S$ coordinates by R_p is also listed.

As observed from Tab. 4.2, the PSB is smaller than EAB, while R_{1max} can be bigger than EAB. Therefore, by considering the nonlinear scaling, the prediction of stability bound is conservative and more accurate. The stability bound predicted by PSB is verified by time-domain simulation as shown in Fig. 4.10 and Fig. 4.11.

Fig. 4.10 shows that when the δ goes beyond the boundary, NNM can predict the instability in the system dynamics, while LNM and NM2 fails. Fig. 4.11 shows that when the δ reaches the stability bound predicted by EAB, the rotor angles keeps still and the frequency of oscillations is zero; PSB indicates that the system is unstable, while LNM and NM2 indicates that the system is still stable.

Therefore, corroborated with the EAB and the time-domain simulations, the PSB conducts a conservative transient stability assessment for the SMIB system.

Table 4.2: The Proposed Stability Bound, E-A Bound and Bound without Considering the Nonlinear Scaling Factor

δ_0	R_{1max} $+\delta_0$	PSB	EAB Bound	Error1 $\frac{Rbound+\delta_0-EAB}{EAB}$	Error2 $\frac{PSB-EAB}{EAB}$
$\frac{\pi}{2}$	1.5708	1.5708	1.5708	0	0
$\frac{\pi}{2.1}$	1.6790	1.6380	1.6456	2.03%	-0.46%
$\frac{\pi}{2.2}$	1.7766	1. 6985	1.7136	3.68%	-0.88%
$\frac{\pi}{2.3}$	1.8643	1.7526	1.7757	4.99%	-1.30%
$\frac{\pi}{2.4}$	1.9430	1.8010	1.8326	6.02%	-1.73%
$\frac{\pi}{2.5}$	2.0136	1.8440	1.8850	6.82%	-2.17%
$\frac{\pi}{2.6}$	2.0769	1.8823	1.9333	7.43%	-2.64%
$\frac{\pi}{2.7}$	2.1337	1.9164	1.9780	7.87%	-3.12%
$\frac{\pi}{2.8}$	2.1848	1.9467	2.0196	8.18%	-3.61%
$\frac{\pi}{2.9}$	2.2307	1.9763	2.0583	8.38%	-4.11%
$\frac{\pi}{3}$	2.2719	1.9976	2.0944	8.48%	-4.62%
$\frac{\pi}{4}$	2.5174	2.2700	2.3562	6.84%	-3.66%
$\frac{\pi}{5}$	2.6100	2.3960	2.5133	3.85%	-4.67%
$\frac{\pi}{6}$	2.6449	2.4587	2.6180	1.03%	-6.08%
$\frac{\pi}{7}$	2.6557	2.4917	2.6928	-1.38%	-7.47%
$\frac{\pi}{8}$	2.6557	2.5096	2.7489	-3.39%	-8.71%
$\frac{\pi}{9}$	2.6508	2.5192	2.7925	-5.07%	-9.79%
$\frac{\pi}{10}$	2.6438	2.5241	2.8274	-6.50%	-10.73%
$\frac{\pi}{11}$	2.6359	2.5262	2.8560	-7.71%	-11.55%
$\frac{\pi}{12}$	2.6278	2.5267	2.8798	-8.75%	-12.26%
$\frac{\pi}{13}$	2.6200	2.5261	2.8999	-9.65%	-12.89%

4.4.2 Multi-Machine Multi-Area Case: IEEE 4 Machine Test System

In the multi-machine case, the E-A criterion doesn't work any more. However, the PSB still works.

The test system selected for this work is a well known IEEE standard system, Kundur's 2–area 4–machine system, shown in Fig. 4.12.

It is a classical system suitable for the analysis of modal oscillations for the validation
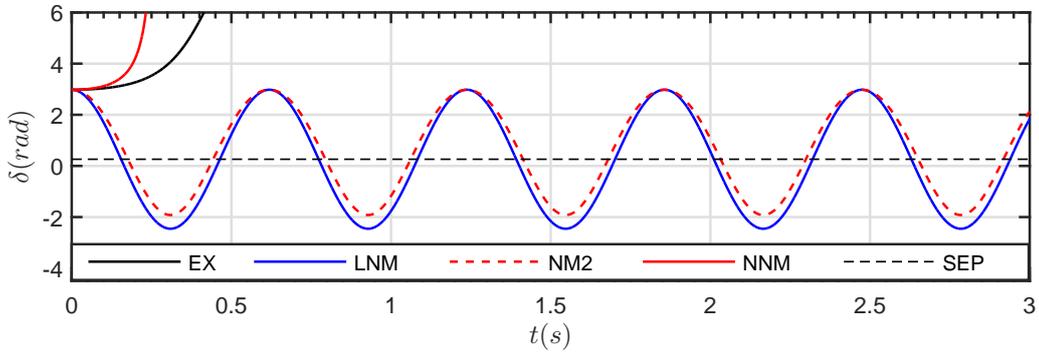
Figure 4.10: When the oscillation amplitude is beyond the bound, $\delta_{max} = 2.9798$ for $\delta_{ep} = \frac{\pi}{12}$
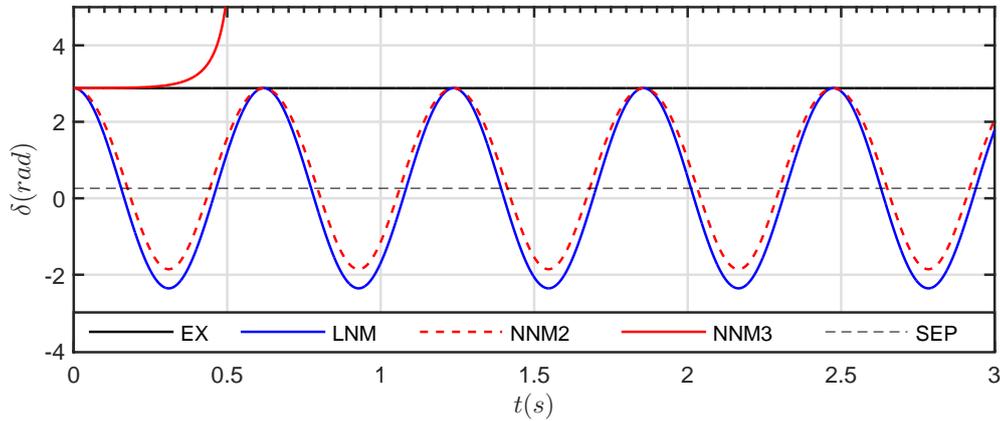
Figure 4.11: When the oscillation amplitude is beyond the bound, $\delta_{max} = 2.9798$ for $\delta_{ep} = \frac{\pi}{12}$

of small-signal analysis [1], and for the validation of 2nd order Normal Form analysis [48]. In the renewable energy generation case, the power generated by G1 and G2 is unbalanced due to the unified distribution of wind energy. And there is a power flow around $415MW$ through the tie line between Area 1 and Area 2. The mechanical damping is weak to obtain the fast response to capture the maximum wind energy. The generators are modelled using classical model [73], assuming that the excitation voltage is constant. The loads L1 and L2 are modelled as constant impedance, and no PSS is equipped. The data for the system and selected case are provided in Appendix. Open source Matlab toolbox PSAT v1.2.10 is used to do the eigen analysis and the full numerical time domain simulation, based on the well validated demo $d\_kundur1$.

As indicated before, dynamics of state-variable δ_i can not reveal the stability property of the whole system. Because there is no infinite bus, it is the synchronization determines the stability, i.e., the relative motion between δ_i and δ_j.
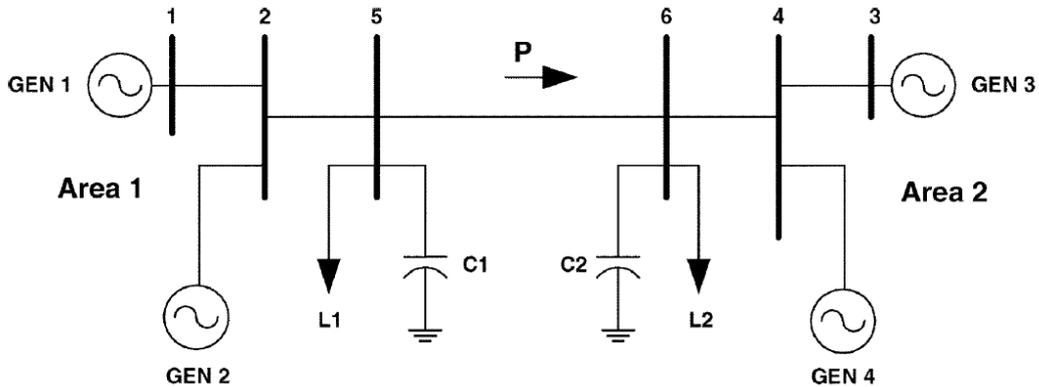
Figure 4.12: IEEE 4 machine test system

In this sense, rotor angle of the 4th generator is served as the reference. And the stability is decided $\delta_{14}, \delta_{24}, \delta_{34}$. It is a weakly damped and highly stressed large-scale interconnected power system. It has one inter-area mode and two local modes.
The case of concern is interarea oscillations.

Case: There is a three-phase short-circuit fault at Bus 5, after a certain time, the fault is cleared, the rotor angles are measured as δ_{max}. In this case, only the inter-area mode is excited.

Fig. 4.13 shows that when the interarea oscillations are under the stability bound, among all the methods, NNM approximates the system dynamics ('EX') to the best. As observed from Figs. 4.14, 4.15 and 4.16, the PSB predicts a conservative stability bound.

4.5 Conclusion and Future Work

4.5.1 Significance of this Research

The PSB can suggest a conservative stability bound for both the SMIB system and the interconnected system, i.e., this proposed method can be used to study not only the case where the fault is caused by *loss of a machine* but also *the loss of one area*.

4.5.2 On-going Work

Two things are due to done to complete the tests:
- Testing the PSB on larger networks, e.g, the New England New York 16 Machine 5 Area System;
- Comparing the performance of method NNM with the TEF methods.
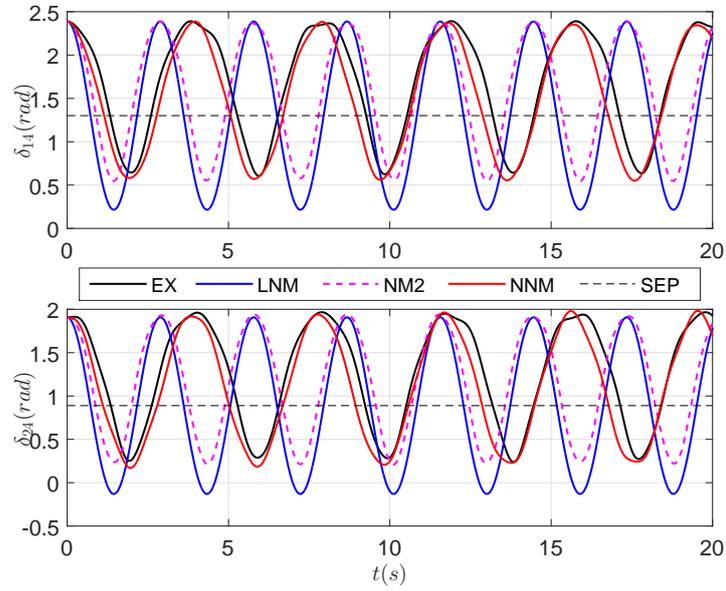
Figure 4.13: Different Models to Approximate the Reference Model
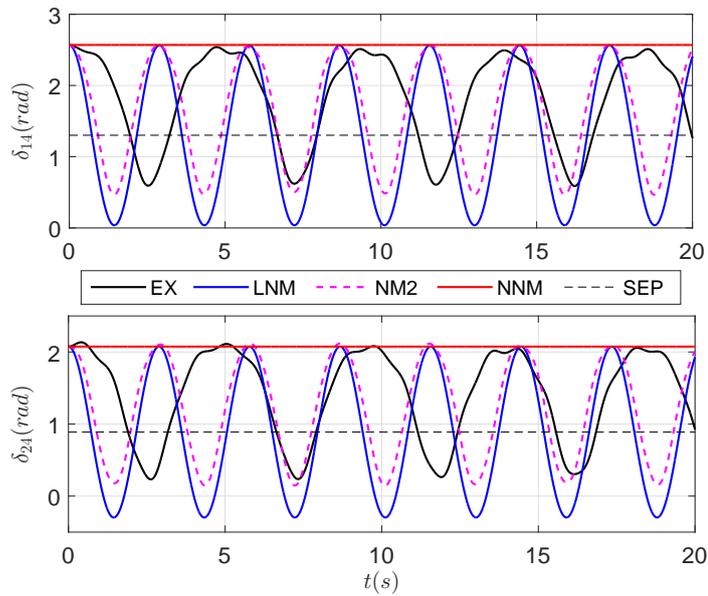
Figure 4.14: At the Stability Bound
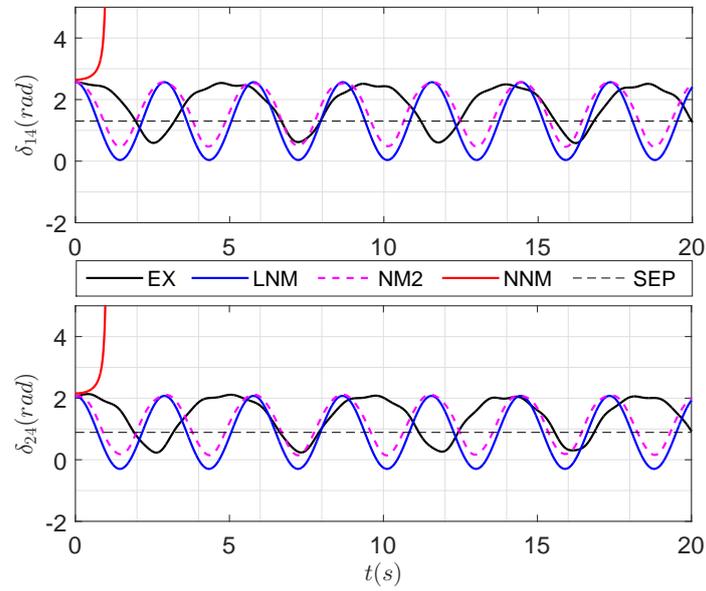
Figure 4.15: Exceeding 2% Bound
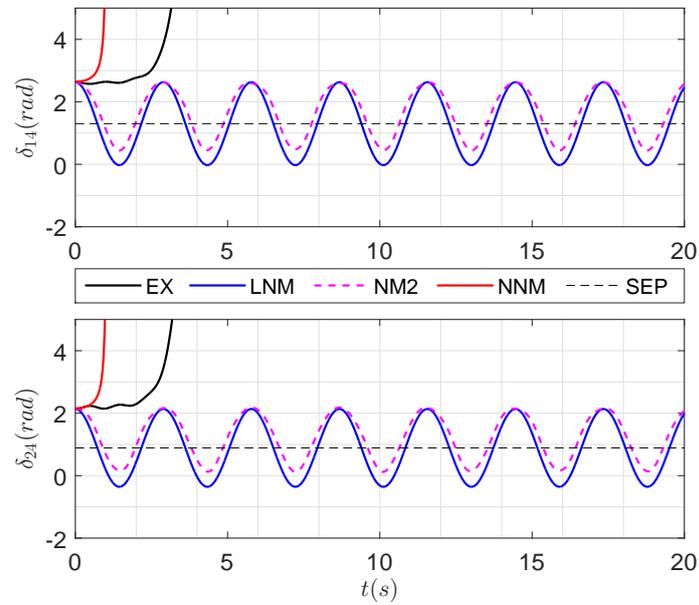
Figure 4.16: Exceeding 5% Bound

4.5.3 Originality and Perspective

It is for the first time that the transient stability is assessed by taking the nonlinearities simplified by normal form transformations. In the sense of "simplest form" (the principle of MNFs), it makes possible to calculate a minimum of nonlinearities and therefore develop a tool more applicable for larger networks composed with more generators. The current work is to test the applicability of the proposed tool on larger networks and to work in the engineering part. The perspective of this research task is to make possible:

On-Line Transient Stability Assessment of Large Interconnected Power Systems

From Analysis to Control and Explorations on Forced Oscillations

In previous chapter, nonlinear analysis using the proposed methodologies are made with investigations on the advantages and limitations. The objective of nonlinear analysis is to have a clear picture of the system dynamics.

The next step is to improve the system dynamic performances, i.e, to the control techniques to enhance the system stability. Concerning nonlinear control, two approaches are proposed. One is the nonlinear analysis based control, the other is the nonlinear model decoupling basis control.

The first approach is to improve the system dynamic response based on the extra information offered by the nonlinear analysis, which is recently popular. The principle of the second approach is to decouple the nonlinear system and is named as "Nonlinear Modal Control". The second approach is for the first time proposed in this PhD work and it is very original and innovative

Besides the explorations on the control, analytical investigations on the forced oscillations are conducted, which is the first step to implement the nonlinear modal control. And the derivation of Normal Forms under forced oscillations illustrates further the philosophy of normal form theory.

For both approaches, a literature review of similar works are conducted, to show the necessity and expected scientific contribution of the proposals.

As several novel concepts concerning the nonlinear modal control are proposed in this chapter and in order to facilitate the reader's comprehension, their linear counterpart are firstly illustrated and then extended to the nonlinear domain. This PhD research may kick the door for future researches or another couple of PhD dissertations.

In the final section, it also provides an innovative proposal in research of normal form theory– the derivation of the control form of normal form.

Keywords: Conclusion of Nonlinear Analysis, On-going Works, Nonlinear Modal Control

5.1 From Nonlinear Analysis to Nonlinear Control

This PhD research works on the very fundamental problems concerning nonlinear systems having multiple input with coupled dynamics. Multiple input system with coupled dynamics almost cover all the modern industrial systems, since high-performance industrial electromechanical systems are often composed of a collection of interconnected subsystems working in collaboration. These dynamical systems can be found everywhere and contribute largely to our daily life, to the national economy and global development.

In the previous chapters of this PhD dissertation, methodologies to analyze the dynamics of some types of multiple input systems with coupled dynamics are proposed and validated with case-studies of interconnected power systems.

However, the more important thing in this work, is to point out the way to use the information obtained from the analysis to improve the dynamic performance of the system, such as enhancing the system stability, damping the interarea oscillations and etc. This can be partly done by designing the parameters of the system using the analysis results as a reference, partly done by controlling the existing system.

In Chapter 2 with the case study of interconnected VSCs, method NNM has already shown its ability to quantify the influence of physical parameters the nonlinearity in the system. Therefore, a rather simple but rude way is to design the physical parameters such that the system can work in a region where it can be viewed as a linear system. Then all the advantages of linear systems would be granted. (Of course, method 3-3-3 can do a similar job.)

However, it is very difficult or expensive to design parameters in such a way, or impossible, especially for the electric power system. Therefore, the main technique to improve the system dynamics is to control it.

Based on EMR + IBC (which is introduced in Chapter 1), once the system's behaviours can be quantified by the analytical analysis, the control strategies can be developed to improve the system dynamic performance, since the relationship between control and analysis can be described as Fig. 5.1:
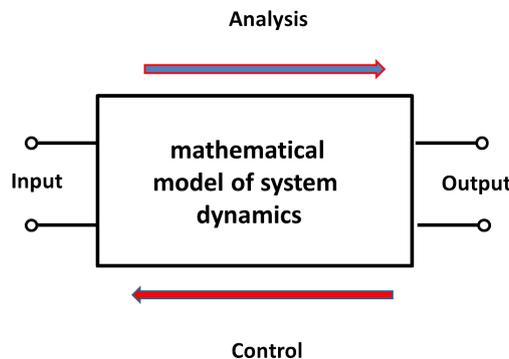
Figure 5.1: Control and Analysis

- **For the analysis, it is to predict the "output" from the given "input";**
- **For the control, it is Analysis + Feedback.**

where the "output" is system dynamic performance, such as the motion, the oscillation and etc; and the "input" can be the design parameter of the physical system, such as the parameters of the controller, the placement of the stabilizers,..., and the external force.

5.2 Two Approaches to Propose the Control Strategies

There are innumerable approaches to develop the control strategies to improve the system dynamic performances. Based on the accumulated experience in linear control, there are two typical approaches:

- *Analysis based control strategy:* the principle of this type of control strategy is to obtain the best analysis results. Examples can be found in tuning the controller parameters. The mathematical model of the system including the controllers is firstly formed, and secondly the indexes quantifying the system dynamics are calculated, thirdly the search algorithm is lanced to search to optimizes the indexes to ensure a best dynamic performance. Examples of linear control can be found in tuning the controllers and aid in the location of controllers.
- *Decoupling basis control strategy:* the principle of this type of control strategy is to decouple the multiple input system with coupled dynamics into independent subsystems, and control strategies are proposed to control those subsystems independently by imposing the command force. The command force are calculated by inverse the mathematical model of the system dynamics and plus the compensation. Examples of linear control strategies belonging to this type can be found in vector control, and modal space control.

In this chapter, the linear control is extended to the nonlinear domain. To illustrate this, the concerned linear control strategies are reviewed and then the methods to extend the linear controls to the nonlinear domain are outlined.

5.3 Approach I: Analysis Based Control Strategy

5.3.0.1 Tuning the controllers:

a. Tuning the controller or stabilizers by linear small signal analysis:
In the linear analysis and control, analysis-based control strategies are widely used to tune the controller parameters, such as tuning the controller parameters based on sensitivity-analysis. The model is based on $\boldsymbol{x} = \boldsymbol{Ax}$, since the eigenvalues of A decides the stability of the system and the time needed to reach steady state, the objective is to obtain the wanted eigenvalues. This method is especially efficient for automatic tuning of controller composed of cascaded loops, as shown in Fig. 5.2. Fig. 5.2 indicates an example coming from the Virtual Synchronous Machine control of voltage source converter (VSC) [29]. The objective is to reduce the time constant of the critical eigenvalues (the eigenvalues with the biggest time constant), therefore the system will have fastest possible dynamic response. It is a heuristic process

to tune the parameters with the highest sensibility factor (i.e the parameters that contribute the most to the critical eigenvalues), as shown in Fig. 5.3. More details can be found in [29, 80].
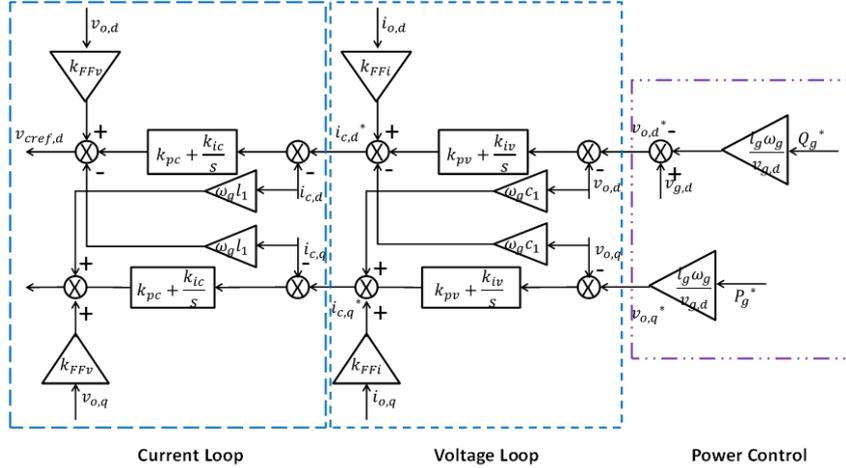
Figure 5.2: The Controller Composed of Cascaded Loops

b. Tuning the controllers or stabilizers based on the nonlinear indexes: As indicated in the previous sections, the stability and the oscillation of the nonlinear systems can be quantified by the nonlinear indexes. And it is the nonlinear indexes such as SI and $MI3$ that predict accurately the system dynamic performance (such as stability and modal oscillations), rather than the eigenvalues. Therefore, the principle to tune the controller parameters taking into account the nonlinear properties is to obtain the desired nonlinear indexes. To enhance the stability is to reduce the real part of SI, and to damp the oscillation is to reduce $MI3$. An example can be found in [16], where the parameters of PSS are tuned to obtain the best nonlinear stability performance.

The nonlinear sensitivity-analysis based algorithm for tuning the controllers is shown in Fig. 5.4

5.3.0.2   Aid in the Location of Stabilizers:

The stabilizer can damp the oscillations in the dynamical system, such as the Power System Stabilizer (PSS) for power systems. However, the stabilizers can be expensive and difficult to be equipped. An important issue in power system is to damp the oscillations to the maximum with a minimum number of PSSs. One choice to place the stabilizer on the symtem component that contributes the most to the oscillations in the system dynamics. And the principle of this type of control strategies is to damp the oscillations by locating the stabilizer on the system component containing the states that have largest participation factors.

a. Locating the stabilizer using linear participation factor We take New England New York 16 machine 5 area system as an example, which is presented in
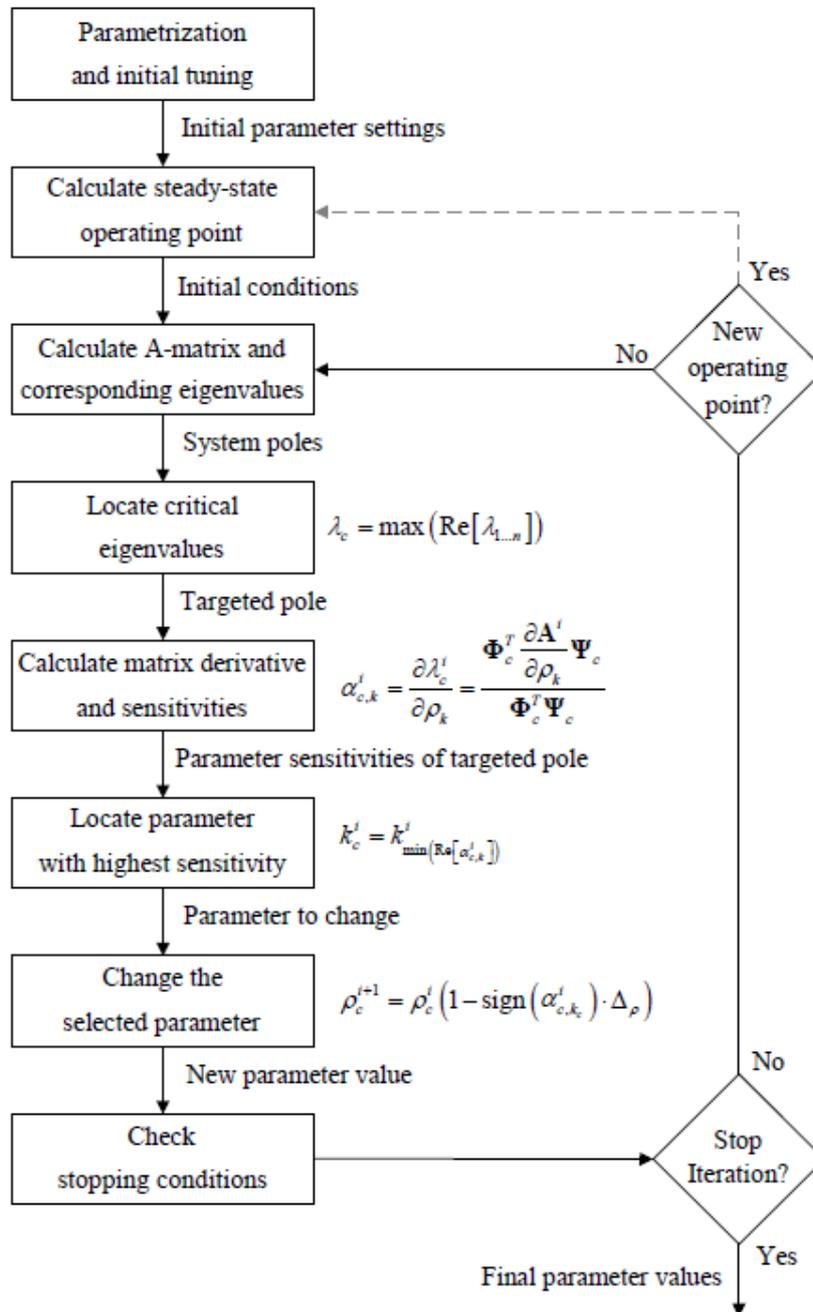
Figure 5.3: The Sensitivity-Analysis Based Algorithm of Tuning the Controllers
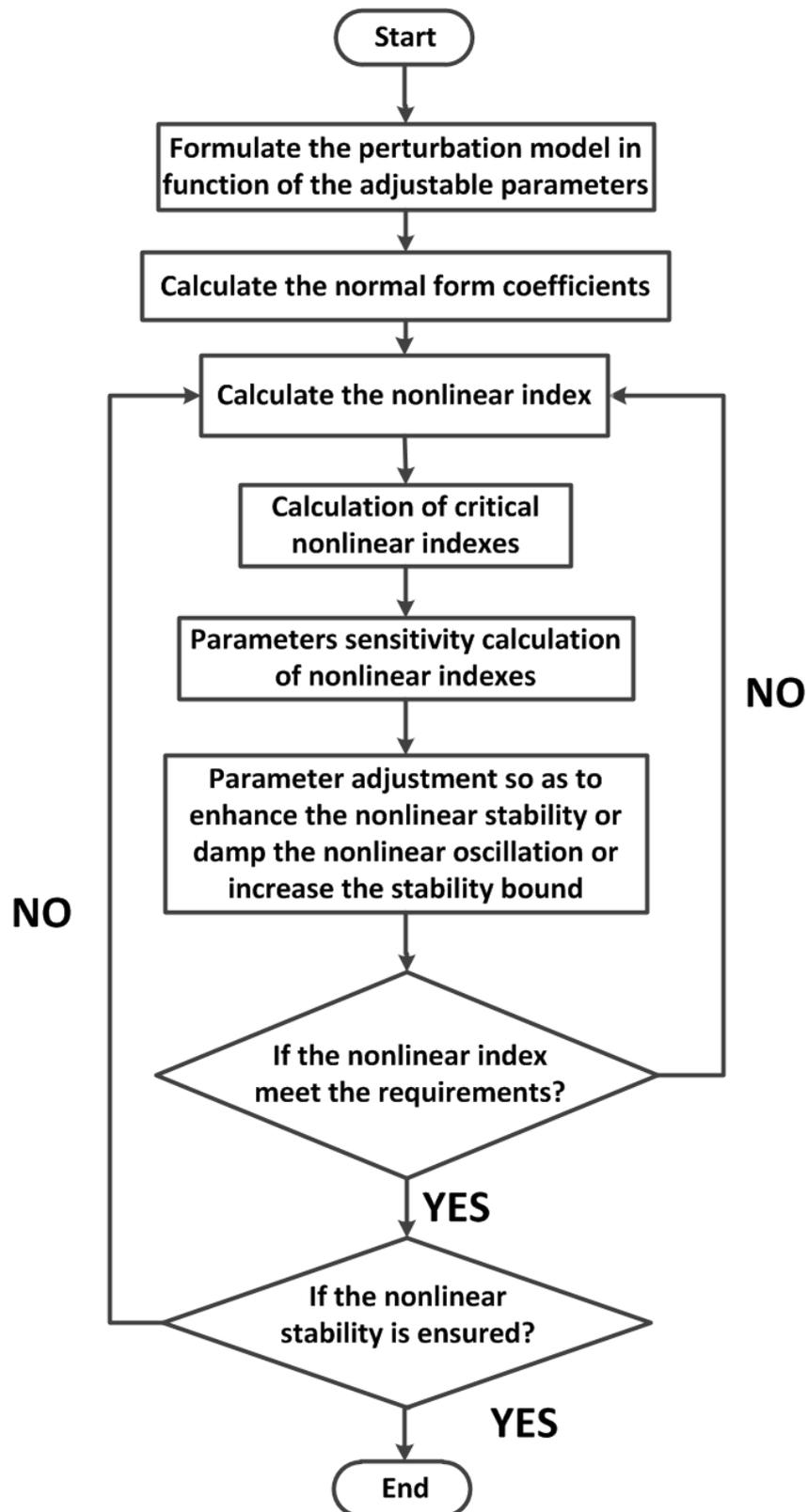
Figure 5.4: The Proposed Nonlinear Sensitivity-Analysis Based Algorithm for Tuning the Controllers

Chapter 1 & Chapter 3. The PSSs are equipped on the generators with the highest participation factor in the oscillations. As in Chapter 3, by locating the PSSs on the G6 and G9 (whose electromechanical states contributes much to the oscillations in the interconnected power system).

b. Locating the stabilizer based on the nonlinear indexes Since the nonlinear oscillations can be quantified by analytical nonlinear sollutions, nonlinear participation factor can be proposed. And the nonlinear oscillations can be damped to the maximum by placing the stabilizers on the system component with the highest nonlinear participation factor.

Second participation factors have been proposed by several literatures [32, 48, 58]. And the third participation factors can be similarly proposed. For sake of compactness, the third participation factors are not listed in this PhD dissertation, and the reader can easily deduce them under the light of [48, 58].

5.3.0.3 Assigning the Power Generation

Indicated by Chapter 3 & Chapter 4, the power transfer limit can be predicted more accurately by taking into account of the nonlinearities. In the interconnected power system, there may be numerous generators or electric sources which work in collaboration to deliver the load. Knowing the power transfer limit can help us to optimize the power generation assignments, to exploit the system's working capacity to the maximum, which is crucial for optimal operation and planning processes of modern power systems. This problem is more economical than technical.

5.4 Approach II: the Nonlinear Modal Control

The first approach is almost an off-line approach, is there an approach to do the

5.4.1 State-of-Art: The Applied Nonlinear Control

In the milestone book *"Applied Nonlinear Control"*, whose first edition is published in 1991 by Slotine,a professor in MIT, the nonlinear control strategies in practice are reviewed [81] and can be classified into three groups [82].

1. The most common control method is to ignore the nonlinearities and assume their effects are negligible relative to the linear approximation and then design a control law based on the linear model. Despite numerous other methods devised for finding "equivalent" linear systems, the most popular procedure is the Taylor series of the equations of motion around the stable equilibrium point and abandoning the nonlinear terms. It is the most common method, since it is the simplest method to be implemented and can be applied to systems with large numbers of degrees of freedom. However, as Nayfeh and Mook mentioned, a number of detrimental effects can be over looked when nonlinearities are ignored [55]. "von Kármán observed that certain parts of an airplane can be violently excited by an engine running at an angular speed much larger

than their natural frequencies, and Lefschetz described a commercial aircraft in which the propellers induced a subharmonic vibration in the wings which in turn induced a subharmonic vibration in the rudder. The oscillations were violent enough to cause tragic consequences."

2. The second most common control method is to apply linearizing control to the system such that the system acts as if it is linear. By changing the state variables and/or applying a control which linearizes the system, the nonlinear equations of motion are transformed into an equivalent set of linear equations of motion, such as the feedback linearization control. The main benefits of linearizing control are that the full range of powerful linear control methodologies can be applied. However, major limitations exist for linearizing control [83]. Firstly, it cannot be used for all systems. Secondly, strict controllability and observability conditions must be met. And finally, robustness of the controlled system is not guaranteed in the presence of parameter uncertainty. Any error in the nonlinear part of the model will prevent the linearizing control from linearizing the dynamics of the structure.

3. A third method is to apply robust control, such as H_∞, and include the nonlinearities as uncertainties. Although this will lead to robust stability, it will not provide robust performance. Clearly the best control law should come from design using all of the available model information, which is not applicable in industry practice [82].

5.4.2   The Limitations

Although the development of computation technology and microprocessors brought numerous new methods to deal with nonlinear control, their principles still belong to the above three groups.

As concluded from the their principles, these control methods either neglect the nonlinearities or only add some compensations in the amplitudes. And they all fail to consider the qualitative aspect of the non-linear behaviour accurately but just endeavor increase the quantitative resolution. Those applied controls were very practical, because at the moment when those nonlinear control strategies were proposed, the analytical analysis results hadn't been available.

However, nowadays by the nonlinear analysis, nonlinear properties are exacted such as the amplitude-dependent frequency-shift (which will influence the frequency of the oscillations), the higher-order modal interaction and the nonlinear stability (which will influnce the decaying of the oscillations) . Therefore, control techniques may be proposed to accurately take into account the nonlinearities.

5.4.3   Decoupling Basis Control

The decoupling basis control methods are very popular since they decompose the complex multiple-input system having coupled dynamics into decoupled single input single output (SISO) subsystems. One then needs only to control the SISO system,

which is a solved problem. The techniques are easy to comprehend since it has clear physical meanings.

5.4.3.1 Vector Control in Electrical Domain

Among the decoupling basis control methods, one famous example is the dq decoupling vector control based on the Park transformation proposed in 1929 by Robert H. Park. It is firstly applied to analyze the dynamics of electric drives by decomposing the physical state variables into dq components, where d component contributes to the magnetic flux of the motor, the q component contributes the torque. By independently controlling the dq components, the dynamic performance of electric drives have been largely improved. Nowadays it has been generally applied in modelling, analyzing and controlling of electrical systems, such as electrical drives, generators, power electronics and etc. Even in this PhD dissertation, the test systems are modelled in the dq synchronous frame, such as indicated by the equations in Chapter 3. And another example can be found in Fig. 5.2. The vector control is almost the most popular, classic and well konwn control method in electrical engineering.

In the vector control, the N-dimensional dynamical system are decoupled into first-order 1-dimensional differential equations and the control strategies are implemented independently based on each equation.

5.4.3.2 Modal Space Control in Mechanical Engineering

Similar to the analysis part, there are decoupling control methods for system modelled as second-order differential equations, which are implemented in the modal space.

Modal space control is very popular in the mechanical engineering, which can be classified into Independent Modal Space Control and Dependent Modal Space Control(DMSC). The modal approach has a more clear physical meaning, as it decouples the N dimensional system (the original system) into N 1-dimensional subsystem, and then all the subsystems are second-order oscillators. The solution in the modal form can indicates the physical motion of the system, which is called as normal mode. The modes are normal in the sense that they can move independently, that is to say that an excitation of one mode will never cause motion of a different mode. In mathematical terms, linear normal modes are orthogonal to each other. The most general motion of a linear system is a superposition of its normal modes. Therefore the original N-dimensional problem is reduced to a series of 1-dimensional problems. The problem complexity is largely reduced.

Inversely speaking, when each mode can be independently studied, the contribution of each input to the dynamics of this system can be figured out, and by imposing different inputs, desired response of the system can be obtained. The precision of positioning control is largely increased. This is the principle of modal control. To the author's knowledge, the linear modal control is firstly realized by Balas in 1978 [84]. And the idea of "decoupling" and the concept "independent modal space control" was first proposed by [85]. After that, linear modal control has been widely studied

and applied. Normally, there are two types of linear modal control, Independent Modal Space Control (IMSC) and Dependent Modal Space Control (DMSC) [86]. Both of them belong to linear modal control.

Compared to vector control, the advantage of modal space control is that it can be implemented with fewer controllers and fewer loops. Controlling a system composed of one second-order equation, two control loops should be implemented if vector control is adopted; however, only one PID controller may be needed if modal space control is adopted.

In this PhD dissertation, some explorations are made to generalize the linear modal control into the nonlinear modal control.

5.4.4 A Linear Example of Independent Modal Space Control Strategy

An example can be found in [87], whose principle can be shown in Fig. 5.5.
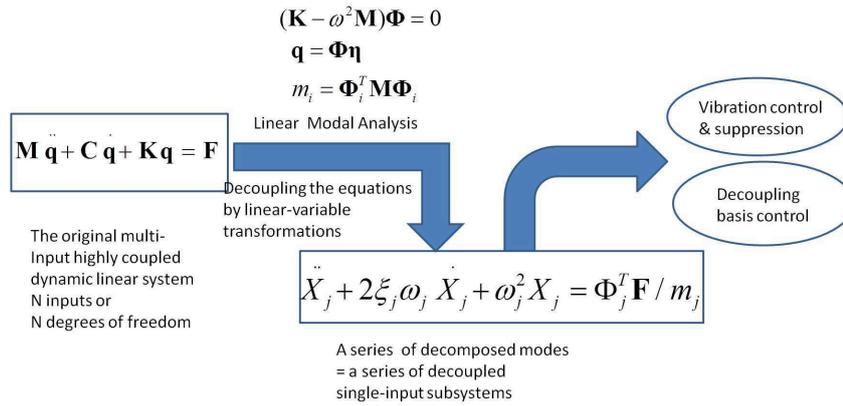
Figure 5.5: The Topology of the Linear Modal Control

It decouples the system under excitation represented by (5.1):

$$M\ddot{\boldsymbol{q}} + D\dot{\boldsymbol{q}} + K\boldsymbol{q} = \boldsymbol{F} \tag{5.1}$$

into a set of 1-dimensional second-order equations as (5.2).

$$\ddot{X}_j + 2\xi_j\omega_j\dot{X}_j + \omega_j^2 X_j = \frac{\Phi_j^T F_j}{M_j} \tag{5.2}$$

Therefore, by intelligently choosing the F_j, the dynamics of X_j will be controlled as desired. To compensate the time-delay and uncertainties in the system dynamics, the feedfoward and feedback controllers are implemented to improve the control performance [87]. Those technical details will not be addressed here and the reader can refer to [87].

As shown in Fig. 5.6, the IMSC, which is based on the equation of the dynamical system is a linear version of the equation studied in Chapter 2 and Chapter 4.

Therefore, it can be generalized to nonlinear domain.

5.4.5   Nonlinear Modal Control

A schema of the proposed nonlinear modal control can be found in Fig. 5.6. The principle is to decouple the nonlinear system into several nonlinear subsystems, and independently control those subsystems or damp the desired modes.
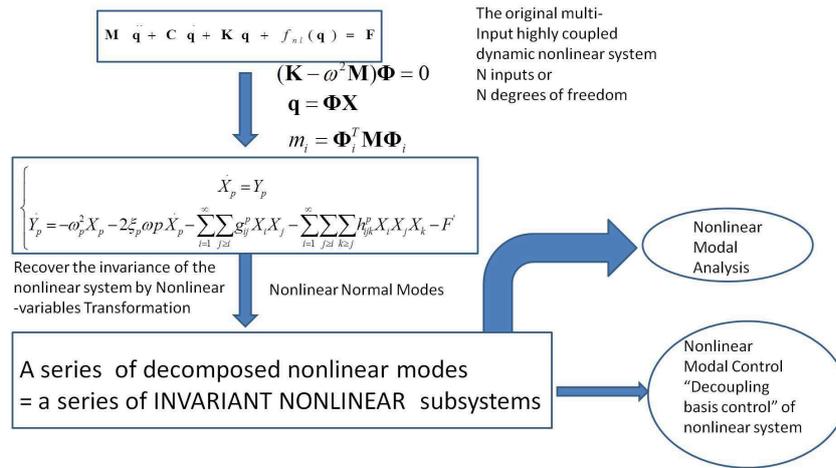
Figure 5.6: The Topology of the Nonlinear Modal Control

5.4.6   How to do the nonlinear modal control ?

As shown in Fig. 5.6, we control the system dynamics by imposing the nonlinear modal force. To implement the nonlinear modal control, there are two questions to answer:
  - What is the nonlinear modal force for each decoupled nonlinear mode ?
  - How to impose the force ?

To answer the first question, we need to investigate the system dynamics under the excitation. This is the first step.

To answer the second question, we use the inversion-based control (IBC) strategy. This is the second step.

5.5   Step I: Analytical Investigation of Nonlinear Power System Dynamics under Excitation

As presented in the Chapter 4, we essentially study the system dynamics modelled by Eq. (5.3).

$$\boldsymbol{M\ddot{q}} + \boldsymbol{C\dot{q}} + \boldsymbol{Kq} + \boldsymbol{f}_{nl}(\boldsymbol{q}) = 0 \qquad\qquad (5.3)$$

Table 5.1: Comparison of Existing and Proposed Normal Form Approximations

Method	Transformation	Decoupled/Invariant	Normal Dynamics	Free Oscillations / Excited systems
LNM [55]	linear	decoupled	linear	free and forced
NNM [21,22]	order 3	decoupled	order 3	free
FDNF3	order 3	decoupled	order 3	free and forced

with $\boldsymbol{M}$ and $\boldsymbol{D}$ are constant symmetric inertia and damping matrix, whose values depend on the physical parameters of the power system and controller parameters. $\boldsymbol{K}$ and $\boldsymbol{f}_{nl}$ indicate the coupling between the variables, where $\boldsymbol{K}$ is a constant matrix, including the linear terms and $\boldsymbol{f}_{nl}$ gathers the nonlinear terms.

As observed from (6.2) and (5.3), the input is null. Therefore, the methodologies presented in Chapters 2, 3, 4 focus on the case that the system is not excited, or the excitation is constant. Or speaking from the perspective of mechanical engineering, what we studied before are free-oscillations.

If we want to influence the system's nonlinear dynamics by imposing the force, analytical investigation should be conducted on system dynamics under excitation.

5.5.1 Limitations and Challenges to Study the System Dynamics under Excitation

Nonlinear analysis can replace the linear analysis as it does a better job in all the three issues: describing the dynamic response, modal interactions and stability analysis. However, the existing nonlinear analysis tools only deal with the case of free oscillations (e.g the post-fault case after the fault is cleared), and not with excited systems (i.e the oscillations caused by variable power references or variable loads). This largely limits the scope of the NF analysis. This is a big disadvantage compared to the linear analysis, which can deal with the case when there are changes in the input (voltage reference, power reference, load, etc) as well as when there are no excitation (free oscillations).

The challenge is to take into account the force vector when doing the normal form transformations. A methodology is proposed in Section 5.5 to overcome such a challenge.

5.5.2 Originality

In this PhD work, a method is introduced to study the power system nonlinear forced oscillations. To the author's knowledge, it is for the first time that an analytical analysis tool based on NF theory is proposed to analyze the nonlinear power system dynamic under excitation. This enlarges the scope of NF analysis and lays the foundation for the lately proposed nonlinear modal control.

5.5.3   Theoretical Formulation

The oscillatory modes of power system can be modeled by (5.4). If the variables of
the system are gathers in a N dimensional vector $\boldsymbol{q}$, the motion equation writes as:

$$\boldsymbol{M}\ddot{\boldsymbol{q}} + \boldsymbol{C}\dot{\boldsymbol{q}} + \boldsymbol{K}\boldsymbol{q} + \boldsymbol{f_{nl}}(\boldsymbol{q}) = \boldsymbol{F} \tag{5.4}$$

where $\boldsymbol{M}, \boldsymbol{C}$ are constant diagonal inertia and damping matrices, whose values
depend on the physical and controller parameters of the system. $\boldsymbol{K}$ and $\boldsymbol{f_{nl}}$ indicate
the coupling between the variables, where $\boldsymbol{K}$ is a constant matrix including the linear
terms and $\boldsymbol{f_{nl}}$ gathers the nonlinear terms coming from the 2nd and 3rd order terms
of the Taylor series. $\boldsymbol{F}$ is the excitation vector.

5.5.4   Linear Transformation: Modal Expansion

A modal expansion $\boldsymbol{q}(t) = \boldsymbol{\Phi}^T \boldsymbol{x}(t)$ can transform (5.4) into modal coordinates with
decoupled linear part [55].

$$\ddot{X}_p + 2\xi_p\omega_p\dot{X}_p + \omega_p^2 X_p \tag{5.5}$$
$$+ \sum_{i=1}^{N}\sum_{j\geq i}^{N} g_{ij}^p X_i X_j + \sum_{i=1}^{N}\sum_{j\geq i}^{N}\sum_{k\geq j}^{N} h_{ijk}^p X_i X_j X_k = F_p$$

where ξ_p is the p-th modal damping ratio, and g_{ij}^p and h_{ijk}^p are quadratic and cubic
nonlinearities coming from $\boldsymbol{f_{nl}}$ in Taylor series. Neglecting the nonlinear terms in
(5.5), a linear model called LNM [55] is obtained and can be used both for analysis
and control of multi-input systems.

5.5.5   Normal Form Transformation in Modal Coordinates

A normal form transformation is proposed in [17, 19], which reads, $\forall p = 1 \ldots N$:

$$X_p = R_p + \mathcal{R}^{(2)}(R_i, S_i) + \mathcal{R}^{(3)}(R_i, S_i), \qquad Y_p = S_p + \mathcal{S}^{(2)}(R_i, S_i) + \mathcal{S}^{(3)}(R_i, S_i), \tag{5.6}$$

where $Y_p = \dot{X}_p$, $S_p = \dot{R}_p$ and $\mathcal{R}^{(3)}, \mathcal{S}^{(3)}$ and $\mathcal{R}^{(3)}, \mathcal{S}^{(3)}$ are second order polynomials
and third order polynomials in R_i ans S_i respectively, fully defined in [17, 19] and
are functions of the g_{ij}^p and h_{ijk}^p coefficients present in (5.5).

5.5.5.1   Normal Dynamics

Up to order 3 and keeping all the terms after the transformation, it leads to a set
of invariant oscillators (if no internal resonance occurs) defined as FNNM [17, 19].
FNNM separates the nonlinear terms into cross-coupling terms and self-coupling
terms. Neglecting the cross-coupling terms, the equations defining the normal dy-
namics are decoupled and defined as NNM and FDNF3.

5.5.5.2   NNM

Free-damped Oscillations

$$\ddot{R}_p + 2\xi_p\omega_p\dot{R}_p + \omega_p^2 R_p \tag{5.7}$$
$$+ (h_{ppp}^p + A_{ppp}^p)R_p^3 + B_{ppp}^p R_p \dot{R}_p^2 + C_{ppp}^p R_p^2 \dot{R}_p = 0$$

5.5.5.3   FDNF3

Systems under excitation

$$\dot{R}_p = S_p - 2b_{pp}^p S_p F_p - c_{pp}^p F_p R_p \tag{5.8}$$
$$\dot{S}_p = -\omega_p^2 R_p - 2\xi_p\omega_p\dot{R}_p$$
$$- (h_{ppp}^p + A_{ppp}^p)R_p^3 - B_{ppp}^p R_p \dot{R}_p^2 - C_{ppp}^p R_p^2 \dot{R}_p$$
$$+ F_p - 2\beta_{pp}^p S_p F_p - 2\gamma_{pp}^p F_p R_p$$

It is shown that, when F is zero, (5.8) becomes (5.7). In other words, (5.7) is a specific case of (5.8) or (5.8) is a generalization of (5.7). (5.8) shows that transforming variables expressed in $X - Y$ coordinates into $R - S$ coordinates will add coupling terms in the excitation vector F ($2\beta_{pp}^p S_p F_p - 2\gamma_{pp}^p F_p R_p$ terms). The NF approximation decouples the state-variables but adds some coupling terms in the excitation vector components.

5.5.5.4   Reconstructing the Results for the Original System

Multi-scale calculating methods can be used to compute an approximate analytical solution of (5.7) and (5.8). From R_p, S_p variables, X_p, Y_p can be reconstructed using transformations (5.6). The efficiency of FDNF3 is validated by a case-study based on interconnected VSCs and compared to the classical linear analysis tool LNM.

5.5.6   Case–Study: interconnected VSCs under Excitation

5.5.6.1   Test System

Modern girds are more and more composed of renewable-energy-based power generators that can be interconnected to the grid through long transmission lines [88]. This weak grid configuration can lead to nonlinear oscillations [22, 89]. To illustrate this particular case, a test case composed of two interconnected VSCs to a transmission grid as been chosen, as shown in Fig. 5.7.
VSC_1 and VSC_2 are interconnected by a short connection line having a reactance X_{12} and are both connected to the transmission grid by long transmission lines having reactances X_1, X_2.
To study the nonlinear interactions under disturbances or variable references or loads, a detailed mathematical model is firsly made, which consists of the physical structure as well as the current, voltage and power loops. To design the power
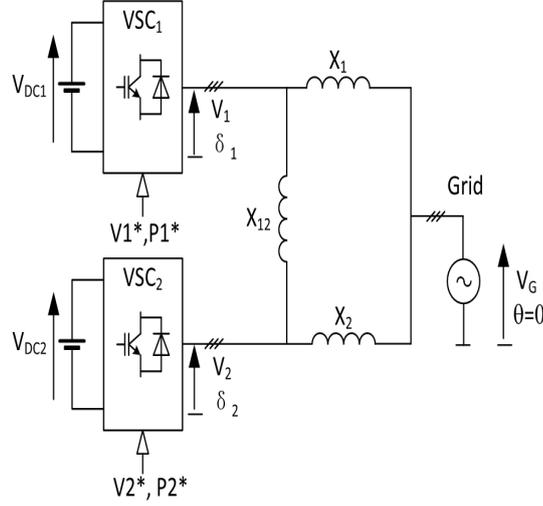
Figure 5.7: Test System Composed of interconnected VSCs

loop, since the conventional PLL controller can cause synchronization problems when facing connections using long transmission lines [66], the Virtual Synchronous Machine (VSM) control strategy is adopted [29].

For the chosen test case, the equivalent switching frequency of VSCs is set as $1700Hz$ and the control loops are tuned with time constants as $T_{current} = 5ms$, $T_{voltage} = 60ms$, $T_{power} = 1.47s$. Large Volume Capacitor is installed to avoid the voltage collapse.

The electromagnetic model of one VSC is a set of 13th order equations [29], and the order of the overall system model can be higher than 26. Considering that the current and voltage loops are linear and that the time constants of the three loops respect $T_{power} \gg T_{voltage} \gg T_{current}$, the voltage V_1 and V_2 at the Point of Common Couplings (PCC) of VSCs are assumed sinusoidal with constant amplitudes and power flows are represented by dynamics in power angles. Thus, a reduced model to study the nonlinear interactions of the system presented in Fig. 5.7, can be described as (5.4). A *4th* order model is then chosen to govern the nonlinear dynamics of the system.

$$M_1 \frac{d^2\delta_1}{dt^2} + D_1 \frac{d\delta_1}{dt} + \frac{V_1 V_g}{X_1} \sin\delta_1 + \frac{V_1 V_2}{X_{12}} \sin(\delta_1 - \delta_2) = P_1^*$$

$$M_2 \frac{d^2\delta_2}{dt^2} + D_2 \frac{d\delta_2}{dt} + \frac{V_2 V_g}{X_2} \sin\delta_2 + \frac{V_1 V_2}{X_{12}} \sin(\delta_2 - \delta_1) = P_2^*$$

(5.9)

In (5.3), δ_1 and δ_2 represent the power angles. X_1 and X_2 are the reactances of the transmission lines which connect the two VSCs to the transmission grid. X_{12} is the reactance of the line interconnecting the two VSCs. V_1, V_2, V_g are the RMS voltages at the PCC of the VSCs and at the grid. Finally, P_1^* and P_2^* are the active power
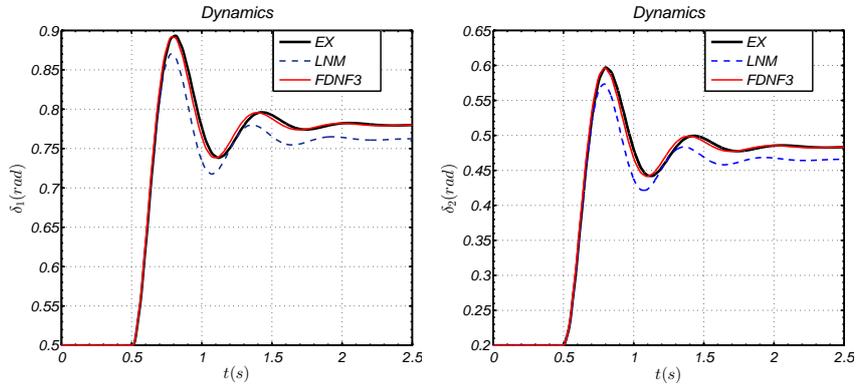
Figure 5.8: System Dynamics under Step Excitation

references, which are set according to the expected operating points.

5.5.6.2 Selected Case Study

A case is selected to test the proposed method. Step Excitation in the Power Reference: VSC_1 and VSC_2 respectively transfer an amount of power as $0.68pu$ and $0.28pu$. It is supposed that there is an increase in the wind energy supply, which implies a step in the power reference of $0.2pu$ for both VSCs. The system experiences then oscillations due to excitation.
The time-domain simulation is done by using a EMT software to assess the performance of the proposed method.

5.5.6.3 Original Results

The dynamics in the power angles of the VSCs, δ_1 and δ_2 are shown in Fig. 5.8. The step excitation in $P_1^* = P^*$ equal to 0.2pu happens at the time $t = 0.5$.
Fig. 5.9 shows that, as proposed by the classical linear analysis, the system dynamic can be decoupled into 2 simpler ones $Ex \approx Sub1 + Sub2$, making it possible to identify that $Sub1$ has a lower frequency and $Sub2$ has a much higher frequency.
As a generalization of NNM, FDNF3 has the property of decomposing a N-dimensional nonlinear system into a nonlinear sum of nonlinear 1-dimensional nonlinear systems, analogous to linear analysis that decompose a N-dimensional linear system into a linear sum of 1-dimensional linear systems. In this way, the complex power dynamics can be reviewed as the combination simpler ones.
It is shown in Fig. 5.8 that FDNF3 can describe the system dynamic response much more accurately than the linear analysis LNM, especially the overshoot, which corresponds to the limit cycles [55] or the stability bound of system's nonlinear dynamics [5].
Also, as shown in Fig. 5.10, even both VSCs are excited, only one nonlinear mode is excited in $R - S$ coordinates. Therefore, inversely, by controlling $R1, R2$ we can make the decoupling control of VSC_1 and VSC_2 possible even if they work in the
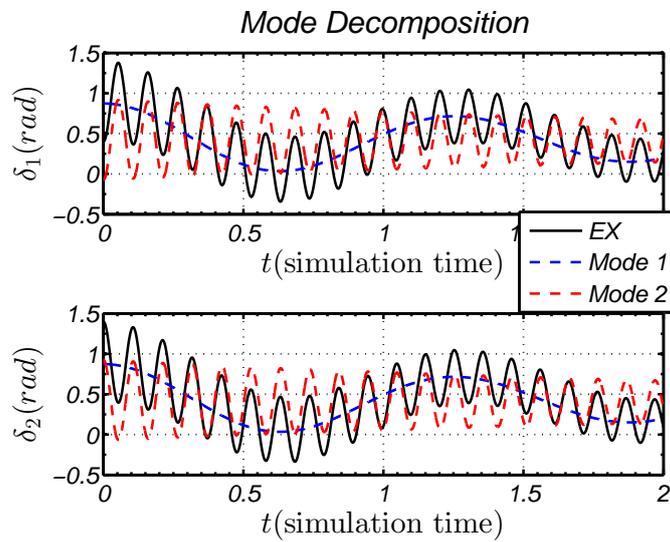
Figure 5.9: System Dynamics Decomposed by NNM
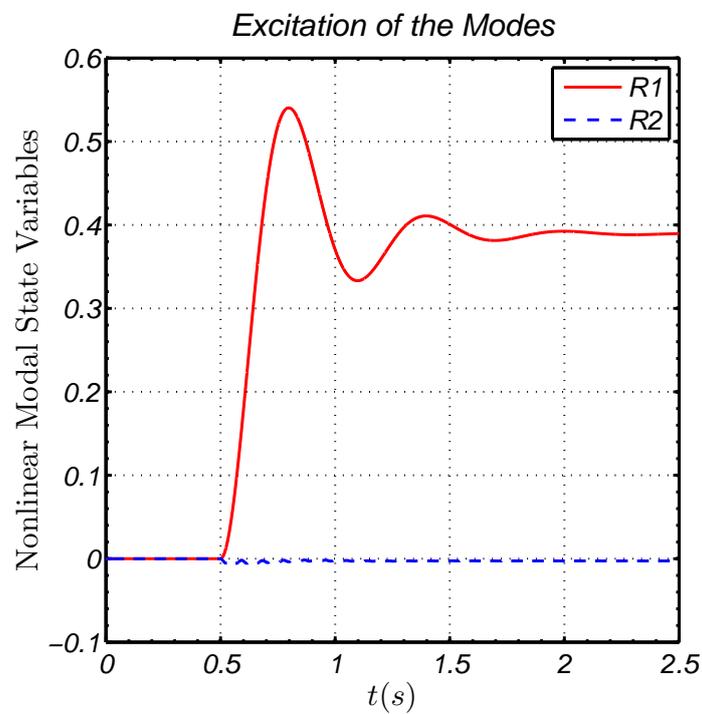
Figure 5.10: Decomposition the Modes under Excitation: R_1, R_2

nonlinear region. It could be one way to overcome the difficulty on how to control VSCs independently when they work in nonlinear regions.

5.5.7   Significance of the Proposed Method

Transforming the original system dynamic into its normal dynamics, it gives a clear picture on how the excitation influences the system dynamics. Compared to the classical linear analysis LNM and the NNM, the advantages of FDNF3 approach can be summarized as:

1. Describing more exactly the power system dynamics under disturbances or under excitation by decomposition of the complex system dynamics into simpler ones;
2. Making possible to independently control interconnected systems even if there are working in highly nonlinear regions.

In this PhD work, to the author's knowledge, it is the first time that Normal Form theory is applied to study the power system dynamics under excitation (i.e. with variable references or loads). The proposed method is validated by comparing results with time-domain simulations based on an EMT software. For the sake of simplicity, only the results under the case $N = 2$ are presented, but the possibility of working with large-scale problems will be investigated by the methodology suggested in this dissertation.

Although the chosen test case is composed of inteconnected VSCs, since the system model is the same as groups of generators working in parallel, the proposed methodology can be applied for studying the modal oscillations between classical generators working in parallel.

The proposed method only shows its ability to describe the power system response by decomposing the complex dynamics. Further applications may be found in modal structural analysis under excitation or stability analysis. This lays the foundation of the future work that:

5.5.7.1   Analysis of Dynamical System under Excitation

The proposed FDNF3 gives the normal forms of the dynamical system under excitation. It makes possible to do stability analysis when there is a change in the input (such as an increase of load or power generation). Also, when measuring the system's oscillations with experiments, it is important to impose the "correct" force. Previously, the nonlinear analysis under excitation is conducted by imposing the force on the free-oscillation Normal Forms:

$$\ddot{R}_p + 2\xi_p\omega_p\dot{R}_p + \omega_p^2 R_p \qquad\qquad (5.10)$$
$$+ (h_{ppp}^p + A_{ppp}^p)R_p^3 + B_{ppp}^p R_p\dot{R}_p^2 + C_{ppp}^p R_p^2\dot{R}_p = F$$

Comparing (5.10) with (5.8), (5.10) fails to take into account the couplings in the F. For the experimental measurements, this will cause large error, since other

modes than p may also excited imposing F_p, i.e, the energy is not only injected into mode p and the *invariance* is broken.

5.5.7.2 Significance in the Control of Dynamical System

The decomposition of nonlinear system makes it possible to control the two VSCs independently in the nonlinear $R - S$ coordinates to reduce the oscillations in the system dynamics. However, this is a open-loop control. To increase the resolution and compensate for the uncertainties, closed-loop control should be implemented.

5.6 Step II: Implementing Nonlinear Modal Control by EMR+IBC

Presented in the previous section, the nonlinear transformation can approximately decouple the system dynamics into nonlinear modes that can be independently controlled by imposing the nonlinear modal force. The next step is to implement the control strategy, which can be realized by EMR+IBC.

5.6.1 The Control Schema Implemented by Inversion-Based Control Strategy

If we represent the decoupling process of the system dynamic model by Energetic Macroscopic Representation (EMR), we can then develop the control schema by inversion-based control (IBC) strategy.

The topology of the nonlinear modal control is shown as Fig. 5.11, considering the nonlinearities up to 3rd order. The linear transformation decouples the linear transformations, and the nonlinear transformation weakens the linear coupling rendering:
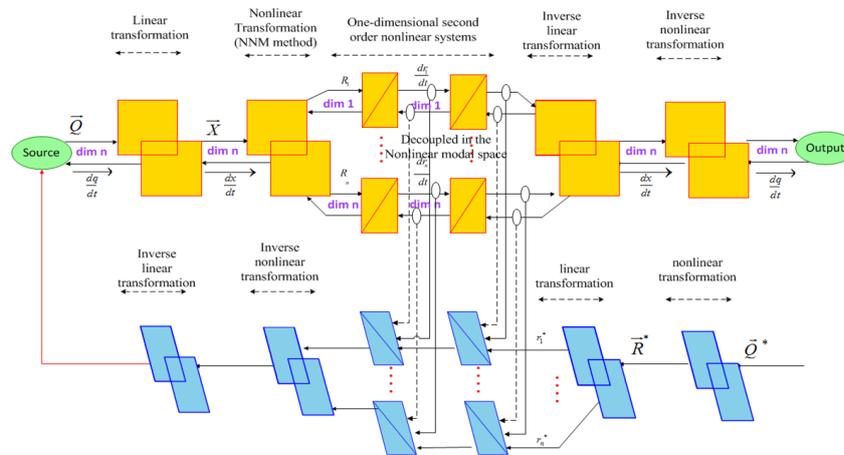
Figure 5.11: The Control Schema of the Nonlinear Modal Control Implemented by Inversion-Based Control Strategy

As observed from the Fig. 5.11, by decomposing the nonlinear system into 1 dimensional subsystems, the nonlinear modal force needed to excite the desired mode can be calculated. Then the force should be imposed on the system is a nonlinear combination of the nonlinear modal force obtained using the Normal Form transformation.

5.6.2   Primitive Results

The exploration of nonlinear modal control is conducted on a gantry system, as shown in Fig. 5.12.
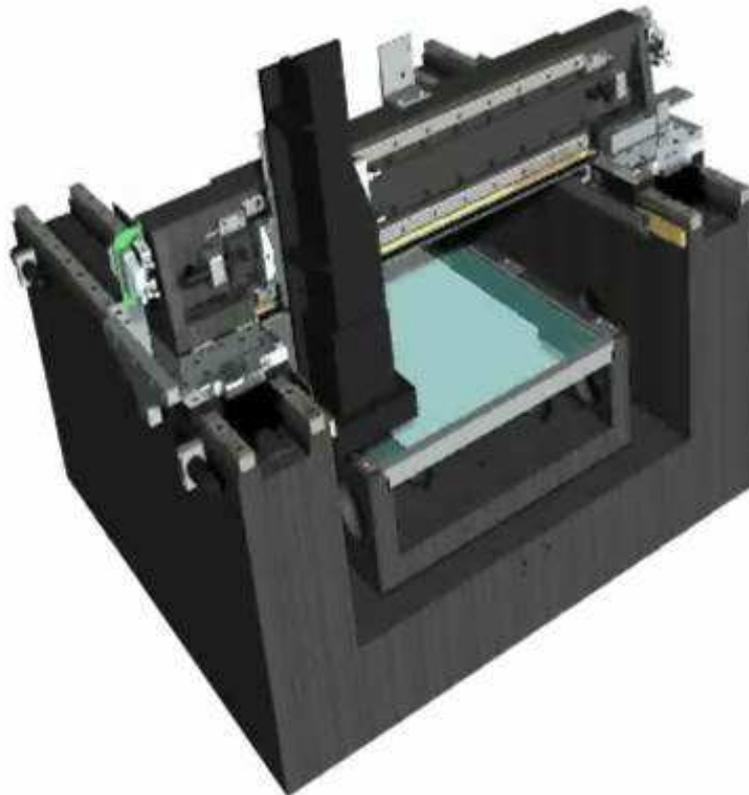
Figure 5.12: An Example of Gantry System

which can be simplified as Fig. 5.13.
For such a system, closed loop control strategy is proposed, as shown in Fig. 5.14 [90].

However, the nonlinear modal control implemented in this way doesn't ensure a good performance, even for nonlinear modal control up to 2nd order where the normal form is a linear system controlled by PID controller. More investigations should be conducted.
The bottle neck may lay in:
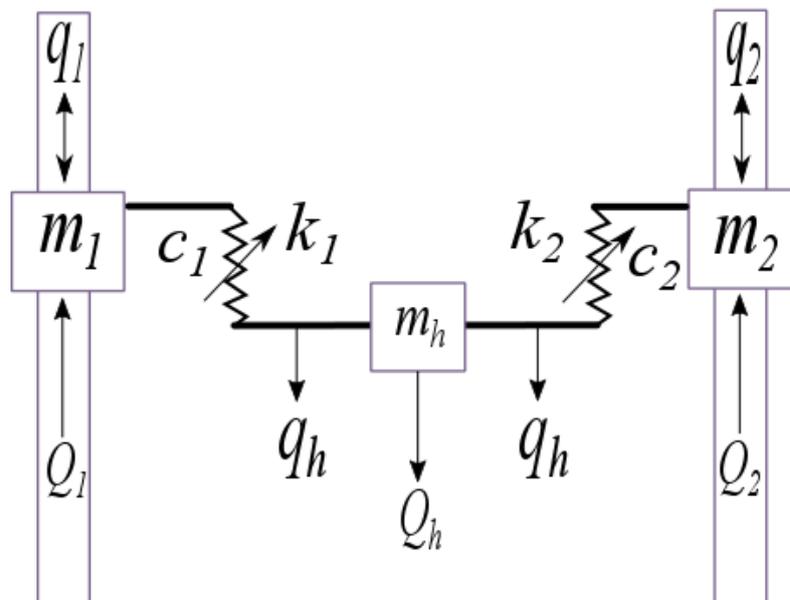
Figure 5.13: The Simplified System of the Gantry System
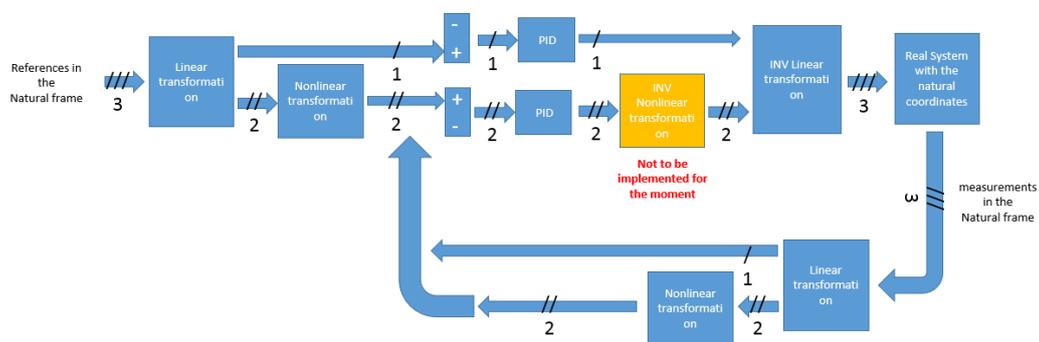
Figure 5.14: The Topology of the Nonlinear Modal Control

- the inverse nonlinear transformation. The way to do the inverse nonlinear transformation has been attached in the Appendix B, for the future researches;
- the validity region of normal form transformations;
- the way to implement the PID controller for the decoupled subsystems.

5.7 Exploration in the Control Form of Normal Forms

If NF can simplify the analysis by transforming the variables into the normal form coordinates, is it possible to simplify the control by the same principle?
This question gives birth to the Normal Form control, for which Poincaré didn't give out any theory or mathematical expressions.

5.7.1 A Literature Review

It is well-known that a state space description of a controllable linear system can be transformed to controllable or controller form by a linear change of state variables. In the sense of being transformed into a "simpler" form, it would be referred to as *Linear Controller Normal Form* [91].
If a nonlinear control system admits a controller normal form, it can be transformed into a linear system by a change of coordinates and feedback. Therefore, the design of a locally stabilizing state feedback control low is a straightforward task. In such a case, we say the system is feedback linearizable. On the other hand, most nonlinear systems do not admit a controller normal form under change of coordinates and invertible state feedback. The nonlinear generalization of the linear controller normal forms, which can be referred to as *Nonlinear Controller Normal Form* (NCNF) has been systematically studied since 1980's by Krener [91]. This approach was extended to control systems in continuous-time by Kang and Krener ([92], see also [93] for a survey) and Tall and Respondek ([94], see [95] for a survey), and by Monaco et all [96] and Hamzi [97] et al. in discretetime. However, this approach mainly focuses on single input system. NCNF for multi-input system is awaited to be developed to cater for the studied case in this thesis.
On another side, the emphasis is on the reduction of the number of monomials in the Taylor expansion, one of the main reasons for the success of normal forms lies in the fact that it allows to analyze a dynamical system based on a simpler form and a simpler form doesn't necessarily mean to remove the maximum number of terms in the Taylor series expansion. This observation, led to introduce the so-called "inner-product normal forms" in [92]. They are based on properly choosing an inner product that allows to simplify the computations. This inner-product will characterize the space overwhich one performs the Taylor series expansion.
The methods reviewed brought several mathematical achievements while their applicability are limited mainly in system having controllable linearization, and in adding the feedback linearization nonlinear control.

5.7.2   A Nouvel Proposed Methodology to Deduce the Normal Form of Control System

In fact, all those methods referred to in the above focus on the generalization of linear controller normal form to the nonlinear domain, the objective is to render a linear normal form by the normal form transformation to aid in the feedback linearization control. However, as shown in Chapter 2, Chapter 3 and Chapter 4, a linear normal form is not ensured for all the cases. And taking into the 3rd order nonlinear terms in the normal forms can suggest more information in the analysis of both the nonlinear modal interaction and nonlinear stability.

Therefore, inspired by the normal form analysis, another approach is proposed to derive the control forms of normal forms, i.e, similar to the analysis, we take the control form:

$$\dot{\boldsymbol{x}} = f(\boldsymbol{x}, \boldsymbol{u}) \tag{5.11}$$

the dimension of the system $T \in R_n \times R_m$ and $u \in R_m$ representing the control And by the cloased-loop control, the u can be represented by

$$\boldsymbol{u} = f_c(\boldsymbol{x}) \tag{5.12}$$

Therefore, the control system can be rewritten as:

$$\dot{\boldsymbol{x}} = f(\boldsymbol{x}, f_c(\boldsymbol{x})) \tag{5.13}$$

5.8   Conclusion

In this chapter, explorations from nonlinear analysis to nonlinear control are conducted. Two approaches and three proposals are illustrated and investigated. Due to the time limit of the PhD, the control strategy is not fully implemented yet. However, those proposal are very innovative and can inspire further investigations. It lays the foundations for future researches. What's more, to the author's knowledge, analytical investigations of nonlinear system dynamics under excitation are conducted for the first time on the power systems.

Conclusions and Perspectives

In this chapter, conclusions on achievements of nonlinear analysis and
The assumptions of methods of normal forms are discussed and investigated. The
classes of the
Unfortunately, the author doesn't have enough time to fully develop the methodology
of nonlinear modal control during the 3 years' PhD period. This PhD research may
kick the door for future researches or another couple of PhD dissertations.
Keywords: Nonlinear Analysis, Nonlinear Modal Control, Multiple Input
System with Coupled Dynamics

6.1 A Summary of the Achievements

This PhD research works on the very fundamental problems concerning nonlinear systems having multiple input with coupled dynamics. Multiple input system with coupled dynamics almost cover all the modern industrial systems, since high-performance industrial electromechanical systems are often composed of a collection of interconnected subsystems working in collaboration. These dynamical systems can be found everywhere and contribute largely to our daily life, to the national economy and global development.

Having made some achievements in the nonlinear analysis to have a clear picture of the system dynamics, several proposals of nonlinear control are investigated which kicks the door for the future investigations.

The achievements can be summarized below, and more detailed discussions are put in the following sections.

- Practical (Application): study of the **nonlinear modal interaction and the stability assessment** of interconnected power systems. This solved a long-time existing problem and explained some nonlinear phenomenon.

  In the previous chapters of this PhD dissertation, methodologies to analyze the stability of some types of multiple input systems with coupled dynamics are proposed and validated with case-studies based on interconnected power systems.

- Foundation for control:
  2 innovative approaches are proposed, investigated and discussed. It opens the way for further developments in both application and normal form theory.

- Theoretical (Methodology): A systematic methodology is proposed, which is innovative and general for nonlinear dynamical systems.
  - development of mathematically accurate normal forms up to **3rd order** for analysis and control of nonlinear dynamical systems with coupled dynamics by **both the PoincarÃ©'s approach and TouzÃ©'s approach**.
  - nonlinear indexes are proposed to quantify the nonlinear properties

6.2 Conclusions of Analysis of Power System Dynamics

The applications of this PhD work are to study the rotor angle dynamics of interconnected power systems when there is disturbance in the transmission line. The methodologies are established in Chapter 2 and are applied to study the interarea oscillations in Chapter 3 and assess the transient stability in Chapters 3 & 4.

Some achievements are made in this PhD research, and a transaction paper has submitted with revision and another transaction is going to be proposed.

Some conclusions are made in this chapter as follows.

6.2.1 Analysis of Nonlinear Interarea Oscillation

Nowadays power systems are composed of a collection of interconnected subsystems working in collaboration to supply a common load, such as groups of generators [1] or interconnected Voltage Sources Converters working in parallel [21,22,98]. One of the most important issue in large-scale interconnected power systems under stress is the oscillations in the power system dynamics [28].
As the oscillations are essentially caused by the modal interactions between the system components, they are called "Modal Oscillations". The complexity of analyzing such oscillations lays in the strong couplings between the components of the system. Understanding of the essence of such oscillations is necessary to help stabilizing and controlling power systems.
To cater for the above demands, analytical analysis tools are developed in this PhD work for:
1. Dynamic performance analysis: suggesting approximate analytical solutions;
2. Modal analysis: describing and quantifying how the system components interact with each other;
3. Nonlinear Stability analysis: predicting the stability of the nonlinear system by taking into account the nonlinear terms in the Taylor series.

6.2.2 Transient Stability Assessment

Transient stability has become a major operating constraint of the interconnected power system. The existing practical tools for transient stability analysis are either time-domain simulations, or direct methods based on energy-function and Lyapunov direct method– the methods of Transient Energy Function (TEF). Though there are numerous meticulous researches on TEF, this method is difficult to implement with large system.
In this PhD research, the stability is assessed by using nonlinear indexes based on 3rd order Normal Forms.
The Transient stability assessment can be done either by the vector field approach, or by the normal mode approach.
The Poincaré's approach (vector field approach) using the nonlinear index SI has the applicability for all generator models whose dynamics can be formulated as $\boldsymbol{x} = f(\boldsymbol{x})$. Unlike the TEF method, it is an easy-to-implement tool with systematic procedures that doesn't need further discussions in the implementation.
Developed in this PhD work, the Touzé's approach (normal mode approach) using the index PSB has been presented to be efficient on the classical models and also possible to be extended to work with more complex models. Since it is rather easy to implement, it can be expected to solve the TSA problem with bright perspectives. One would like to ask a question:

What are the differences between the stability assessments made by the two approaches ? Are they essentially the same ?

In fact, the SI is more accurate than PSB since SI takes into accunt both the

coupled nonlinearities and decoupled nonlinearities and PSB neglects the coupled nonlinearities in the normal forms. SI is based on method 3-3-3, PSB is based on method NNM which is somewhat equivalent to method 3-3-3(S).

However, for the applications, PSB is more adept for multi-machine systems, since it has a much less computational burden and much easier to be calculated.

6.2.3 A Summary of the Procedures

For both methodologies, the procedures of analyzing the power system can be summarized as the flowchart in Fig. 6.1.

To do the Normal Form analysis of electric power systems, there are two stages. The first stage is to formulate the differential equations containing polynomial nonlinearities by perturbing the system around the stable equilibrium point (SEP) by Taylor series, which is labelled as "SEP Initialization"; once the perturbation model is fixed, the Normal Form coefficients are fixed.

After the "SEP Initialization", the second stage is to calculate the initial conditions in the Normal Form coordinates, which is labelled as "Disturbance Initialization". It depends on the disturbance which the system experiences.

6.2.4 Issues Concerned with the Methods of Normal Forms in Practice

To make the methodologies practical for the readers (mathematicians, engineers...), the issues to implement the Normal Form analysis are discussed in Section 2.8 and Section 3.6, such as the search for initial conditions, computational burden, model dependence and etc. The scalability problem and applicability to large-scale systems are also discussed in Section 3.5. Also, the help the readers to implement the methodologies, programs and simulation files are made available online. More details can be found in the appendixes.

6.3 Conclusions of the Control Proposals

In this PhD dissertation, it points out two approaches to implement the nonlinear control in Chapter 5.

The first is automatic tuning the controller parameters to obtain the desired nonlinear dynamic performance quantified by the nonlinear indexes, which is named as the analysis based approach.

The second is imposing the nonlinear modal force on the approximately decoupled nonlinear modes, which is named as the decoupling-basis approach.

Due to the time limit of the PhD, those control proposals are not fully implemented yet, however, the presented investigations and discussions lay the foundation of future researches.
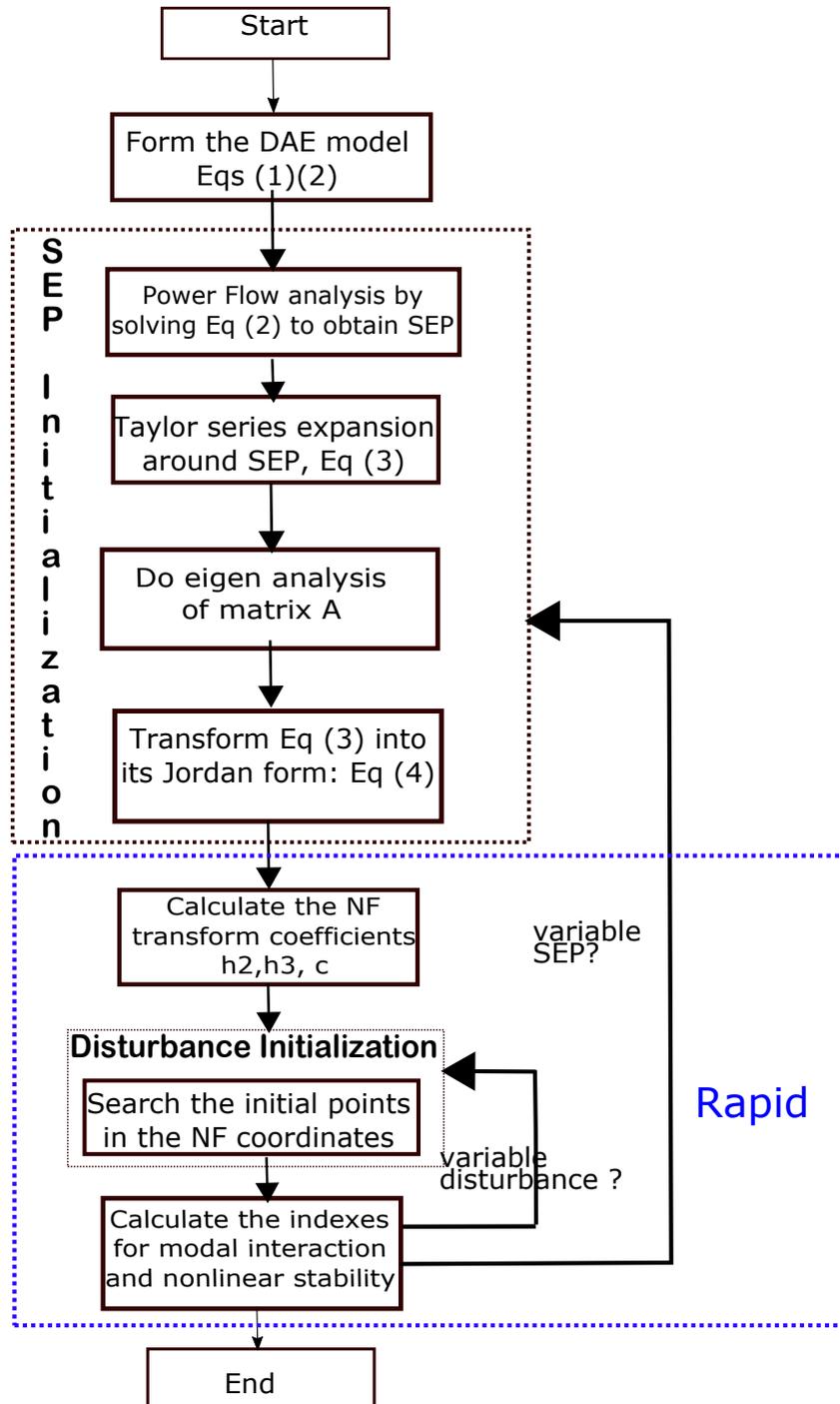
Figure 6.1: The Flowchart of Applying Methods of Normal Forms in Analysis of System Dynamics

6.4   Conclusions of the Existing and Proposed Methodologies

The most important achievements of this PhD research work is the proposed methodologies. The proposed methodologies in this PhD work has been successfully applied to nonlinear analysis of interconnected power system. However, the applicability of the proposed methodologies is not limited in electrical domain. As presented in Chapter 2, the proposed method 3-3-3 and method NNM are general methodologies for study of dynamical systems and the extracted nonlinear properties are universal in multiple input system with nonlinear coupled dynamics.
However, to use the proposed

6.4.1   Validity region

One important concern of methods of normal forms is the validity region. From the numerical results, it can be concluded that the methods of normal forms are valid in the entire working regions of the power system.
For other systems, we can employ the methodology proposed in [51] to investigate the validity region of the methods of normal forms.
It should be noted that if the amplitudes of the state-variables go beyond the validity region, then the information extracted from the normal forms is NONSENSE.

6.4.2   Resonance

In this PhD work, when deducing the normal forms, internal resonances due to the coincidences of the eigenvalue frequencies are not considered. If there exists internal resonance other than the trivially resonant terms, the normal form may include more 2nd-order and 3rd-order terms, and therefore the stability assessment will become difficult. However, the quantification of the nonlinear modal interaction will not become more difficult. Investigations should be done on the resonant cases.

6.4.3   Possibility to do the Physical Experiments

Since the researches in power systems are mainly validated by numerical simulations, one question may arise:

Is it possible to validate the proposed methodologies by physical experiments?

Conducting physical experiments on interconnected power systems is much more expensive then conducting experiments on mechanical systems. However, since the electromechanical oscillations can be measured from the rotor which may contain nonlinear modal interactions. It is possible to validate the conclusions drawn in this PhD dissertation by physical experiments.

6.5 Multiple Input Systems with Coupled Dynamics

In this PhD research dissertation, we only focus on system with coupled dynamics on the state-variables. However, there can be other type of coupled dynamics.

6.5.1 Classes of Multiple-input Systems with Coupled Dynamics Studied by the Proposed Methodologies

Two approaches are established, which cover the studies of a large number of nonlinear dynamical systems composed of interconnected subsystems working in collaboration, as far as their dynamics can be modelled by either (6.1) or (5.3).

6.5.1.1 Class of System Studied by Poincaré's Approach

$$\dot{\boldsymbol{x}} = \boldsymbol{f}(\boldsymbol{x}, \boldsymbol{u}) \tag{6.1}$$

where $\boldsymbol{x}$ is the state-variables vector, $\boldsymbol{u}$ is the system's inputs vector and $\boldsymbol{f}$ is a differentiable nonlinear vector field. Expanding this system in Taylor series around a stable equilibrium point (SEP), $u = u_{SEP}$, $x = x_{SEP}$, one obtains:

$$\triangle\dot{\boldsymbol{x}} = \boldsymbol{H1}(\triangle\boldsymbol{x}) + \frac{1}{2!}\boldsymbol{H2}(\triangle\boldsymbol{x}) + \frac{1}{3!}\boldsymbol{H3}(\triangle\boldsymbol{x}) + \mathcal{O}(4) \tag{6.2}$$

where $\boldsymbol{Hq}$ gathers the qth-order partial derivatives of f. i.e., for $j = 1, 2, \cdots, n$, $H1_k^j = \partial f_j/\partial x_k$, $H2_{kl}^j = \left[\partial^2 f_j/\partial x_k \partial x_l\right]$, $H3_{klm}^j = \left[\partial^3 f_j/\partial x_k \partial x_l \partial x_m\right]$ and $\mathcal{O}(4)$ are terms of order 4 and higher.

6.5.1.2 Class of System Studied by Touzé's Approach

$$\boldsymbol{M}\ddot{\boldsymbol{q}} + \boldsymbol{C}\dot{\boldsymbol{q}} + \boldsymbol{K}\boldsymbol{q} + \boldsymbol{f}_{nl}(\boldsymbol{q}) = \boldsymbol{F} \tag{6.3}$$

where $\boldsymbol{M}, \boldsymbol{C}$ are constant diagonal inertia and damping matrices, whose values depend on the physical and controller parameters of the system. $\boldsymbol{K}$ and $\boldsymbol{f}_{nl}$ indicate the coupling between the variables, where $\boldsymbol{K}$ is a constant matrix including the linear terms and $\boldsymbol{f}_{nl}$ gathers the nonlinear terms coming from the 2nd and 3rd order terms of the Taylor series. $\boldsymbol{F}$ is the excitation vector.

6.5.2 System with Coupled Dynamics in the First-Order Differential of State-Variables of System

If there is a system with coupled dynamics in the first-order differential of state-variables of systems, as modelled by Eq. (6.4)

$$\dot{\boldsymbol{x}} = f(\boldsymbol{x}, \dot{x}) \tag{6.4}$$

or Eq. (6.5)

$$\boldsymbol{M}\ddot{\boldsymbol{q}} + \boldsymbol{C}_{nl}(\dot{\boldsymbol{q}}) + \boldsymbol{K}\boldsymbol{q} + \boldsymbol{f}\boldsymbol{q} = \boldsymbol{F} \tag{6.5}$$

we can also endeavour to study the system dynamics by methods of normal forms. By Poincaré's approach, one solution is to define the auxiliary state variables as $\dot{\boldsymbol{x}} = \boldsymbol{x_s}$. However, this may lead to zero eigenvalues in the Jordan form. If $\lambda_j = 0$, trivial resonance may occur in second-order nonlinear terms, since the conjugate pairs $(\lambda_{2k}, \lambda_{2k-1})$ satisfy $\omega_j = \omega_{2k} + \omega_{2k-1}$ and therefore the second-order nonlinear terms must be kept in the normal forms. Its normal forms are more complicated and the stability assessment may be different than what we have proposed. However, the study of nonlinear modal interaction can employ the procedures and the nonlinear indexes will be in the similar form.

By Touzé's approach, we can still try to use the procedures proposed in previous Chapters to decouple the system dynamics. This may take another 3 years' PhD work. However, it deserves that. Such type of coupled dynamics can be found in electrical machine which are electromagnetically coupled, and for a long time, no analytical investigation is available to study its nonlinear dynamics according to the author's knowledge. Solving such a system can overcome a great ever-existing problem in electrical engineering.

6.5.3 System with Coupled Dynamics in the Second-Order Differential of State-Variables of System

If there is a system with coupled dynamics in the first-order differential of state-variables of systems, as modelled by Eq. (6.6):

$$\dot{\boldsymbol{x}} = f(\boldsymbol{x}, \ddot{x}) \tag{6.6}$$

or Eq. (6.7)

$$\boldsymbol{M_{cl}}\ddot{\boldsymbol{q}} + \boldsymbol{C}(\dot{\boldsymbol{q}}) + \boldsymbol{K}\boldsymbol{q} + \boldsymbol{f}\boldsymbol{q} = \boldsymbol{F} \tag{6.7}$$

I hold the similar opinions as in the last section. However, investigations should be conducted to make a more rigorous conclusion.

6.6 The End, or a new Start ?

In this chapter, achievements are summarized. Also, due to the limited time of the PhD and the limited talents of the PhD student, there are still a lot things to do to complete the theory and enlarge the range of applications.

More questions are asked then answered. For the questions that are not answered, this PhD dissertation has pointed out the possible way to answer them. It is the end of this PhD dissertation, but it is a new start of more interesting researches.

Interconnected VSCs

This part of appendix is dedicated to the interconnected VSCs.

Section A.1 illustrates how the reduced 4th order model is formulated.

In this part of Appendix, the crucial files are presented to facilitate the reader's comprehension of the PhD dissertation.

All the programs and files associated with interconnected VSCs can be found in:
https://drive.google.com/drive/folders/0B2onGI-yt3FwRVZQbUFkcGl5enc?usp=sharing

A.1 Reduced Model of the Interconnected VSCs

As stated in Chapter 1, nonlinear oscillations are predominant in stressed power system, such as the weak grid with long transmission line.

Therefore, to test the proposed methodologies, a renewable energy transmission system is chosen, where predominant nonlinear oscillations are involved. It is of practical significance to study such a case, as renewable energy is our future source, environmentally friendly and sustainable and has a very bright prospect. European Community has proposed to reach 20% energy share in 2020, while the US proposed 22%. With 35%, policies in Asia and Pacific countries rank as the most encouraging.

A.1.1 A Renewable Transmission System

Among all the renewable energy sources, wind energy takes a large part in the market. A typical off-shore wind farm is shown as Fig. A.1, the generators are situated in remote areas, convert the mechanical energy into electricity integrated into the great grid by voltage source converters (VSC) and transferred by long cables.To improve the reliability, the generators are interconnected.Because when the cables are long, it is likely to be broken, that means, the fault level is low. Moreover, unlike the coral energy,which is always constant, the uncertainty and variability of wind and solar generation can pose challenges for grid operators. And the reliability of both the generation and transmission of renewable energy should be enforced. One solution is to connect the different VSCs together. The effective interaction between the VSCs reduce peak and fill valley of the generation and ensure the power stability even if one cable is cut-off.

This topology effectively solves the transmission problem and enforces the reliability of power supply, but it leads to nonlinear oscillations. Because a) the long cables connecting the generators to the great grid has very high impedance,make the power system very weak, called "weak grid", meaning that it is very sensitive to the dis-

Figure A.1: Renewable Distributed Energy Located in Remote Areas [99]

turbance in the power system; b) the line connecting generators to each other has a very low impedance in the high voltage transmission system, this will cause strong coupling of the generators when there is some large disturbance.

To study the oscillations in power system, a popular method is to linearizing the system around the equilibrium point and study its eigenmodes [1]. That is, assume the system to exhibit linear oscillation under small disturbance. In our case, the conventional small disturbance method is not applicable any more. Nonlinear modal analysis should be done.

A.1.1.1 The Basic Unit

As the generator can be modeled as DC source, so the simplest unit of such a system can be modeled two grid-connected voltage source converters interconnected to each other, shown as Figure A.2. As Voltage Source Converters can be used to control the voltage, currents as well as power flows, this topology can represent the principle functions of the orignal large-scale system.
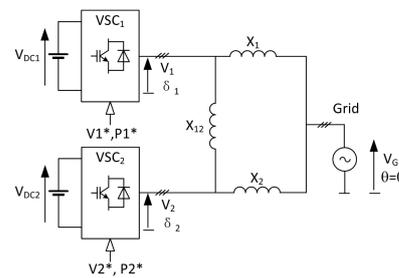
Figure A.2: The Basic Unit to Study the Inter-oscillations in Weak Grid

A.1.2 Methodology

The steps of this methodology can be summarized as below.

1. Model the System(Section A.1.3): it contains three parts:

a). Establish the mathematical model of the studied system by EMR, develop inversion-based control strategy correspondingly, use linear modal analysis to tune linear controllers;

b). Reduce the model to focus on nonlinear behavior;

c). Make the disturbance model to study the damped free vibration around the equilibrium under large disturbance.

2. Modal Analysis: Do linear modal analysis, then nonlinear modal analysis based on nonlinear normal modes(NNM) to decouple the N-dimensional Equation into 1-dimensional Equations (decouple the linear and nonlinear coupling).

3. Solve the 1-dimensional problem: by numerical integration to obtain numerical results or use perturbation method to obtain analytical results.

A.1.3 Modeling the System

A.1.3.1 The Detailed Model

To start the case study, a single classic VSC is modeled and controlled.

Fig. A.3 [29] presents a classical physical configuration of grid-connected VSC, and the currents and voltages as well as power injected into the grid should be controlled. There are two crucial issues concerning the control of the grid-connected VSC.First problem is the low frequency resonances that can interact with the vector control. Second problem is due to the PLL dynamics when the power converter is synchronized to a weak grid. To handle the first issue, the controller parameters will be tuned by iterative tuning based on linear modal analysis [80].To handle the second issue, the virtual synchronous machine power control will be adopted [29].
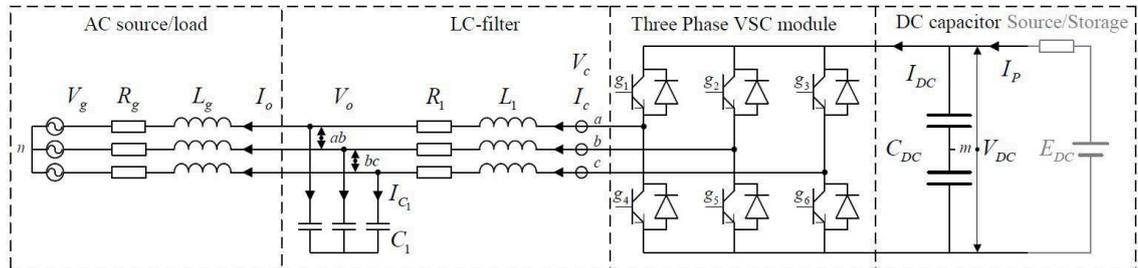
Figure A.3: Grid-side-VSC Configuration [29]

According to Figure A.3, the equations of the components can be written as Equation (A.1)(A.2)(A.3)(A.4). For simplicity,all the varialbes and parameters are expressed in per unit.

AC Load/Source

$$\frac{l_g}{\omega_b} \cdot s \cdot i_{o,d} = v_{o,d} - r_g \cdot i_{o,d} + \omega_g \cdot l_g \cdot i_{o,q} - v_{g,d} \quad \frac{l_g}{\omega_b} \cdot s \cdot i_{o,q} = v_{o,q} - r_g \cdot i_{o,q} - \omega_g \cdot l_g \cdot i_{o,d} - v_{g,q}$$
$$(A.1)$$

LC Filter Filter L:

$$\frac{l_1}{\omega_b} \cdot s \cdot i_{c,d} = v_{o,d} - r_1.i_{c,d} + \omega_g.l_1.i_{c,q} - v_{o,d} \quad \frac{l_1}{\omega_b} \cdot s \cdot i_{c,q} = v_{o,q} - r_1.i_{c,q} - \omega_g.l_1.i_{c,d} - v_{o,q}$$
$$(A.2)$$

Filter C:

$$\frac{c_1}{\omega_b} \cdot s \cdot v_{o,d} = i_{c,d} + \omega_g \cdot c_1 \cdot v_{o,q} - i_{o,d} \quad \frac{c_1}{\omega_b} \cdot s \cdot v_{o,q} = i_{c,q} - \omega_g \cdot c_1 \cdot v_{o,d} - i_{o,q}$$
$$(A.3)$$

Power Estimation:(Neglecting the resistance r_g of the grid impedance)

$$P_g = \frac{v_{g,d} \cdot v_{o,q}}{l_g \cdot \omega_g} \quad Q_g = \frac{v_{g,d} \cdot (v_{o,q} - v_{g,d})}{l_g \cdot \omega_g} \tag{A.4}$$

To model and decide the control structure, Energetic Macroscopic Representation(EMR) is used. EMR is multi-physical graphical description based on the interaction principle (systemic) and the causality principle (energy). It vivifies the relations between the subsystems as action and reaction decided by the inputs and outputs flowing between each other. It classifies subsystems into source, accumulation, conversion and distribution by their energetic functions [100]. It uses blocks in different color and shapes to represent subsystems with different functions correspondingly.

From the configuration and the equations, we can see that the LC filter and the AC source are energetic accumulation systems.For the inductance of LC filter, the inputs are the voltages v_o, v_c imposed by c_1 and the converter,and the output is i_c. For the capacitance,the inputs are the currents i_c, i_o injected from l_1 and the grid. For the AC source/load, it is similar to the inductance of LC filter, the inputs are the voltages v_g, v_o while the output is i_o.

The converter is a conversion block,of which the inputs are tunable. The grid voltage source and the DC-link Bus serve as the sources to the system.

Thus, the representation of the physical system is accomplished, shown as the Figure.A.4. The output of the converter is v_c and the variables to be controlled are v_o, i_o as well as the power injected into the grid. There are different ways to estimate the power, leading to different inversion-based control strategies. According to the inversion-based control theory [100], the reference voltage v_{cref} to the converter is produced by current loop via inversion the equation of inductance component of the LC filter, the reference current i_c^* to the current loop can be calculated by inverting
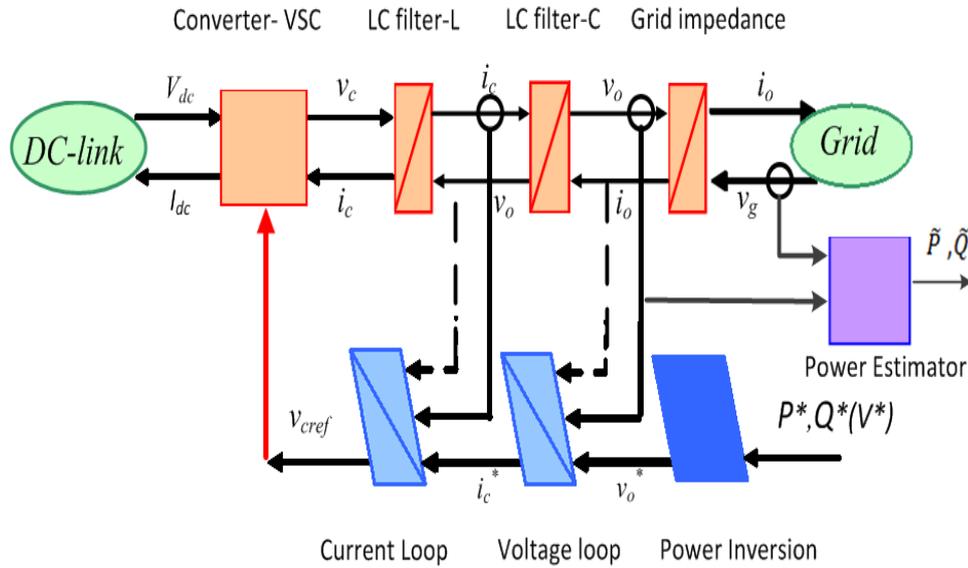
Figure A.4: EMR and Inversion Based Control Strategy
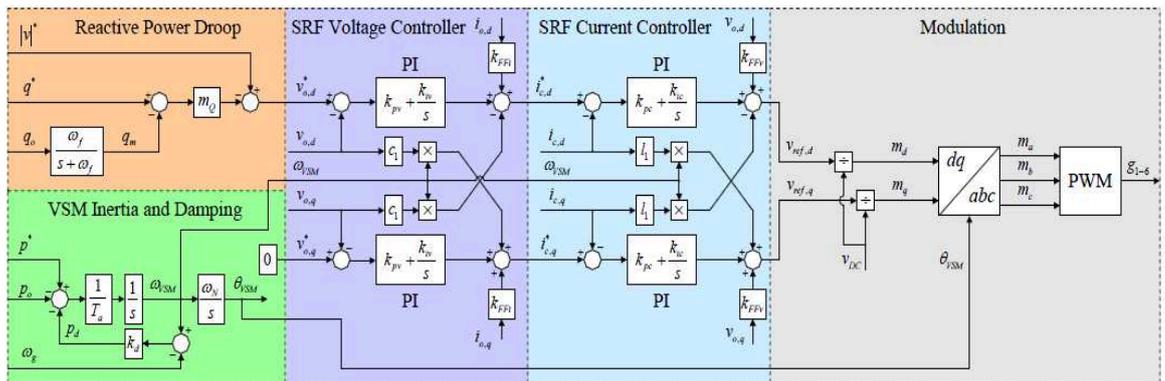
Figure A.5: The cascaded control loops [29]

the equation of the capacitance component of the LC filter, the power is controlled by estimator virtual synchronous machine (VSM), avoiding the unsynchronization. Then the cascaded control loops are decided, shown in Figure A.5 [29].

To tune the control parameters, the whole system is tuned by sensitivity analysis based on linear modal analysis,where the whole system is expressed in statespace, and controller parameters are tuned to obtain desired eigenvalues(corresponding to linear modes) [29] [80].

This section illustrates the analysis and control of a single VSC, and it also serves as an example to the application of linear modal analysis. However, seen from this section, we can see the control structure is complex enough and the whole system is 13th-order. If we use such analytical model to study two VSCs interconnected to each other, the complexity will be at least twice, and it is impossible to use such a complex model to study the system. One would like to reduce the model to just

focus on the nonlinearities.

A.1.3.2 The Reduced Model

One way to reduce the model is to reduce the voltage loop and current loop as, $V_{o,d}^* = V_{o,d}, V_{o,d}^* = V_{o,d}, i_{o,d}^* = i_{o,d}, i_{o,q}^* = i_{o,q}$, as the time constants of the current loop, voltage loop and power loop verify that $T_{power} \gg T_{voltage} \gg T_{current}$. This is done by simplifying the loops one by one, first the current loop, secondly the voltage loop. The process to reduce the model is illustrated in Figure A.6, where the loops are the mathematics expression of $i_{o,d}, v_{o,d}$ is demonstrated to analyze the system dynamics.

One should note that, the process to reduce the model is not a simple deleting out the loops and poles. The eigenvalues of the current loop and voltage loop can be complex; the eigenvalues of the power loop are real.

It is based on two important pre-conditions: a)there are big gaps between the time constant of the three loops; b)the voltage loop and the current loop are conservative and linear; c)the nonlinearities must be reserved. After reducing the model,the system can be expressed as Equation (A.5).

$$
\begin{aligned}
J_1 \frac{d^2\delta_1}{dt^2} + D_1(\omega_1 - \omega_g) + \frac{V_1 V_g}{L_1}\sin\delta_1 + \frac{V_1 V_2}{L_{12}}\sin(\delta_1 - \delta_2) = P_1^* \\
J_2 \frac{d^2\delta_1}{dt^2} + D_2(\omega_2 - \omega_g) + \frac{V_2 V_g}{L_2}\sin\delta_2 + \frac{V_1 V_2}{L_{12}}\sin(\delta_2 - \delta_1) = P_2^*
\end{aligned}
\tag{A.5}
$$

Where J_1, D_1, J_2, D_2 are the controller parameters of the power loop, δ_1, δ_2 are the power angles, V_1, V_2 are the voltages, P_1^*, P_2^* are the references values of the power, ω_1, ω_2 are angular frequencies of the two VSCs. ω_g is the angular frequency of the grid, and L_1, L_2 is the impedance of the cable connecting VSC to the grid, and L_{12} is the impedance of the transmission line connecting the two VSCs to each other. L_1, L_2 is very high $(0.7pu)$, leading a very big power angle of VSC to transfer the electricity. L_{12} is very low due to high voltage of the transmission system, leading to strong coupling between the two VSCs. When there is a large disturbance on one VSC, there will be drastic nonlinear oscillations between the two VSCs, which is verified by the simulation results.

A.1.4 The Disturbance Model

As stated before, we would like to study the nonlinear oscillations of the studied case under large disturbance. So, we need a disturbance model. This is done by making Taylor's Series Expansion around the equilibrium point. Assume:
$V_1 = const, V_2 = const, V_g = const, \omega_g = const$
The equilibrium point: $\omega_{10}, \omega_{20}, \delta_{10}, \delta_{20}$ As $\omega_g = \omega_{10} = \omega_{20} = const$ so $\omega_1 = \widetilde{\omega_1} + \omega_{10}, \omega_2 = \widetilde{\omega_2} + \omega_{20} \frac{d\omega_1}{dt} = \frac{d(\omega_1 - \omega_g)}{dt}, \frac{d\omega_2}{dt} = \frac{d(\omega_2 - \omega_g)}{dt} \theta_1 - \theta_g = \delta_1, \theta_2 - \theta_g = \delta_2, \theta_1 - \theta_2 = \delta_1 - \delta_2 = \delta_{12} = \widetilde{\delta_1} + \delta_{10} - \widetilde{\delta_2} + \delta_{20} = \widetilde{\delta_1} - \widetilde{\delta_2} + \delta_{120} \frac{d\omega_1}{dt} = \frac{d(\widetilde{\omega_1} + \omega_{10})}{dt} = \frac{d\widetilde{\omega_1}}{dt}, \frac{d\omega_2}{dt} = \frac{d(\widetilde{\omega_2} + \omega_{20})}{dt} = \frac{d\widetilde{\omega_2}}{dt}, \frac{d\delta_1}{dt} = \frac{d(\widetilde{\delta_1} + \delta_{10})}{dt} = \frac{d\widetilde{\delta_1}}{dt} = \omega_b\widetilde{\omega_1}, \frac{d\delta_2}{dt} = \frac{d(\widetilde{\delta_2} + \delta_{20})}{dt} = \frac{d\widetilde{\delta_2}}{dt} = \omega_b\widetilde{\omega_2}$ And, as
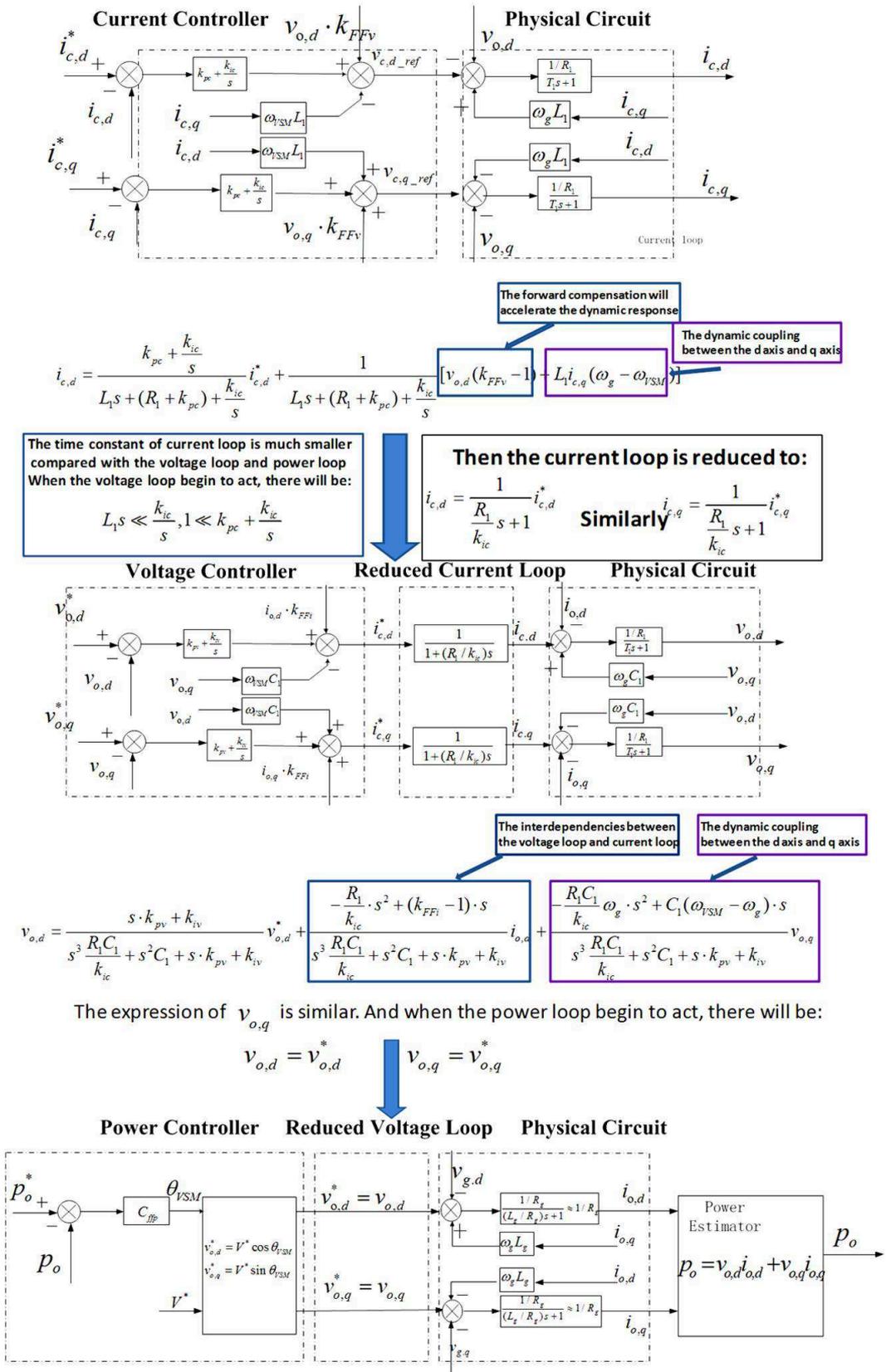
Figure A.6: How the three-loops system can be reduced to one-loop

Table A.1: The parameters of the Interconnected VSCs

J_1	16	$L_1(pu)$	0.7	V_1	1
J_2	16	$L_2(pu)$	0.7	V_2	1
D_1	10	$L_{12}(pu)$	0.01	V_g	1
D_2	10	w_b	314		

the system operates at the equilibrium point,there will be:

$$P_1^* = \frac{V_1 V_g}{L_1}\sin\delta_{10} + \frac{V_1 V_2}{L_{12}}\sin\delta_{120}, P_2^* = \frac{V_1 V_g}{L_2}\sin\delta_{20} + \frac{V_1 V_2}{L_{12}}\sin\delta_{210}$$

Therefore the system can be expressed as Equation(A.6).

$$\frac{J_1}{\omega_b}\frac{d^2\widetilde{\delta_1}}{dt^2} + \frac{D_1}{\omega_b}\frac{d\widetilde{\delta_1}}{dt} + \frac{V_1 V_g}{L_1}(\sin(\widetilde{\delta_1}+\delta_{10}) - \sin\delta_{10}) + \frac{V_1 V_2}{L_{12}}(\sin(\widetilde{\delta_1}-\widetilde{\delta_2}+\delta_{120}) - \sin\delta_{120}) = 0$$

$$\frac{J_2}{\omega_b}\frac{d^2\widetilde{\delta_2}}{dt^2} + \frac{D_2}{\omega_b}\frac{d\widetilde{\delta_2}}{dt} + \frac{V_2 V_g}{L_2}(\sin(\widetilde{\delta_2}+\delta_{20}) - \sin\delta_{10}) + \frac{V_1 V_2}{L_{12}}(\sin(\widetilde{\delta_2}-\widetilde{\delta_1}+\delta_{210}) - \sin\delta_{210}) = 0$$

$$\text{(A.6)}$$

To simulate the system under a large disturbance, and then damped to the equilibrium point, we need to expand the power in the expression of: $\sin(\widetilde{\delta}+\delta_0) - \sin(\delta_0)$
There are two methods to do the Taylor's Series Expansion around the equilibrium:δ_0

- a)Just keep the linear term:
  $\sin(\widetilde{\delta}+\delta_0) - \sin\delta_0 = \cos\delta_0\widetilde{\delta}$
- b)Keep the quadratic and cubic terms:
  $\sin(\widetilde{\delta}+\delta_0) - \sin\delta_0 = \cos\delta_0\widetilde{\delta} - \frac{\sin\delta_0}{2}\widetilde{\delta}^2 - \frac{\cos\delta_0}{6}\widetilde{\delta}^3$;

In our study, we keep the nonlinearities to the cubic order. In the previous researches concerning power system,only quadratic terms are considered. The type of nonlinearities(quadratic or cubic) depends on the initial state, δ_{10}, δ_{20}. So,by setting different values for δ_{10}, δ_{20}, we can study the impacts of the nonlinearities on the system dynamics. The results of the disturbance model is put in next section for modal analysis.

A.2   Parameters and Programs

A.2.1   Parameters of Interconnected VSCs

A.2.2   Initial File for Interconnected VSCs

```
delta10=input('Type in the stable equibrium point: delta10 ');
delta20=input('Type in the stable equilibrium point: delta20 ');
disturbance1=input('Type in the disturbance around the equilibrium point: disturbance1 ')
```

```
disturbance2=input('Type in the disturbance around the equilibrium point: disturbance2
J1=0.2*16;D1=20;J2=0.2*16;D2=20;w_b=100*3.14;
g1=J1/w_b;
g2=J2/w_b;
d1=D1/w_b;
d2=D2/w_b;
%syms g1 g2 d1 d2;

%syms w_b delta10 delta20 P1 P2;
delta120=delta10-delta20;
delta210=-delta120;
L1=0.7;L2=0.7;L12=0.01;wg=1;w_b=50*2*3.14;
%AC source/load parameters
V1=1;V2=1;Vg=1;w10=1;w20=1;
k1=V1*Vg/L1;k2=V2*Vg/L2;k12=V1*V2/L12;
%compensation of springs efforts

%%
%Natural frequencies
M=[g1 0;0 g2];
K=[k1*cos(delta10)+k12*cos(delta120) -k12*cos(delta120);
-k12*cos(delta120) k2*cos(delta20)+k12*cos(delta210)];
D=[d1 0;0 d2];
%modal matrix and eigenvalues matrix
[Tr,E]=eig(inv(M)*K);
%natural frequencies matrix
OMEGA=[sqrt(E(1,1)) sqrt(E(2,2))];
%Normalisation of T
Tr=Tr/det(Tr);
leg=sqrt(sum(Tr.^2));
Tr=Tr./leg(ones(1,2),:);
%%
%normalization
%[ Tn]=normalization(T);
%modal matrices
Mm=Tr.'*M*Tr;
Dm=Tr.'*D*Tr;
Km=Tr.'*K*Tr;
T11=Tr(1,1);
T12=Tr(1,2);
T21=Tr(2,1);
T22=Tr(2,2);
%division by Mm
```

```
Dm_div=inv(Mm)*Dm;
OMEGA=double(OMEGA);

for i=1:2
xi(i)=0.5*Dm_div(i,i)/OMEGA(i);
end

TEQ(1,1,1)=k1*(-sin(delta10)/2)+k12*(-sin(delta120)/2);
TEQ(1,1,2)=k12*sin(delta120);
TEQ(1,2,2)=k12*(-sin(delta120)/2);
TEQ(2,1,1)=k12*(-sin(delta210)/2);
TEQ(2,1,2)=k12*sin(delta210);
TEQ(2,2,2)=k2*(-sin(delta20)/2)+k12*(-sin(delta210)/2);
TEC(1,1,1,1)=k1*(-cos(delta10)/6)+k12*(-cos(delta120)/6);
TEC(1,1,1,2)=k12*(cos(delta120)/2);
TEC(1,1,2,2)=k12*(-cos(delta120)/2);
TEC(1,2,2,2)=k12*(cos(delta120)/6);
TEC(2,1,1,1)=k12*(cos(delta210)/6);
TEC(2,1,1,2)=k12*(-cos(delta210)/2);
TEC(2,1,2,2)=k12*(cos(delta210)/2);
TEC(2,2,2,2)=k2*(-cos(delta20)/6)+k12*(-cos(delta210)/6);
%%Auxilliary tensors of quadratic and cubic coefficients
Gg=zeros(2,2,2,2);
Gg(1,1,1)=TEQ(1,1,1)*T11^2+TEQ(1,1,2)*T11*T21+TEQ(1,2,2)*T21^2;
Gg(1,1,2)=TEQ(1,1,1)*2*T11*T12+TEQ(1,1,2)*(T11*T22+ T12*T21)+TEQ(1,2,2)*2*T21*T22;
Gg(1,2,2)=TEQ(1,1,1)*T12^2+TEQ(1,1,2)*T12*T22+TEQ(1,2,2)*T22^2;
Hg(1,1,1,1)=TEC(1,1,1,1)*T11^3+TEC(1,1,1,2)*T21*T11^2+...
TEC(1,1,2,2)*T11*T21^2+TEC(1,2,2,2)*T21^3;
Hg(1,1,1,2)=TEC(1,1,1,1)*3*T11^2*T12+TEC(1,1,1,2)*(T22*T11^2+2*T21*T11*T12)+...
TEC(1,1,2,2)*(T12*T21^2+2*T11*T21*T22)+TEC(1,2,2,2)*3*T21^2*T22;
Hg(1,1,2,2)=TEC(1,1,1,1)*3*T11*T12^2+TEC(1,1,1,2)*(2*T22*T11*T12+T21*T12^2)+...
TEC(1,1,2,2)*(2*T12*T21*T22+T11*T22^2)+TEC(1,2,2,2)*3*T21*T22^2;
Hg(1,2,2,2)=TEC(1,1,1,1)*T12^3+TEC(1,1,1,2)*T22*T12^2+...
TEC(1,1,2,2)*T12*T22^2+TEC(1,2,2,2)*T22^3;
%%
Gg(2,1,1)=TEQ(2,1,1)*T11^2+TEQ(2,1,2)*T11*T21+TEQ(2,2,2)*T21^2;
Gg(2,1,2)=TEQ(2,1,1)*2*T11*T12+TEQ(2,1,2)*(T11*T22+ T12*T21)+TEQ(2,2,2)*2*T21*T22;
Gg(2,2,2)=TEQ(2,1,1)*T12^2+TEQ(2,1,2)*T12*T22+TEQ(2,2,2)*T22^2;
Hg(2,1,1,1)=TEC(2,1,1,1)*T11^3+TEC(2,1,1,2)*T21*T11^2+TEC(2,1,2,2)*T11*T21^2+...
TEC(2,2,2,2)*T21^3;
Hg(2,1,1,2)=TEC(2,1,1,1)*3*T11^2*T12+TEC(2,1,1,2)*(T22*T11^2+2*T21*T11*T12)+...
TEC(2,1,2,2)*(T12*T21^2+2*T11*T21*T22)+TEC(2,2,2,2)*3*T21^2*T22;
Hg(2,1,2,2)=TEC(2,1,1,1)*3*T11*T12^2+TEC(2,1,1,2)*(2*T22*T11*T12+T21*T12^2)+...
TEC(2,1,2,2)*(2*T12*T21*T22+T11*T22^2)+TEC(2,2,2,2)*3*T21*T22^2;
```

```
Hg(2,2,2,2)=TEC(2,1,1,1)*T12^3+TEC(2,1,1,2)*T22*T12^2+TEC(2,1,2,2)*T12*T22^2+...
TEC(2,2,2,2)*T22^3;
%%
%%G: tensor of quadratic coefficients
%%H: tensor of cubic coefficients
G=zeros(2,2,2);
H=zeros(2,2,2,2);
%G(1,1,1)=(T11*Gg(1,1,1)*T21*Gg(2,1,1))/Mm(1,1);
%G(1,1,2)=(T11*Gg(1,1,2)*T21*Gg(2,1,2))/Mm(1,1);
%G(1,2,2)=(T11*Gg(1,2,2)*T21*Gg(2,2,2))/Mm(1,1);
%G(2,1,1)=(T12*Gg(2,1,1)*T22*Gg(2,1,1))/Mm(2,2);
%G(2,1,2)=(T12*Gg(2,1,2)*T22*Gg(2,1,2))/Mm(2,2);
%G(2,2,2)=(T12*Gg(2,2,2)*T22*Gg(2,2,2))/Mm(2,2);
for p=1:2
    for k=1:2
        for j=k:2
                G(p,k,j)=(Tr(1,p)*Gg(1,k,j)+Tr(2,p)*Gg(2,k,j))/Mm(p,p);
                ++j;
        end
        ++k;

    end
 ++p;
end
for p=1:2
for i=1:2
    for k=i:2
        for j=k:2
                H(p,i,k,j)=(Tr(1,p)*Hg(1,i,k,j)+Tr(2,p)*Hg(2,i,k,j))/Mm(p,p);
                ++j;
        end
        ++k;
    end
    ++i;
     end
 ++p;
end
H=zeros(2,2,2,2);
c1=[G(1,1,1) G(1,1,2) G(1,2,2) H(1,1,1,1) H(1,1,1,2) H(1,1,2,2) H(1,2,2,2)];
c2=[G(2,1,1) G(2,1,2) G(2,2,2) H(2,1,1,1) H(2,1,1,2) H(2,1,2,2) H(2,2,2,2)];
[A,B,C,ALPHA,BETA,GAMMA,AA,BB,CC,R,S,T,U,LAMBDA,MU,NU,ZETA]=forcedcoef(OMEGA,G,H,xi);
sim('Damped_free_vibration_interconnectedVSCs');
```

A.2.3   M-file to Calculate the Coef

```
%File calculating the coefs of the NNM considering a linear damping of the
%system
%/calling/system_parameters.m: OMEGA xi G H
%calculating A,B,C,ALPHA,BETA,GAMMA,AA,BB,CC,R,S,T,U,LAMBDA,MU,NU,ZETA
%Created the 07/05 by Ghofrane BH using coefdirect_dampc_XK_forcee.m
function [A,B,C,ALPHA,BETA,GAMMA,AA,BB,CC,R,S,T,U,LAMBDA,MU,NU,ZETA]=...
forcedcoef(OMEGA,G,H,xi);

N=length(OMEGA);
correction=1;

%%
%quadratic coefs
A=zeros(N,N,N);
B=zeros(N,N,N);
C=zeros(N,N,N);
ALPHA=zeros(N,N,N);
BETA=zeros(N,N,N);
GAMMA=zeros(N,N,N);

for p=1:N
for i=1:N
    A(p,i,i) = -(64*OMEGA(i)^4*xi(i)^4+8*OMEGA(i)^4-...
96*OMEGA(i)^3*xi(i)^3*xi(p)*OMEGA(p)-8*OMEGA(i)^3*xi(p)*OMEGA(p)*xi(i)
...+20*xi(i)^2*OMEGA(i)^2*OMEGA(p)^2+32*OMEGA(i)^2*xi(i)^2*xi(p)^2*OMEGA(p)^2-...
6*OMEGA(i)^2*OMEGA(p)^2+8*xi(p)^2*OMEGA(p)^2*OMEGA(i)^2-12*xi(p)*OMEGA(p)^3*...
xi(i)*OMEGA(i)+OMEGA(p)^4)*G(p,i,i)/(64*OMEGA(i)^6*xi(i)^2-32*OMEGA(i)^4*xi(i)^2*...
OMEGA(p)^2+64*xi(i)^4*OMEGA(i)^4*OMEGA(p)^2+20*xi(i)^2*OMEGA(i)^2*OMEGA(p)^4+...
16*OMEGA(i)^2*OMEGA(p)^4*xi(p)^2+16*OMEGA(i)^4*OMEGA(p)^2-8*OMEGA(i)^2*OMEGA(p)^4
+OMEGA(p)^6-128*OMEGA(i)^5*xi(i)^3*xi(p)*OMEGA(p)+192*OMEGA(i)^4*xi(i)^2*...
xi(p)^2*OMEGA(p)^2-96*xi(i)^3*OMEGA(i)^3*OMEGA(p)^3*xi(p)-12*xi(i)*OMEGA(i)*...
OMEGA(p)^5*xi(p)+32*xi(i)^2*OMEGA(i)^2*OMEGA(p)^4*xi(p)^2-64*OMEGA(i)^5*...
xi(p)*OMEGA(p)*xi(i)-64*OMEGA(i)^3*xi(p)^3*OMEGA(p)^3*xi(i));

B(p,i,i) = -2*G(p,i,i)*(4*OMEGA(i)^2+8*xi(i)^2*OMEGA(i)^2-OMEGA(p)^2-12*...
xi(p)*OMEGA(p)*xi(i)*OMEGA(i)+4*xi(p)^2*OMEGA(p)^2)/(64*OMEGA(i)^6*xi(i)^2-...
32*OMEGA(i)^4*xi(i)^2*OMEGA(p)^2+64*xi(i)^4*OMEGA(i)^4*OMEGA(p)^2+20*...
xi(i)^2*OMEGA(i)^2*OMEGA(p)^4+16*OMEGA(i)^2*OMEGA(p)^4*xi(p)^2+16*...
OMEGA(i)^4*OMEGA(p)^2-8*OMEGA(i)^2*OMEGA(p)^4+OMEGA(p)^6-128*OMEGA(i)^5*...
xi(i)^3*xi(p)*OMEGA(p)+192*OMEGA(i)^4*xi(i)^2*xi(p)^2*OMEGA(p)^2-96*xi(i)^3*...
OMEGA(i)^3*OMEGA(p)^3*xi(p)-12*xi(i)*OMEGA(i)*OMEGA(p)^5*xi(p)+32*xi(i)^2*...
OMEGA(i)^2*OMEGA(p)^4*xi(p)^2-64*OMEGA(i)^5*xi(p)*OMEGA(p)*xi(i)-64*...
```

```
OMEGA(i)^3*xi(p)^3*OMEGA(p)^3*xi(i));

C(p,i,i) = -4*G(p,i,i)*(4*OMEGA(i)^3*xi(i)+16*xi(i)^3*OMEGA(i)^3-24*xi(i)^2*...
OMEGA(i)^2*xi(p)*OMEGA(p)+xi(i)*OMEGA(i)*OMEGA(p)^2-xi(p)*OMEGA(p)^3+...
8*xi(p)^2*OMEGA(p)^2*xi(i)*OMEGA(i))/(64*OMEGA(i)^6*xi(i)^2-32*OMEGA(i)^4*...
xi(i)^2*OMEGA(p)^2+64*xi(i)^4*OMEGA(i)^4*OMEGA(p)^2+20*xi(i)^2*OMEGA(i)^2*...
OMEGA(p)^4+16*OMEGA(i)^2*OMEGA(p)^4*xi(p)^2+16*OMEGA(i)^4*OMEGA(p)^2-...
8*OMEGA(i)^2*OMEGA(p)^4+OMEGA(p)^6-128*OMEGA(i)^5*xi(i)^3*xi(p)*OMEGA(p)+...
192*OMEGA(i)^4*xi(i)^2*xi(p)^2*OMEGA(p)^2-96*xi(i)^3*OMEGA(i)^3*OMEGA(p)^3*...
xi(p)-12*xi(i)*OMEGA(i)*OMEGA(p)^5*xi(p)+32*xi(i)^2*OMEGA(i)^2*OMEGA(p)^4*...
xi(p)^2-64*OMEGA(i)^5*xi(p)*OMEGA(p)*xi(i)-64*OMEGA(i)^3*xi(p)^3*OMEGA(p)^3*...
xi(i));

GAMMA(p,i,i)=2*(A(p,i,i) - OMEGA(i)^2*B(p,i,i)) -2*xi(i)*OMEGA(i)*C(p,i,i);

ALPHA(p,i,i) = -OMEGA(i)^2*C(p,i,i);

BETA(p,i,i) = -4*xi(i)*OMEGA(i)*B(p,i,i) + C(p,i,i);
end
end


for p=1:N
  for i=1:N
    for j=i+1:N
      D=(OMEGA(i) + OMEGA(j) - OMEGA(p))*(OMEGA(i) + OMEGA(j) + OMEGA(p))*...
(OMEGA(i)- OMEGA(j) + OMEGA(p))*(OMEGA(i) - OMEGA(j) - OMEGA(p));
      if abs(D) < 1e-12
A(p,i,j)=0;
B(p,i,j)=0;
C(p,i,j)=0;
C(p,j,i)=0;
ALPHA(p,i,j)=0;
BETA(p,i,j)=0;
GAMMA(p,i,j)=0;
GAMMA(p,j,i)=0;
      else
A2=[OMEGA(j)^2+OMEGA(i)^2-OMEGA(p)^2, -2*OMEGA(j)^2*OMEGA(i)^2, -2*OMEGA(j)^3*...
xi(j)+2*xi(p)*OMEGA(p)*OMEGA(j)^2, -2*OMEGA(i)^3*xi(i)+2*xi(p)*OMEGA(p)*...
OMEGA(i)^2 ;  -2, -4*xi(i)^2*OMEGA(i)^2-8*xi(i)*OMEGA(i)*xi(j)*OMEGA(j)-4*...
xi(j)^2*OMEGA(j)^2+OMEGA(i)^2+OMEGA(j)^2-OMEGA(p)^2+4*xi(p)*OMEGA(p)*...
xi(i)*OMEGA(i)+4*xi(p)*OMEGA(p)*xi(j)*OMEGA(j), 2*xi(i)*OMEGA(i)+...
4*xi(j)*OMEGA(j)-2*xi(p)*OMEGA(p), 4*xi(i)*OMEGA(i)+2*xi(j)*OMEGA(j)-2*...
xi(p)*OMEGA(p) ; 2*xi(j)*OMEGA(j)-2*xi(p)*OMEGA(p), -2*OMEGA(i)^3*xi(i)-...
```

```
4*OMEGA(i)^2*xi(j)*OMEGA(j)+2*xi(p)*OMEGA(p)*OMEGA(i)^2, OMEGA(j)^2+OMEGA(i)^2-...
4*xi(j)^2*OMEGA(j)^2-OMEGA(p)^2+4*xi(p)*OMEGA(p)*xi(j)*OMEGA(j), 2*OMEGA(i)^2 ;
2*xi(i)*OMEGA(i)-2*xi(p)*OMEGA(p), -4*OMEGA(j)^2*xi(i)*OMEGA(i)-2*OMEGA(j)^3*...
xi(j)+2*xi(p)*OMEGA(p)*OMEGA(j)^2, 2*OMEGA(j)^2, OMEGA(i)^2+OMEGA(j)^2-...
4*xi(i)^2*OMEGA(i)^2-OMEGA(p)^2+4*xi(p)*OMEGA(p)*xi(i)*OMEGA(i)];

B2=[G(p,i,j) ; 0 ; 0; 0];
%solabcij=inv(A2)*B2;
        solabcij=A2\B2;
A(p,i,j)=solabcij(1);
B(p,i,j)=solabcij(2);
C(p,i,j)=solabcij(3);
C(p,j,i)=solabcij(4);
ALPHA(p,i,j) = -C(p,i,j)*OMEGA(j)^2 - C(p,j,i)*OMEGA(i)^2;
BETA(p,i,j)  = -2*(xi(i)*OMEGA(i) + xi(j)*OMEGA(j))*B(p,i,j)+ C(p,i,j) + C(p,j,i);
GAMMA(p,i,j) = A(p,i,j) - OMEGA(i)^2*B(p,i,j) - 2*xi(j)*OMEGA(j)*C(p,i,j);
GAMMA(p,j,i) = A(p,i,j) - OMEGA(j)^2*B(p,i,j) - 2*xi(i)*OMEGA(i)*C(p,j,i);
      end
    end
  end
end

%%
%Calcul interm\'ediaire : AA, BB et CC

AA=zeros(N,N,N,N);
BB=zeros(N,N,N,N);
CC=zeros(N,N,N,N);
AA2=zeros(N,N,N,N);
BB2=zeros(N,N,N,N);
CC2=zeros(N,N,N,N);

for p=1:N
for i=1:N
for j=1:N
for k=1:N
V1=squeeze(G(p,i,i:N));
V2=squeeze(A(i:N,j,k));
V3=squeeze(G(p,1:i,i));
V4=squeeze(A(1:i,j,k));
AA(p,i,j,k)=V1'*V2 + V3*V4;
V5=squeeze(G(p,i,i:N));
V6=squeeze(B(i:N,j,k));
V7=squeeze(G(p,1:i,i));
```

```
V8=squeeze(B(1:i,j,k));
BB(p,i,j,k)=V5'*V6 + V7*V8;
V9=squeeze(G(p,i,i:N));
V10=squeeze(C(i:N,j,k));
V11=squeeze(G(p,1:i,i));
V12=squeeze(C(1:i,j,k));
CC(p,i,j,k)=V9'*V10 + V11*V12;
end
end
end
end



%%
%cubic coefs
R=zeros(N,N,N,N);
S=zeros(N,N,N,N);
T=zeros(N,N,N,N);
U=zeros(N,N,N,N);
LAMBDA=zeros(N,N,N,N);
MU=zeros(N,N,N,N);
NU=zeros(N,N,N,N);
ZETA=zeros(N,N,N,N);



%treated in different loops to express all the particular cases

for p=1:N
for i=1:N
if i~=p
D1=(OMEGA(p)^2-OMEGA(i)^2)*(OMEGA(p)^2-9*OMEGA(i)^2);
if abs(D1) < 1e-12
R(p,i,i,i)=0;
S(p,i,i,i)=0;
T(p,i,i,i)=0;
U(p,i,i,i)=0;
LAMBDA(p,i,i,i)=0;
MU(p,i,i,i)=0;
NU(p,i,i,i)=0;
ZETA(p,i,i,i)=0;
else
A3iii=[-OMEGA(p)^2+3*OMEGA(i)^2, 0, 2*xi(p)*OMEGA(p)*OMEGA(i)^2-...
2*OMEGA(i)^3*xi(i), -2*OMEGA(i)^4 ;  0, -OMEGA(p)^2+12*xi(p)*OMEGA(p)*...
```

```
xi(i)*OMEGA(i)+ 3*OMEGA(i)^2-36*xi(i)^2*OMEGA(i)^2, -2, -2*xi(p)*OMEGA(p)+...
10*xi(i)*OMEGA(i) ; -6*xi(p)*OMEGA(p)+6*xi(i)*OMEGA(i), -6*OMEGA(i)^4, ...
-OMEGA(p)^2+4*xi(p)*OMEGA(p)*xi(i)*OMEGA(i)+7*OMEGA(i)^2-4*xi(i)^2*OMEGA(i)^2,...
4*xi(p)*OMEGA(p)*OMEGA(i)^2-12*OMEGA(i)^3*xi(i) ; -6, 6*xi(p)*OMEGA(p)*...
OMEGA(i)^2-30*OMEGA(i)^3*xi(i), -4*xi(p)*OMEGA(p)+12*xi(i)*OMEGA(i),...
-OMEGA(p)^2+8*xi(p)*OMEGA(p)*xi(i)*OMEGA(i)+7*OMEGA(i)^2-16*xi(i)^2*OMEGA(i)^2];

B3iii=[H(p,i,i,i)+AA(p,i,i,i) ; 0 ; CC(p,i,i,i) ;  BB(p,i,i,i)];
%sol3iii=inv(A3iii)*B3iii;
                sol3iii=A3iii\B3iii;
R(p,i,i,i)=sol3iii(1);
S(p,i,i,i)=sol3iii(2);
T(p,i,i,i)=sol3iii(3);
U(p,i,i,i)=sol3iii(4);
LAMBDA(p,i,i,i) = -OMEGA(i)^2*T(p,i,i,i);
MU(p,i,i,i) = U(p,i,i,i) -6*xi(i)*OMEGA(i)*S(p,i,i,i);
NU(p,i,i,i)=3*R(p,i,i,i)-2*xi(i)*OMEGA(i)*T(p,i,i,i)-2*OMEGA(i)^2*U(p,i,i,i);
ZETA(p,i,i,i)= -3*OMEGA(i)^2*S(p,i,i,i)+2*T(p,i,i,i)-4*xi(i)*OMEGA(i)*U(p,i,i,i);
end
end
end
end

for p=1:N
for i=1:N-1
if i~=p
for j=i+1:N
D2=(OMEGA(p)+OMEGA(i)-2*OMEGA(j))*(OMEGA(p)+OMEGA(i)+2*OMEGA(j))*...
(-OMEGA(p)+OMEGA(i)+2*OMEGA(j))*(-OMEGA(p)+OMEGA(i)-2*OMEGA(j));
if ((abs(D2) < 1e-12) | (abs(OMEGA(i)^2-OMEGA(p)^2)<1e-12))
R(p,i,j,j) = 0;
S(p,i,j,j) = 0;
T(p,i,j,j) = 0;
T(p,j,i,j) = 0;
U(p,i,j,j) = 0;
U(p,j,i,j) = 0;
LAMBDA(p,i,j,j)=0;
MU(p,i,j,j) = 0;
NU(p,i,j,j) =0;
NU(p,j,i,j) =0;
ZETA(p,i,j,j) = 0;
 %b 21n132
           ZETA(p,j,i,j) = 0;
else
```

```
  Aip=[-OMEGA(p)^2+2*OMEGA(j)^2+OMEGA(i)^2, 0,2*xi(p)*OMEGA(p)*OMEGA(i)^2-...
2*OMEGA(i)^3*xi(i), 2*xi(p)*OMEGA(p)*OMEGA(j)^2-2*OMEGA(j)^3*xi(j), ...
-2*OMEGA(j)^4, -2*OMEGA(j)^2*OMEGA(i)^2 ;  0, -OMEGA(p)^2+4*xi(p)*...
OMEGA(p)*xi(i)*OMEGA(i)+8*xi(p)*OMEGA(p)*xi(j)*OMEGA(j)+2*OMEGA(j)^2+...
OMEGA(i)^2-4*xi(i)^2*OMEGA(i)^2-16*xi(i)*OMEGA(i)*xi(j)*OMEGA(j)-...
16*xi(j)^2*OMEGA(j)^2, -2,  -2, -2*xi(p)*OMEGA(p)+8*xi(j)*OMEGA(j)+2*...
xi(i)*OMEGA(i), -2*xi(p)*OMEGA(p)+4*xi(i)*OMEGA(i)+6*xi(j)*OMEGA(j) ;
-2*xi(p)*OMEGA(p)+2*xi(i)*OMEGA(i), -2*OMEGA(j)^4, -OMEGA(p)^2+4*xi(p)*...
OMEGA(p)*xi(i)*OMEGA(i)+OMEGA(i)^2+2*OMEGA(j)^2-4*xi(i)^2*OMEGA(i)^2,
2*OMEGA(j)^2, 0, 2*xi(p)*OMEGA(p)*OMEGA(j)^2-4*OMEGA(j)^2*xi(i)*OMEGA(i)-...
2*OMEGA(j)^3*xi(j) ;  -4*xi(p)*OMEGA(p)+4*xi(j)*OMEGA(j), -4*OMEGA(j)^2*...
OMEGA(i)^2, 4*OMEGA(i)^2, -OMEGA(p)^2+4*xi(p)*OMEGA(p)*xi(j)*OMEGA(j)+...
4*OMEGA(j)^2-4*xi(j)^2*OMEGA(j)^2+OMEGA(i)^2, 4*xi(p)*OMEGA(p)*...
OMEGA(j)^2-12*OMEGA(j)^3*xi(j), 2*xi(p)*OMEGA(p)*OMEGA(i)^2-4*OMEGA(i)^2*...
xi(j)*OMEGA(j)-2*OMEGA(i)^3*xi(i) ;  -2, 2*xi(p)*OMEGA(p)*OMEGA(i)^2-...
2*OMEGA(i)^3*xi(i)-8*OMEGA(i)^2*xi(j)*OMEGA(j), 0, -2*xi(p)*OMEGA(p)+...
6*xi(j)*OMEGA(j), -OMEGA(p)^2+8*xi(p)*OMEGA(p)*xi(j)*OMEGA(j)+OMEGA(i)^2+...
2*OMEGA(j)^2-16*xi(j)^2*OMEGA(j)^2, 2*OMEGA(i)^2 ;  -4, -12*OMEGA(j)^3*...
xi(j)+4*xi(p)*OMEGA(p)*OMEGA(j)^2-8*OMEGA(j)^2*xi(i)*OMEGA(i), 8*xi(i)*...
OMEGA(i)+4*xi(j)*OMEGA(j)-4*xi(p)*OMEGA(p), 4*xi(j)*OMEGA(j)-2*xi(p)*...
OMEGA(p)+2*xi(i)*OMEGA(i), 4*OMEGA(j)^2, -OMEGA(p)^2-4*xi(j)^2*...
OMEGA(j)^2+OMEGA(i)^2+4*OMEGA(j)^2-8*xi(i)*OMEGA(i)*xi(j)*OMEGA(j)-...
4*xi(i)^2*OMEGA(i)^2+4*xi(p)*OMEGA(p)*xi(i)*OMEGA(i)+4*xi(p)*OMEGA(p)*...
xi(j)*OMEGA(j)];

Bip=[H(p,i,j,j)+AA(p,i,j,j)+AA(p,j,i,j) ;0; CC(p,j,j,i) ;CC(p,j,i,j)+...
CC(p,i,j,j) ;BB(p,i,j,j) ;  BB(p,j,i,j)];
  %solrstuip=inv(Aip)*Bip;
                          solrstuip=Aip\Bip;
  R(p,i,j,j) = solrstuip(1);
  S(p,i,j,j) = solrstuip(2);
  T(p,i,j,j) = solrstuip(3);
  T(p,j,i,j) = solrstuip(4);
  U(p,i,j,j) = solrstuip(5);
  U(p,j,i,j) = solrstuip(6);
  LAMBDA(p,i,j,j) = -OMEGA(j)^2*T(p,j,i,j)-OMEGA(i)^2*T(p,i,j,j);
  ZETA(p,i,j,j) = -OMEGA(i)^2*S(p,i,j,j)+T(p,j,i,j)-4*xi(j)*OMEGA(j)*U(p,i,j,j);
  NU(p,i,j,j) = R(p,i,j,j)-OMEGA(j)^2*U(p,j,i,j)-2*xi(i)*OMEGA(i)*T(p,i,j,j);
  MU(p,i,j,j) = U(p,j,i,j)+U(p,i,j,j)-2*xi(i)*OMEGA(i)*S(p,i,j,j)-...
4*xi(j)*OMEGA(j)*S(p,i,j,j);

NU(p,j,i,j) = 2*R(p,i,j,j)-2*xi(j)*OMEGA(j)*T(p,j,i,j)-OMEGA(i)^2*U(p,j,i,j)-...
2*OMEGA(j)^2*U(p,i,j,j);
```

```
ZETA(p,j,i,j) = -2*OMEGA(j)^2*S(p,i,j,j)+2*T(p,i,j,j)+T(p,j,i,j)-...
2*xi(i)*OMEGA(i)*U(p,j,i,j)-2*xi(j)*OMEGA(j)*U(p,j,i,j);
end
end
end
end
end

for p=1:N
for i=1:N-1
for j=(i+1):N
if j~=p
D3= (OMEGA(p)+2*OMEGA(i)-OMEGA(j))*(OMEGA(p)+2*OMEGA(i)+OMEGA(j))*...
(-OMEGA(p)+2*OMEGA(i)+OMEGA(j))*(-OMEGA(p)+2*OMEGA(i)-OMEGA(j));
if ((abs(D3) < 1e-12) | (abs(OMEGA(p)^2 -OMEGA(j)^2)<1e-12))
R(p,i,i,j) =0;
S(p,i,i,j) =0;
T(p,j,i,i) =0;
T(p,i,i,j) =0;
U(p,j,i,i) =0;
U(p,i,i,j) =0;
LAMBDA(p,i,i,j)=0;
NU(p,j,i,i) =0;
NU(p,i,i,j) =0;
MU(p,i,i,j) =0;
ZETA(p,j,i,i) =0;
ZETA(p,i,i,j) =0;
else
  Ajpp=[-OMEGA(p)^2+OMEGA(j)^2+2*OMEGA(i)^2, 0, 2*xi(p)*OMEGA(p)*OMEGA(i)^2-...
2*OMEGA(i)^3*xi(i), 2*xi(p)*OMEGA(p)*OMEGA(j)^2-2*OMEGA(j)^3*xi(j),  ...
-2*OMEGA(j)^2*OMEGA(i)^2, -2*OMEGA(i)^4 ;  0,  -OMEGA(p)^2+8*xi(p)*OMEGA(p)*...
xi(i)*OMEGA(i)+4*xi(p)*OMEGA(p)*xi(j)*OMEGA(j)+OMEGA(j)^2+2*OMEGA(i)^2-...
16*xi(i)^2*OMEGA(i)^2-16*xi(i)*OMEGA(i)*xi(j)*OMEGA(j)-4*xi(j)^2*OMEGA(j)^2,...
-2, -2, -2*xi(p)*OMEGA(p)+6*xi(i)*OMEGA(i)+4*xi(j)*OMEGA(j), ...
-2*xi(p)*OMEGA(p)+8*xi(i)*OMEGA(i)+2*xi(j)*OMEGA(j) ;
-4*xi(p)*OMEGA(p)+4*xi(i)*OMEGA(i), -4*OMEGA(j)^2*OMEGA(i)^2, -OMEGA(p)^2+...
4*xi(p)*OMEGA(p)*xi(i)*OMEGA(i)+4*OMEGA(i)^2-4*xi(i)^2*OMEGA(i)^2+OMEGA(j)^2,
4*OMEGA(j)^2, 2*xi(p)*OMEGA(p)*OMEGA(j)^2-4*OMEGA(j)^2*xi(i)*OMEGA(i)-...
2*OMEGA(j)^3*xi(j), 4*xi(p)*OMEGA(p)*OMEGA(i)^2-12*OMEGA(i)^3*xi(i) ;
-2*xi(p)*OMEGA(p)+2*xi(j)*OMEGA(j), -2*OMEGA(i)^4, 2*OMEGA(i)^2, -OMEGA(p)^2+...
4*xi(p)*OMEGA(p)*xi(j)*OMEGA(j)+OMEGA(j)^2-4*xi(j)^2*OMEGA(j)^2+2*OMEGA(i)^2,
2*xi(p)*OMEGA(p)*OMEGA(i)^2-4*OMEGA(i)^2*xi(j)*OMEGA(j)-2*OMEGA(i)^3*xi(i), 0 ;
-4, -12*OMEGA(i)^3*xi(i)+4*xi(p)*OMEGA(p)*OMEGA(i)^2-8*OMEGA(i)^2*xi(j)*OMEGA(j),
4*xi(i)*OMEGA(i)+2*xi(j)*OMEGA(j)-2*xi(p)*OMEGA(p), 8*xi(j)*OMEGA(j)+4*xi(i)*OMEGA(i)
```

```
-4*xi(p)*OMEGA(p), -OMEGA(p)^2+OMEGA(j)^2+4*OMEGA(i)^2-4*xi(j)^2*OMEGA(j)^2-...
4*xi(i)^2*OMEGA(i)^2+4*xi(p)*OMEGA(p)*xi(i)*OMEGA(i)+4*xi(p)*OMEGA(p)*...
xi(j)*OMEGA(j)-8*xi(i)*OMEGA(i)*xi(j)*OMEGA(j), 4*OMEGA(i)^2 ; -2,
2*xi(p)*OMEGA(p)*OMEGA(j)^2-8*OMEGA(j)^2*xi(i)*OMEGA(i)-2*OMEGA(j)^3*xi(j),
-2*xi(p)*OMEGA(p)+6*xi(i)*OMEGA(i), 0, 2*OMEGA(j)^2, -OMEGA(p)^2+8*xi(p)*...
OMEGA(p)*xi(i)*OMEGA(i)+OMEGA(j)^2+2*OMEGA(i)^2-16*xi(i)^2*OMEGA(i)^2];

Bjpp=[H(p,i,i,j)+AA(p,i,i,j)+AA(p,j,i,i) ; 0; CC(p,j,i,i)+CC(p,i,j,i); CC(p,i,i,j);
BB(p,i,i,j); BB(p,j,i,i)];
  %solrstujpp=inv(Ajpp)*Bjpp;
  solrstujpp=Ajpp\Bjpp;
                   R(p,i,i,j) =solrstujpp(1);
  S(p,i,i,j) =solrstujpp(2);
  T(p,i,i,j) =solrstujpp(3);
  T(p,j,i,i) =solrstujpp(4);
  U(p,i,i,j) =solrstujpp(5);
  U(p,j,i,i) =solrstujpp(6);
  NU(p,j,i,i) = R(p,i,i,j)-2*xi(j)*OMEGA(j)*T(p,j,i,i)-OMEGA(i)^2*U(p,i,i,j);
  ZETA(p,j,i,i) = -OMEGA(j)^2*S(p,i,i,j)+T(p,i,i,j)-4*xi(i)*OMEGA(i)*U(p,j,i,i);
  LAMBDA(p,i,i,j) = -OMEGA(j)^2*T(p,j,i,i)-OMEGA(i)^2*T(p,i,i,j);
  MU(p,i,i,j) = U(p,j,i,i)+U(p,i,i,j)-4*xi(i)*OMEGA(i)*S(p,i,i,j)-...
2*xi(j)*OMEGA(j)*S(p,i,i,j);
  NU(p,i,i,j) = 2*R(p,i,i,j)-2*xi(i)*OMEGA(i)*T(p,i,i,j)-2*OMEGA(i)^2*U(p,j,i,i)-...
OMEGA(j)^2*U(p,i,i,j);

ZETA(p,i,i,j) = -2*OMEGA(i)^2*S(p,i,i,j)+2*T(p,j,i,i)+T(p,i,i,j)-...
2*xi(i)*OMEGA(i)*U(p,i,i,j)-2*xi(j)*OMEGA(j)*U(p,i,i,j);
end
end
end
end
end

for p=1:N
for i=1:N-2
for j=(i+1):N-1
for k=(j+1):N
D4=(OMEGA(p)+OMEGA(j)+OMEGA(k)-OMEGA(i))*(-OMEGA(p)+OMEGA(j)-OMEGA(k)+...
OMEGA(i))*(OMEGA(p)+OMEGA(j)+OMEGA(k)+OMEGA(i))*(-OMEGA(p)+OMEGA(j)-...
OMEGA(k)-OMEGA(i))*(OMEGA(p)+OMEGA(j)-OMEGA(k)-OMEGA(i))*(-OMEGA(p)+OMEGA(j)+...
OMEGA(k)+OMEGA(i))*(OMEGA(p)+OMEGA(j)-OMEGA(k)+OMEGA(i))*(-OMEGA(p)+OMEGA(j)+...
OMEGA(k)-OMEGA(i));
if abs(D4) < 1e-12
U(p,i,j,k) =0;
```

```
U(p,j,i,k) =0;
U(p,k,i,j) =0;
R(p,i,j,k) =0;
MU(p,i,j,k) =0;
NU(p,k,i,j) =0;
NU(p,j,i,k) =0;
NU(p,i,j,k) =0;
else
  Alastijkp=[-OMEGA(p)^2+OMEGA(k)^2+OMEGA(j)^2+OMEGA(i)^2, 0, 2*xi(p)*...
OMEGA(p)*OMEGA(i)^2-2*OMEGA(i)^3*xi(i), 2*xi(p)*OMEGA(p)*OMEGA(j)^2-...
2*OMEGA(j)^3*xi(j), 2*xi(p)*OMEGA(p)*OMEGA(k)^2-2*OMEGA(k)^3*xi(k), ...
-2*OMEGA(k)^2*OMEGA(j)^2, -2*OMEGA(k)^2*OMEGA(i)^2,-2*OMEGA(j)^2*OMEGA(i)^2;
0, OMEGA(i)^2+ OMEGA(j)^2-OMEGA(p)^2+OMEGA(k)^2+4*xi(p)*OMEGA(p)*...
xi(i)*OMEGA(i)+4*xi(p)*OMEGA(p)*xi(j)*OMEGA(j)+4*xi(p)*OMEGA(p)*xi(k)*...
OMEGA(k)-4*xi(i)^2*OMEGA(i)^2-4*xi(j)^2*OMEGA(j)^2-4*xi(k)^2*OMEGA(k)^2-...
8*xi(i)*OMEGA(i)*xi(j)*OMEGA(j)-8*xi(i)*OMEGA(i)*xi(k)*OMEGA(k)-8*xi(j)*...
OMEGA(j)*xi(k)*OMEGA(k), -2, -2, -2, 4*xi(j)*OMEGA(j)+4*xi(k)*OMEGA(k)-...
2*xi(p)*OMEGA(p)+2*xi(i)*OMEGA(i), 4*xi(i)*OMEGA(i)+4*xi(k)*OMEGA(k)-...
2*xi(p)*OMEGA(p)+2*xi(j)*OMEGA(j), 4*xi(i)*OMEGA(i)+4*xi(j)*OMEGA(j)-...
2*xi(p)*OMEGA(p)+2*xi(k)*OMEGA(k) ;  -2*xi(p)*OMEGA(p)+2*xi(i)*OMEGA(i), ...
-2*OMEGA(k)^2*OMEGA(j)^2, -OMEGA(p)^2+4*xi(p)*OMEGA(p)*xi(i)*OMEGA(i)+...
OMEGA(i)^2-4*xi(i)^2*OMEGA(i)^2+OMEGA(j)^2+OMEGA(k)^2, 2*OMEGA(j)^2, ...
2*OMEGA(k)^2, 0, 2*xi(p)*OMEGA(p)*OMEGA(k)^2-4*xi(i)*OMEGA(i)*OMEGA(k)^2-...
2*OMEGA(k)^3*xi(k), 2*xi(p)*OMEGA(p)*OMEGA(j)^2-4*xi(i)*OMEGA(i)*...
OMEGA(j)^2-2*OMEGA(j)^3*xi(j) ; -2*xi(p)*OMEGA(p)+2*xi(j)*OMEGA(j),
-2*OMEGA(k)^2*OMEGA(i)^2, 2*OMEGA(i)^2, -OMEGA(p)^2+4*xi(p)*OMEGA(p)*...
xi(j)*OMEGA(j)+OMEGA(j)^2-4*xi(j)^2*OMEGA(j)^2+OMEGA(i)^2+OMEGA(k)^2,
2*OMEGA(k)^2, 2*xi(p)*OMEGA(p)*OMEGA(k)^2-4*xi(j)*OMEGA(j)*OMEGA(k)^2-...
2*OMEGA(k)^3*xi(k), 0, 2*xi(p)*OMEGA(p)*OMEGA(i)^2-4*xi(j)*OMEGA(j)*...
OMEGA(i)^2-2*OMEGA(i)^3*xi(i) ; -2*xi(p)*OMEGA(p)+2*xi(k)*OMEGA(k),
-2*OMEGA(j)^2*OMEGA(i)^2, 2*OMEGA(i)^2, 2*OMEGA(j)^2, -OMEGA(p)^2+4*...
xi(p)*OMEGA(p)*xi(k)*OMEGA(k)+OMEGA(k)^2-4*xi(k)^2*OMEGA(k)^2+...
OMEGA(i)^2+OMEGA(j)^2, 2*xi(p)*OMEGA(p)*OMEGA(j)^2-4*xi(k)*OMEGA(k)*...
OMEGA(j)^2-2*OMEGA(j)^3*xi(j), 2*xi(p)*OMEGA(p)*OMEGA(i)^2-4*xi(k)*...
OMEGA(k)*OMEGA(i)^2-2*OMEGA(i)^3*xi(i), 0 ; -2, 2*xi(p)*OMEGA(p)*...
OMEGA(i)^2-2*OMEGA(i)^3*xi(i)-4*xi(j)*OMEGA(j)*OMEGA(i)^2-4*xi(k)*...
OMEGA(k)*OMEGA(i)^2, 0, -2*xi(p)*OMEGA(p)+4*xi(j)*OMEGA(j)+2*xi(k)*...
OMEGA(k), -2*xi(p)*OMEGA(p)+4*xi(k)*OMEGA(k)+2*xi(j)*OMEGA(j), -OMEGA(p)^2+...
4*xi(p)*OMEGA(p)*xi(j)*OMEGA(j)+4*xi(p)*OMEGA(p)*xi(k)*OMEGA(k)+OMEGA(i)^2+...
OMEGA(j)^2+OMEGA(k)^2-4*xi(j)^2*OMEGA(j)^2-8*xi(j)*OMEGA(j)*xi(k)*OMEGA(k)-...
4*xi(k)^2*OMEGA(k)^2, 2*OMEGA(i)^2, 2*OMEGA(i)^2 ; -2, 2*xi(p)*OMEGA(p)*...
OMEGA(j)^2-4*xi(i)*OMEGA(i)*OMEGA(j)^2-2*OMEGA(j)^3*xi(j)-4*xi(k)*...
OMEGA(k)*OMEGA(j)^2, -2*xi(p)*OMEGA(p)+4*xi(i)*OMEGA(i)+2*xi(k)*OMEGA(k),
0, -2*xi(p)*OMEGA(p)+4*xi(k)*OMEGA(k)+2*xi(i)*OMEGA(i), 2*OMEGA(j)^2, ...
```

```
-OMEGA(p)^2+4*xi(p)*OMEGA(p)*xi(i)*OMEGA(i)+4*xi(p)*OMEGA(p)*xi(k)*...
OMEGA(k)+OMEGA(j)^2+OMEGA(i)^2+OMEGA(k)^2-4*xi(i)^2*OMEGA(i)^2-8*xi(i)*...
OMEGA(i)*xi(k)*OMEGA(k)-4*xi(k)^2*OMEGA(k)^2, 2*OMEGA(j)^2 ; -2, ...
2*xi(p)*OMEGA(p)*OMEGA(k)^2-4*xi(i)*OMEGA(i)*OMEGA(k)^2-4*xi(j)*...
OMEGA(j)*OMEGA(k)^2-2*OMEGA(k)^3*xi(k), -2*xi(p)*OMEGA(p)+4*xi(i)*OMEGA(i)+...
2*xi(j)*OMEGA(j), -2*xi(p)*OMEGA(p)+4*xi(j)*OMEGA(j)+2*xi(i)*OMEGA(i), 0,
2*OMEGA(k)^2, 2*OMEGA(k)^2, -OMEGA(p)^2+4*xi(p)*OMEGA(p)*xi(i)*OMEGA(i)+...
4*xi(p)*OMEGA(p)*xi(j)*OMEGA(j)+OMEGA(k)^2+OMEGA(i)^2+OMEGA(j)^2-...
4*xi(i)^2*OMEGA(i)^2-8*xi(i)*OMEGA(i)*xi(j)*OMEGA(j)-4*xi(j)^2*OMEGA(j)^2];


Blastijkp=[H(p,i,j,k)+AA(p,i,j,k)+AA(p,k,i,j)+AA(p,j,i,k) ; 0 ;
CC(p,k,j,i)+CC(p,j,k,i) ; CC(p,k,i,j)+CC(p,i,k,j) ;
CC(p,j,i,k)+CC(p,i,j,k) ; BB(p,i,j,k) ; BB(p,j,i,k)  ; BB(p,k,i,j)];
  %Am1=inv(Alastijkp);
  solrstu=Alastijkp\Blastijkp;
  R(p,i,j,k)=solrstu(1);
  S(p,i,j,k)=solrstu(2);
  T(p,i,j,k)=solrstu(3);
  T(p,j,i,k)=solrstu(4);
  T(p,k,i,j)=solrstu(5);
  U(p,i,j,k)=solrstu(6);
  U(p,j,i,k)=solrstu(7);
  U(p,k,i,j)=solrstu(8);

NU(p,k,i,j)= R(p,i,j,k)-2*xi(k)*OMEGA(k)*T(p,k,i,j)-OMEGA(i)^2*U(p,j,i,k)-...
OMEGA(j)^2*U(p,i,j,k);

ZETA(p,k,i,j)= -OMEGA(k)^2*S(p,i,j,k)+T(p,j,i,k)+T(p,i,j,k)-...
2*(xi(i)*OMEGA(i)+xi(j)*OMEGA(j))*U(p,k,i,j);

LAMBDA(p,i,j,k)=-OMEGA(k)^2*T(p,k,i,j)-OMEGA(j)^2*T(p,j,i,k)-...
OMEGA(i)^2*T(p,i,j,k);

MU(p,i,j,k)=U(p,k,i,j)+U(p,j,i,k)+U(p,i,j,k)-2*(xi(i)*OMEGA(i)+xi(j)*...
OMEGA(j)+xi(k)*OMEGA(k))*S(p,i,j,k);

NU(p,j,i,k)=R(p,i,j,k)-2*xi(j)*OMEGA(j)*T(p,j,i,k)-OMEGA(i)^2*U(p,k,i,j)-...
OMEGA(k)^2*U(p,i,j,k);

NU(p,i,j,k)=R(p,i,j,k)-2*xi(i)*OMEGA(i)*T(p,i,j,k)-OMEGA(j)^2*U(p,k,i,j)-...
OMEGA(k)^2*U(p,j,i,k);

ZETA(p,j,i,k)=-OMEGA(j)^2*S(p,i,j,k)+T(p,k,i,j)+T(p,i,j,k)-2*(xi(i)*OMEGA(i)+...
xi(k)*OMEGA(k))*U(p,j,i,k);
```

```
ZETA(p,i,j,k)=-OMEGA(i)^2*S(p,i,j,k)+T(p,k,i,j)+T(p,j,i,k)-2*(xi(j)*OMEGA(j)+...
xi(k)*OMEGA(k))*U(p,i,j,k);
end
end
end
end
end
disp('end')
```

A.3   Simulation Files

The simulation files can be found in https://drive.google.com/open?id= 0B2onGI-yt3FwRVZQbUFkcGl5enc with:
1. "Damped_free_vibration_interconnectedVSCs.mdl" to study the free oscillations;
2. "Forced_damped_vibration_interconnectedVSCs.mdl" to study the forced oscillations.

Inverse Nonlinear Transformation on Real-time

This part is dedicated to illustrate the real-time algorithm of inverting nonlinear transformation

B.1 Theoretical Formulation

A nonlinear transformation is proposed to obtain the Normal Forms of the system of equations, which is proposed to render the simplest Normal Forms and reads:

$$
\begin{cases}
X_p = R_p + \sum_{i=1}^{N} \sum_{j \geq i}^{N} (a_{ij}^p R_i R_j + b_{ij}^p S_i S_j) + \sum_{i=1}^{N} \sum_{j=1}^{N} c_{ij}^p R_i S_j \\
\quad + \sum_{i=1}^{N} \sum_{j \geq i}^{N} \sum_{k \geq j}^{N} (r_{ijk}^p R_i R_j R_k + s_{ijk}^p S_i S_j S_k) \\
\quad + \sum_{i=1}^{N} \sum_{j=1}^{N} \sum_{k \geq j}^{N} (t_{ijk}^p S_i R_j R_k + u_{ijk}^p R_i S_j S_k) \\
Y_p = S_p + \sum_{i=1}^{N} \sum_{j \geq i}^{N} (\alpha_{ij}^p R_i R_j + \beta_{ij}^p S_i S_j) + \sum_{i=1}^{N} \sum_{j=1}^{N} \gamma_{ij}^p R_i S_j \\
\quad + \sum_{i=1}^{N} \sum_{j \geq i}^{N} \sum_{k \geq j}^{N} (\lambda_{ijk}^p R_i R_j R_k + \mu_{ijk}^p S_i S_j S_k) \\
\quad + \sum_{i=1}^{N} \sum_{j=1}^{N} \sum_{k \geq j}^{N} (\nu_{ijk}^p S_i R_j R_k + \zeta_{ijk}^p R_i S_j S_k)
\end{cases}
$$

The difficulty to implement in inverting the matrix is the nonlinearities. However, in real-time, in each step, the R_p and S_p increase slightly. Thus, the real-time (RT) values can be approximated with great accuracy as $X_p^{RT} = X_p^{init} + \triangle X_p, Y_p^{RT} = Y_p^{init} + \triangle Y_p, R_p^{RT} = R_p^{init} + \triangle R_p, S_p^{RT} = S_p^{init} + \triangle S_p$. Keeping terms up to degree $\triangle$, and neglect terms with higher degrees, Eq. (B.1) leads a linearization of the nonlinear transformation.

B.2   Linearization of the Nonlinear Transformation

The linearization of the nonlinear transformation can be done as (B.1).

$$
\begin{cases}
\triangle X_p = \triangle R_p + \displaystyle\sum_{i=1}^{N} PR(1)_{pi}\triangle R_i + \sum_{i=1}^{N} PS(1)_{pi}\triangle S_i \\[2ex]
\quad \displaystyle\sum_{i=1}^{N} PR(R2)_{pi}\triangle R_i + \sum_{i=1}^{N} PS(S2)_{pi}\triangle S_i \\[2ex]
\quad \displaystyle\sum_{i=1}^{N} PR(S2)_{pi}\triangle R_i + \sum_{i=1}^{N} PS(R2)_{pi}\triangle S_i \\[2ex]
\triangle Y_p = \triangle S_p + \displaystyle\sum_{i=1}^{N} QR(1)_{pi}\triangle R_i + \sum_{i=1}^{N} QS(1)_{pi}\triangle S_i \\[2ex]
\quad \displaystyle\sum_{i=1}^{N} QR(R2)_{pi}\triangle R_i + \sum_{i=1}^{N} QS(S2)_{pi}\triangle S_i \\[2ex]
\quad \displaystyle\sum_{i=1}^{N} QR(S2)_{pi}\triangle R_i + \sum_{i=1}^{N} QS(R2)_{pi}\triangle S_i
\end{cases}
$$

with

$$
PR(1)_{pi} = \sum_{j=1}^{i} a_{ji}^{p} R_j + \sum_{j\geq i}^{N} a_{ij}^{p} R_j + \sum_{j=1}^{N} c_{ij}^{p} S_j \tag{B.1}
$$

$$
PS(1)_{pi} = \sum_{j=1}^{i} b_{ji}^{p} S_j + \sum_{j\geq i}^{N} b_{ij}^{p} S_j + \sum_{j=1}^{N} c_{ji}^{p} R_j
$$

$$
PR(R2)_{pi} = \sum_{j=1}^{i}\sum_{k\geq j}^{i} r_{kji}^{p} R_j R_k + \sum_{j=1}^{i}\sum_{k\geq i}^{N} r_{jik}^{p} R_j R_k + \sum_{j\geq i}^{N}\sum_{k\geq j}^{N} r_{ijk}^{p} R_j R_k
$$

$$
PS(S2)_{pi} = \sum_{j=1}^{i}\sum_{k\geq j}^{i} s_{kji}^{p} S_j S_k + \sum_{j=1}^{i}\sum_{k\geq i}^{N} s_{jik}^{p} S_j S_k + \sum_{j\geq i}^{N}\sum_{k\geq j}^{N} s_{ijk}^{p} S_j S_k
$$

$$
PR(S2)_{pi} = \sum_{j=1}^{N}\sum_{k=1}^{i} t_{jki}^{p} S_j R_k + \sum_{j=1}^{N}\sum_{k\geq i}^{N} t_{jik}^{p} S_j R_k + \sum_{j=1}^{N}\sum_{k\geq j}^{N} u_{ijk}^{p} S_j S_k
$$

$$
PS(R2)_{pi} = \sum_{j=1}^{N}\sum_{k=1}^{i} u_{jki}^{p} R_j S_k + \sum_{j=1}^{N}\sum_{k\geq i}^{N} u_{jik}^{p} R_j S_k + \sum_{j=1}^{N}\sum_{k\geq j}^{N} t_{ijk}^{p} R_j R_k
$$

$$QR(1)_{pi} = \sum_{j=1}^{i} \alpha_{ji}^{p} R_j + \sum_{j \geq i}^{N} \alpha_{ij}^{p} R_j + \sum_{j=1}^{N} \gamma_{ij}^{p} S_j \qquad \text{(B.2)}$$

$$QS(1)_{pi} = \sum_{j=1}^{i} \beta_{ji}^{p} S_j + \sum_{j \geq i}^{N} \beta_{ij}^{p} S_j + \sum_{j=1}^{N} \gamma_{ji}^{p} R_j$$

$$QR(R2)_{pi} = \sum_{j=1}^{i} \sum_{k \geq j}^{j} \lambda_{kji}^{p} R_j R_k + \sum_{j=1}^{i} \sum_{k \geq i}^{N} \lambda_{jik}^{p} R_j R_k + \sum_{j \geq i}^{N} \sum_{k \geq j}^{N} \lambda_{ijk}^{p} R_j R_k$$

$$QS(S2)_{pi} = \sum_{j=1}^{i} \sum_{k \geq j}^{i} \mu_{kji}^{p} S_j S_k + \sum_{j=1}^{i} \sum_{k \geq i}^{N} \mu_{jik}^{p} S_j S_k + \sum_{j \geq i}^{N} \sum_{k \geq j}^{N} \mu_{ijk}^{p} S_j S_k$$

$$QR(S2)_{pi} = \sum_{j=1}^{N} \sum_{k=1}^{i} \nu_{jki}^{p} S_j R_k + \sum_{j=1}^{N} \sum_{k \geq i}^{N} \nu_{jik}^{p} S_j R_k + \sum_{j=1}^{N} \sum_{k \geq j}^{N} \zeta_{ijk}^{p} S_j S_k$$

$$QS(R2)_{pi} = \sum_{j=1}^{N} \sum_{k=1}^{i} \zeta_{jki}^{p} R_j S_k + \sum_{j=1}^{N} \sum_{k \geq i}^{N} \zeta_{jik}^{p} R_j S_k + \sum_{j=1}^{N} \sum_{k \geq j}^{N} \nu_{ijk}^{p} R_j R_k$$

Let

$$XR = PR(1) + PR(R2) + PR(S2) \quad XS = PS(1) + PS(R2) + PS(S2)$$

$$YR = QR(1) + QR(R2) + QR(S2) \quad YS = QS(1) + QS(R2) + QS(S2)$$

(B.3)

Then we obtain

$$\begin{bmatrix} \triangle X \\ \triangle Y \end{bmatrix} = \begin{bmatrix} I + XR & XS \\ YR & YS \end{bmatrix} \begin{bmatrix} \triangle R \\ \triangle S \end{bmatrix} \qquad \text{(B.4)}$$

and

$$\begin{bmatrix} \triangle R \\ \triangle S \end{bmatrix} = \begin{bmatrix} I + XR & XS \\ YR & YS \end{bmatrix}^{-1} \begin{bmatrix} \triangle X \\ \triangle Y \end{bmatrix} = \begin{bmatrix} NL^{RT} \end{bmatrix}^{-1} \begin{bmatrix} \triangle X \\ \triangle Y \end{bmatrix} \qquad \text{(B.5)}$$

The initial values can be searched off-line, which will need dozen's of steps. And after that, the change in the variable $\triangle R, \triangle S$ can be calculated from $\triangle X, \triangle Y$ at real-time. And after the calculation, matrix NL^{RT} will be updated for the calculation at next sampling time.

Kundur's 4 Machine 2 Area System

C.1 Parameters of Kundur's Two Area Four Machine System

Table C.1: Generator Data in PU on Machine Base

Parameter	Value	Parameter	Value
R_a	0.0025	x_l	0.002
x_d	1.80	τ'_{d0}	8.0
x_q	1.70	τ'_{q0}	0.40
x'_d	0.3	τ''_{d0}	0.0
x'_q	0.3	τ''_{d0}	0.0
x''_d	0.0	MVA_{base}	900
x''_q	0.0	H	6.5

Table C.2: Power Flow Data for Case 1 and Case 2 in Steady State after the fault is cleared: Load

Load Bus	Voltage (pu/230kv)	Z_{shunt}
$B5$	$1.029\angle 19.75°$	$P = 665.84MW, Q = -350.82Mvar$
$B6$	$0.987\angle -47.37°$	$P = 1443.38MW, Q = -350.02Mvar$

Table C.3: Power Flow Data for Case 1 and Case 2 in Steady State after the fault is cleared:Generator

Generator	Bus Type	Terminal Voltage (pu/20kv)	P (MW)	Q (Mvar)
G1	*PV*	$1.00\angle 14.02°$	747.50	49.94
G2	*swingbus*	$1.000\angle 0.0°$	406.50	140.74
G3	*PV*	$1.00\angle -58.17°$	539.25	113.99
G4	*PV*	$1.00\angle -66.11°$	525.00	143.14

Table C.4: Mechanical Damping and Exciter Gain of Generators for case 1, case 2 and case 3

Generator	Mechanical Damping			Exciter Gain		
	Case 1	Case 2	Case 3	Case 1	Case 2	Case 3
Gen 1	15	3.5	3.5	150	150	240
Gen 2	15	3.5	3.5	150	150	240
Gen 3	11	2	2	150	150	240
Gen 4	10	2	2	150	150	240

C.2   Programs and Simulation Files

This part of appendix is dedicated to the interconnected VSCs.

Section A.1 illustrates how the reduced 4th order model is formulated.

In this part of Appendix, the crucial files are presented to facilitate the reader's comprehension of the PhD dissertation.

All the programs and files associated with interconnected VSCs can be found in:
https://drive.google.com/open?id=0B2onGI-yt3FwdnBZQnJ6SUQ1UHM

C.2.1   SEP Initialization

```
--file Reduce27thOrderEquation.m --
%% Created by Tian TIAN, PhD in EE, 07/09/16
%% This is a symboic program of IEEE 4 machine system composed of :
```

```
%% the 4th order generator model+ 3rd oder Exciter model with AVR
clear all;
close all
%% Load the system.
%% The admittance matrix
% clear all

%% This program is used to calculate the interconnected power system with
%% a number of Gn generators.

%% Define the system
Gn=4 %% This is the 4 generator case.
omega_s=120*pi;

delta_Syn_1=1.8477; delta_Syn_2=1.2081; delta_Syn_3=0.78541; delta_Syn_4=0.53684;
omega_Syn_1=1;omega_Syn_2=1;omega_Syn_3=1; omega_Syn_4=1;

elq_Syn_1=0.8652; elq_Syn_2=1.0067; elq_Syn_3=0.88605;elq_Syn_4=0.91746;
eld_Syn_1=0.6477;     eld_Syn_2=0.33037; eld_Syn_3=0.5998; eld_Syn_4=0.52695;
vm_Exc_1=1.03;    vr3_Exc_1=0;            vf_Exc_1=1.8658;
vm_Exc_2=1.01;      vr3_Exc_2=0;            vf_Exc_2=1.4058;
vm_Exc_3=1.03;      vr3_Exc_3=0;            vf_Exc_3=1.6747;
vm_Exc_4=1.03;      vr3_Exc_4=0;            vf_Exc_4=1.5975;


Yt=[3.9604-39.5821i  -3.9604+39.6040i   0.0000+0.0000i   0.0000+0.0000i;
   -3.9604+39.6040i  10.3914-42.4178i   0.0000+0.0000i   0.4578+4.1671i;
    0.0000+0.0000i   0.0000+0.0000i   3.9604-39.5821i  -3.9604+39.6040i;
    0.0000+0.0000i   0.4578+4.1671i  -3.9604+39.6040i  18.2758-43.1388i];


Gt=real(Yt);
Bt=imag(Yt);
%% The admittance matrix of the network reduced to the
%% internal bus of the generators



%%Parameters for mechanical part of generators

H=[6.5;6.5;6.5;6.5];%% Inertial constant
D=[3.5;3.5;2;2];%% Mechanical damping

%%Parameters for electrical part of generators in steady state
```

```
Ra=ones(4,1)*0; Xd=ones(4,1)*1.80; Xq=ones(4,1)*1.70;
%% Stator resist ance, Equivalent reactance in the d axis,
%% Equivalent reactance in the q axis




%%Parameters for electromagentic transient process
Tld0=ones(4,1)*8.0;%% Transient time constant in the d axis
Tlq0=ones(4,1)*0.40;%% Transient time constant in the q axis
Xld=ones(4,1)*0.3;%% Equivalent transient reactance in the d axis
Xlq=ones(4,1)*0.3;%% Equivalent transient reactance in the q axis


%% Parameters for the exciters equipped with AVR(automatic voltage regulator)
K_A=[150;150;150;150];%% Exciter gain
T_e=ones(4,1)*0.01;
T_1=ones(4,1)*10;
T_2=ones(4,1)*1;
T_r=ones(4,1)*0.01;%% Delay for sampling of Vt



%% Define the variables for each generator:
%%  $\delta_{i}$, $\omega_{i}$, $e'q$,e'd,Efd,XE1,XE2
deltaG = sym('deltaG', [Gn-1 1]);

delta=[deltaG;0]+delta_Syn_4*ones(Gn,1);
omega= sym('omega', [Gn 1]);
elq= sym('elq', [Gn 1]);
eld= sym('eld', [Gn 1]);
Vf= sym('Vf', [Gn 1]);
Vm= sym('Vm', [Gn 1]);
Vr= sym('Vr', [Gn 1]);



Yr=zeros(2*Gn,2*Gn);
for l=1:Gn
    for m=1:Gn
        Yr(2*l-1,2*m-1)=Gt(l,m);
        Yr(2*l-1,2*m)=-Bt(l,m);
        Yr(2*l,2*m-1)=Bt(l,m);
        Yr(2*l,2*m)=Gt(l,m);
    end
end
```

```
%% Transformation matrices
%% T1: from the $dq_{i}$ reference frame to the common reference frame
%% T2: from the bus terminal to the generator transient axes
%% T1 and T2 are defined in Chapter 3
for l=1:Gn
        T1(2*l-1,2*l-1)=sin(delta(l));  T1(2*l-1,2*l)=cos(delta(l));
        T1(2*l,2*l-1)=-cos(delta(l));  T1(2*l,2*l)=sin(delta(l));
        T2(2*l-1,2*l-1)=Ra(l);  T2(2*l-1,2*l)=-Xlq(l);
        T2(2*l,2*l-1)=Xld(l);  T2(2*l,2*l)=Ra(l);
end

Y=inv(inv(Yr)+T2/9);
for l=1:Gn
    for m=1:Gn
        G1(l,m)=Y(2*l-1,2*m-1);
        B1(l,m)=-Y(2*l-1,2*m);
        B1(l,m)=Y(2*l,2*m-1);
        G1(1,m)=Y(2*l,2*m);
    end
end
Ydelta=inv(T1)*Y*T1;

for j=1:Gn
    eldq(2*j-1)=eld(j);
    eldq(2*j)=elq(j);
end

Idq=Ydelta*eldq.';

%% Auxiliary variable--id,iq
for j=1:Gn
    id(j)=Idq(2*j-1);
    iq(j)=Idq(2*j);
end

for j=1:Gn
    Vt(j)=sqrt((elq(j)-Xld(j)*id(j)/9)^2+(eld(j)+Xlq(j)*iq(j)/9)^2);
    Pe(j)=eld(j)*id(j)+elq(j)*iq(j);
    elx(j)=sin(delta(j))*eld(j)+cos(delta(j))*elq(j);
    ely(j)=-cos(delta(j))*eld(j)+sin(delta(j))*elq(j);
end
for j=1:Gn
```

```
        elxy(2*j-1,1)=elx(j);
        elxy(2*j,1)=ely(j);
end

Ixy=Y*elxy;


%%Initial conditions of the physical state variables
vf_Syn_1=1.8658;        pm_Syn_1=7.4911;        p_Syn_1=7.4911;        q_Syn_1=0.71811;
vf_Syn_2=1.4058;        pm_Syn_2=2.9291;        p_Syn_2=2.9291;        q_Syn_2=1.3674;
vf_Syn_3=1.6747;        pm_Syn_3=6.2548;        p_Syn_3=6.2548;        q_Syn_3=0.63815;
vf_Syn_4=1.5975;        pm_Syn_4=5.258;         p_Syn_4=5.258;         q_Syn_4=1.0209;

Pm=[pm_Syn_1;pm_Syn_2;pm_Syn_3;pm_Syn_4];
Pe0=[p_Syn_1;p_Syn_2;p_Syn_3;p_Syn_4];
Qe0=[q_Syn_1;q_Syn_2;q_Syn_3;q_Syn_4];
Vref=zeros(Gn,1);
Vref_Exc_1=1.03;
Vref_Exc_2=1.01;
Vref_Exc_3=1.03;
Vref_Exc_4=1.01;
Vref=[Vref_Exc_1;Vref_Exc_2;Vref_Exc_3;Vref_Exc_4];

delta0=[delta_Syn_1-delta_Syn_4;delta_Syn_2-delta_Syn_4;delta_Syn_3-delta_Syn_4];
omega0=[omega_Syn_1;omega_Syn_2;omega_Syn_3;omega_Syn_4];
elq0=[elq_Syn_1;elq_Syn_2;elq_Syn_3;elq_Syn_4];
eld0=[eld_Syn_1;eld_Syn_2;eld_Syn_3;eld_Syn_4];
Vm0=[vm_Exc_1;vm_Exc_2;vm_Exc_3;vm_Exc_4];
Vr0=[vr3_Exc_1;vr3_Exc_2;vr3_Exc_3;vr3_Exc_4];
Vf0=[vf_Exc_1;vf_Exc_2;vf_Exc_3;vf_Exc_4];

for j=1:Gn-1
    ddelta_Gn(j)=omega_s*(omega(j)-omega(Gn));
    domega(j)=1/(2*H(j))*(Pm(j)/9-Pe(j)/9-D(j)*(omega(j)-1));
    delq(j)=1/Tld0(j)*(Vf(j)-(Xd(j)-Xld(j))*id(j)/9-elq(j));
    deld(j)=1/Tlq0(j)*((Xq(j)-Xlq(j))/9*iq(j)-eld(j));
    dVm(j)=(Vt(j)-Vm(j))/T_r(j);
    dVr(j)=(K_A(j)*(1-T_1(j)/T_2(j))*(Vref(j)-Vm(j))-Vr(j))/T_2(j);
    dVf(j)=(Vr(j)+K_A(j)*T_1(j)/T_2(j)*(Vref(j)-Vm(j))+Vf0(j)-Vf(j))/T_e(j);
end
for j=Gn
    domega(j)=1/(2*H(j))*(Pm(j)/9-Pe(j)/9-D(j)*(omega(j)-1));
    delq(j)=1/Tld0(j)*(Vf(j)-(Xd(j)-Xld(j))*id(j)/9-elq(j));
    deld(j)=1/Tlq0(j)*((Xq(j)-Xlq(j))/9*iq(j)-eld(j));
```

```
    dVm(j)=(Vt(j)-Vm(j))/T_r(j);
    dVr(j)=(K_A(j)*(1-T_1(j)/T_2(j))*(Vref(j)-Vm(j))-Vr(j))/T_2(j);
    dVf(j)=(Vr(j)+K_A(j)*T_1(j)/T_2(j)*(Vref(j)-Vm(j))+Vf0(j)-Vf(j))/T_e(j);
end


for j=1:Gn-1
    X27(7*j-6:7*j)=[deltaG(j),omega(j),elq(j),eld(j),Vm(j),Vr(j),Vf(j)];
    F27(7*j-6:7*j)=[ddelta_Gn(j),domega(j),delq(j),deld(j),dVm(j),dVr(j),dVf(j)];
end
for j=Gn
    X27(7*j-6:7*j-1)=[omega(j),elq(j),eld(j),Vm(j),Vr(j),Vf(j)];
    F27(7*j-6:7*j-1)=[domega(j),delq(j),deld(j),dVm(j),dVr(j),dVf(j)];
end

%%%---- Input of the operating point obtained from the power flow analysis
%% run by the software PSAT ----------

for j=1:Gn-1
    x027(7*j-6:7*j)=[delta0(j),omega0(j),elq0(j),eld0(j),Vm0(j),Vr0(j),Vf0(j)];
end


for j=Gn
    x027(7*j-6:7*j-1)=[omega0(j),elq0(j),eld0(j),Vm0(j),Vr0(j),Vf0(j)];
end
x027=x027.';

Fv_R=vpa(F27);
FvS_R=simplify(Fv_R);

TS_R=taylor(FvS_R,X27,x027,'Order',4);
%TStest=subs(TS,X,X+x0);
%x0test=zeros(28,1);
[F1t_R,F2t_R,F3t_R]=EqNl2Matrix(TS_R,X27,x027.');

%[F1t,F2t,F3t]=EqNl2Matrix(F27,X27,x027.');

EIV_R=eig(F1t_R);
[Tu,Lambda,F2N_R,F3N_R]=NLcoefJordan(F1t_R,F2t_R,F3t_R);
```

C.2.1.1 Doing the Taylor's Expansion Series

```
----function [F1,F2,F3]=EqNl2Matrix(F,X,x0)----

%% Created by Tian TIAN, PhD in EE, ENSAM, Lille, 2017
```

```
 function [F1,F2,F3]=EqNl2Matrix(F,X,x0)
%% This functions is used to do the taylor's expansion of
%% a set of nonlinear functions of multi-variables
%% X=[x1,x2,...,xn] around the Equilibrium Point x0=[x10,x20,...,xn0]
%% i.e
%%     F(x)=F(x0)+F1*(X-x0)+F2*(X-x0)^{2}+F3*(X-x0)^{3}+terms higher than 3rd-order
%% Input: the nonlinear equations--F, the variable vector--X, the equilibrium point-- x0
%% Output: first-order derivative matrix--F1,
%% second derivative matrix-- F2 (0.5*Hessin matrix),
%% third-order derivative matrix-- F3(1/6 H3 matrix),
%% In fact, this function can be extended to calculate the Taylor's series
%% coefficients matrix to order higher than 3, such as n+1th order
%% What is needed is to derivate the matrix n-th order derivative matrix
%% repetitively until to the expected order
%% i.e H(n+1)(p,q,r,...n,:)=jacobian(H(n)(p,q,r,...,n),X)
%TS3=taylor(F,X,x0,'Order',3);

L=length(X);%% Get the length of the matrix

J = jacobian(F,X);%% Jocobian matrix, obtaining the first-order derivative
N1 = double(subs(J,X,x0)); %% Obtain the matrix F1 at the equilibirum point x0
for p=1:L
H2(p,:,:) = hessian(F(p),X);
end

for p=1:L
    for k=1:L
            H3(p,k,:,:)=hessian(J(p,k),X);
    end
end


N2=double(subs(H2,X,x0));

N3=double(subs(H3,X,x0));

F1=N1;
F2=0.5*N2; %% Return the 0.5 Hessian Matrix
F3=1/6*N3; %% Return the 1/6 Tensor Matrix
```

C.2.1.2 Calculating the Nonlinear Matrices in Jordan Form

```
%% Created by Tian TIAN, PhD in EE, ENSAM, Lille, 2017
function [Tu,Lambda,F2,F3]=NLcoefJordan(A,N2,N3)
```

```
%% This function is used to change the nonlinear matrix of
%% the original system dynamics in the jordan coordinate
%% i.e form \dot{x}=Ax+N2(x)+N3(x)
%% to \dot{y}=\lambda y+F2(y)+F3(y)
L=length(A);%%get the dimension of the system of equations.
[Tu,Lambda]=eig(A);
%Tu=Tu/(det(Tu))^(1/27);
invTu=inv(Tu);
%% Calculate F2
F21=zeros(L,L,L);
F2=zeros(L,L,L);
for p=1:L
    %F2(p,:,:)=invTu.'*(Tu.'*squeeze(N2(p,:,:))*Tu);
        F21(p,:,:)=Tu.'*squeeze(N2(p,:,:))*Tu;

end

for p=1:L
        for j=1:L
            for k=1:L
                F2(p,j,k)=invTu(p,:)*F21(:,j,k);
            end
        end
end

%% Calculate F3
F31=zeros(L,L,L,L);
F3=zeros(L,L,L,L);

for j=1:L
    for p=1:L
        for q=1:L
            for r=1:L

                for l=1:L
                        for m=1:L
                            for n=1:L
        F31(j,p,q,r)=F31(j,p,q,r)+N3(j,l,m,n)*Tu(l,p)*Tu(m,q)*Tu(n,r);
                            end
                        end
                end
            end
        end
    end
```

```
end

for j=1:L
      for p=1:L
         for q=1:L
              for r=1:L
                  F3(j,p,q,r)=invTu(j,:)*F31(:,p,q,r);
              end
         end
      end
end
```

C.3   Calculation of Normal Form Coefficients

C.3.1   Calculating the NF Coefficients $h2^{j}_{kl}$ of Method 2-2-1

```
%% Created by Tian TIAN, PhD in EE, ENSAM, Lille, 2017

function h2=classic_coef(EIV,CG)
%File calculating the coefs of the normal from transformation (VF)
N=length(EIV);
%%
%quadratic coefs
Cla=zeros(N,N,N);
 for p=1:N
 for j=1:N
        for k=1:N
        Cla(p,j,k) = CG(p,j,k)/(EIV(j) + EIV(k)-EIV(p));
        end
    end
 end
 disp('end to find the coefficients ')
end


\subsection{Finding the Oscillatory Modes}
\begin{verbatim}
%% Created by Tian TIAN, PhD in EE, ENSAM, Lille, 2017

function ModeNumber=OsciModeNO(EIV)
%% This function is to get the numerical order of oscillatory modes from
%% the eigenvalue vector.
ModeNumber=[];
%% This vector is used to record the numerical order
```

```
%% of the oscillatory modes
m=0;
ModeSize=length(EIV);
for j=1:ModeSize
    if abs(imag(EIV(j)))>1e-3
        m=m+1;
        ModeNumber(m)=j;
    end
end
```

C.3.2   Calculation the NF Coefficients of Method 3-3-3

```
function [h2 h3 C3 F2H2 c3]=NF_coef333R(EIV,F2,F3,ModeNumber)
%File calculating the coefs of the normal from transformation (VF)
L=length(EIV);
M=length(ModeNumber);
MN=ModeNumber;
 N1718=0;

xdot=zeros(L,1);
c3=zeros(L,L);
term_3=zeros(L,1);

F2H2=zeros(L,L,L,L);
F2c=zeros(L,L);
C3=zeros(L,L,L,L);

h2=zeros(L,L,L);
h3=zeros(L,L,L,L);


for p=1:M
    for l=1:M
        for m=1:M
            for n=1:M
h2(MN(p),MN(l),MN(m))= F2(MN(p),MN(l),MN(m))/(EIV(MN(l))+EIV(MN(m))-EIV(MN(p)));
            end
        end
    end
end


for p=1:L
    for l=1:L
            for k=1:L
```

```
                        F2c(p,l)=F2c(p,l)+F2(p,l,k)+F2(p,k,l);
                end
                for m=1:L
                        for n=1:L
                            F2H2(p,l,m,n)=F2c(p,l)*h2(p,m,n);
                            C3(p,l,m,n)=F2H2(p,l,m,n)+F3(p,l,m,n);
                        end
                end
        end
end


for i=1:(M/2)
    for j=1:(M/2)
        if j~=i
                c3(MN(2*i),MN(2*j))=C3(MN(2*i),MN(2*i),MN(2*j),MN(2*j-1))+...
C3(MN(2*i),MN(2*j),MN(2*i),MN(2*j-1))+...
C3(MN(2*i),MN(2*j),MN(2*j-1),MN(2*i))+...
C3(MN(2*i),MN(2*i),MN(2*j-1),MN(2*j))+...
C3(MN(2*i),MN(2*j-1),MN(2*i),MN(2*j))+...
C3(MN(2*i),MN(2*j-1),MN(2*j),MN(2*i));

    c3(MN(2*i-1),MN(2*j))=C3(MN(2*i-1),MN(2*i)-1,MN(2*j),MN(2*j-1))+...
C3(MN(2*i-1),MN(2*j),MN(2*i-1),MN(2*j-1))+...
C3(MN(2*i-1),MN(2*j),MN(2*j-1),MN(2*i-1))+...
C3(MN(2*i-1),MN(2*i-1),MN(2*j-1),MN(2*j))+...
C3(MN(2*i-1),MN(2*j-1),MN(2*i-1),MN(2*j))+...
C3(MN(2*i-1),MN(2*j-1),MN(2*j),MN(2*i-1));
            else
                c3(MN(2*i),MN(2*i))=C3(MN(2*i),MN(2*i),MN(2*i),MN(2*i-1))+...
C3(MN(2*i),MN(2*i),MN(2*i-1),MN(2*i))+...
C3(MN(2*i),MN(2*i-1),MN(2*i),MN(2*i));
                c3(MN(2*i-1),MN(2*i))=C3(MN(2*i-1),MN(2*i-1),MN(2*i),MN(2*i-1))+...
C3(MN(2*i-1),MN(2*i-1),MN(2*i-1),MN(2*i))+...
C3(MN(2*i-1),MN(2*i),MN(2*i-1),MN(2*i-1));
        %xdot(2*i-1)=conj(x(2*i));
            end
    end
end

  for p=1:M
    for l=1:M
        for m=1:M
            for n=1:M
```

```
              h3(MN(p),MN(l),MN(m),MN(n))= C3(MN(p),MN(l),MN(m),MN(n))/...
(EIV(MN(l))+EIV(MN(m))+EIV(MN(n))-EIV(MN(p))));
            end
         end
      end
   end
   for k=1:(M/2)
      for l=1:(M/2)
         for m=1:(M/2)
            for n=1:(M/2)

if l~=k
  h3(MN(2*k),MN(2*k),MN(2*l),MN(2*l-1))=0;h3(MN(2*k),MN(2*l),MN(2*k),MN(2*l-1))=0;
  h3(MN(2*k),MN(2*l),MN(2*l-1),MN(2*k))=0;h3(MN(2*k),MN(2*k),MN(2*l-1),MN(2*l))=0;
  h3(MN(2*k),MN(2*l-1),MN(2*k),MN(2*l))=0;h3(MN(2*k),MN(2*l-1),MN(2*l),MN(2*k))=0;

h3(MN(2*k-1),MN(2*k-1),MN(2*l),MN(2*l-1))=0;
h3(MN(2*k-1),MN(2*l),MN(2*k-1),MN(2*l-1))=0;
         h3(MN(2*k-1),MN(2*l),MN(2*l-1),MN(2*k-1))=0;
h3(MN(2*k-1),MN(2*k-1),MN(2*l-1),MN(2*l))=0;
         h3(MN(2*k-1),MN(2*l-1),MN(2*k-1),MN(2*l))=0;
h3(MN(2*k-1),MN(2*l-1),MN(2*l),MN(2*k-1))=0;

else

h3(MN(2*k),MN(2*k),MN(2*k),MN(2*k-1))=0;
h3(MN(2*k),MN(2*k),MN(2*k-1),MN(2*k))=0;
         h3(MN(2*k),MN(2*k-1),MN(2*k),MN(2*k))=0;
h3(MN(2*k-1),MN(2*k-1),MN(2*k),MN(2*k-1))=0;
         h3(MN(2*k-1),MN(2*k),MN(2*k-1),MN(2*k-1))=0;
h3(MN(2*k-1),MN(2*k-1),MN(2*k-1),MN(2*k))=0;

end
            end
         end
      end
   end

disp('------------------------End to find the coefficients for method 3-3-3----------
end
```

C.3.3   Calculation of Nonlinear Indexes *MI3*

```
--file calculationnonlinearindexes.m--
```

```
%% Created by Tian TIAN, 30/01/2017
%% This file is used to calculate the files for h2, h3 in the proposed 3-3-3 method
%function [h2,h3,C3,F2H2,c3]=NonlinearIndex(EIV,F2,F3,ModeNumber)
%File calculating the coefs of the normal from transformation (VF)
L=length(EIV_R);%%The number of modes
M=length(ModeNumber);%%The number of oscillatory modes
MN=ModeNumber;
M=L/2;

EIV=EIV_R;
w=imag(EIV);
sigma=real(EIV);
F2=F2N_R;
F3=F3N_R;
%quadratic coefs

h3=h3test_R;
 for j=1:L
    for p=1:L
        h3(j,p,p,p)=h3(j,p,p,p);
        for q=(p+1):L
            h3(j,p,q,q)=h3(j,p,q,q)+h3(j,q,p,q)+h3(j,q,q,p);
            for r=(q+1):L
            h3(j,p,q,r)=h3(j,p,q,r)+h3(j,p,r,q)+h3(j,r,p,q)+h3(j,q,p,r)+...
h3(j,q,r,p)+h3(j,r,q,p);
            end
        end
    end
end

for j=1:L
    for p=1:L
        for q=1:L
            for r=1:L
        MI333(j,p,q,r)=abs(h3(j,p,q,r)*z0333(p)*z0333(q)*z0333(r))/abs(z0333(j));
            end
        end
    end
end
MaxMI333=zeros(27,7);
for j=1:L
[Ch3,Ih3] = max(MI333(j,:));
[Ih3_1,Ih3_2,Ih3_3] = ind2sub([27 27 27],Ih3);
MaxMI333(j,:)=[j,Ih3_1,Ih3_2,Ih3_3,EIV_R(j),(EIV_R(Ih3_1)+EIV_R(Ih3_2)+EIV_R(Ih3_3)),...
```

```
MI3(j,Ih3_1,Ih3_2,Ih3_3)];
end

disp('-----------End to calculate the nonlinear indexes for method 3-3-3

-----------------------')
```

C.3.4 Normal Dynamics

Solving the Normal Dynamics, the solution of the normal forms will be obtained, which contains the properties of the system in the normal form coordinates and whose reconstruction by the NF transformation can approximate the original system dynamics.

C.3.4.1 Normal Dynamics for method 3-2-3S and method 3-3-3

```
%% Created by Tian TIAN, PhD in EE, ENSAM, Lille, 2017

function xdot=NF_333(t,x,CE,c3)
L=length(CE);
xdot=zeros(L,1);
term_3=zeros(L,1);
%% Cam=zeros(4,2);
F2H2=zeros(L,L,L,L);
F2c=zeros(L,L);
C3=zeros(L,L,L,L);


for i=1:(L/2)
    for j=1:(L/2)
        term_3(2*i)=term_3(2*i)+c3(2*i,j)*x(2*i)*x(2*j)*x(2*j-1);
        term_3(2*i-1)=term_3(2*i-1)+c3(2*i-1,j)*x(2*i-1)*x(2*j)*x(2*j-1);
        %xdot(2*i-1)=conj(x(2*i));
      end
end
for p=1:L
        xdot(p)=CE(p,p)*x(p)+term_3(p);
end

end
```

C.3.4.2 Normal Dynamics for method 3-3-1 and 2-2-1

```
function xdot=NF_1(t,x,CE)
```

```
L=length(CE);
xdot=zeros(L,1);


for p=1:L
        xdot(p)=CE(p,p)*x(p);
end


end
```

C.3.5   Search for Initial Conditions

C.3.5.1   Newton Raphson's Method [67]

```
function [x, resnorm, F, exitflag, output, jacob] = newtonraphson(fun,x0,options)
% NEWTONRAPHSON Solve set of non-linear equations using Newton-Raphson method.
%
% [X, RESNORM, F, EXITFLAG, OUTPUT, JACOB] = NEWTONRAPHSON(FUN, X0, OPTIONS)
% FUN is a function handle that returns a vector of residuals equations, F,
% and takes a vector, x, as its only argument. When the equations are
% solved by x, then F(x) == zeros(size(F(:), 1)).
%
% Optionally FUN may return the Jacobian, Jij = dFi/dxj, as an additional
% output. The Jacobian must have the same number of rows as F and the same
% number of columns as x. The columns of the Jacobians correspond to d/dxj and
% the rows correspond to dFi/d.
%
%   EG:  J23 = dF2/dx3 is the 2nd row ad 3rd column.
%
% If FUN only returns one output, then J is estimated using a center
% difference approximation,
%
%   Jij = dFi/dxj = (Fi(xj + dx) - Fi(xj - dx))/2/dx.
%
% NOTE: If the Jacobian is not square the system is either over or under
% constrained.
%
% X0 is a vector of initial guesses.
%
% OPTIONS is a structure of solver options created using OPTIMSET.
% EG: options = optimset('TolX', 0.001).
%
% The following options can be set:
% * OPTIONS.TOLFUN is the maximum tolerance of the norm of the residuals.
%   [1e-6]
```

```
% * OPTIONS.TOLX is the minimum tolerance of the relative maximum stepsize.
%   [1e-6]
% * OPTIONS.MAXITER is the maximum number of iterations before giving up.
%   [100]
% * OPTIONS.DISPLAY sets the level of display: {'off', 'iter'}.
%   ['iter']
%
% X is the solution that solves the set of equations within the given tolerance.
% RESNORM is norm(F) and F is F(X). EXITFLAG is an integer that corresponds to
% the output conditions, OUTPUT is a structure containing the number of
% iterations, the final stepsize and exitflag message and JACOB is the J(X).
%
% See also OPTIMSET, OPTIMGET, FMINSEARCH, FZERO, FMINBND, FSOLVE, LSQNONLIN
%
% References:
% * http://en.wikipedia.org/wiki/Newton's_method
% * http://en.wikipedia.org/wiki/Newton's_method_in_optimization
% * 9.7 Globally Convergent Methods for Nonlinear Systems of Equations 383,
%   Numerical Recipes in C, Second Edition (1992),
%   http://www.nrbook.com/a/bookcpdf.php

% Version 0.5
% * allow sparse matrices, replace cond() with condest()
% * check if Jstar has NaN or Inf, return NaN or Inf for cond() and return
%   exitflag: -1, matrix is singular.
% * fix bug: max iteration detection and exitflag reporting typos
% Version 0.4
% * allow lsq curve fitting type problems, IE non-square matrices
% * exit if J is singular or if dx is NaN or Inf
% Version 0.3
% * Display RCOND each step.
% * Replace nargout checking in funwrapper with ducktypin.
% * Remove Ftyp and F scaling b/c F(typx)->0 & F/Ftyp->Inf!
% * User Numerical Recipies minimum Newton step, backtracking line search
%   with alpha = 1e-4, min_lambda = 0.1 and max_lambda = 0.5.
% * Output messages, exitflag and min relative step.
% Version 0.2
% * Remove 'options.FinDiffRelStep' and 'options.TypicalX' since not in MATLAB.
% * Set 'dx = eps^(1/3)' in 'jacobian' function.
% * Remove 'options' argument from 'funwrapper' & 'jacobian' functions
%   since no longer needed.
% * Set typx = x0; typx(x0==0) = 1; % use initial guess as typx, if 0 use 1.
% * Replace 'feval' with 'evalf' since 'feval' is builtin.
```

```
%% initialize
% There are no argument checks!
x0 = x0(:); % needs to be a column vector
% set default options
oldopts = optimset( ...
    'TolX', 1e-8, 'TolFun', 1e-5, 'MaxIter', 2000, 'Display', 'iter');
if nargin<3
    options = oldopts; % use defaults
else
    options = optimset(oldopts, options); % update default with user options
end
FUN = @(x)funwrapper(fun, x); % wrap FUN so it always returns J
%% get options
TOLX = optimget(options, 'TolX'); % relative max step tolerance
TOLFUN = optimget(options, 'TolFun'); % function tolerance
MAXITER = optimget(options, 'MaxIter'); % max number of iterations
DISPLAY = strcmpi('iter', optimget(options, 'Display')); % display iterations
TYPX = max(abs(x0), 1); % x scaling value, remove zeros
ALPHA = 1e-4; % criteria for decrease
MIN_LAMBDA = 0.1; % min lambda
MAX_LAMBDA = 0.5; % max lambda
%% set scaling values
% TODO: let user set weights
weight = ones(numel(FUN(x0)),1);
J0 = weight*(1./TYPX'); % Jacobian scaling matrix
%% set display
if DISPLAY
    fprintf('\n%10s %10s %10s %10s %10s %12s\n', 'Niter', 'resnorm', 'stepnorm', ...
        'lambda', 'rcond', 'convergence')
    for n = 1:67,fprintf('-'),end,fprintf('\n')
    fmtstr = '%10d %10.4g %10.4g %10.4g %10.4g %12.4g\n';
    printout = @(n, r, s, l, rc, c)fprintf(fmtstr, n, r, s, l, rc, c);
end
%% check initial guess
x = x0; % initial guess
[F, J] = FUN(x); % evaluate initial guess
Jstar = J./J0; % scale Jacobian
if any(isnan(Jstar(:))) || any(isinf(Jstar(:)))
    exitflag = -1; % matrix may be singular
else
    exitflag = 1; % normal exit
end
if issparse(Jstar)
    rc = 1/condest(Jstar);
```

```
else
    if any(isnan(Jstar(:)))
        rc = NaN;
    elseif any(isinf(Jstar(:)))
        rc = Inf;
    else
        rc = 1/cond(Jstar); % reciprocal condition
    end
end
resnorm = norm(F); % calculate norm of the residuals
dx = zeros(size(x0));convergence = Inf; % dummy values
%% solver
Niter = 0; % start counter
lambda = 1; % backtracking
if DISPLAY,printout(Niter, resnorm, norm(dx), lambda, rc, convergence);end
while (resnorm>TOLFUN || lambda<1) && exitflag>=0 && Niter<=MAXITER
    if lambda==1
        %% Newton-Raphson solver
        Niter = Niter+1; % increment counter
        dx_star = -Jstar\F; % calculate Newton step
        % NOTE: use isnan(f) || isinf(f) instead of STPMAX
        dx = dx_star.*TYPX; % rescale x
        g = F'*Jstar; % gradient of resnorm
        slope = g*dx_star; % slope of gradient
        fold = F'*F; % objective function
        xold = x; % initial value
        lambda_min = TOLX/max(abs(dx)./max(abs(xold), 1));
    end
    if lambda<lambda_min
        exitflag = 2; % x is too close to XOLD
        break
    elseif any(isnan(dx)) || any(isinf(dx))
        exitflag = -1; % matrix may be singular
        break
    end
    x = xold+dx*lambda; % next guess
    [F, J] = FUN(x); % evaluate next residuals
    Jstar = J./J0; % scale next Jacobian
    f = F'*F; % new objective function
    %% check for convergence
    lambda1 = lambda; % save previous lambda
    if f>fold+ALPHA*lambda*slope
        if lambda==1
            lambda = -slope/2/(f-fold-slope); % calculate lambda
```

```
            else
                A = 1/(lambda1 - lambda2);
                B = [1/lambda1^2,-1/lambda2^2;-lambda2/lambda1^2,lambda1/lambda2^2];
                C = [f-fold-lambda1*slope;f2-fold-lambda2*slope];
                coeff = num2cell(A*B*C);
                [a,b] = coeff{:};
                if a==0
                    lambda = -slope/2/b;
                else
                    discriminant = b^2 - 3*a*slope;
                    if discriminant<0
                        lambda = MAX_LAMBDA*lambda1;
                    elseif b<=0
                        lambda = (-b+sqrt(discriminant))/3/a;
                    else
                        lambda = -slope/(b+sqrt(discriminant));
                    end
                end
                lambda = min(lambda,MAX_LAMBDA*lambda1); % minimum step length
            end
    elseif isnan(f) || isinf(f)
        % limit undefined evaluation or overflow
        lambda = MAX_LAMBDA*lambda1;
    else
        lambda = 1; % fraction of Newton step
    end
    if lambda<1
        lambda2 = lambda1;f2 = f; % save 2nd most previous value
        lambda = max(lambda,MIN_LAMBDA*lambda1); % minimum step length
        continue
    end
    %% display
    resnorm0 = resnorm; % old resnorm
    resnorm = norm(F); % calculate new resnorm
    convergence = log(resnorm0/resnorm); % calculate convergence rate
    stepnorm = norm(dx); % norm of the step
    if any(isnan(Jstar(:))) || any(isinf(Jstar(:)))
        exitflag = -1; % matrix may be singular
        break
    end
    if issparse(Jstar)
        rc = 1/condest(Jstar);
    else
        rc = 1/cond(Jstar); % reciprocal condition
```

```
    end
    if DISPLAY,printout(Niter, resnorm, stepnorm, lambda1, rc, convergence);end
end
%% output
output.iterations = Niter; % final number of iterations
output.stepsize = dx; % final stepsize
output.lambda = lambda; % final lambda
if Niter>=MAXITER
    exitflag = 0;
    output.message = 'Number of iterations exceeded OPTIONS.MAXITER.';
elseif exitflag==2
    output.message = 'May have converged, but X is too close to XOLD.';
elseif exitflag==-1
    output.message = 'Matrix may be singular. Step was NaN or Inf.';
else
    output.message = 'Normal exit.';
end
jacob = J;
end


function [F, J] = funwrapper(fun, x)
% if nargout<2 use finite differences to estimate J
try
    [F, J] = fun(x);
    catch
    F = fun(x);
    J = jacobian(fun, x); % evaluate center diff if no Jacobian
end
F = F(:); % needs to be a column vector
end


function J = jacobian(fun, x)
% estimate J
dx = eps^(1/3); % finite difference delta
nx = numel(x); % degrees of freedom
nf = numel(fun(x)); % number of functions
J = zeros(nf,nx); % matrix of zeros
    for n = 1:nx
    % create a vector of deltas, change delta_n by dx
        delta = zeros(nx, 1); delta(n) = delta(n)+dx;
        dF = fun(x+delta)-fun(x-delta); % delta F
        J(:, n) = dF(:)/dx/2; % derivatives dF/d_n
    end
end
```

C.3.5.2   Mismatch function for Method 3-3-3 and Method 3-3-1

```
%% Created by Tian TIAN, PhD in EE, ENSAM, Lille
function f=fzinit3(z,h2,h3,y0)
%% Reconstruction the system dynamics(SD) from the normal dynamics(ND).
%% From the z coordinate to the x coordinate.
%% dynamics=linear system+second order dynamics+non-resonant 3rd order dynamics+...
%% resonant 3rd order dynamics
%%from z to y: y=z+h2(z)+h3(z)+c3(z); for y to x: x=U*y
%% The input is the solution in the time-series,
%% the time length of data(discretation):tt;
%% N=length(tt);
L=length(y0);
ynl=zeros(L,1);
ynl3=zeros(L,1);
H3=zeros(L,1);

for l=1:L
    for p=1:L
        for q=1:L
            for r=1:L
                    H3(l)=H3(l)+h3(l,p,q,r)*z(p)*z(q)*z(r);
            end
        end
    end
end

for l=1:L
     ynl3(l)=z(l)+z.'*squeeze(h2(l,:,:))*z+H3(l);
end

f=ynl3-y0;
```

C.3.5.3   Mismatch Equation for method 2-2-1 and 3-2-3S

```
%% Created by Tian TIAN, PhD in EE, ENSAM, Lille, 2017
function f=fzinit2(z,h2,y0)
%% Reconstruction the system dynamics(SD) from the normal dynamics(ND).
%% From the z coordinate to the x coordinate.
%% dynamics=linear system+second order dynamics+non-resonant 3rd order dynamics+...
%% resonant 3rd order dynamics
%%from z to y: y=z+h2(z)+h3(z)+c3(z); for y to x: x=U*y
%% The input is the solution in the time-series,
%% the time length of data(discretation):tt;
%% N=length(tt);
```

```
L=length(y0);
ynl=zeros(L,1);
ynl3=zeros(L,1);

for l=1:L
    ynl3(l)=z(l)+z.'*squeeze(h2(l,:,:))*z;
end

f=ynl3-y0;
```

C.4   Simulation files

The simulation files can be found in https://drive.google.com/open?id=0B2onGI-yt3FwdnBZQnJ6SUQ1UHM with:
- "power_PSS3_unbalanced.slx" to assess the performance of the presented methods by numerical step-by-step integration based on the demo "power_PSS".

New England New York 16 Machine 5 Area System

This part of appendix is dedicated to New England New York 16 Machine 5 Area System.

In this part of Appendix, the crucial files are presented to facilitate the reader's comprehension of the PhD dissertation.

All the programs and files associated with interconnected VSCs can be found in:
https://drive.google.com/open?id=0B2onGI-yt3FwdnBZQnJ6SUQ1UHM

D.1 Programs

–Initial File of New England New York 16 Machine 5 Area System –
--Init_16m_NFanalysis.m --

```
% This is the initi alization and modal analysis file for
% the 68-Bus Benchmark system with 16-machines and
% 86-lines. It requires following files to successfully run:
% 1. calc.m
% 2. chq_lim.m
% 3. data16m_benchmark.m
% 4. form_jac.m
% 5. loadflow.m
% 6. y_sparse.m
% 7. Benchmark_IEEE_standard.mdl
% Version:     3.3
% Authors:     Abhinav Kumar Singh, Bikash C. Pal
% Affiliation: Imperial College London
% Date:        December 2013
%% Largely modified by Tian TIAN, PhD in EE, ENSAM, Lille, 2017
%% to obtain the nonlinear matrices in Jordan Form, in preparation
%% for the Normal Form Analysis

clear all;
clc;
MVA_Base=100.0;
f=60.0;
deg_rad = pi/180.0;    % degree to radian,
```

```
rad_deg = 180.0/pi;   % radian to degree.
j=sqrt(-1);


%%%%%%%%%Load Data%%%%%%%%%%%%%%%%%%%%%%%%%%%%%%%%%%%%%%%%
data16m_benchmark;
N_Machine=size(mac_con,1);
N_Bus=size(bus,1);
N_Line=size(line,1);
%%%%%%%%%Loading Data Ends%%%%%%%%%%%%%%%%%%%%%%%%%%%%%%%%

%%%%%%%%%Run Load Flow%%%%%%%%%%%%%%%%%%%%%%%%%%%%%%%%%%%%
tol = 1e-12;iter_max = 50; vmin = 0.5; vmax = 1.5; acc = 1.0;
disply='y';flag = 2;
svolt = bus(:,2); stheta = bus(:,3)*deg_rad;
bus_type = round(bus(:,10));
swing_index=find(bus_type==1);
    [bus_sol,line_sol,line_flow,Y1,y,tps,chrg] = ...
        loadflow(bus,line,tol,iter_max,acc,disply,flag);
clc;
display('Running..');
%%%%%%%%%Load Flow End%%%%%%%%%%%%%%%%%%%%%%%%%%%%%%%%%%%%

%%%%%%%%%Initialize Machine Variables%%%%%%%%%%%%%%%%%%%%
BM=mac_con(:,3)/MVA_Base;%uniform base conversion matrix
xls=mac_con(:,4)./BM;
Ra=mac_con(:,5)./BM;
xd=mac_con(:,6)./BM;
xdd=mac_con(:,7)./BM;
xddd=mac_con(:,8)./BM;
Td0d=mac_con(:,9);
Td0dd=mac_con(:,10);
xq=mac_con(:,11)./BM;
xqd=mac_con(:,12)./BM;
xqdd=mac_con(:,13)./BM;
Tq0d=mac_con(:,14);
Tq0dd=mac_con(:,15);
H=mac_con(:,16).*BM;
D=mac_con(:,17).*BM;
M=2*H;
wB=2*pi*f;
Tc=0.01*ones(N_Machine,1);
Vs=0.0*ones(N_Machine,1);
if xddd~=0 %#ok<BDSCI>
    Zg= Ra + j*xddd;%Zg for sub-transient model
```

```
else
    Zg= Ra + j*xdd;
end
Yg=1./Zg;
%%%%%%%%Machine Variables initialization ends%%%%%%%%

%%%%%%%%%%%%%%AVR Initialization%%%%%%%%%%%%%%%%%%%%
Tr=ones(N_Machine,1);
KA=zeros(N_Machine,1);
Kp=zeros(N_Machine,1);
Ki=zeros(N_Machine,1);
Kd=zeros(N_Machine,1);
Td=ones(N_Machine,1);
Ka=ones(N_Machine,1);
Kad=zeros(N_Machine,1);%for DC4B Efd0 initialization
Ta=ones(N_Machine,1);
Ke=ones(N_Machine,1);
Aex=zeros(N_Machine,1);
Bex=zeros(N_Machine,1);
Te=ones(N_Machine,1);
Kf=zeros(N_Machine,1);
Tf=ones(N_Machine,1);
Efdmin=zeros(N_Machine,1);
Efdmax=zeros(N_Machine,1);
Efdmin_dc=zeros(N_Machine,1);
Efdmax_dc=zeros(N_Machine,1);
len_exc=size(exc_con);
Vref_Manual=ones(N_Machine,1);
for i=1:1:len_exc(1)
    Exc_m_indx=exc_con(i,2);%present machine index
    Vref_Manual(Exc_m_indx)=0;
    if(exc_con(i,3)~=0)
        Tr(Exc_m_indx)=exc_con(i,3);
    end;
    if(exc_con(i,5)~=0)
        Ta(Exc_m_indx)=exc_con(i,5);
    end;
    if(exc_con(i,1)==1)
        Kp(Exc_m_indx)=exc_con(i,16);
        Kd(Exc_m_indx)=exc_con(i,17);
        Ki(Exc_m_indx)=exc_con(i,18);
        Td(Exc_m_indx)=exc_con(i,19);
        Ke(Exc_m_indx)=exc_con(i,8);
        Te(Exc_m_indx)=exc_con(i,9);
```

```
        Kf(Exc_m_indx)=exc_con(i,14);
        Tf(Exc_m_indx)=exc_con(i,15);
        Bex(Exc_m_indx)=log(exc_con(i,11)/exc_con(i,13))/(exc_con(i,10)-exc_con(i,12));
        Aex(Exc_m_indx)=exc_con(i,11)*exp(-Bex(Exc_m_indx)*exc_con(i,10));
        Ka(Exc_m_indx)=exc_con(i,4);
        Kad(Exc_m_indx)=1;
        Efdmin_dc(Exc_m_indx)=exc_con(i,7);
        Efdmax_dc(Exc_m_indx)=exc_con(i,6);
    else
        KA(Exc_m_indx)=exc_con(i,4);
        Efdmin(Exc_m_indx)=exc_con(i,7);
        Efdmax(Exc_m_indx)=exc_con(i,6);
    end;
end;
%%%%%%%%%%%%%%AVR initialization ends%%%%%%%%%%%%%%

%%%%%%%%%%%%%%%%%%%PSS initialization%%%%%%%%%%%%%%%%%
Ks=zeros(N_Machine,1);
Tw=ones(N_Machine,1);
T11=ones(N_Machine,1);
T12=ones(N_Machine,1);
T21=ones(N_Machine,1);
T22=ones(N_Machine,1);
T31=ones(N_Machine,1);
T32=ones(N_Machine,1);
Vs_max=zeros(N_Machine,1);
Vs_min=zeros(N_Machine,1);
len_pss=size(pss_con);
for i=1:1:len_pss(1)
    Pss_m_indx=pss_con(i,2);%present machine index
    Ks(Pss_m_indx)=pss_con(i,3);%pssgain
    Tw(Pss_m_indx)=pss_con(i,4);%washout time constant
    T11(Pss_m_indx)=pss_con(i,5);%first lead time constant
    T12(Pss_m_indx)=pss_con(i,6);%first lag time constant
    T21(Pss_m_indx)=pss_con(i,7);%second lead time constant
    T22(Pss_m_indx)=pss_con(i,8);%second lag time constant
    T31(Pss_m_indx)=pss_con(i,9);%third lead time constant
    T32(Pss_m_indx)=pss_con(i,10);%third lag time constant
    Vs_max(Pss_m_indx)=pss_con(i,11);%maximum output limit
    Vs_min(Pss_m_indx)=pss_con(i,12);%minimum output limit
end
%%%%%%%%%%%%%%%%%%%PSS initialization ends%%%%%%%%%%%%

%%%%%%%%%Initialize Network Variables%%%%%%%%%%%%%%%%%
```

```
Y=full(Y1);%sparse to full matrix
MM=zeros(N_Bus,N_Machine,'double');
%Multiplying matrix to convert Ig into vector of correct length
for i=1:1:N_Machine
    MM(mac_con(i,2),mac_con(i,1))=1;
end
YG=MM*Yg;
YG=diag(YG);
V=bus_sol(:,2);
theta=bus_sol(:,3)*pi/180;
YL=diag((bus(:,6)-j*bus(:,7))./V.^2);%Constant Impedence Load model
Y_Aug=Y+YL+YG;
Z=inv(Y_Aug);%%% It=
Y_Aug_dash=Y_Aug;
%%%%%%%%Network Variables initialization ends%%%%%%%

%%%%%%%%%%%%%%%%%%%Initial Conditions%%%%%%%%%%%%%%%%%%%
Vg=MM'*V;thg=MM'*theta;
P=MM'*bus_sol(:,4);Q=MM'*bus_sol(:,5);
mp=2;
mq=2;
kp=bus_sol(:,6)./V.^mp;
kq=bus_sol(:,7)./V.^mq;
V0=V.*(cos(theta)+ j*sin(theta));
y_dash=y;
from_bus = line(:,1);
to_bus = line(:,2);
MW_s = V0(from_bus).*conj((V0(from_bus) - tps.*V0(to_bus)).*y_dash ...
    + V0(from_bus).*(j*chrg/2))./(tps.*conj(tps)));
P_s = real(MW_s);      % active power sent out by from_bus
Q_s = imag(MW_s);
voltage = Vg.*(cos(thg) + j*sin(thg));
current = conj((P+j*Q)./voltage);
Eq0 = voltage + (Ra+j.*xq).*current;
id0 = -abs(current) .* (sin(angle(Eq0) - angle(current)));
iq0 = abs(current) .* cos(angle(Eq0) - angle(current));
vd0 = -abs(voltage) .* (sin(angle(Eq0) - angle(voltage)));
vq0 = abs(voltage) .* cos(angle(Eq0) - angle(voltage));
Efd0 = abs(Eq0) - (xd-xq).*id0;
Eq_dash0 = Efd0 + (xd - xdd) .* id0;
Ed_dash0 = -(xq-xqd) .* iq0;
Psi1d0=Eq_dash0+(xdd-xls).*id0;
Psi2q0=-Ed_dash0+(xqd-xls).*iq0;
Edc_dash0=(xddd-xqdd).*iq0;
```

```
Te0 = Eq_dash0.*iq0.*(xddd-xls)./(xdd-xls) + Ed_dash0.*id0.*(xqdd-xls)./...
(xqd-xls)+(xddd-xqdd).*id0.*iq0 - Psi2q0.*id0.*(xqd-xqdd)./(xqd-xls) +...
 Psi1d0.*iq0.*(xdd-xddd)./(xdd-xls);

delta0 = angle(Eq0);
IG0 = (Yg.*(vq0+j.*vd0)+ (iq0+j.*id0)).*exp(j.*delta0);%% The sum of currents.
IQ0 = real((iq0+j.*id0).*exp(j.*delta0));
ID0 = imag((iq0+j.*id0).*exp(j.*delta0));
VDQ=MM'*(Y_Aug_dash\(MM*IG0));
VD0=imag(VDQ);
VQ0=real(VDQ);
Vref=Efd0;
V_Ka0=zeros(N_Machine,1);
V_Ki0=zeros(N_Machine,1);
for i=1:1:len_exc(1)
    Exc_m_indx=exc_con(i,2);
    if(exc_con(i,1)==1)
        V_Ka0(Exc_m_indx)=...
Efd0(Exc_m_indx)*(Ke(Exc_m_indx)+Aex(Exc_m_indx)*exp(Efd0(Exc_m_indx)*Bex(Exc_m_indx)));
        V_Ki0(Exc_m_indx)=V_Ka0(Exc_m_indx)/Ka(Exc_m_indx);
        Vref(Exc_m_indx)=Vg(Exc_m_indx);
    else
        Vref(Exc_m_indx)=(Efd0(Exc_m_indx)/KA(Exc_m_indx))+Vg(Exc_m_indx);
    end
end
Tm0=Te0;
Pm0=Tm0;
Sm0=0.0*ones(N_Machine,1);

Gn=16;
delta = sym('delta', [Gn 1]);

%delta=[deltaG;0]+delta_Syn_16*ones(Gn,1);
Sm= sym('Sm', [Gn 1]);
Eq_dash=sym('Eq_dash',[N_Machine 1]);
Ed_dash=sym('Ed_dash',[N_Machine 1]);
Eq_dash=sym('Eq_dash',[N_Machine 1]);
Edc_dash=sym('Edc_dash',[N_Machine 1]);



Psi1d=sym('Psi1d',[N_Machine 1]);
Psi2q=sym('Psi2q',[N_Machine 1]);
```

```
Efd=sym('Efd',[N_Machine 1]);

PSS1=sym('PSS1',[N_Machine 1]);
PSS2=sym('PSS2',[N_Machine 1]);
PSS3=sym('PSS3',[N_Machine 1]);
PSS4=sym('PSS4',[N_Machine 1]);

V_r=sym('V_f',[N_Machine 1]);
V_Ki=sym('V_Ki',[N_Machine 1]);
V_Kd=sym('V_Kd',[N_Machine 1]);
V_a=sym('V_a',[N_Machine 1]);
V_f=sym('V_f',[N_Machine 1]);

Efdd2=sym('Efdd2',[N_Machine 1]);


ig=(Eq_dash.*(xddd-xls)./(xdd-xls)+Psi1d.*(xdd-xddd)./(xdd-xls)+...
1i*(Ed_dash.*(xqdd-xls)./(xqd-xls)-...
Psi2q.*(xqd-xqdd)./(xqd-xls)+Edc_dash)).*Yg;

Vdq=MM'*Z*(MM*(ig.*exp(j*delta))).*exp(-j*delta);

Vq=real(Vdq);

Vd=imag(Vdq);

idq=(Eq_dash.*(xddd-xls)./(xdd-xls)+Psi1d.*(xdd-xddd)./(xdd-xls)+...
1i*(Ed_dash.*(xqdd-xls)./(xqd-xls)-Psi2q.*(xqd-xqdd)./(xqd-xls)+Edc_dash)-(Vq+1i*Vd)).*

iq=real(idq);
id=imag(idq);
TeG=Eq_dash.*iq.*(xddd-xls)./(xdd-xls)+Ed_dash.*id.*(xqdd-xls)./(xqd-xls)+...
(xddd-xqdd).*id.*iq-Psi2q.*id.*(xqd-xqdd)./(xqd-xls)+Psi1d.*iq.*(xdd-xddd)./(xdd-xls);


%%% Differential Equations of the Electromechanical Part
    ddelta=wB*Sm;
    dSm=1./(2*H).*(Tm0-TeG-D.*Sm);

dEd_dash=1./Tq0d.*(-Ed_dash+(xq-xqd).*(-iq+(xqd-xqdd)./(xqd-xls).^2.*((xqd-xls).*id-...
Ed_dash-Psi2q)));

dEdc_dash=1./Tc.*(iq.*(xddd-xqdd)-Edc_dash);
dEq_dash=1./Td0d.*(Efd-Eq_dash+(xd-xdd).*(id+(xdd-xddd)./(xdd-xls).^2....
```

```
*(Psi1d-(xdd-xls).*id-Eq_dash)));
    dPsi1d=1./Td0dd.*(Eq_dash+(xdd-xls).*id-Psi1d);
    dPsi2q=1./Tq0dd.*(-Ed_dash+(xqd-xls).*iq-Psi2q);


%ddelta_Gn(Gn)=[];

%% Differential Equations of the PSS

KPSS1=(T11-T12)./T12; KPSS3=(T21-T22)./T22; KPSS6=(T31-T32)./T32;

PSS_in1=Ks.*Sm-PSS1;
PSS_in2=PSS_in1+(PSS_in1-PSS2).*KPSS1;
%PSS_in3=PSS_in2+(PSS_in2-PSS3).*KPSS3;
PSS_in3=PSS_in2+(PSS_in2-PSS3).*KPSS3;
Vs=PSS_in3+(PSS_in3-PSS4).*KPSS6;

N_PSS=[]; %% This vector records the numer of machines on which the PSSs are equipped.
for i=1:1:len_pss(1)
    Pss_m_indx=pss_con(i,2);%present machine index
    dPSS1(Pss_m_indx)=1/Tw(Pss_m_indx)*(Sm(Pss_m_indx)*Ks(Pss_m_indx)-PSS1(Pss_m_indx));
    dPSS2(Pss_m_indx)=1/T12(Pss_m_indx)*(PSS_in1(Pss_m_indx)-PSS2(Pss_m_indx));
    dPSS3(Pss_m_indx)=1/T22(Pss_m_indx)*(PSS_in2(Pss_m_indx)-PSS3(Pss_m_indx));
   %dPSS3(i)=1/T22(i)*(((Ks*Sm-PSS1)*T11./T12-PSS2(i))*(T11(i)-T12(i))/T12(i)-PSS3(i));
    dPSS4(Pss_m_indx)=1/T32(Pss_m_indx)*(PSS_in3(Pss_m_indx)-PSS4(Pss_m_indx));
    N_PSS=[N_PSS i];
end

Vt=sqrt(Vd.^2+Vq.^2);
%% Differential Equations of the Exciter.
N_ST1A=[];%% This vector record the number of machines equipped with exciter type ST1A
N_DC4B=[];%% Tihs vector record the number of machines equipped with exciter type DC4B
for i=1:1:len_exc(1)
    Exc_m_indx=exc_con(i,2);
    if(exc_con(i,1)==1)%% The differential equations for exciter type DC4B

    DC4B_in1(Exc_m_indx)=Vs(Exc_m_indx)+Vref(Exc_m_indx)-V_r(Exc_m_indx)-...
Kf(Exc_m_indx)/Tf(Exc_m_indx)*(Efd(Exc_m_indx)-V_f(Exc_m_indx));

DC4B_in2(Exc_m_indx)=DC4B_in1(Exc_m_indx)*Kp(Exc_m_indx)+V_Ki(Exc_m_indx)+...
DC4B_in1(Exc_m_indx)*Kd(Exc_m_indx)/Td(Exc_m_indx)-V_Kd(Exc_m_indx);

dEfd(Exc_m_indx)=1/Te(Exc_m_indx)*(V_a(Exc_m_indx)-(Ke(Exc_m_indx)*Efd(Exc_m_indx)+...
Efd(Exc_m_indx)*Aex(Exc_m_indx)*exp(Bex(Exc_m_indx)*Efd(Exc_m_indx))));
```

```
dV_r(Exc_m_indx)=1/Tr(Exc_m_indx)*(Vt(Exc_m_indx)-V_r(Exc_m_indx));

dV_Ki(Exc_m_indx)=DC4B_in1(Exc_m_indx)*Ki(Exc_m_indx );

dV_Kd(Exc_m_indx)=(DC4B_in1(Exc_m_indx)*Kd(Exc_m_indx)/Td(Exc_m_indx)-...
V_Kd(Exc_m_indx))*1/Td(Exc_m_indx);

dV_a(Exc_m_indx)=(DC4B_in2(Exc_m_indx)*Ka(Exc_m_indx)-...
V_a(Exc_m_indx))*1/Ta(Exc_m_indx);

dV_f(Exc_m_indx)=(Efd(Exc_m_indx)-V_f(Exc_m_indx))*1/Tf(Exc_m_indx);
   N_DC4B=[N_DC4B Exc_m_indx];
    else
    dEfdd2(Exc_m_indx)=(Vt(Exc_m_indx)-Efdd2(Exc_m_indx))*1/Tr(Exc_m_indx);
    Efd(Exc_m_indx)=KA(Exc_m_indx)*(Vs(Exc_m_indx)+Vref(Exc_m_indx)-Efdd2(Exc_m_indx));
    N_ST1A=[N_ST1A Exc_m_indx];
     end
end
   V_r0=Vg; V_f0=Efd0.*Kad;   V_Kd0=zeros(N_Machine,1);
 Efdd20=Vg;PSS10=zeros(N_Machine,1); PSS20=zeros(N_Machine,1);
PSS30=zeros(N_Machine,1); PSS40=zeros(N_Machine,1);
%Cla2=classic_coef(EIV,CG,CH);
F=[ddelta;dSm;dEd_dash;dEdc_dash;dEq_dash;dPsi1d;dPsi2q;dEfd(N_DC4B).';
dV_r(N_DC4B).';dV_Ki(N_DC4B).';dV_Kd(N_DC4B).';dV_a(N_DC4B).';dV_f(N_DC4B).';
dEfdd2(N_ST1A).';dPSS1(N_PSS).';dPSS2(N_PSS).';dPSS3(N_PSS).';dPSS4(N_PSS).'];

X=[delta;Sm;Ed_dash;Edc_dash;Eq_dash;Psi1d;Psi2q;Efd(N_DC4B);V_r(N_DC4B);
V_Ki(N_DC4B);V_Kd(N_DC4B);V_a(N_DC4B);V_f(N_DC4B);Efdd2(N_ST1A);PSS1(N_PSS);
PSS2(N_PSS);PSS3(N_PSS);PSS4(N_PSS)];

x0=[delta0;Sm0;Ed_dash0;Edc_dash0;Eq_dash0;Psi1d0;Psi2q0;Efd0(N_DC4B);
V_r0(N_DC4B);V_Ki0(N_DC4B);V_Kd0(N_DC4B);V_Ka0(N_DC4B);V_f0(N_DC4B);
Efdd20(N_ST1A);PSS10(N_PSS);PSS20(N_PSS);PSS30(N_PSS);PSS40(N_PSS)];


EIV=eig(F1t);
[Tu,Lambda,F2N,F3N]=NLcoefJordan(F1t,F2t,F3t);

damping_ratioP=-real(EIV)./abs(EIV);

N_State=size(EIV,1);
for i=1:1:N_State
    if(abs(EIV(i))<=1e-10)
```

```
      damping_ratioP(i)=1;
    end
end
[DrP,IdxP]=sort(damping_ratioP*100);%% value calculated by the m-file
--clac.m--

function [delP,delQ,P,Q,conv_flag] = ...
                calc(V,ang,Y,Pg,Qg,Pl,Ql,sw_bno,g_bno,tol)
% Syntax:   [delP,delQ,P,Q,conv_flag] =
%                calc(V,ang,Y,Pg,Qg,Pl,Ql,sw_bno,g_bno,tol)
%
% Purpose: calculates power mismatch and checks convergence
%          also determines the values of P and Q based on the
%          supplied values of voltage magnitude and angle
% Version: 2.0 eliminates do loop
% Input:    nbus       - total number of buses
%           bus_type   - load_bus(3), gen_bus(2), swing_bus(1)
%           V          - magnitude of bus voltage
%           ang        - angle(rad) of bus voltage
%           Y          - admittance matrix
%           Pg         - real power of generation
%           Qg         - reactive power  of generation
%           Pl         - real power of load
%           Ql         - reactive power of load
%  sw_bno - a vector having zeros at all  swing_bus locations ones otherwise
%  g_bno  - a vector having zeros at all  generator bus locations ones otherwise
%           tol        - a tolerance of computational error
%
% Output:   delP       - real power mismatch
%           delQ       - reactive power mismatch
%           P          - calculated real power
%           Q          - calculated reactive power
%           conv_flag  - 0, converged
%                        1, not yet converged
%
% See also:
%
% Calls:
%
% Called By:   loadflow

% (c) Copyright 1991 Joe H. Chow - All Rights Reserved
%
% History (in reverse chronological order)
```

```
% Version:    2.0
% Author:     Graham Rogers
% Date:       July 1994
%
% Version:    1.0
% Author:     Kwok W. Cheung, Joe H. Chow
% Date:       March 1991
%
% *********************************************************
jay = sqrt(-1);
swing_bus = 1;
gen_bus = 2;
load_bus = 3;
% voltage in rectangular coordinate
V_rect = V.*exp(jay*ang);
% bus current injection
cur_inj = Y*V_rect;
% power output based on voltages
S = V_rect.*conj(cur_inj);
P = real(S); Q = imag(S);
delP = Pg - Pl - P;
delQ = Qg - Ql - Q;
% zero out mismatches on swing bus and generation bus
delP=delP.*sw_bno;
delQ=delQ.*sw_bno;
delQ=delQ.*g_bno;
%  total mismatch
[pmis,ip]=max(abs(delP));
[qmis,iq]=max(abs(delQ));
mism = pmis+qmis;
if mism > tol,
    conv_flag = 1;
  else
    conv_flag = 0;
end
return
--chq_lim.m--

function f = chq_lim(qg_max,qg_min)
%Syntax:
%       f = chq_lim(qg_max,qg_min)
% function for detecting generator vars outside limit
% sets Qg to zero if limit exceded, sets Ql to negative of limit
% sets bus_type to 3, and recalculates ang_red and volt_red
```

```
% changes  generator bus_type to type 3
% recalculates the generator index
% inputs: qg_max and qg_min are the last two clumns of the bus matrix
% outputs:f is set to zero if no limit reached, or to 1 if a limit is reached
% Version:  1.1
% Author: Graham Rogers
% Date:   May 1997
% Purpose: Addition of var limit index
% Version:  1.0
% Author:   Graham Rogers
% Date:     October 1996
%
% (c) copyright Joe Chow 1996
global Qg bus_type g_bno PQV_no PQ_no ang_red volt_red
global Ql
global gen_chg_idx
%         gen_chg_idx indicates those generators changed to PQ buses
%         gen_cgq_idx = ones(n of bus,1) if no gen at vars limits
%                     = 0 at the corresponding bus if generator at var limit

f = 0;
lim_flag = 0;% indicates whether limit has been reached
gen_idx = find(bus_type ==2);
qg_max_idx = find(Qg(gen_idx)>qg_max(gen_idx));
qg_min_idx = find(Qg(gen_idx)<qg_min(gen_idx));
if ~isempty(qg_max_idx)
  %some q excedes maximum
  %set Qg to zero
  Qg(gen_idx(qg_max_idx)) = zeros(length(qg_max_idx),1);
  % modify Ql
  Ql(gen_idx(qg_max_idx)) = Ql(gen_idx(qg_max_idx))...
                                - qg_max(gen_idx(qg_max_idx));
  % modify bus_type to PQ bus
  bus_type(gen_idx(qg_max_idx)) = 3*ones(length(qg_max_idx),1);
  gen_chg_idx(gen_idx(qg_max_idx)) = zeros(length(qg_max_idx),1);
  lim_flag = 1;
end
if ~isempty(qg_min_idx)
  %some q less than minimum
  %set Qg to zero
  Qg(gen_idx(qg_min_idx)) = zeros(length(qg_min_idx),1);
  % modify Ql
  Ql(gen_idx(qg_min_idx)) = Ql(gen_idx(qg_min_idx))...
                                - qg_min(gen_idx(qg_min_idx));
```

```
  % modify bus_type to PQ bus
  bus_type(gen_idx(qg_min_idx)) = 3*ones(length(qg_min_idx),1);
  gen_chg_idx(gen_idx(qg_min_idx)) = zeros(length(qg_min_idx),1);
  lim_flag = 1;
end
if lim_flag == 1
  %recalculate g_bno
  nbus = length(bus_type);
  g_bno = ones(nbus,1);
  bus_zeros=zeros(nbus,1);
  bus_index=(1:1:nbus)';
  PQV_no=find(bus_type >=2);
  PQ_no=find(bus_type==3);
  gen_index=find(bus_type==2);
  g_bno(gen_index)=bus_zeros(gen_index);
  % construct sparse angle reduction matrix
  il = length(PQV_no);
  ii = (1:1:il)';
  ang_red = sparse(ii,PQV_no,ones(il,1),il,nbus);
  % construct sparse voltage reduction matrix
  il = length(PQ_no);
  ii = (1:1:il)';
  volt_red = sparse(ii,PQ_no,ones(il,1),il,nbus);
end
f = lim_flag;
return
--Benchmark_IEEE_standard.m--
% This is the data file for the 68-Bus Benchmark system with 16-machines
% and 86-lines. The data is partially taken from the book "Robust Control
% in Power Systems" by B. Pal and B. Chaudhuri, with some of the parameters
% modified to account for a more realistic model.
% Version:     3.3
% Authors:     Abhinav Kumar Singh, Bikash C. Pal
% Affiliation: Imperial College London
% Date:        December 2013

%********************** BUS DATA STARTS ********************************
% bus data format
% bus: number, voltage(pu), angle(degree), p_gen(pu), q_gen(pu),
%      p_load(pu), q_load(pu),G-shunt (p.u), B shunt (p.u); bus_type
%      bus_type - 1, swing bus
%               - 2, generator bus (PV bus)
%               - 3, load bus (PQ bus)
system_base_mva = 100.0;
```

```
bus = [...
    01 1.045    0.00     2.50   0.00    0.00    0.00      0.00 0.00   2  999   -999;
    02 0.98     0.00     5.45   0.00    0.00    0.00      0.00 0.00   2  999   -999;
    03 0.983    0.00     6.50   0.00    0.00    0.00      0.00 0.00   2  999   -999;
    04 0.997    0.00     6.32   0.00    0.00    0.00      0.00 0.00   2  999   -999;
    05 1.011    0.00     5.05   0.00    0.00    0.00      0.00 0.00   2  999   -999;
    06 1.050    0.00     7.00   0.00    0.00    0.00      0.00 0.00   2  999   -999;
    07 1.063    0.00     5.60   0.00    0.00    0.00      0.00 0.00   2  999   -999;
    08 1.03     0.00     5.40   0.00    0.00    0.00      0.00 0.00   2  999   -999;
    09 1.025    0.00     8.00   0.00    0.00    0.00      0.00 0.00   2  999   -999;
    10 1.010    0.00     5.00   0.00    0.00    0.00      0.00 0.00   2  999   -999;
    11 1.000    0.00    10.000  0.00    0.00    0.00      0.00 0.00   2  999   -999;
    12 1.0156   0.00    13.50   0.00    0.00    0.00      0.00 0.00   2  999   -999;
    13 1.011    0.00    35.91   0.00    0.00    0.00      0.00 0.00   2  999   -999;
    14 1.00     0.00    17.85   0.00    0.00    0.00      0.00 0.00   2  999   -999;
    15 1.000    0.00    10.00   0.00    0.00    0.00      0.00 0.00   2  999   -999;
    16 1.000    0.00    40.00   0.00    0.00    0.00      0.00 0.00   1   0    0;
    17 1.00     0.00     0.00   0.00   60.00    3.00      0.00 0.00   3   0    0;
    18 1.00     0.00     0.00   0.00   24.70    1.23      0.00 0.00   3   0    0;
    19 1.00     0.00     0.00   0.00    0.00    0.00      0.00 0.00   3   0    0;
    20 1.00     0.00     0.00   0.00    6.800   1.03      0.00 0.00   3   0    0;
    21 1.00     0.00     0.00   0.00    2.740   1.15      0.00 0.00   3   0    0;
    22 1.00     0.00     0.00   0.00    0.00    0.00      0.00 0.00   3   0    0;
    23 1.00     0.00     0.00   0.00    2.480   0.85      0.00 0.00   3   0    0;
    24 1.00     0.00     0.00   0.00    3.09   -0.92      0.00 0.00   3   0    0;
    25 1.00     0.00     0.00   0.00    2.24    0.47      0.00 0.00   3   0    0;
    26 1.00     0.00     0.00   0.00    1.39    0.17      0.00 0.00   3   0    0;
    27 1.00     0.00     0.00   0.00    2.810   0.76      0.00 0.00   3   0    0;
    28 1.00     0.00     0.00   0.00    2.060   0.28      0.00 0.00   3   0    0;
    29 1.00     0.00     0.00   0.00    2.840   0.27      0.00 0.00   3   0    0;
    30 1.00     0.00     0.00   0.00    0.00    0.00      0.00 0.00   3   0    0;
    31 1.00     0.00     0.00   0.00    0.00    0.00      0.00 0.00   3   0    0;
    32 1.00     0.00     0.00   0.00    0.00    0.00      0.00 0.00   3   0    0;
    33 1.00     0.00     0.00   0.00    1.12    0.00      0.00 0.00   3   0    0;
    34 1.00     0.00     0.00   0.00    0.00    0.00      0.00 0.00   3   0    0;
    35 1.00     0.00     0.00   0.00    0.00    0.00      0.00 0.00   3   0    0;
    36 1.00     0.00     0.00   0.00    1.02   -0.1946    0.00 0.00   3   0    0;
    37 1.00     0.00     0.00   0.00    0.00    0.00      0.00 0.00   3   0    0;
    38 1.00     0.00     0.00   0.00    0.00    0.00      0.00 0.00   3   0    0;
    39 1.00     0.00     0.00   0.00    2.67    0.126     0.00 0.00   3   0    0;
    40 1.00     0.00     0.00   0.00    0.6563  0.2353    0.00 0.00   3   0    0;
    41 1.00     0.00     0.00   0.00   10.00    2.50      0.00 0.00   3   0    0;
    42 1.00     0.00     0.00   0.00   11.50    2.50      0.00 0.00   3   0    0;
    43 1.00     0.00     0.00   0.00    0.00    0.00      0.00 0.00   3   0    0;
```

```
      44 1.00      0.00     0.00     0.00     2.6755 0.0484   0.00 0.00   3   0   0;
      45 1.00      0.00     0.00     0.00     2.08    0.21     0.00 0.00   3   0   0;
      46 1.00      0.00     0.00     0.00     1.507   0.285    0.00 0.00   3   0   0;
      47 1.00      0.00     0.00     0.00     2.0312 0.3259    0.00 0.00   3   0   0;
      48 1.00      0.00     0.00     0.00     2.4120 0.022     0.00 0.00   3   0   0;
      49 1.00      0.00     0.00     0.00     1.6400 0.29      0.00 0.00   3   0   0;
      50 1.00      0.00     0.00     0.00     1.00    -1.47    0.00 0.00   3   0   0;
      51 1.00      0.00     0.00     0.00     3.37    -1.22    0.00 0.00   3   0   0;
      52 1.00      0.00     0.00     0.00     1.58    0.30     0.00 0.00   3   0   0;
      53 1.00      0.00     0.00     0.00     2.527   1.1856   0.00 0.00   3   0   0;
      54 1.00      0.00     0.00     0.00     0.00    0.00     0.00 0.00   3   0   0;
      55 1.00      0.00     0.00     0.00     3.22    0.02     0.00 0.00   3   0   0;
      56 1.00      0.00     0.00     0.00     2.00    0.736    0.00 0.00   3   0   0;
      57 1.00      0.00     0.00     0.00     0.00    0.00     0.00 0.00   3   0   0;
      58 1.00      0.00     0.00     0.00     0.00    0.00     0.00 0.00   3   0   0;
      59 1.00      0.00     0.00     0.00     2.34    0.84     0.00 0.00   3   0   0;
      60 1.00      0.00     0.00     0.00     2.088   0.708    0.00 0.00   3   0   0;
     61 1.00     0.00      0.00      0.00     1.04    1.25     0.00 0.00   3   0   0;
     62 1.00     0.00      0.00      0.00     0.00    0.00     0.00 0.00   3   0   0;
      63 1.00      0.00     0.00     0.00     0.00    0.00     0.00 0.00   3   0   0;
      64 1.00      0.00     0.00     0.00     0.09    0.88     0.00 0.00   3   0   0;
      65 1.00      0.00     0.00     0.00     0.00    0.00     0.00 0.00   3   0   0;
      66 1.00      0.00     0.00     0.00     0.00    0.00     0.00 0.00   3   0   0;
      67 1.00      0.00     0.00     0.00     3.200   1.5300   0.00 0.00   3   0   0;
      68 1.00      0.00     0.00     0.00     3.290   0.32     0.00 0.00   3   0   0
      ];
%********************** BUS DATA ENDS ********************************

%********************** LINE DATA STARTS ****************************
line =[...
      01   54        0    0.0181        0    1.0250        0;
      02   58        0    0.0250        0    1.0700        0;
      03   62        0    0.0200        0    1.0700        0;
      04   19    0.0007   0.0142        0    1.0700        0;
      05   20    0.0009   0.0180        0    1.0090        0;
      06   22        0    0.0143        0    1.0250        0;
      07   23    0.0005   0.0272        0         0        0;
      08   25    0.0006   0.0232        0    1.0250        0;
      09   29    0.0008   0.0156        0    1.0250        0;
      10   31        0    0.0260        0    1.0400        0;
      11   32        0    0.0130        0    1.0400        0;
      12   36        0    0.0075        0    1.0400        0;
      13   17        0    0.0033        0    1.0400        0;
      14   41        0    0.0015        0    1.0000        0;
```

15	42	0	0.0015	0	1.0000	0;
16	18	0	0.0030	0	1.0000	0;
17	36	0.0005	0.0045	0.3200	0	0;
18	49	0.0076	0.1141	1.1600	0	0;
18	50	0.0012	0.0288	2.0600	0	0;
19	68	0.0016	0.0195	0.3040	0	0;
20	19	0.0007	0.0138	0	1.0600	0;
21	68	0.0008	0.0135	0.2548	0	0;
22	21	0.0008	0.0140	0.2565	0	0;
23	22	0.0006	0.0096	0.1846	0	0;
24	23	0.0022	0.0350	0.3610	0	0;
24	68	0.0003	0.0059	0.0680	0	0;
25	54	0.0070	0.0086	0.1460	0	0;
26	25	0.0032	0.0323	0.5310	0	0;
27	37	0.0013	0.0173	0.3216	0	0;
27	26	0.0014	0.0147	0.2396	0	0;
28	26	0.0043	0.0474	0.7802	0	0;
29	26	0.0057	0.0625	1.0290	0	0;
29	28	0.0014	0.0151	0.2490	0	0;
30	53	0.0008	0.0074	0.4800	0	0;
30	61	0.00095	0.00915	0.5800	0	0;
31	30	0.0013	0.0187	0.3330	0	0;
31	53	0.0016	0.0163	0.2500	0	0;
32	30	0.0024	0.0288	0.4880	0	0;
33	32	0.0008	0.0099	0.1680	0	0;
34	33	0.0011	0.0157	0.2020	0	0;
34	35	0.0001	0.0074	0	0.9460	0;
36	34	0.0033	0.0111	1.4500	0	0;
36	61	0.0011	0.0098	0.6800	0	0;
37	68	0.0007	0.0089	0.1342	0	0;
38	31	0.0011	0.0147	0.2470	0	0;
38	33	0.0036	0.0444	0.6930	0	0;
40	41	0.0060	0.0840	3.1500	0	0;
40	48	0.0020	0.0220	1.2800	0	0;
41	42	0.0040	0.0600	2.2500	0	0;
42	18	0.0040	0.0600	2.2500	0	0;
43	17	0.0005	0.0276	0	0	0;
44	39	0	0.0411	0	0	0;
44	43	0.0001	0.0011	0	0	0;
45	35	0.0007	0.0175	1.3900	0	0;
45	39	0	0.0839	0	0	0;
45	44	0.0025	0.0730	0	0	0;
46	38	0.0022	0.0284	0.4300	0	0;

```
47   53   0.0013    0.0188   1.3100          0        0;
48   47   0.00125   0.0134   0.8000          0        0;
49   46   0.0018    0.0274   0.2700          0        0;

51   45   0.0004    0.0105   0.7200          0        0;
51   50   0.0009    0.0221   1.6200          0        0;
52   37   0.0007    0.0082   0.1319          0        0;
52   55   0.0011    0.0133   0.2138          0        0;
54   53   0.0035    0.0411   0.6987          0        0;
55   54   0.0013    0.0151   0.2572          0        0;
56   55   0.0013    0.0213   0.2214          0        0;
57   56   0.0008    0.0128   0.1342          0        0;
58   57   0.0002    0.0026   0.0434          0        0;
59   58   0.0006    0.0092   0.1130          0        0;
60   57   0.0008    0.0112   0.1476          0        0;
60   59   0.0004    0.0046   0.0780          0        0;
61   60   0.0023    0.0363   0.3804          0        0;
63   58   0.0007    0.0082   0.1389          0        0;
63   62   0.0004    0.0043   0.0729          0        0;
63   64   0.0016    0.0435        0     1.0600        0;
65   62   0.0004    0.0043   0.0729          0        0;
65   64   0.0016    0.0435        0     1.0600        0;
66   56   0.0008    0.0129   0.1382          0        0;
66   65   0.0009    0.0101   0.1723          0        0;
67   66   0.0018    0.0217   0.3660          0        0;
68   67   0.0009    0.0094   0.1710          0        0;
27   53   0.0320    0.3200   0.4100          0        0;

     ];
%********************* LINE DATA ENDS ****************************

% ********************* MACHINE DATA STARTS **************************
% Machine data format
%        1. machine number,
%        2. bus number,
%        3. base mva,
%        4. leakage reactance x_l(pu),
%        5. resistance r_a(pu),
%        6. d-axis sychronous reactance x_d(pu),
%        7. d-axis transient reactance x'_d(pu),
%        8. d-axis subtransient reactance x"_d(pu),
%        9. d-axis open-circuit time constant T'_do(sec),
%       10. d-axis open-circuit subtransient time constant
%               T"_do(sec),
```

```
%       11. q-axis sychronous reactance x_q(pu),
%       12. q-axis transient reactance x'_q(pu),
%       13. q-axis subtransient reactance x"_q(pu),
%       14. q-axis open-circuit time constant T'_qo(sec),
%       15. q-axis open circuit subtransient time constant
%              T"_qo(sec),
%       16. inertia constant H(sec),
%       17. damping coefficient d_o(pu),
%       18. dampling coefficient d_1(pu),
%       19. bus number
%       20. saturation factor S(1.0)
%       21. saturation factor S(1.2)
% note: all the following machines use subtransient reactance model
mac_con = [

01 01  100 0.0125 0.0  0.1    0.031   0.025    10.2  0.05 0.069 0.0416667   0.025   1.5
    0.035 42.   0  0   01    0 0;

02 02  100 0.035  0.0  0.295  0.0697  0.05     6.56  0.05 0.282 0.0933333   0.05    1.5
    0.035 30.2 0  0   02    0 0;

03 03  100 0.0304 0.0  0.2495 0.0531  0.045    5.7   0.05 0.237 0.0714286   0.045   1.5
    0.035 35.8 0  0   03    0 0

04 04  100 0.0295 0.0  0.262  0.0436  0.035    5.69  0.05 0.258 0.0585714   0.035   1.5
    0.035 28.6 0  0   04    0 0;

05 05  100 0.027  0.0  0.33   0.066   0.05     5.4   0.05 0.31  0.0883333   0.05    0.44
 0.035 26.   0  0   05    0 0;

06 06  100 0.0224 0.0  0.254  0.05    0.04     7.3   0.05 0.241 0.0675000   0.04    0.4
 0.035 34.8 0  0   06    0 0;

07 07  100 0.0322 0.0  0.295  0.049   0.04     5.66  0.05 0.292 0.0666667   0.04    1.5
    0.035 26.4 0  0   07    0 0;

08 08  100 0.028  0.0  0.29   0.057   0.045    6.7   0.05 0.280 0.0766667   0.045   0.41
    0.035 24.3 0  0   08    0 0;

09 09  100 0.0298 0.0  0.2106 0.057   0.045    4.79  0.05 0.205 0.0766667   0.045   1.96
    0.035 34.5 0  0   09    0 0;

10 10  100 0.0199 0.0  0.169  0.0457  0.04     9.37  0.05 0.115 0.0615385   0.04    1.
    0.035 31.0 0  0   10    0 0;
```

```
11 11   100 0.0103 0.0   0.128   0.018    0.012    4.1    0.05 0.123  0.0241176    0.012    1


12 12   100 0.022  0.0   0.101   0.031    0.025    7.4    0.05 0.095  0.0420000    0.025    1


13 13   200 0.0030 0.0   0.0296  0.0055   0.004    5.9    0.05 0.0286 0.0074000    0.004    1


14 14   100 0.0017 0.0   0.018   0.00285  0.0023   4.1    0.05 0.0173 0.0037931    0.0023   1


15 15   100 0.0017 0.0   0.018   0.00285  0.0023   4.1    0.05 0.0173 0.0037931    0.0023   1


 16 16   200 0.0041 0.0   0.0356  0.0071   0.0055   7.8    0.05 0.0334 0.0095000    0.0055   1
                            ] ;
% *********************** MACHINE DATA ENDS ***************************

% *********************** EXCITER DATA STARTS ***********************
% Description of Exciter data starts
% exciter data DC4B,ST1A model
%      1 - exciter type (1 for DC4B, 0 for ST1A)
%      2 - machine number
%      3 - input filter time constant T_R
%      4 - voltage regulator gain K_A
%      5 - voltage regulator time constant T_A
%      6 - maximum voltage regulator output V_Rmax
%      7 - minimum voltage regulator output V_Rmin
%      8 - exciter constant K_E
%      9 - exciter time constant T_E
%     10 - E_1
%     11 - S(E_1)
%     12 - E_2
%     13 - S(E_2)
%     14 - stabilizer gain K_F
%     15 - stabilizer time constant T_F
%     16 - K_P
%     17 - K_I
%     18 - K_D
%     19 - T_D
%% 1 2 3     4     5    6    7     8      9     10     11     12     13    14      15  16
exc_con = [...
1 1  0.01 1.   0.02 10.  -10.  1.0     .785 3.9267 0.070 5.2356 0.910 0.030 1.0 200 50 5
.01;
1 2  0.01 1.   0.02 10.  -10.  1.0     .785 3.9267 0.070 5.2356 0.910 0.030 1.0 200 50 5
.01;
```

```
1 3  0.01 1.    0.02 10.   -10.   1.0      .785 3.9267 0.070 5.2356 0.910 0.030 1.0 200 50 50
.01;
1 4  0.01 1.    0.02 10.   -10.   1.0      .785 3.9267 0.070 5.2356 0.910 0.030 1.0 200 50 50
.01;
1 5  0.01 1.    0.02 10.   -10.   1.0      .785 3.9267 0.070 5.2356 0.910 0.030 1.0 200 50 50
.01;
1 6  0.01 1.    0.02 10.   -10.   1.0      .785 3.9267 0.070 5.2356 0.910 0.030 1.0 200 50 50
.01;
1 7  0.01 1.    0.02 10.   -10.   1.0      .785 3.9267 0.070 5.2356 0.910 0.030 1.0 200 50 50
.01;
1 8  0.01 1.    0.02 10.   -10.   1.0      .785 3.9267 0.070 5.2356 0.910 0.030 1.0 200 50 50
.01;
0 9  0.01 200   0.00 5.0   -5.0   0.0       0   0      0     0     0     0     0   0  0  0
0;
1 10 0.01 1.    0.02 10.   -10.   1.0      .785 3.9267 0.070 5.2356 0.910 0.030 1.0 200 50 50
.01;
1 11 0.01 1.    0.02 10.   -10.   1.0      .785 3.9267 0.070 5.2356 0.910 0.030 1.0 200 50 50
.01;
1 12 0.01 1.    0.02 10.   -10.   1.0      .785 3.9267 0.070 5.2356 0.910 0.030 1.0 200 50 50
.01;
           ];
 %*********************** EXCITER DATA ENDS ***********************

% *********************** PSS DATA STARTS ***********************
%1-S. No.
%2-present machine index
%3-pssgain
%4-washout time constant
%5-first lead time constant
%6-first lag time constant
%7-second lead time constant
%8-second lag time constant
%9-third lead time constant
%10-third lag time constant
%11-maximum output limit
%12-minimum output limit
pss_con = [
     1   1   12   10   0.15   0.04   0.15   0.04   0.15   0.04 0.2 -0.05 ;
     2   2   20   15   0.15   0.04   0.15   0.04   0.15   0.04 0.2 -0.05 ;
     3   3   20   15   0.15   0.04   0.15   0.04   0.15   0.04 0.2 -0.05 ;
     4   4   20   15   0.15   0.04   0.15   0.04   0.15   0.04 0.2 -0.05 ;
     5   5   12   10   0.15   0.04   0.15   0.04   0.15   0.04 0.2 -0.05 ;
     6   6   12   10   0.15   0.04   0.15   0.04   0.15   0.04 0.2 -0.05 ;
     7   7   20   15   0.15   0.04   0.15   0.04   0.15   0.04 0.2 -0.05 ;
```

```
    8    8    20   15  0.15  0.04   0.15  0.04   0.15   0.04 0.2 -0.05 ;
    %9   9    12   10  0.15  0.04   0.15  0.04   0.15   0.04 0.2 -0.05 ;


    9    9    15   10  0.09  0.02   0.09  0.02   1      1    0.2 -0.05 ;
    10   10   20   15  0.15  0.04   0.15  0.04   0.15   0.04 0.2 -0.05 ;
    11   11   20   15  0.15  0.04   0.15  0.04   0.15   0.04 0.2 -0.05 ;
    12   12   20   15  0.09  0.04   0.15  0.04   0.15   0.04 0.2 -0.05 ;
    ];
%********************** PSS DATA ENDS ************************
--file: form_jac.m--

function [Jac11,Jac12,Jac21,Jac22]=form_jac(V,ang,Y,ang_red,volt_red)
% Syntax:   [Jac] = form_jac(V,ang,Y,ang_red,volt_red)
%           [Jac11,Jac12,Jac21,Jac22] = form_jac(V,ang,Y,...
%                                       ang_red,volt_red)
%
% Purpose: form the Jacobian matrix using sparse matrix techniques
%
% Input:    V        - magnitude of bus voltage
%           ang      - angle(rad) of bus voltage
%           Y        - admittance matrix
%           ang_red  - matrix to eliminate swing bus  voltage magnitude and angle
%                      entries
%           volt_red - matrix to eliminate generator bus voltage magnitude
%                      entries
% Output:   Jac      - jacobian matrix
%           Jac11,Jac12,Jac21,Jac22 - submatrices of
%                                     jacobian matrix
% See also:
%
% Calls:
%
% Called By:   vsdemo loadflow

% (c) Copyright 1991-1996 Joe H. Chow - All Rights Reserved
%
% History (in reverse chronological order)
% Version:   2.0
% Author:    Graham Rogers
% Date:      March 1994
% Purpose:   eliminated do loops to improve speed
% Version:   1.0
% Author:    Kwok W. Cheung, Joe H. Chow
% Date:      March 1991
```

```
%
% ********************************************************
jay = sqrt(-1);
exp_ang = exp(jay*ang);
% Voltage rectangular coordinates
V_rect = V.*exp_ang;
CV_rect=conj(V_rect);
Y_con = conj(Y);
%vector of conjugate currents
i_c=Y_con*CV_rect;
% complex power vector
S=V_rect.*i_c;
S=sparse(diag(S));
Vdia=sparse(diag(V_rect));
CVdia=conj(Vdia);
Vmag=sparse(diag(abs(V)));
S1=Vdia*Y_con*CVdia;
t1=((S+S1)/Vmag)*volt_red';
t2=(S-S1)*ang_red';
J11=-ang_red*imag(t2);
J12=ang_red*real(t1);
J21=volt_red*real(t2);
J22=volt_red*imag(t1);
if nargout > 3
   Jac11 = J11; clear J11
   Jac12 = J12; clear J12
   Jac21 = J21; clear J21
   Jac22 = J22; clear J22
else
   Jac11 = [J11 J12;
       J21 J22];
end
--loadflow.m--



function [bus_sol,line_sol,line_flow,Y,y,tps,chrg] = ...
   loadflow(bus,line,tol,iter_max,acc,display,flag)
% Syntax:    [bus_sol,line_sol,line_flow] =
% loadflow(bus,line,tol,iter_max,acc,display,flag)
% 8/12/97
% Purpose:   solve the load-flow equations of power systems
%            modified to eliminate do loops and improve the use
%            sparse matices
% Input:    bus        - bus data
```

```
%               line      - line data
%               tol       - tolerance for convergence
%               iter_max  - maximum number of iterations
%               acc       - acceleration factor
%               display   - 'y', generate load-flow study report
%                             else, no load-flow study report
%               flag      - 1, form new Jacobian every iteration
%                           2, form new Jacobian every other
%                                iteration
%
% Output:   bus_sol   - bus solution (see report for the
%                          solution format)
%           line_sol  - modified line matrix
%           line_flow - line flow solution (see report)
%
% See also:
%
% Algorithm: Newton-Raphson method using the polar form of
%    the equations for P(real power) and Q(reactive power).
%
% Calls:     Y_sparse, calc, form_jac chq_lim
%
%
% (c) Copyright 1991 Joe H. Chow - All Rights Reserved
%
% History (in reverse chronological order)
% Modification to correct generator var error on output
% Graham Rogers November 1997
% Version:   2.1
% Author:      Graham Rogers
% Date:        October 1996
% Purpose:   To add generator var limits and on-load tap changers
% Version:   2.0
% Author:    Graham Rogers
% Date:      March 1994
% Version:   1.0
% Authors:   Kwok W. Cheung, Joe H. Chow
% Date:      March 1991
%
% ************************************************************
global bus_int
global Qg bus_type g_bno PQV_no PQ_no ang_red volt_red
global Q Ql
global gen_chg_idx
```

```
global ac_line n_dcl
tt = clock;      % start the total time clock
jay = sqrt(-1);
load_bus = 3;
gen_bus = 2;
swing_bus = 1;
if exist('flag') == 0
   flag = 1;
end
lf_flag = 1;
% set solution defaults
if isempty(tol);tol = 1e-9;end
if isempty(iter_max);iter_max = 30;end
if isempty(acc);acc = 1.0; end;
if isempty(display);display = 'n';end;

if flag <1 || flag > 2
   error('LOADFLOW: flag not recognized')
end
[nline nlc] = size(line);    % number of lines and no of line cols
[nbus ncol] = size(bus);     % number of buses and number of col
% set defaults
% bus data defaults
if ncol<15
   % set generator var limits
   if ncol<12
      bus(:,11) = 9999*ones(nbus,1);
      bus(:,12) = -9999*ones(nbus,1);
   end
   if ncol<13;bus(:,13) = ones(nbus,1);end
   bus(:,14) = 1.5*ones(nbus,1);
   bus(:,15) = 0.5*ones(nbus,1);
   volt_min = bus(:,15);
   volt_max = bus(:,14);
else
   volt_min = bus(:,15);
   volt_max = bus(:,14);
end
no_vmin_idx = find(volt_min==0);
if ~isempty(no_vmin_idx)
   volt_min(no_vmin_idx) = 0.5*ones(length(no_vmin_idx),1);
end
no_vmax_idx = find(volt_max==0);
if ~isempty(no_vmax_idx)
```

```
   volt_max(no_vmax_idx) = 1.5*ones(length(no_vmax_idx),1);
end
no_mxv = find(bus(:,11)==0);
no_mnv = find(bus(:,12)==0);
if ~isempty(no_mxv);bus(no_mxv,11)=9999*ones(length(no_mxv),1);end
if ~isempty(no_mnv);bus(no_mnv,12) = -9999*ones(length(no_mnv),1);end
no_vrate = find(bus(:,13)==0);
if ~isempty(no_vrate);bus(no_vrate,13) = ones(length(no_vrate),1);end
tap_it = 0;
tap_it_max = 10;
no_taps = 0;
% line data defaults, sets all tap ranges to zero - this fixes taps
if nlc < 10
   line(:,7:10) = zeros(nline,4);
   no_taps = 1;
   % disable tap changing
end

% outer loop for on-load tap changers

mm_chk=1;
while (tap_it<tap_it_max&&mm_chk)
   tap_it = tap_it+1;
   % build admittance matrix Y
   [Y,nSW,nPV,nPQ,SB] = y_sparse(bus,line);
   % process bus data
   bus_no = bus(:,1);
   V = bus(:,2);
   ang = bus(:,3)*pi/180;
   Pg = bus(:,4);
   Qg = bus(:,5);
   Pl = bus(:,6);
   Ql = bus(:,7);
   Gb = bus(:,8);
   Bb = bus(:,9);
   bus_type = round(bus(:,10));
   qg_max = bus(:,11);
   qg_min = bus(:,12);
   sw_bno=ones(nbus,1);
   g_bno=sw_bno;
   % set up index for Jacobian calculation
   %% form PQV_no and PQ_no
   bus_zeros=zeros(nbus,1);
   swing_index=find(bus_type==1);
```

```
sw_bno(swing_index)=bus_zeros(swing_index);
PQV_no=find(bus_type >=2);
PQ_no=find(bus_type==3);
gen_index=find(bus_type==2);
g_bno(gen_index)=bus_zeros(gen_index);
%sw_bno is a vector having ones everywhere but the swing bus locations
%g_bno is a vector having ones everywhere but the generator bus locations

% construct sparse angle reduction matrix
il = length(PQV_no);
ii = (1:1:il)';
ang_red = sparse(ii,PQV_no,ones(il,1),il,nbus);

% construct sparse voltage reduction matrix
il = length(PQ_no);
ii = (1:1:il)';
volt_red = sparse(ii,PQ_no,ones(il,1),il,nbus);

iter = 0;      % initialize iteration counter

% calculate the power mismatch and check convergence

[delP,delQ,P,Q,conv_flag] =...
   calc(V,ang,Y,Pg,Qg,Pl,Ql,sw_bno,g_bno,tol);



st = clock;      % start the iteration time clock
%% start iteration process for main Newton_Raphson solution
while (conv_flag == 1 && iter < iter_max)
   iter = iter + 1;
   % Form the Jacobean matrix
   clear Jac
   Jac=form_jac(V,ang,Y,ang_red,volt_red);
   % reduced real and reactive power mismatch vectors
   red_delP = ang_red*delP;
   red_delQ = volt_red*delQ;
   clear delP delQ
   % solve for voltage magnitude and phase angle increments
   temp = Jac\[red_delP; red_delQ];
   % expand solution vectors to all buses
   delAng = ang_red'*temp(1:length(PQV_no),:);
   delV = volt_red'*temp(length(PQV_no)+1:length(PQV_no)+length(PQ_no),:);
   % update voltage magnitude and phase angle
   V = V + acc*delV;
```

```
        V = max(V,volt_min);  % voltage higher than minimum
        V = min(V,volt_max);  % voltage lower than maximum
        ang = ang + acc*delAng;
        % calculate the power mismatch and check convergence
        [delP,delQ,P,Q,conv_flag] =...
            calc(V,ang,Y,Pg,Qg,Pl,Ql,sw_bno,g_bno,tol);
        % check if Qg is outside limits
        gen_index=find(bus_type==2);
        Qg(gen_index) = Q(gen_index) + Ql(gen_index);
        lim_flag = chq_lim(qg_max,qg_min);
        if lim_flag == 1;
            disp('Qg at var limit');
        end
    end
     if iter == iter_max
        imstr = int2str(iter_max);
        disp(['inner ac load flow failed to converge after ', imstr,' iterations'])
        tistr = int2str(tap_it);
        disp(['at tap iteration number ' tistr])
    else
        disp('inner load flow iterations')
        disp(iter)
    end
    if no_taps == 0
        lftap
    else
        mm_chk = 0;
    end
end
if tap_it >= tap_it_max
    titstr = int2str(tap_it_max);
    disp(['tap iteration failed to converge after',titstr,' iterations'])
else
    disp(' tap iterations ')
    disp(tap_it)
end
ste = clock;      % end the iteration time clock
vmx_idx = find(V==volt_max);
vmn_idx = find(V==volt_min);
if ~isempty(vmx_idx)
    disp('voltages at')
    bus(vmx_idx,1)'
    disp('are at the max limit')
end
```

```
if ~isempty(vmn_idx)
   disp('voltages at')
   bus(vmn_idx,1)'
   disp('are at the min limit');
end
gen_index=find(bus_type==2);
load_index = find(bus_type==3);
Pg(gen_index) = P(gen_index) + Pl(gen_index);
Qg(gen_index) = Q(gen_index) + Ql(gen_index);
gend_idx = find((bus(:,10)==2)&(bus_type~=2));
if ~isempty(gend_idx)
   disp('the following generators are at their var limits')
   disp('    bus#    Qg')
   disp([bus(gend_idx,1)  Q(gend_idx)])
   Qlg = Ql(gend_idx)-bus(gend_idx,7);% the generator var part of the load
   Qg(gend_idx)=Qg(gend_idx)-Qlg;% restore the generator vars
   Ql(gend_idx)=bus(gend_idx,7);% restore the original load vars
end
Pl(load_index) = Pg(load_index) - P(load_index);
Ql(load_index) = Qg(load_index) - Q(load_index);

Pg(SB) = P(SB) + Pl(SB); Qg(SB) = Q(SB) + Ql(SB);
VV = V.*exp(jay*ang);   % solution voltage
% calculate the line flows and power losses
tap_index = find(abs(line(:,6))>0);
tap_ratio = ones(nline,1);
tap_ratio(tap_index)=line(tap_index,6);
phase_shift(:,1) = line(:,7);
tps = tap_ratio.*exp(jay*phase_shift*pi/180);
from_bus = line(:,1);
from_int = bus_int(round(from_bus));
to_bus = line(:,2);
to_int = bus_int(round(to_bus));
r = line(:,3);
rx = line(:,4);
chrg = line(:,5);
z = r + jay*rx;
y = ones(nline,1)./z;


MW_s = VV(from_int).*conj((VV(from_int) - tps.*VV(to_int)).*y ...
   + VV(from_int).*(jay*chrg/2))./(tps.*conj(tps));
P_s = real(MW_s);      % active power sent out by from_bus
% to to_bus
```

```
Q_s = imag(MW_s);     % reactive power sent out by
% from_bus to to_bus
MW_r = VV(to_int).*conj((VV(to_int) ...
   - VV(from_int)./tps).*y ...
   + VV(to_int).*(jay*chrg/2));
P_r = real(MW_r);     % active power received by to_bus
% from from_bus
Q_r = imag(MW_r);     % reactive power received by
% to_bus from from_bus
iline = (1:1:nline)';
line_ffrom = [iline from_bus to_bus P_s Q_s];
line_fto   = [iline to_bus from_bus P_r Q_r];
% keyboard
P_loss = sum(P_s) + sum(P_r) ;
Q_loss = sum(Q_s) + sum(Q_r) ;
bus_sol=[bus_no  V  ang*180/pi Pg Qg Pl Ql Gb Bb...
      bus_type qg_max qg_min bus(:,13) volt_max volt_min];
line_sol = line;
line_flow(1:nline, :)  =[iline from_bus to_bus P_s Q_s];
line_flow(1+nline:2*nline,:) = [iline to_bus from_bus P_r Q_r];
% Give warning of non-convergence
if conv_flag == 1
   disp('ac load flow failed to converge')
   error('stop')
end

% display results
if display == 'y',
   clc
   disp('                            LOAD-FLOW STUDY')
   disp('                   REPORT OF POWER FLOW CALCULATIONS ')
   disp(' ')
   disp(date)
   fprintf('SWING BUS                 : BUS %g \n', SB)
   fprintf('NUMBER OF ITERATIONS      : %g \n', iter)
   fprintf('SOLUTION TIME             : %g sec.\n',etime(ste,st))
   fprintf('TOTAL TIME                : %g sec.\n',etime(clock,tt))
   fprintf('TOTAL REAL POWER LOSSES   : %g.\n',P_loss)
   fprintf('TOTAL REACTIVE POWER LOSSES: %g.\n\n',Q_loss)
   if conv_flag == 0,
      disp('                              GENERATION          LOAD')
      disp('    BUS    VOLTS    ANGLE    REAL  REACTIVE    REAL  REACTIVE ')
      disp(bus_sol(:,1:7))
```

```
      disp('                        LINE FLOWS                    ')
      disp('      LINE  FROM BUS    TO BUS       REAL  REACTIVE   ')
      disp(line_ffrom)
      disp(line_fto)
   end
end; %
if iter > iter_max,
   disp('Note: Solution did not converge in %g iterations.\n', iter_max)
   lf_flag = 0
end

return


--file: y_sparse.m--

function    [Y,nSW,nPV,nPQ,SB] = y_sparse(bus,line)
% Syntax:    [Y,nSW,nPV,nPQ,SB] = y_sparse(bus,line)
%
% Purpose:   build sparse admittance matrix Y from the line data
%
% Input:     bus  - bus data
%            line - line data
%
% Output:    Y    - admittance matrix
%            nSW  - total number of swing buses
%            nPV  - total number generator buses
%            nPQ  - total number of load buses
%            SB   - internal bus numbers of swing bus
%
% See also:
%
% Calls:
%
% Called By:   loadflow, form_j, calc

% (c) Copyright 1994-1996 Joe Chow - All Rights Reserved
%
% History (in reverse chronological order)
%
% Version:   2.0
% Author:    Graham Rogers
% Date:      April 1994
% Version:   1.0
% Author:    Kwok W. Cheung, Joe H. Chow
```

```
% Date:      March 1991
%
% ***********************************************************
global bus_int

jay = sqrt(-1);
swing_bus = 1;
gen_bus = 2;
load_bus = 3;

nline = length(line(:,1));     % number of lines
nbus = length(bus(:,1));     % number of buses
r=zeros(nline,1);
rx=zeros(nline,1);
chrg=zeros(nline,1);
z=zeros(nline,1);
y=zeros(nline,1);

Y = sparse(1,1,0,nbus,nbus);

% set up internal bus numbers for second indexing of buses
busmax = max(bus(:,1));
bus_int = zeros(busmax,1);
ibus = (1:nbus)';
bus_int(round(bus(:,1))) = ibus;


% process line data and build admittance matrix Y
  r = line(:,3);
  rx = line(:,4);
  chrg =jay*sparse(diag( 0.5*line(:,5)));
  z = r + jay*rx;     % line impedance
  y = sparse(diag(ones(nline,1)./z));

% determine connection matrices including tap changers and phase shifters
  from_bus = round(line(:,1));
  from_int = bus_int(from_bus);
  to_bus = round(line(:,2));
  to_int = bus_int(to_bus);
  tap_index = find(abs(line(:,6))>0);
  tap=ones(nline,1);
  tap(tap_index)=1. ./line(tap_index,6);
  phase_shift = line(:,7);
  tap = tap.*exp(-jay*phase_shift*pi/180);
```

```
  % sparse matrix formulation
  iline = [1:1:nline]';
  C_from = sparse(from_int,iline,tap,nbus,nline,nline);
  C_to = sparse(to_int,iline,ones(nline,1),nbus,nline,nline);
  C_line = C_from - C_to;

% form Y matrix from primative line ys and connection matrices
  Y=C_from*chrg*C_from' + C_to*chrg*C_to' ;
  Y = Y + C_line*y*C_line';
  Gb = bus(:,8);      % bus conductance
  Bb = bus(:,9);      % bus susceptance

% add diagonal shunt admittances
  Y = Y + sparse(ibus,ibus,Gb+jay*Bb,nbus,nbus);

if nargout > 1
  % count buses of different types
  nSW = 0;
  nPV = 0;
  nPQ = 0;
  bus_type=round(bus(:,10));
  load_index=find(bus_type==3);
  gen_index=find(bus_type==2);
  SB=find(bus_type==1);
  nSW=length(SB);
  nPV=length(gen_index);
  nPQ=length(load_index);
end

return
```

D.2   Simulation Files

The simulation files can be found in https://drive.google.com/open?id=0B2onGI-yt3FwcTBQWFgwQTYwRU0 with:
- "Benchmark_IEEE_standard.mdl" to study the system dynamics by step-by-step numerical integration;

and "Init_MultiMachine13fault.m" is the initial file to simulate the case when there is a fault near Generator 13.

Bibliography

[1] A. K. Singh and B. C. Pal, "Ieee pes task force on benchmark systems for stability controls report on the 68-bus, 16-machine, 5-area system."

[2] "Ieee recommended practice for excitation system models for power system stability studies," *IEEE Std 421.5-1992*, 1992.

[3] K. Morrison, *Transient Stability*, 2nd ed. Boca Raton: CRC Press LLC, 2001, 2001, ch. 11.2.

[4] *http://mainstreamrp.com/supergrid/*.

[5] S. D'Arco, J. Suul, and O. Fosso, "Automatic tuning of cascaded controllers for power converters using eigenvalue parametric sensitivities," *Industry Applications, IEEE Transactions on*, vol. 51, no. 2, pp. 1743–1753, March 2015.

[6] P. Kundur, N. J. Balu, and M. G. Lauby, *Power system stability and control.* McGraw-hill New York, 1994, vol. 7.

[7] H. Alkhatib, "Etude de la stabilite aux petites perturbations dans les grands reseaux electriques : Optimisation de la regulation par une methode metaheuristique." Ph.D. dissertation, Automatique/Robotique. Université Paul Cézanne -Aix-Marseille III, 2008. Fracançais. <tel-00408160v2>, 2008.

[8] H.-D. Chang, C.-C. Chu, and G. Cauley, "Direct stability analysis of electric power systems using energy functions: theory, applications, and perspective," *Proceedings of the IEEE*, vol. 83, no. 11, pp. 1497–1529, Nov 1995.

[9] B. Wang and K. Sun, "Formulation and characterization of power system electromechanical oscillations," *IEEE Transactions on Power Systems*, vol. 31, no. 6, pp. 5082–5093, Nov 2016.

[10] H. Amano, T. Kumano, and T. Inoue, "Nonlinear stability indexes of power swing oscillation using normal form analysis," *IEEE Transactions on Power Systems*, vol. 21, no. 2, pp. 825–834, May 2006.

[11] C.-M. Lin, V. Vittal, W. Kliemann, and A. A. Fouad, "Investigation of modal interaction and its effects on control performance in stressed power systems using normal forms of vector fields," *IEEE Transactions on Power Systems*, vol. 11, no. 2, pp. 781–787, May 1996.

[12] Y. X. Ni, V. Vittal, W. Kliemann, and A. A. Fouad, "Nonlinear modal interaction in hvdc/ac power systems with dc power modulation," *IEEE Transactions on Power Systems*, vol. 11, no. 4, pp. 2011–2017, Nov 1996.

[13] J. Thapar, V. Vittal, W. Kliemann, and A. A. Fouad, "Application of the normal form of vector fields to predict interarea separation in power systems," *IEEE Transactions on Power Systems*, vol. 12, no. 2, pp. 844–850, May 1997.

[14] S. Saha, A. A. Fouad, W. H. Kliemann, and V. Vittal, "Stability boundary approximation of a power system using the real normal form of vector fields," *IEEE Transactions on Power Systems*, vol. 12, no. 2, pp. 797–802, May 1997.

[15] S. K. Starrett and A. A. Fouad, "Nonlinear measures of mode-machine participation [transmission system stability]," *IEEE Transactions on Power Systems*, vol. 13, no. 2, pp. 389–394, May 1998.

[16] G. Jang, V. Vittal, and W. Kliemann, "Effect of nonlinear modal interaction on control performance: use of normal forms technique in control design. i. general theory and procedure," *IEEE Transactions on Power Systems*, vol. 13, no. 2, pp. 401–407, May 1998.

[17] ——, "Effect of nonlinear modal interaction on control performance: use of normal forms technique in control design. ii. case studies," *IEEE Transactions on Power Systems*, vol. 13, no. 2, pp. 408–413, May 1998.

[18] V. Vittal, W. Kliemann, Y. X. Ni, D. G. Chapman, A. D. Silk, and D. J. Sobajic, "Determination of generator groupings for an islanding scheme in the manitoba hydro system using the method of normal forms," *IEEE Transactions on Power Systems*, vol. 13, no. 4, pp. 1345–1351, Nov 1998.

[19] S. Zhu, V. Vittal, and W. Kliemann, "Analyzing dynamic performance of power systems over parameter space using normal forms of vector fields-part i: identification of vulnerable regions," *IEEE Transactions on Power Systems*, vol. 16, no. 3, pp. 444–450, Aug 2001.

[20] ——, "Analyzing dynamic performance of power systems over parameter space using normal forms of vector fields part ii: Comparison of the system structure," *IEEE Power Engineering Review*, vol. 21, no. 6, pp. 71–71, June 2001.

[21] H. Amano and T. Inoue, "A new pss parameter design using nonlinear stability analysis," in *Power Engineering Society General Meeting, 2007. IEEE*, June 2007, pp. 1–8.

[22] C. Touzé, O. Thomas, and A. Chaigne, "Hardening/softening behaviour in non-linear oscillations of structural systems using non-linear normal modes," *Journal of Sound Vibration*, vol. 273, no. 1-2, pp. 77–101, 2004.

[23] C. Touzé and M. Amabili, "Non-linear normal modes for damped geometrically non-linear systems: application to reduced-order modeling of harmonically forced structures," *Journal of Sound and Vibration*, vol. 298, no. 4-5, pp. 958–981, 2006.

[24] C. Touzé, "Normal form theory and nonlinear normal modes: theoretical settings and applications," in *Modal Analysis of nonlinear Mechanical Systems*, G. Kerschen, Ed. Springer Series CISM courses and lectures, vol. 555, ISBN 978-3-7091-1790-2, 2014.

[25] S. Liu, A. R. Messina, and V. Vittal, "Assessing placement of controllers and nonlinear behavior using normal form analysis," *IEEE Transactions on Power Systems*, vol. 20, no. 3, pp. 1486–1495, Aug 2005.

[26] T. Tian, X. Kestelyn, and O. Thomas, "Third-order based analytical investigation of nonlinear interactions between voltage source converters interconnected to a transmission grid," in *2016 18th European Conference on Power Electronics and Applications (EPE'16 ECCE Europe)*, Sept 2016, pp. 1–10.

[27] T. Tian, X. Kestelyn, G. Denis, X. Guillaud, and O. Thomas, "Analytical investigation of nonlinear interactions between voltage source converters interconnected to a transmission grid," in *2016 IEEE Power and Energy Society General Meeting (PESGM)*, July 2016, pp. 1–5.

[28] F. Milano, "An open source power system analysis toolbox," *IEEE Transac-*

tions on Power Systems, vol. 20, no. 3, pp. 1199–1206, Aug 2005.

[29] F. p. D. Mello, P. J. Nolan, T. F. Laskowski, and J. M. Undrill, "Coordinated application of stabilizers in multimachine power systems," *IEEE Transactions on Power Apparatus and Systems*, vol. PAS-99, no. 3, pp. 892–901, May 1980.

[30] I. J. Perez-arriaga, G. C. Verghese, and F. C. Schweppe, "Selective modal analysis with applications to electric power systems, part i: Heuristic introduction," *IEEE Transactions on Power Apparatus and Systems*, vol. PAS-101, no. 9, pp. 3117–3125, Sept 1982.

[31] F. L. Pagola, I. J. Perez-Arriaga, and G. C. Verghese, "On sensitivities, residues and participations: applications to oscillatory stability analysis and control," *IEEE Transactions on Power Systems*, vol. 4, no. 1, pp. 278–285, Feb 1989.

[32] N. Martins and L. T. G. Lima, "Determination of suitable locations for power system stabilizers and static var compensators for damping electromechanical oscillations in large scale power systems," *IEEE Transactions on Power Systems*, vol. 5, no. 4, pp. 1455–1469, Nov 1990.

[33] V. Vittal, N. Bhatia, and A. A. Fouad, "Analysis of the inter-area mode phenomenon in power systems following large disturbances," *IEEE Transactions on Power Systems*, vol. 6, no. 4, pp. 1515–1521, Nov 1991.

[34] A. H. Nayfeh, *A Method of Normal Forms*. New-York: John Wiley & sons, inc., 2011.

[35] I. Martínez, A. Messina, and E. Barocio, "Perturbation analysis of power systems: effects of second- and third-order nonlinear terms on system dynamic behavior," *Electric Power Systems Research*, vol. 71, no. 2, pp. 159 – 167, 2004. [Online]. Available: http://www.sciencedirect.com/science/article/pii/S037877960400029X

[36] Q. Huang, Z. Wang, and C. Zhang, "Evaluation of the effect of modal interaction higher than 2nd order in small-signal analysis," in *Power Energy Society General Meeting, 2009. PES '09. IEEE*, July 2009, pp. 1–6.

[37] L. Jezequel and C. Lamarque, "Analysis of non-linear dynamical systems by the normal form theory," *Journal of Sound and Vibration*, vol. 149, no. 3, pp. 429 – 459, 1991. [Online]. Available: http://www.sciencedirect.com/science/article/pii/0022460X9190446Q

[38] N. Pariz, H. Shanechi, and E. Vaahedi, "Explaining and validating stressed power systems behavior using modal series," *Power Systems, IEEE Transactions on*, vol. 18, no. 2, pp. 778–785, May 2003.

[39] H. M. Shanechi, N. Pariz, and E. Vaahedi, "General nonlinear modal representation of large scale power systems," *IEEE Transactions on Power Systems*, vol. 18, no. 3, pp. 1103–1109, Aug 2003.

[40] R. Z. Davarani, R. Ghazi, and N. Pariz, "Nonlinear modal analysis of interaction between torsional modes and {SVC} controllers," *Electric Power Systems Research*, vol. 91, pp. 61 – 70, 2012. [Online]. Available: http://www.sciencedirect.com/science/article/pii/S0378779612001277

[41] S. Soltani, N. Pariz, and R. Ghazi, "Extending the perturbation technique

to the modal representation of nonlinear systems," *Electric Power Systems Research*, vol. 79, no. 8, pp. 1209 – 1215, 2009. [Online]. Available: http://www.sciencedirect.com/science/article/pii/S0378779609000650

[42] F. Wu, H. Wu, Z. Han, and D. Gan, "Validation of power system non-linear modal analysis methods," *Electric Power Systems Research*, vol. 77, no. 10, pp. 1418 – 1424, 2007. [Online]. Available: http://www.sciencedirect.com/science/article/pii/S0378779606002574

[43] S. Shaw and C. Pierre, "Normal modes for non-linear vibratory systems," *Journal of Sound and Vibration*, vol. 164, no. 1, pp. 85 – 124, 1993. [Online]. Available: http://www.sciencedirect.com/science/article/pii/S0022460X83711983

[44] R. Betancourt, E. Barocio, A. Messina, and I. MartÃnez, "Modal analysis of inter-area oscillations using the theory of normal modes," *Electric Power Systems Research*, vol. 79, no. 4, pp. 576 – 585, 2009. [Online]. Available: http://www.sciencedirect.com/science/article/pii/S0378779608002332

[45] M. Ribbens-Pavella and F. J. Evans, "Direct methods for studying dynamics of large-scale electric power systems-a survey," *Automatica*, vol. 21, no. 1, pp. 1–21, Jan. 1985. [Online]. Available: http://dx.doi.org/10.1016/0005-1098(85)90095-0

[46] P. M. Anderson and A. Bose, "A probabilistic approach to power system stability analysis," *IEEE Transactions on Power Apparatus and Systems*, vol. PAS-102, no. 8, pp. 2430–2439, Aug 1983.

[47] A. D. Patton, "Assessment of the security of operating electric power systems using probability methods," *Proceedings of the IEEE*, vol. 62, no. 7, pp. 892–901, July 1974.

[48] Y. Akimoto, H. Tanaka, J. Yoshizawa, D. B. Klapper, W. W. Price, and K. A. Wirgau, "Transient stability expert system," *IEEE Transactions on Power Systems*, vol. 4, no. 1, pp. 312–320, Feb 1989.

[49] H. Hakim, "Application of pattern recognition in transient security assessment," *Electric Machines & Power Systems*, vol. 20, no. 1, pp. 1–15, 1992. [Online]. Available: http://dx.doi.org/10.1080/07313569208909564

[50] L. Wehenkel, *Automatic learning techniques in power systems.* Boston: Kluwer Academic, 1998. [Online]. Available: http://www.montefiore.ulg.ac.be/services/stochastic/pubs/1998/Weh98

[51] I. Dobson and E. Barocio, "Scaling of normal form analysis coefficients under coordinate change," *IEEE Transactions on Power Systems*, vol. 19, no. 3, pp. 1438–1444, Aug 2004.

[52] J. Sanchez-Gasca, V. Vittal, M. Gibbard, A. Messina, D. Vowles, S. Liu, and U. Annakkage, "Inclusion of higher order terms for small-signal (modal) analysis: committee report-task force on assessing the need to include higher order terms for small-signal (modal) analysis," *Power Systems, IEEE Transactions on*, vol. 20, no. 4, pp. 1886–1904, Nov 2005.

[53] M. A. GÃ©rard Iooss, *Topics in Bifurcation Theory and Applications*, 2nd ed., ser. Advanced Series in Nonlinear Dynamics: Volume 3. World Scientific,

1999. [Online]. Available: http://www.worldscientific.com/worldscibooks/10.1142/3990

[54] H. Poincaré, *Les méthodes nouvelles de la mécanique céleste.* Gauthiers-Villars, Paris, 1899.

[55] C.-H. Lamarque, C. Touzé, and O. Thomas, "An upper bound for validity limits of asymptotic analytical approaches based on normal form theory," *Nonlinear Dynamics*, vol. 70, no. 3, pp. 1931–1949, 2012. [Online]. Available: http://dx.doi.org/10.1007/s11071-012-0584-y

[56] F. Dumortier, "Singularities of vector fields on the plane," *Journal of Differential Equations*, vol. 23, no. 1, pp. 53 – 106, 1977. [Online]. Available: http://www.sciencedirect.com/science/article/pii/002203967790136X

[57] J. Guckenheimer and P. Holmes, *Nonlinear oscillations, dynamical systems and bifurcations of vector fields.* New-York: Springer-Verlag, 1983.

[58] I. Martínez, A. R. Messina, and V. Vittal, "Normal form analysis of complex system models: A structure-preserving approach," *IEEE Transactions on Power Systems*, vol. 22, no. 4, pp. 1908–1915, Nov 2007.

[59] A. H. Nayfeh and D. T. Mook, *Nonlinear oscillations.* New-York: John Wiley & sons, inc., 1979.

[60] C. Touz'e, "A normal form approach for nonlinear normal modes," *[Research Report] Publications du LMA*, no. 156, 2003. [Online]. Available: https://hal-ensta.archives-ouvertes.fr/hal-01154702/document

[61] H. Dulac, "Solutions d'un systéme d'équations différentielles dans le voisinage de valeurs singuliéres," *Bulletin de la Société Mathématique de France*, vol. 42, pp. 324–383, 1912, http://www.numdam.org/item?id=BSMF_1912__40__324_0.

[62] S. Liu, "Assessing placement of controllers and nonlinear behavior of electrical power system using normal form information," Ph.D. dissertation, Iowa State University, Retrospective Theses and Dissertations. Paper 1280., 2006.

[63] R. Zeinali Davarani, R. Ghazi, and N. Pariz, "Non-linear analysis of dfig based wind farm in stressed power systems," *Renewable Power Generation, IET*, vol. 8, no. 8, pp. 867–877, 2014.

[64] R. Zeinali, R. Ghazi, and N. Pariz, "Nonlinear interaction problems of large capacity wind farms," in *Smart Grids (ICSG), 2012 2nd Iranian Conference on*, May 2012, pp. 1–6.

[65] R. Rosenberg, "On nonlinear vibrations of systems with many degrees of freedom," *Advances in Applied Mechanics*, vol. 9, pp. 155 – 242, 1966. [Online]. Available: http://www.sciencedirect.com/science/article/pii/S0065215608700085

[66] C. Pierre and s. shaw, "Non-linear normal modes and invariant manifolds," *Journal of Sound and Vibration*, vol. 150, no. 1, pp. 170–173, 1991. [Online]. Available: https://hal.archives-ouvertes.fr/hal-01310674

[67] A. Luongo, "Center manifold and normal form theories," in *3rd Sperlonga Summer School on Mechanics and Engineering Sciences*, 23-27 Spetember,2013, pp. 6–9. [Online]. Available: http://memocs.univaq.it/

wp-content/uploads/2013/10/Sperlonga_2013_Lect_3+.pdf

[68] A. Messina and E. Barocio, "Assessment of non-linear modal interaction in stressed power networks using the method of normal forms," *International Journal of Electrical Power & Energy Systems*, vol. 25, no. 1, pp. 21 – 29, 2003. [Online]. Available: http://www.sciencedirect.com/science/article/pii/S0142061502000157

[69] O. Rodríguez, A. Medina, and G. Andersson, "Closed-form analytical characterisation of non-linear oscillations in power systems incorporating unified power flow controller," *Generation, Transmission Distribution, IET*, vol. 9, no. 11, pp. 1019–1032, 2015.

[70] A. Egea-Alvarez, S. Fekriasl, F. Hassan, and O. Gomis-Bellmunt, "Advanced vector control for voltage source converters connected to weak grids," *Power Systems, IEEE Transactions on*, vol. 30, no. 6, pp. 3072–3081, Nov 2015.

[71] M. Mikofski. (2014) Newton-raphson solver. [Online]. Available: https://fr.mathworks.com/matlabcentral/fileexchange/43097-newton-raphson-solver

[72] G. Iooss and M. Adelmeyer, *Topics in Bifurcation Theory and Applications*. World Scientific, 1992.

[73] W. Kang, "Normal form, invariants, and bifurcations of nonlinear control systems in the particle deflection plane," in *Dynamics, Bifurcations, and Control*, D. L. G. Professor Fritz Colonius, Ed. Berlin; Heidelberg; NewYork; Barcelona; Hong Kong; London; Milano; Paris; Tokyo: Springer, 2002, ch. 5, pp. 67–87.

[74] R. Betancourt, E. Barocio, J. Arroyo, and A. Messina, "A real normal form approach to the study of resonant power systems," *Power Systems, IEEE Transactions on*, vol. 21, no. 1, pp. 431–432, Feb 2006.

[75] H. Lomei, M. Assili, D. Sutanto, and K. M. Muttaqi, "A new approach to reduce the nonlinear characteristics of a stressed power system by using the normal form technique in the control design of the excitation system," *IEEE Transactions on Industry Applications*, vol. 53, no. 1, pp. 492–500, Jan 2017.

[76] B. Wang and K. Sun, "Power system differential-algebraic equations," *CoRR*, vol. abs/1512.05185, 2015. [Online]. Available: http://arxiv.org/abs/1512.05185

[77] P. M. Anderson and A. A. Fouad, *Power system Control and Stability,2nd Edition*. Wiley-IEEE Press, 2002.

[78] B. Wang, X. Su, and K. Sun, "Properties of the frequency-amplitude curve," *IEEE Transactions on Power Systems*, vol. 32, no. 1, pp. 826–827, Jan 2017.

[79] [Online]. Available: http://www.sel.eesc.usp.br/ieee/

[80] C. B. Pal Bikash, *Robust Control in Power Systems*. Springer US, 2005.

[81] T. Tian, Y. Liao, and X. Kestelyn, "A systematic methodology based on emr and modal analysis to analyze and control modern systems," in *JCGE2015seeds,Cherburg, France*, June 11-12 2015. [Online]. Available: https://www.researchgate.net/publication/301228019_A_Systematic_Methodology_Based_on_EMR_and_Modal_Analysis_to_Analyze_and_Control_Modern_Systems

[82] J.-J. E. Slotine and W. Li, *Applied nonlinear control.* Upper Saddle River, NJ: Pearson, 1991, the book can be consulted by contacting: BE-ABP-CC3: Pfingstner, Juergen. [Online]. Available: https://cds.cern.ch/record/1228283

[83] J. C. Slater and D. J. Inman, "Nonlinear modal control method," *Journal of Guidance, Control, and Dynamics*, vol. 18, no. 3, pp. 433–440., 1995. [Online]. Available: http://www.sciencedirect.com/science/article/pii/S0967066112002328

[84] S. Joo and J. H. Seo, "Design and analysis of the nonlinear feedback linearizing control for an electromagnetic suspension system," *IEEE Transactions on Control Systems Technology*, vol. 5, no. 1, pp. 135–144, Jan 1997.

[85] M. J. Balas, "Active control of flexible systems," *Journal of Optimization Theory and Applications*, vol. 25, no. 3, pp. 415–436, 1997. [Online]. Available: http://dx.doi.org/10.1007/BF00932903

[86] L. Meirovitch, H. Baruh, , and H.Oz, "A comparison of control techniques for large flexible systems," *Journal of Guidance, Control*, vol. 6, no. 4, pp. 302–310, 1997.

[87] M. Serra, F. Resta, and F. Ripamonti, "A comparison between the imsc and the dmsc for vibration suppression of smart flexible structures," *Proc. SPIE*, vol. 8688, pp. 868 823–868 823–12, 2013. [Online]. Available: http://dx.doi.org/10.1117/12.2009670

[88] I. García-Herreros, X. Kestelyn, J. Gomand, R. Coleman, and P.-J. Barre, "Model-based decoupling control method for dual-drive gantry stages: A case study with experimental validations," *Control Engineering Practice*, vol. 21, no. 3, pp. 298 – 307, 2013. [Online]. Available: http://www.sciencedirect.com/science/article/pii/S0967066112002328

[89] C. L. Archer and M. Z.Jacobson, "Supplying baseload power and reducing transmission requirements by interconnecting wind farms," *Journal of Applied Meteorology and Climatology*, nov 2007.

[90] R. Piwko, N. Miller, J. Sanchez-Gasca, X. Yuan, R. Dai, and J. Lyons, "Integrating large wind farms into weak power grids with long transmission lines," in *Power Electronics and Motion Control Conference, 2006. IPEMC 2006. CES/IEEE 5th International*, vol. 2, Aug 2006, pp. 1–7.

[91] [Online]. Available: https://www.researchgate.net/publication/310600111_Investigation_of_nonlinear_modal_control_of_multi_input_systems_with_nonlinear_coupled_dynamics_Comparison_of_control_algorithms_suitable_for_a_Gantry_pick-n-place_system

[92] J. Krener, "Normal forms for linear and nonlinear systems," *Contemporary Mathematics*, vol. 68, 1987.

[93] W. Kang and A. J. Krener, "Extended quadratic controller normal form and dynamic state feedback linearization of nonlinear systems," *SIAM Journal on Control and Optimization*, vol. 30, no. 6, pp. 1319–1337, 1992. [Online]. Available: https://doi.org/10.1137/0330070

[94] W.Kang and A.J.Krener, "Normal forms of nonlinear control systems," in *Chaos and Automatic Control.* W. Perruquetti and J-P. Barbot (Eds), 2006,

pp. 345–376.

[95] I.A.Tall and W.Respondek, "Feedback classification of nonlinear single-input control systems with controllable linearization: Normal forms, canonical forms, and invariants," *SIAM Journal on Control and Optimization*, vol. 41, no. 5, pp. 1498–1531, 2003.

[96] ——, *Feedback Equivalence of Nonlinear Control Systems: A Survey on Formal Approach*, 2006, pp. 137–262.

[97] S. Monaco and D. Normand-Cyrot, "Normal forms and approximated feedback linearization in discrete time," *Systems & Control Letters*, vol. 55, no. 1, pp. 71 – 80, 2006. [Online]. Available: http://www.sciencedirect.com/science/article/pii/S0167691105000915

[98] B. Hamzi, W. Kang, and J.-P. Barbot, "Analysis and control of hopf bifurcations," *SIAM Journal on Control and Optimization*, vol. 42, no. 6, pp. 2200–2220, 2004. [Online]. Available: https://doi.org/10.1137/S0363012900372714

[99] J. Quintero, V. Vittal, G. Heydt, and H. Zhang, "The impact of increased penetration of converter control-based generators on power system modes of oscillation," *Power Systems, IEEE Transactions on*, vol. 29, no. 5, pp. 2248–2256, Sept 2014.

[100] [Online]. Available: http://www.emrwebsite.org

Analysis and control of nonlinear multiple-input systems with coupled dynamics by the method of Normal Forms

Application to nonlinear modal interactions and transient stability assessment of interconnected power systems

Analyse et contrôle de systèmes non linéaires à entrées multiples et à dynamiques couplées par la méthode des formes normales

Les systèmes composés d'une somme de sous-systèmes interconnectés offrent les avantages majeurs de flexibilité d'organisation et de redondance synonyme de fiabilité accrue. Une des plus belles réalisations basée sur ce concept réside dans les réseaux électriques qui sont reconnus à ce jour comme la plus grande et la plus complexe des structures existantes jamais développées par l'homme.

Les phénomènes de plus en plus non linéaires rencontrés dans l'étude des nouveaux réseaux électriques amènent au développement de nouveaux outils permettant l'étude des interactions entre les différents éléments qui les composent. Parmi les outils d'analyse existants, ce mémoire présente le développement et l'application de la théorie des Formes Normales à l'étude des interactions présentes dans un réseau électrique. Les objectifs spécifiques de cette thèse concernent le développement de la méthode des Formes Normales jusqu'à l'ordre 3, l'application de cette méthode à l'étude des oscillations présentes dans des réseaux tests et l'apport de la méthode développée dans l'étude de la stabilité des réseaux.

Mots clés : Non linéaire, Analyse modale, Contrôle, Modes non linéaires, réseau électrique, stabilité

Analysis and control of nonlinear multiple-input systems with coupled dynamics by the method of Normal Forms

Systems composed with a sum of interconnected sub-systems offer the advantages of a better flexibility and redundancy for an increased reliability. One of the largest and biggest system based on this concept ever devised by man is the interconnected power system.

Phenomena encountered in the newest interconnected power systems are more and more nonlinear and the development of new tools for their study is od major concern. Among the existing tools, this PhD work presents the development and the application of the Normal Form theory to the study of the interactions existing on an interconnected power system. The specific objectives of this PhD work are the development of the Normal Form theory up to the third order, the application of this method to study power system interarea oscillations and the gain of the developed method for the study of stability of power systems.

Keywords : Nonlinear, Modal analysis, Control, Nonlinear modes, power system, stability